**Czech Technical University in Prague**

**Faculty of Electrical Engineering**

# Doctoral Thesis

*March,2017*

*Ing. Ghaeth Fandi*

Czech Technical University in Prague

Faculty of Electrical Engineering

Department of Electrical Power Engineering

# *Intelligent Distribution Systems with Dispersed Electricity Generation*

**Doctoral Thesis**

*Ing. Ghaeth Fandi*

Prague, 2017

Ph.D. Programme: Electrical Engineering and Information Technology

Branch of study: Electric Power Engineering

**Supervisor: Ing. Jan Švec, Ph.D.**

**Supervisor - specialist: Prof. Ing. Josef Tlustý, CSc.**

# Declaration

I hereby declare that I worked out the presented thesis independently and I quoted all used sources of information in accord with Methodical instructions about ethical principles for writing academic thesis.

...........................

Ing. Ghaeth Fandi

# Acknowledgment

On the first place, I would like to express my special gratitude to my supervisor, Ing. Jan Švec, Ph.D. and my Supervisor - specialist, Professor Josef Tlustý for their supervision, advice and guidance from the very early stage of this work as well as giving me extraordinary experience throughout the work.

I would like to thank my colleagues and all members of staff in the Department of Electrical Power Engineering for their assistance, kindness and helpful discussions.

I would also like to thank my friends for their encouragement.

Peace and quiet to the soul of the professor Jiří Tůma for his assistance, kindness, support and helpful discussions.

Last, but not least, my greatest gratitude goes to my parents and siblings for their encouragement and support during my studies.

Finally, I wish to express my utmost gratitude to my dear wife Farah for her support and love.

My research has been partially supported by the Ministry of Education, Youth and Sports of the Czech Republic, and by the Grants Agency of the Czech Technical University in Prague: SGS12/139/OHK3/2T/13, SGS14/188/OHK3/3T/13 and SGS17/181/OHK3/3T/13.

# Abstrakt

Velké množství energie dodávané z větrných elektráren představuje potenciál využití energie větru pomocí větrných farem do rozlehlých oblastí na Zemi. Již bylo navrženo mnoho konceptů větrných farem, ale stále je potřeba vykonat hodně práce při vývoji inteligentních distribučních systémů s rozptýlenou výrobou elektrické energie.

V této práci je uveden vývoj komplexního simulačního nástroje pro modelování dynamické odezvy větrných farem, ověření tohoto simulačního nástroje srovnáním modelů a jeho aplikace na skutečný komerční integrovaný systém. Dále jsou provedeny analýzy zatížení pro navržené systémové koncepty bez větrných farem a s farmami. Simulační nástroj v prostředí MATLAB/Simulink byl vyvinut pro kalibrovaný energetický systém, má vlastnosti požadované k provedení analýzy zatížení, ať s připojenými větrnými farmami, či bez nich. Příznivé výsledky všech ověřovacích úloh poskytují věrohodnost výsledků napěťových profilů v síti a snížení výkonových ztrát.

Simulační nástroj byl poté aplikován v předběžné analýze zatížení větrných farem. Analýza zatížení se zaměřuje na dynamickou odezvu a identifikaci potenciálních odběrů a nestabilit vyplývajících z dynamických vazeb větrných farem. Jako odezva vazeb mezi větrnými farmami, zejména s většími výkony bylo zjištěno, že zlepšení napěťové nestability lze dosáhnout instalací větrných farem v různých vzdálenostech a umístění v systému.

Modifikace návrhu zlepšením odezvy větrných farem v různých vzdálenostech a umístěních byly schopny eliminovat napěťové nestability systému. Cílem bylo dosažení efektivního návrhu, aby bylo dosaženo příznivých vlivů na energetickou soustavu, tedy zlepšení napěťových profilů a snížení výkonových ztrát.

**Klíčová slova:** Větrná farma, Insulated gate bipolar transistors (IGBT), výkonové elektronické měniče, Synchronní generátor s permanentními magnety (PSMG), napěťová stabilita, výkonové ztráty

# Abstract

The huge wind energy resource represents a potential to use wind farms to power vast area of the earth with renewable energy. Many wind farm concepts have been proposed, but much work still need to be done on Intelligent Distribution Systems with Dispersed Electricity Generation.

This work presents the development of a comprehensive simulation tool for modeling the dynamic response of wind farms, the verification of the simulation tool through model-to-model comparisons, and the application of the simulation tool to an integrated real commercial power system loads analysis for the promising system concepts without and with wind farm. A MATLAB/Simulink simulation tool was developed from a benchmark commercial power system and to have the features required to perform loads analyses for without and with wind farm system configurations. The simulation capability was tested using model-to-model comparisons without and with wind farm. The favorable results of all of the verification exercises provided confidence of enhanced voltage profile and reduced power losses.

The simulation tool was then applied in a preliminary loads analysis of a wind farm. The loads analysis aimed to characterize the dynamic response and to identify potential loads and instabilities resulting from the dynamic couplings of the wind farm. The coupling between the wind farm response, in particular, with larger extreme loads experienced voltage instabilities which were then found to be improved with the installation of the wind farm at various distance and location in the system.

The design modifications by improving the wind farm response at various distance and location, was able to eliminate voltage instabilities in the system. This was aimed at obtaining an effective design to achieve favorable performance of the proposed electric power system with regards to improved voltage profile and reduced power losses.

**Keywords:** Wind farm, insulated gate bipolar transistors (IGBT), power electronics converters, permanent magnet synchronous generator (PMSG), voltage stability, power losses.

# Contents

# List of figures

# List of tables

# Notation

## Abbreviations

| | |
|---|---|
| IGBT | Insulated-Gate Bipolar Transistor |
| PMSG | Permanent Magnet Synchronous Generator |
| PV | Photovoltaic |
| MV | Medium Voltage |
| DR | Demand Response |
| VVO | Voltage/VAR Optimization |
| LTCs | Load Tap Changers |
| ADMS | Advanced Distribution Management Systems |
| PCC | point of common coupling |
| FACTS | Flexible Alternating Current Transmission System |
| D | Diameter |
| d-axis | direct axis |
| q-axis | quadrature axis |
| PMG | Permanent Magnet Generator |
| DFIG | doubly-fed induction generator |
| SG | synchronous generator |
| THD | Total Harmonic Distortion |
| DC | Direct current |
| AC | Alternating current |
| PWM | Pulse-Width Modulation |
| SST | Solid-State Transformer |
| PCC | power conversion scheme |
| IGCT | Integrated Gate Commutated Thyristor |
| MCT | MOS-Controlled Thyristor |
| MOSFET | Metal Oxide Semiconductor Field Effect Transistor |
| BJT | Bipolar Junction Transistor |
| RC-IGBT | Reverse-Conducting Insulated Gate Bipolar Transistor |
| G | Gate |
| E | Emitter |
| C | Collector |
| P | Positive |
| N | Negative |
| WTSs | Wind Turbine Systems |
| 2L-PWM-VSC | Two-Level Pulse-Width-Modulation Voltage Source Converters |
| 2L-UNI | Two-level unidirectional voltage source converter |
| 2L-BTB | Two-level back-to-back voltage source converter |
| 3L-NPC BTB | Three-Level Neutral-Point Diode Clamped Back-To-Back Topology |
| 3L-HB BTB | Three-Level H-Bridge Back-to-Back Topology |
| 5L-HB BTB | Five-Level H-Bridge Back-to-Back Topology |
| 3L-NPC + 5L-HB | Three-Level Neutral-Point Diode Clamped Topology for Generator Side and Five-Level H-Bridge Topology for Grid Side |
| CHB | Cascaded H-Bridge converter |

| | |
|---|---|
| MFT | medium-frequency transformer |
| MVDC | Medium Voltage Direct Current |
| S-S | Series- Series |
| S-P | Series-Parallel |
| P-S | Parallel- Parallel |
| MP-S | Magnetic parallel- Series |
| S-MP | Series- Magnetic parallel |
| DSO | distribution system operator |
| PCC | Point of Common Coupling |
| TSOs | Transmission System Operators |
| STATCOMs | static synchronous compensator |
| DFAG | Doubly Fed Asynchronous Generator |
| AVR | Automatic Voltage Regulator |
| PFCCs | Power Factor Correction Capacitors |
| MSCs | Mechanical Switched Capacitors |
| SVCs | Static VAR Compensators |
| MSCDN | Mechanically Switched Capacitor with Damping Network |
| TCR | Thyristor-controlled Reactor |
| TSR | Thyristor-switched Reactor |
| VSC | Voltage-Source Converter |
| GTOs | gate turn-off thyristors |
| TCSC | Thyristor-Controlled Series Compensation |
| AG | the asynchronous (induction) generator |
| PCs | power converters |
| S. $S_1$ | substation system |
| E. S | electrical system |
| D. S | distribution systems |

# Symbols

| | |
|---|---|
| $R_S$ | stator resistance |
| $L_S$ | stator inductance |
| $U_S$ | stator voltage |
| e | excited voltage |
| $i_d$ | Instantaneous real power current |
| $i_q$ | Instantaneous reactive power current |
| $i_s$ | whole current |
| $\gamma$ | Angular velocity |
| $\Psi_d$, $\Psi_q$ | components of the magnetic field |
| $\Omega_L$ | electrical angular velocity |
| $\Psi_{pm}$ | synaptic magnetic field with the rotor |
| $M_{MI}$ | torque of the machine |
| $M_W$ | load torque |
| J | whole Torque inertia |
| I | current |
| U | Voltage |

| | |
|---|---|
| P | Active power |
| Q | Reactive power |
| L | Inductance |
| C | Capacity |
| θ | pitch angle |
| $I_{ctr1}$, $I_{ctr2}$, $I_{ctr3}$ | outputs of the control circuit |
| AF | amplitude function |
| $I_{L1}$, $I_{L2}$, $I_{L3}$ | Lines currents |
| $I_\alpha$, $I_\beta$ | stator coordinate currents |
| α, β | stator coordinate system |
| d, q | rotor coordinate system |
| -VD | vector negative adapter |
| PI | Proportional, Integral controller |
| $I_d$, $I_q$ | rotor coordinate currents |
| $V_{ctr1}$,$V_{ctr2}$,$V_{ctr3}$ | Vector drive |
| $Q_{gen}$ | inductive reactive power consumption of the wind turbines |
| X | equivalent series reactance |
| C | equivalent shunt reactance |
| $Q_{comp}$ | reactive-power administered by any centralized reactive power compensation |
| $X_m$ | magnetizing reactance |
| $X_l$ | leakage reactance |
| $\delta$ | power angle |
| $X_L$ | reactance of the electric-power line |
| $X_C$ | admittance of the thyristor-controlled series compensator |
| $U_g$ | voltage of the electricity grid |
| $U_W$ | voltage of the wind farm |
| $\delta$ | angle between $U_g$ and $U_W$. |
| $Q_{ref}$ | Q-reference |
| $r_1$ | Positive resistances |
| $r_0$ | Zero-sequence resistances |
| $l_1$ | Positive inductances |
| $l_0$ | zero-sequence inductances |
| $c_1$ | Positive capacitances |
| $c_0$ | zero-sequence capacitances |
| $f_n$ | Frequency |
| $R_1$ | Phase resistance |
| $X_1$ | Phase Inductive reactance |
| $B$ | Phase susceptance |
| $V_{rms}$ | root mean square of voltage |
| $R$ | Resistance |
| $S_n$ | Nominal Power |
| $R_m$ | Magnetization resistance |
| $L_m$ | Magnetization inductance |
| $P_s$ | Sending active power |
| $P_r$ | Receiving active power |
| $Q_S$ | Sending reactive power |

| | |
|---|---|
| $Q_r$ | Receiving reactive power |
| $U_s$ | Sending voltage |
| $U_r$ | Receiving voltage |
| $\Delta P$ | Active power losses |
| $f(losses)$ | Power losses function |
| $A_{ka}$ | Position of sources, active and reactive power, renewable sources |
| $L_{kl}$ | Parameters of lines and loads |
| $D_{kd}$ | Compensation device |
| $S_{SS}$ | apparent power of the substation system |
| $I_{SS}$ | total line current of the substation system |
| $I_{SLi}$ | line current supplied to the $n^{th}$ number of power lines from the substation |
| $S_{SLi}$ | apparent power supplied to the $n^{th}$ number of power lines from the substation |
| $P_{SLi}$ | active power supplied to the $n^{th}$ number of lines |
| $\Delta P_{LLi}$ | active power losses of the $n^{th}$ number of lines |
| $P_{LTi}$ | active power of the $n^{th}$ number of lines |
| $\Delta P_{ALLi}$ | power losses for $n^{th}$ number of lines for Scenario A |
| $I_{ASSi}$ | line current for $n^{th}$ number of power lines for Scenario A |
| $\Delta P_{AT}$ | total losses of S. $S_1$ for Scenario A |
| $\Delta V_{ALLi}$ | voltage drop on $n^{th}$ number of lines of Scenario A |
| $Z_{LLi}$ | longitudinal impedance of $n^{th}$ number of lines |
| $I_{BW}$ | wind farm line current of Scenario B |
| $I_{BSS}$ | total substation line current of Scenario B |
| $I_{BWi}$ | constituent of the of wind farm line current going through $n^{th}$ number of lines of Scenario B |
| $I_{BSSi}$ | new line current supplied to $n^{th}$ number of power lines of Scenario B. |
| $\Delta P_{BLLi}$ | power losses for $n^{th}$ number of lines of Scenario B. |
| $\Delta P_{BT}$ | total losses of S. $S_1$ for Scenario B |
| $\Delta V_{BLLi}$ | voltage drop of $n^{th}$ number of lines of Scenario B. |
| $I_{CW}$ | total current of wind farm for Scenario C |
| $I_{CSSi}$ | new current for the transmission line number n in scenario C |
| $I_{CWi}$ | constituent of the of wind farm line current going through line number n |
| $\Delta P_{CLLi}$ | power losses for power losses for $n^{th}$ number of lines of Scenario C. |
| $\Delta P_{CT}$ | total losses of S. $S_1$ for Scenario C |
| $\Delta V_{CLLi}$ | voltage drop of $n^{th}$ number of lines of Scenario C. |
| $I_{DSSi}$ | new current for the transmission line number n in scenario D |
| $I_{DWi}$ | constituent of the of wind farm line current going through line number n in scenario D |
| $\Delta P_{DLLi}$ | power losses for $n^{th}$ number of lines of Scenario D |
| $\Delta P_{DT}$ | total losses of S. $S_1$ for Scenario D |
| $\Delta V_{DLLi}$ | voltage drop of $n^{th}$ number of lines of Scenario D |
| $Q_{Li}\,\%$ | increase percentage of reactive power of load number i. |
| $Q_{Li}$ | basic reactive power of load number i |
| $Q_{Twind}$ | total reactive power of wind farm. |
| $K$ | wind farm constant |
| $\Delta V_{allowed}$ | allowed voltage drop for the transmission line |
| $Value_{i1}$ | generated value number 1 from this part of regulator for line i |

| | |
|---|---|
| $V_{system}$ | nominal voltage of the MV substation system. |
| $V_{Sm}$ | measured value of sending voltage. |
| $Value_{i2}$ | generated value number 2 from this part of regulator for line i. |
| $V_{Rm}$ | measured value of receiving voltage. |
| $Value_{i3}$ | generated value number 3 from this part of regulator for line i. |
| $Q_i$ | generated value of line i. |
| $\Delta Q$ | Reactive power losses |
| $cos\,\varphi_s$ | Sending power factor |
| $cos\,\varphi_r$ | Receiving power factor |
| $I_L$ | Line current |

In some parts of the text, an identical symbol is used with different meaning. This was motivated by the aim to follow the symbols given in the cited literature (for clarity). The used symbols are described in the text.

# Chapter 1
# 1 Introduction

Continuity in the development of the human race ultimately need sources of renewable or virtually inexhaustible energy such as wind renewable energy resource. The history of wind energy describes a general evolution from the utilization of simple, light equipment's driven by aerodynamic drag forces; to heavy, material-intensive drag equipment's; to a rise in the utilization of light, material-efficient aerodynamic lift equipment's in the modern period. Wind energy is essentially looked at in the area of public policy, economics and managerial perspectives. The entire world producing potential of wind power increased in size from 13 megawatts in the year 1980 to 17,400 megawatts in the year 2000, and rose almost to 200,000 megawatts in 2010. Nevertheless, wind proportion has been extremely skewed geographically. In 2010 the United States and China solely accounted for 42% of installed global energy potential. The relative significance of wind power in electricity production displays noticeable geographical variation. In 2008, wind provided one-fifth of Denmark's electrical energy, and 13% of Portugal's, and 11% of Spain's. Also, in Britain, France, Italy, and the United States, wind energy provided less than 2% of their electrical power. But in Japan it was just 0.3%. All-in-all, wind renewable energy supplied a meager 1% of the earth's electrical power. Wind is not homogeneous across the earth. The speed of Wind varies in intensity and season. There is a very weak correlation connecting installed wind capacity and wind energy potential. Energy issues is usually political, Policy resolutions basically regarding access to electrical power grids at advantageous prices, alongside tax and additional financial incentives, are broadly seen as key drivers responsible for the wide spread of wind renewable energy usage. The electric-power utilities which supply end-users, the entities which produce wind power i.e. individuals, co-operatives or, more recently large independent electric-power producers which construct large wind farms and the manufacturers who build some or each of the units of turbines that produces electric-power from wind, including of; clutches, gearboxes, rotor bearings, yaw motors, rotor hubs and blades are the three-business enterprise in the renewable wind energy industry. Wind energy has advanced, in spite of that there is still much space for growth [1] – [20]. In the same vein, human being have all the time utilized solar power. Solar renewable energy resource was the theme of scientific investigation during the early twentieth century. The first solar Photovoltaic (PV) device that generated utilizable quantity of electric-power was presented in 1954, and by 1958, solar cells were being utilized in diverse small-scale scientific and commercial practices. The energy catastrophe of 1970s saw the development of significant attraction in utilizing solar cells to generate electric-power in homes and businesses. Industry growth and research has made PV devices more practicable and a cycle of progressive generation and reduced costs began which is carried on with till today [21] – [30].

## 1.1 Background

As a result of industrial revolution worldwide energy consumption has steadily risen as well as economic growth. Non-renewable resources such as coal, natural gas, oil, and nuclear energy are the major sources of power for most parts of the globe. Burning fossil fuels, nevertheless, is hazardous to the environment, and fossil fuel are known to be limited and subject to price volatility. Also, issues of safe storage and discarding of radioactive waste, the possibilities of radioactive pollution from mishaps or vandalism, and the possibility of nuclear proliferation are serious obstacles to the success of nuclear power. Therefore, renewable resources such as wind possess great potential since they are indigenous, nonpolluting, and inexhaustible. Today, there has been progressive advancement in modern renewable wind power plant technology. Specifically, the gearless wind power plant with permanent magnet synchronous generator utilizing full-scale power converter. Electric-power production from renewable energy sources, such as wind, is growingly drawing attraction due to environmental issues, long-term economic advantages and scarcity of conventional energy sources in the near future. The main cost-efficient and practicable disadvantage of wind power is its intermittent characteristics. Wind power requires not only that wind is flowing, all the same it also rely on cut-in and cut-out wind speed, that is the wind speeds at which production starts and is brought to a stop in order to keep away from harm. The production of power from the wind on a large-scale, has become an accepted business. It holds substantial prospect for the future, hoping that wind power will become the most accepted choice and form of renewable energy source. Wind energy technology application has come of age, with numerous nations preparing and establishing extensive wind energy farms, with enormous amount of wind turbines. The strength of wind power technology is that it is clean and inexpensive. As a result of increasing fossil fuel price and state-of-the-art technology, more and more residential and commercial consumers of electricity have been installing wind turbines, the motivation being to cut energy bills and carbon dioxide emissions, and are even vending extra electricity back to the grid network. Another motivation is to adopt a policy for independent electricity production, the aim of this policy is to encourage the involvement of independent power producers in the growth and expansion of environmentally sound and inexpensive electricity supply for end-users while adhering to the robustness of the existing electric-power network [31] – [42]. Wind power is one of the rapidly expanding clean renewable energy resource. Currently, plenty of wind farms have been established in several nations from the thought of global warming and exhaustion of fossil fuels. Huge amount of established renewable electric-power resource is wind generated. Established wind farms are anticipated to expand with time coinciding with reduction in the price of wind power technology [43] - [44]. Also, nations are now going away from fossil-nuclear age and preparing the way for photovoltaics (PV) to contribute a notable part in a future shaped by sustainable energy generation. Some countries have very great opportunity of producing solar power. The explanation being their geographical location on the globe and obtained solar radiation all over the year. Currently, nations have purposeful intention to build huge grid-connected solar energy plants for electric-power production. Solar photovoltaic modules or panels are made of semiconductor materials that permit sunlight be able to be changed directly into electric-power. These modules can supply safe, reliable, maintenance-free and environmentally friendly means of energy for a longer time. A triumphant application of solar PV system requires knowledge of their operational capabilities under varied climatic circumstances [45] – [47].

Hence, to achieve an effective active and reactive power control strategy, a Simulation scheme of a commercial electric-power system and a wind farm with gearless variable speed PMSG insulated gate bipolar transistor (IGBT) power converters connected to a MV distributed network is carried out using MATLAB/Simulink software. The proposed grid system is compared with an existing benchmark commercial grid system in terms of power losses, and voltage stability. Results for the proposed scheme at different loads were assessed showing similar efficiency gains compared to the benchmark commercial electric power grid system. Results for the various scenarios are presented, depicting that integration of the wind farm on the grid network has enhanced active and reactive power control to achieve better voltage profile and system losses.

## 1.2 Aims and Main Contributions of the Work

The overall aim of this thesis is to investigate the possible benefits and adverse impacts of MV Wind Farm location and distance on Distribution Systems (DSs). The focus has been on the benefits for the distribution system and the end-use customers. To address this, in this thesis the generation pattern from wind power is based on existing work and the focus has been on modeling flexible loads with a commercial benchmark system.

The main contributions of this thesis can be summarized as follows:

A model to estimate and schedule flexible load demand.

A complex model of DS with variable load and wind power.

A methodology to evaluate the simulation design.

A methodology to evaluate the effects of different schedule of loads demand and its consequential effect on the distribution system.

A methodology to assess the possible mutual benefits for wind power producers and end use customers.

Probability and statistics of using wind power and load changes with time according to distribution functions.

The developed model is used in a case study of a real benchmark distribution system. The effect on the distribution system is studied using MATLAB/Simulink software, with the focus on steady state conditions, such as power losses and steady state voltage profile performance.

## 1.3 Outline of this Thesis

This thesis is organized as follows:

Chapter 1: This chapter provides a general background on the topics of MV Wind Farm Distribution Systems. In addition, the aims and main contributions of the thesis are provided.

Chapter 2: Current State of Wind Renewable Power Generation and Flexible Load in Distribution System.

Chapter 3: Here, MV Wind Farm Distribution Systems have been extensively studied by the academia and industry. This chapter aims to present the current status in the academia, that is literature review related to MV Wind Farm Distribution Systems

Chapter 4: This chapter presents an overview of the research approaches and models developed in this thesis. It entails detailed description of the design basis

Chapter 5: it entails case studies and simulations were described in this chapter.: Here, Loads analysis overview, description, and discussion of the results were thoroughly dealt with.

Chapter 6: This chapter focused on the verification of the simulation models.

Chapter 7: This is the final chapter, the main conclusions from this thesis are presented together with some possible ideas for future work.

# Chapter 2

# 2 Current State of Wind Renewable Power Generation and Flexible Load in Distribution System

When the idea of conveying meaningful quantity of energy to the electric-power grid with renewable energy resource began, little thought was given to its negative aspect, but now highly variable renewable energy resource, could be triumphantly joined with existing electric-power grid infrastructures. As renewable power becomes a huge percentage of sum total of power generated worldwide, its influence on the quality and reliability of the electricity network have become more demanding, particularly for the utility authorities that must cope with earlier rather than later with power quality issues renewable energy sources can cause. Renewable power sources can bring about variability, intermittency and fluctuations in the utility authority distribution networks. Huge renewable energy installations such as wind or solar farms can have these negative consequences when they represent bulk percentage of the sum total energy generated. Normally, solar or photovoltaic production is the most source of difficulty [48] – [50].

To power distribution load centers, wind farms are installed. Implementation of wind farms distribution system is the future of wind farm projects development. It is such that wind power could represent a reasonable percentage of global electric-power production. Worldwide interest in wind energy is growing owing to the fact that global wind resource is abundant. Potential of wind farm distribution schemes lies close to major urban populations. Other reasons for installing wind energy systems includes; The fact that wind tends to blow more strongly and consistently, with less turbulence intensity and smaller shear depending on wind farm location; The size of wind turbine is not limited by road or rail logistical constraints if it can be manufactured near wind farm sites; The visual and noise annoyances of wind turbines can be avoided if the turbines are installed at a sufficient distance from dwelling places; Vast expanses of uninterrupted open desert and semi-desert places are available for the installations of wind farms, thereby not interfering with other land uses. Also, the demerits of wind farm schemes are that it requires higher capital investment due to the costs associated of the turbine and added complications of installation, and decommissioning; installations are less accessible due to their site in distance location from the end-user, which raises the operations and maintenance costs and possibly increases the downtime of the machines; Wind turbines also experience environmental loading from the wind. As a result, the complexity of the design increases [51] – [53].

Reactive power is necessary to provide a magnetizing field required by motors and other inductive loads to perform their desired functions. Reactive power can also be interpreted as wattles, magnetizing or wasted power and it represents an extra burden on the electricity supply system and on consumer’s bill. An inductive load requires a magnetic field to operate and in creating such a magnetic field causes the current to be out of phase with the voltage, that is current lags voltage. There is need for reactive power compensation of the lagging current by creating a leading current by way of connecting sufficient capacitors to the supply. Inductive loads can be used to keep reactive power low by consumption of more electrical energy. This is so since an inductive load draws reactive power as well as active power. Reactive component is watt less power drawn from the source. We use only active part of the source. It is of benefit to note here that there is no bidding activity for reactive power, electricity end-users do ask for active power but they have to pay for reactive power as well, likewise, electric-power producers provide active and reactive power at a single price but they do bid only for active power and are paid for reactive power as well. Low reactive power also affects other systems in the circuit virtually making the cables under sized by heating them. Lagging Kvars due to the prevalence of large inductive loads has the negative effect of increased energy cost, due to penalties imposed by utility authorities, higher system losses, due to reactive power losses and lower utilization power due to the previously mentioned losses. There are several methods available today to attempt to offset the lagging Kvars imposed by inductive power loads. The two most common methods for improving reactive power is the use of shunt capacitors or synchronous motors. Reactive power compensation can also be provided by locating wind farms at remote locations, this is the focus of this thesis. Reactive power losses bring about voltage drop or sag, voltage sags pose a serious power quality issue for the electric power industry. Much work has been done assessing the effects of voltage sags on power system operation, and on industrial and commercial loads. However, more research has been needed on the effects of voltage sags on residential loads, particularly sensitive equipment such as computers, hence, this research thesis [54] - [57].

The medium voltage system is between 1,000 V to 100 kV. The connection of an electrical installation to a Medium Voltage (MV) utility distribution network is always realized by means of a dedicated MV substation usually designed as the main substation. Depending on its size and specific criteria mainly related to the loads, such as rated voltage, number, power, location, and so on, the installation may include additional substations designed to function as secondary substations. The locations of these substations are carefully selected in order to optimize the budget dedicated to MV power cables. They are supplied from the main substation through the internal MV distribution. The best distribution system is one that will, cost-effectively and safely, supply adequate electric service to both present and future probable loads. The function of the electric power distribution system in an installation site is to receive power at one or more supply points and to deliver it to the individual lamps, motors and all other electrically operated devices. The importance of the distribution system to the function of an installation makes it almost imperative that the best system be designed and installed. In order to design the best distribution system, the system design engineer must have information concerning the loads and a knowledge of the various types of distribution systems that are applicable [58] - [63].

Renewable power resources, like solar and wind, are intermittent and usually unforeseeable as compared to their traditional counterparts. Hence, the incorporation of huge quantities of renewable power resources brings about an increase in the complication of power system functioning and security of provision. In an electricity system where electric-power is purely generated by renewable power sources, electric-power system operators loose notable control over generator dispatch, implying losing vital resource in supporting production to load balance. This increases the function of energy storage, Demand Response (DR) programs, or advanced Voltage/VAR Optimization (VVO) control schemes and intelligence distribution management.

Distribution scheme resources will have to be coordinated and intelligent to effectively adjust to the power source variations by means of remote management. Apart from traditional methods like control of substation Load Tap Changers (LTCs), switched capacitors, and voltage regulators, deployment of huge quantities of small, changeable reactive power equipment's on secondary networks, which would permit finer muting of voltage spikes and drops is another control strategy. Also, compensating consumers for the utilization of their smart inverters to supply voltage/VAR support, would make the possibilities of incorporating huge quantities of distributed power resources less formidable. Furthermore, the full incorporation of traditional voltage and VAR control resources with DR schemes and distributed power resources, which could be controlled by means of algorithms programmed in Advanced Distribution Management Systems (ADMS), would permit electric-power system operators to optimize systems operations by influencing substantial computational power [64] – [68].

Originally, wind energy did not have any important influence on energy network regulation, but now due to its proportion, wind energy has to perform a substantial more functional role in electric-power grid performance and control. The device utilized in wind farms was initially established on squirrel-cage induction generator connected exactly to the electric-power grid. Power pulsating nature in wind energy systems were nearly straight away conveyed to the electrical grid by utilizing squirrel-cage induction generator as its speed is fixed owing to its restricted slip limit. Moreover, no dynamic control of the active and reactive power occurred excepting for not many capacitor banks which assured unity power factor at the point of common coupling (PCC). As the energy ability of wind farms expands, controlling the frequency and the voltage in the electric-power grid happen to be more important, and in then recent paste it has come to be essential to advance power electronics, like IGBT FACTS devices [69] - [74] as a brilliant interface connecting the wind turbine system and the electric-power grid. IGBT FACTS Power electronics devices is altering the fundamental attributes of wind turbine from actually a power source to essentially a reactive power source for the electric-power grid. Owing to the devices utilized in wind farms, the cost per kW of recently developed wind energy plant is now commensurate and indeed lower than coal energy systems; consequently, applications with IGBT power electronics devices are extremely appealing [75] - [78].

# Chapter 3

# 3 Literature Review

This chapter provides an introduction to the electric-power distribution grid, intelligent electric-power distribution systems, dispersed generation, dispersed wind electricity generation, development of wind power generation systems, power electronics for wind power generation systems, active and reactive power control in wind energy systems, promising power converter topologies for wind energy systems, control structure of wind power systems, grid integration of wind power systems, reactive power compensation of wind connected power systems, and voltage stability in wind power conversion systems.

## 3.1 The Electric Power Distribution Grid

The principal function of an electrical power distribution scheme is to supply electricity to individual power consumer buildings, together with its outbuildings. Distribution of electricity to diverse power consumers is done with much low voltage level and it is executed by means of the distribution systems. The distribution systems are composed of the following dominant parts, that is; Distribution substation, Primary distribution feeder; Distribution Transformer; Distributors, and Service mains. Transmitted electricity is stepped down with the aid of step-down transformers in substations, for primary distribution. The stepped down electricity is conveyed to the distribution transformer via primary distribution feeders. Overhead primary distribution feeders are normally supported by iron pole, ideally rail pole. The conductors are strand aluminum conductors and they are installed onto the arms of the pole with the aid of pin insulators. Some times in overcrowded locations, underground cables may equally be utilized for primary distribution purposes. Distribution transformers are predominantly three-phase pole mounted type. The secondary of the transformer is linked to distributors. Different power consumers are fed electricity by means of the service main. These service mains are tapped from individual points of distributors. The distributors can equally be re-classified as distributors and sub distributors. Distributors are exactly joined to the secondary of distribution transformers in contrast with the sub distributors that are tapped from distributors. The service main of the power consumers may either be joined to distributors or sub distributors, this depends on the location and agreement with power consumers. Feeder and distributor convey electrical loads, but they have one fundamental difference. Feeder feeds electric-power from one point to another point without being tapped from any intermediary point. Since there is no tapping point in between, the current at the sending end is equal to the current at the receiving end of the conductor. The distributors are tapped at different points for feeding individual power consumers; and hence current differs throughout the whole length of the conductor. There is the radial and ring main electrical power distribution systems. Diagrams showing the electricity distribution networks can be seen in fig 3.1 and 3.2 [79], [80], [81] and [82].

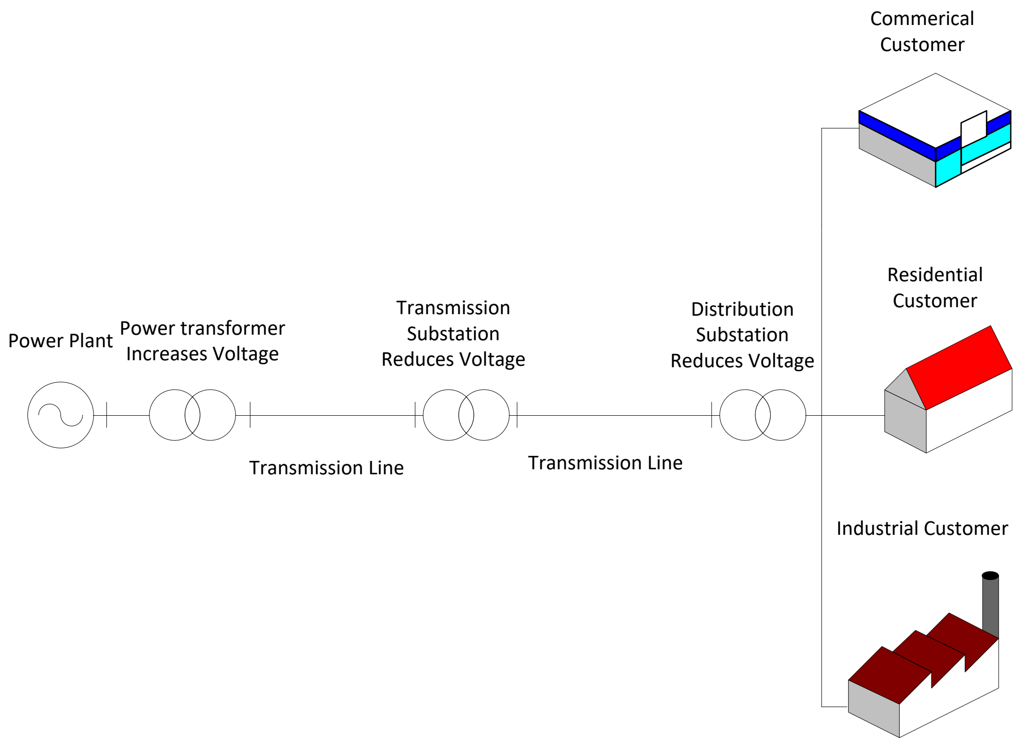


*Fig 3.1 A typical electric-power distribution grid [82]*

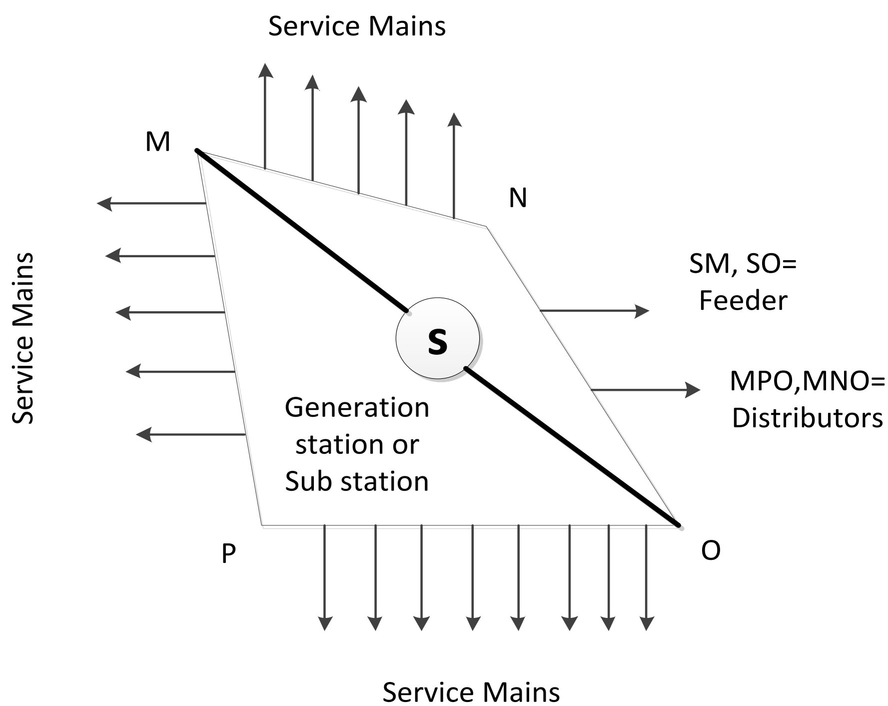


*Fig 3.2 Schematic diagram of an electrical power distribution system [79]*

# 3.2 Intelligent Electric Power Distribution Systems

The term Distribution-intelligence means the section of the smart grid that is concern with electricity utility distribution network, such as, the wires, switches, and transformers that links the utility substation to the electricity consumer. The electric-power lines are part of the electricity distribution network. A major constituent of distribution intelligence is power outage detection and response. Nowadays, most utility authorities depend on power consumer phone calls to know which section of the electricity distribution grid is affected by power outage. Alongside with smart meters, distribution intelligence do assist to immediately identify the source of power outage so that maintenance crews can be dispatched as quickly as possible to the problem section of electric-power networks in order to effect repairs. This will go a long way to improve power utility authority's outage response time. Most utility authorities count on complex electric-power distribution strategy and manual switching to keep electric-power flowing to many power consumers, even when electric-power lines are destroyed. Nevertheless, this approach has its constraints, and in many cases an automated scheme respond more quickly and keep electric-power flowing to more power consumers. By having sensors that can indicate which sections of the electricity distribution network have lost power, and by incorporating automated switching with an intelligent network that decides how best to respond to power outage, electric-power can be redirected to many power consumers in a matter of seconds, or maybe even milliseconds. It might even be feasible to act fast enough to power disturbances so that only electricity consumers in the nearest vicinity are affected, while other electricity consumers power source is redirected fast enough to avert any interference in electric-power. This functioning illustrates the highly commended self-healing characteristic of the smart grid in operation [83].

## 3.2.1 Automation of Electric Power Distribution Systems

The traditional distinct pattern or method of operation of electric-power systems is its unidirectional and top-down orientation. A few number of big electric-power plants feed into the electricity grid and try to keep demand and supply balanced all the time. This balance is extremely an important characteristic in managing an electric-power system. The unpredictable nature of renewable power sources and electro-mobility of electrical power are new impediments to this balance and therefore calls for advanced control techniques. Outage response is one feature of electric-power distribution intelligence that is very often referred to as distribution automation. Electric-power distribution automation might in actual fact be the oldest aspect of the smart grid system, in view of the fact that utility authorities have been automating their electric-power distribution systems since the 1960s. In its early stages distribution automation concentrated just on remote control of switches, but at present distribution intelligence is regarded to mean a fully controllable and flexible electric-power distribution System. Putting together distribution automation elements with a set of intelligent sensors, processors, and communication machinery and devices leads to distribution intelligence. When completely utilized, distribution intelligence will allow electric-power utility authorities to remotely monitor and coordinate its electric-power distribution resources, operating them in an optimal manner by utilizing either manual or automatic controls [83], [84], [85] and [86].

### 3.2.2 The Usefulness of Intelligent Electric Power Distribution Systems

Alongside with outage detection and response, other possible utilization of distribution intelligence is in its capability to make the best or most effective use of the balance between real and reactive power. Equipment's that store and release energy, for example capacitors, or that utilize coils of wire to induce magnetic fields, take for instance the electrical motor, have the capacity to bring about an increment in electrical currents without absorbing real power; this is generally known as reactive power. A specific amount of reactive power is advisable within the electric-power system, but too much of reactive power can result in large current flows that will be of no benefit, bringing about efficiency losses as it heats up the electric-power distribution system conductors. An intelligent distribution system can make use of power electronics to sustain the actual level of reactive power in the electric-power system. Distribution intelligence can as well assist to protect and control the feeder of power lines that make up the electricity distribution network. Most feeder electric-power lines are now protected by either breakers or relays that trip when high currents flow through such electric-power lines, a circumstance normally caused by fault somewhere on the electric-power network. These relays occasionally include time delays to permit temporary or transient flow of high current, which might have been as a result of industrial equipment powering up, rather than a fault. Protection schemes are oftentimes a combination of instantaneous breakers of high current settings and time-delayed breakers or made up of relays with lower settings. These schemes of automated breakers and relays becomes a balancing act for the system: they permit the electric-power scheme to function with high currents when required but protects the electricity scheme and the consumers around the locality from high current flows when faults do occur. Distribution intelligence can present a more effective methodology of protecting feeder power lines, utilizing advanced monitoring and controls to detect and correct faults situations while still sustaining the highest level of system reliability during non-fault situations. An intelligent system can as well detect and isolate faults in specific equipment's and route electric-power through a backup system to maintain electric-power reliability as an alternative. Distribution intelligence can equally combine more advanced ground-fault detectors to reduce the chances of consumers experiencing shocked or being electrocuted when the power lines encounters down time. Many utility authorities are only recently beginning to embrace true distribution intelligence, but the market is anticipated to boom in the near future [83].

## 3.3 Dispersed Generation

Dispersed generation is decentralized electric-power plant, feeding into the electricity distribution power network and usually sized between 10 and 150 MW. Dispersed generation is strategically situated on the electricity transmission grid to deal with issues in the transmission and distribution network and to enhance the stability of the electricity network. In the world of decentralized power technologies, electricity is generated at or near the locality of consumption, comprises both distributed and dispersed kinds of electric-power generation. The main difference between these two types of electric-power generation, is that distributed generation is joined to the electric-power grid but dispersed generation is not. dispersed generators are planned to supply backup power and normally functions exclusively in the time of urgent situation or electric-power system outages [87] and [88].

Electricity utility infrastructure in many countries is usually founded on large electric-power plants system feeding electricity to consumers through an extensive power transmission and distribution network, collectively referred to as the electricity grid. Dispersed generation is an idea where smaller, highly efficient electric-power plants would be built throughout the length of the existing grid, close to the power consumer. It is comparable in conceptualization to the move from the era of bulky central computers to desktop computers on an interconnected system. Nations with strong renewable power potentials such as wind energy, are preferably suited to embrace dispersed generation. Dispersed generation provides a range of advantages for many prospects. Electricity consumers, electric-power providers, and other stakeholders in the industry all have their own rationales for wanting greater acquisition of distributed generation. Distributed electric-power generators are small when compared with normal central station electric-power plants and gives distinctive advantages that are not obtainable from centralized electricity generation. Most of these advantages is as a result of the fact that power generating units are essential modular, which makes distributed electric-power highly accommodating. It can supply electric-power where it is required, and when it is required. Since they normally depend on natural gas or renewable power resources, the generators are usually associated with less noise and therefore less pollution than larger electric-power plants, this makes it appropriate for on-site installation at various locality [87] and [89].

### 3.3.1 Features of Dispersed Generation

Dispersed generation minimizes both power transfers between localities of electric-power systems and power imbalance in every single location. Dispersed generation equally enable uniform distribution of the general electric-power system by responding speedily to electricity demand variation. It gives more flexibility and can be dispatched in incremental blocks of electric-power as required. It brings about reliability and stability of the electric-power system. Complete failure of the network can be averted when the load centers are sustained by dispersed generation. A significant outage in the electric-power line can be forestalled with the aid of dispersed generation connected by reciprocating engines, thereby bringing electricity back onto the power line within minutes [87].

### 3.3.2 Benefits of Dispersed Generation

The drivers for dispersed generation are including of Low cost of electricity -. The fact that power consumers benefits from low cost of electricity could well be the main reasons for embracing dispersed generation; Geographical factors – Due to the overcrowding of power transmission lines and higher electricity price in mainly metropolitan localities, dispersed generation technology is being embraced; Saving on outage cost - The increasing demand for premium electric-power might have force most industrial and commercial power consumers to change to dispersed generation in order to secure consumers from the threat of power outages; Increasing demand in intermediate sector - Flexibility to meet up with intermediate electrical load increases the demand for dispersed generation; Low payback period - Electricity utility authorities are usually disturbed about investing on long-term bases. Hence, they are comfortable with dispersed generation, which is based on lesser investment and lower payback time [87].

### 3.3.3 limitations and Challenges of Dispersed Generation

Just as dispersed generation has its benefits, it equally goes with limitations and challenges, these are: Dispersed Generation Utility attitude - Electricity utility authorities are normally bothered about the recouping of stranded assets, therefore they provide resistance in terms of execution of dispersed generation; Consumer perception – For now, there are few successful stories of dispersed generation, so power consumers are afraid of the future of dispersed generation; Government regulations – The future growth of dispersed generation markets predominantly rely on the regulator's policy and framework; Grid interconnection issues – Issues such as lack of uniform standards, safety, and the influence of grid tear affects dispersed generation [87].

### 3.3.4 The Future of Dispersed Generation

Although decentralized generation of electricity is not likely to absolutely take the place of central power generation, the share of decentralized power generation is hope to rise dramatically in the near future, with significant benefits to all electricity consumers and coupled with its environmental advantages. Dispersed generators are improbable to compare with central power station, consumers are attracted by the crave for reliable electric-power which would be the propelling factor for the future of dispersed generation. Since the quality of the entire centralized electric-power system and its capability to transmit electricity to the loads at where and when required is a concern to stakeholder's in the industry, a mixed portfolio together with dispersed and distributed electric-power generation will help to supplement and improve the reliability of the general electric-power system [87].

## 3.4 Dispersed Wind Electricity Generation

For just about as long as history has been documented human beings have been utilizing wind power to carry out work in one way or another. Nowadays the most widespread use of wind power is for electricity generation; this has been achieved at usually very small scale. Dispersed wind generation is the utilization of wind turbines at homes, businesses, farm and ranches, public and industrial facilities, off-grid and other sites joined either physically or effectively on the consumer side of the meter to counterbalance all or a part of local power consumption. Dispersed wind power systems supply clean, renewable power for on-site utilization and assist to alleviate pressure on the electric-power grid while creating jobs and instrumental to electrical energy security for homes, factories, farms, schools, private and public amenities, distribution utilities, and faraway or isolated localities. Small wind technology was developed in the 1920s, and it is the only renewable power industry segment that still dominates today in terms of world market share, technology, and manufacturing. Dispersed wind systems normally supply electricity on the retail side of the electric meter without requiring power transmission lines, thereby offering a strong, low-cost substitute to photovoltaic electric-power systems that are progressively been utilized in urban communities. Small-scale dispersed wind turbines equally generate electricity at lower wind speeds than large, utility-grade turbines, considerably increasing the accessible land with harvestable wind resource. These elements, joined with rising high retail power prices and demand for on-site electric-power production, have brought about strong market pull for dispersed wind industry, which is confident of a quick market expansion [90], [91], and [92].

# 3.5 Development of Wind Power Generation Systems

The collective wind power production from 1999 to 2020 is shown in fig 3.3, from this diagram, it is observed that wind power has grown rapidly to a capacity of 283 GW with approximately 45 GW put in place only in 2012, this number is anticipated to reach 760 GW in 2020, that is on a moderate situation. Wind power generation has grown more notably than any other renewable power sources and it is becoming actually a significant player in the modern electricity supply system. Today, most countries have a high penetration of wind power, this is to say that electric power consumption is mostly covered by wind energy. Presently, some nations have even the ambition to achieve 100% non-fossil based power generation system in the near future [93], and [94].

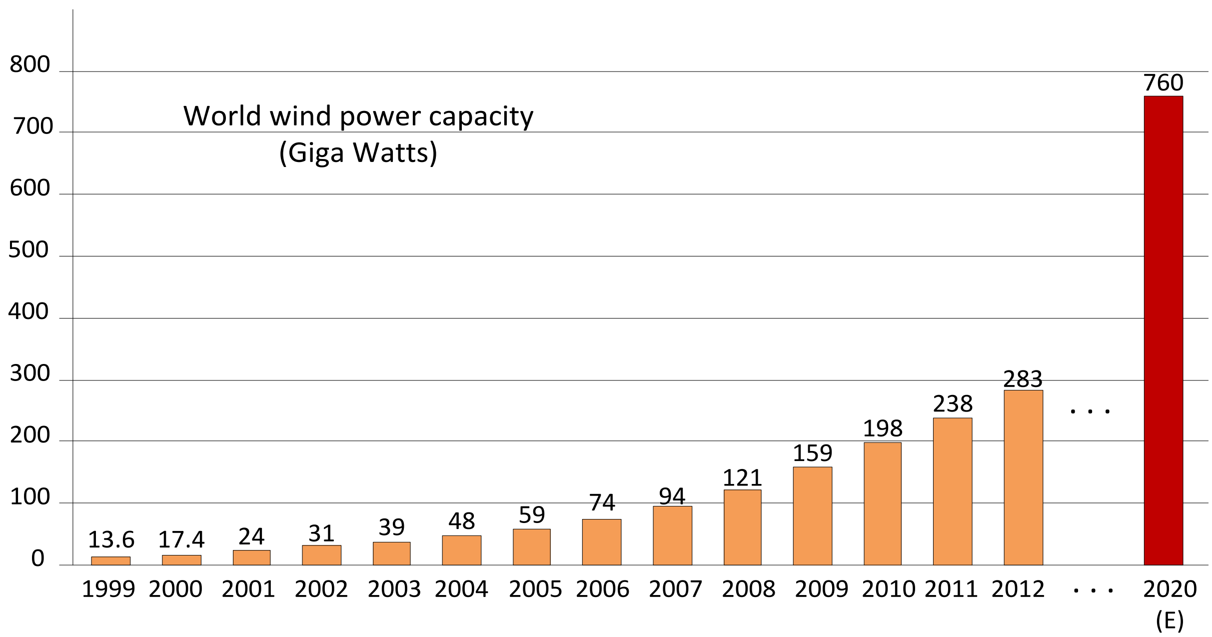


*Fig 3.3 Global collective installed wind power production from 1999 to 2020 [95].*

In inclusion to the quick development in the total installed production of wind power generation, the size of each wind turbine has equally increased dramatically to get a lower price per generated kilowatt hour. In the year 2012, the average turbine size brought into the market was 1.8 MW, out of which the average offshore turbine technology has realized a size of 4-MW. The increasing tendency of emerging wind turbine size between 1980 and 2018 can be vividly seen in fig 3.4, The growth of power electronics in wind turbine systems with its rating coverage and function role is as well shown. It is noticed that the cutting-edge 8-MW wind turbines having a diameter of 164 m have hitherto shown up in 2012. Today, many wind turbine manufacturers are initiating products in the power competence of 4.5–8 MW, and it is presumed that more and more huge wind turbines of multi-megawatt electric-power level, even as large as 10-MW will emerge in 2018, this will be in existence in the following decade driven mainly by the thoughts to bring down the cost of electric-power [93] and [96].

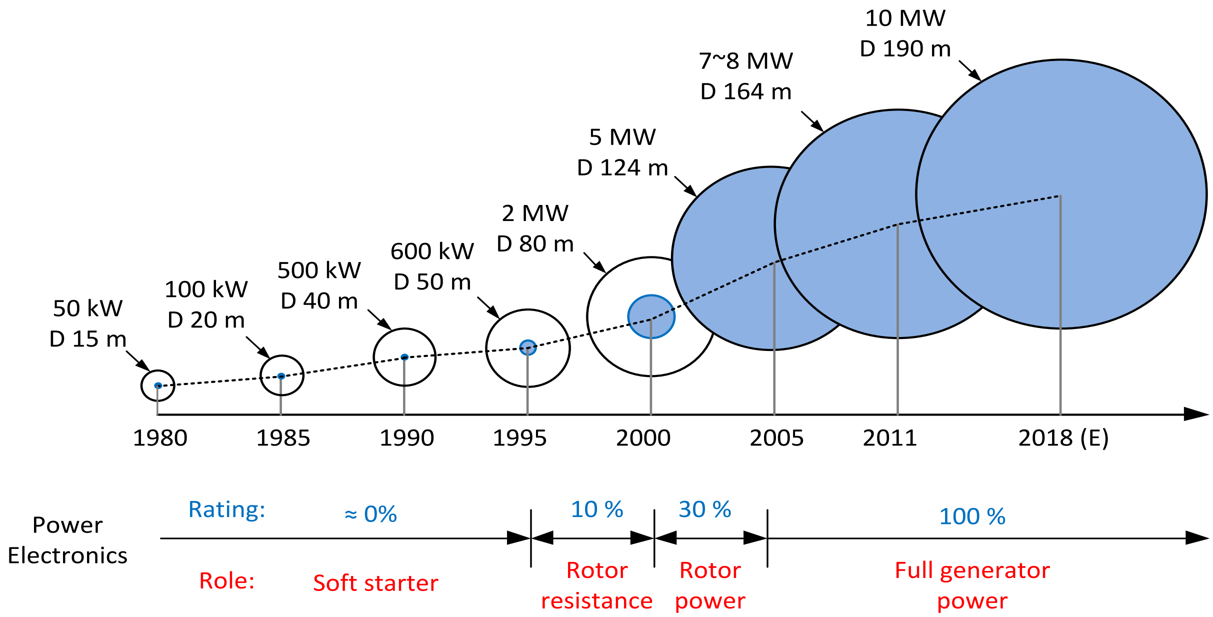


*Fig 3.4 Evolution of wind turbine size and the power electronics seen from 1980 to 2018 (estimated). Blue circle: the power coverage by power electronics [95].*

### 3.5.1 Generators in Wind Power Generation Systems

Synchronous generators, whether externally excited or with permanent magnets, are now becoming the favored technology in the wind power industry. Multipole permanent magnet synchronous generator (PMSG) having a full power back-to-back converter hope to become the predominantly embraced generator in the near future due to its lowered losses and lower weight as compared to the externally excited synchronous generator that has been manufactured successfully by wind turbine manufacturers. In some cases, the generator can be annular generator, and the rotor current is utilized to regulate the direct current link voltage. The change appears to be mainly valid for larger wind turbines from 3–6 MW. Nonetheless, the increment in the prices of rare-earth magnets might transform the philosophy of wind turbine drive trains to keep away from high risk in terms of expenses [76], [97] – [100].

Permanent magnet synchronous generators occupy an important part in direct-drive wind power generation systems for changing mechanical power into electrical power. The dynamic configuration of the permanent magnet synchronous generator is obtained from the two-phase synchronous reference frame, in which the q-axis is 90 (°) degree leading of the d-axis in conformance with the orientation of rotation. The harmonization connecting the (d-q) revolving reference structure and the abc three-phase structure is sustained by utilizing a phase locked loop. A detailed mathematical modelling of the permanent magnet synchronous generator is a necessary condition for the design of the machine control algorithms and the examination of the steady-state and dynamic features of the wind power transformation scheme. Direct drive wind turbine generators, distinguished as highly effective or efficient and requires low maintenance procedures, provides favorable possibilities for future implementations, particularly offshore applications. In order to do away with the gearbox, the generator is constructed for low speed performance maximally between 15-20 (rpm). This characteristic has made synchronous generators the only choice for low speed wind turbine utilizations. Synchronous generators magnetic field is provided with rotor excitation, but in the instance of the permanent magnet synchronous generator the direct current excitation scheme can be removed, which necessitate minimizing losses and exclusion of slip rings and consequently the maintenance requirements of the system. To realize independent control strategy of the active and reactive power, the d-axis and q-axis equivalent circuits is utilized in the drive converter arrangements [32], [37], [101] – [106].

The phasor diagram of a PMSG model is shown in fig 3.5 While the mathematical model of the PMSG in both natural (abc) three-phase stationary reference frame and (d, q) synchronously rotating reference frame is developed as follows:

Writing the stator voltage equation in time domain:

$$u_s = R_s . i_s + L_s \frac{di_s}{dt} + e \quad (3.1)$$

If (α, β) is the stator coordinate system, we can write the equation (3.1) in these coordinates:

$$u_s(\alpha,\beta) = R_s . i_s(\alpha,\beta) + L_s \frac{di_s(\alpha,\beta)}{dt} + e \quad (3.2)$$

Then the voltage and current equations in the rotor coordinate system become:

$$\widehat{U}_s(d,q) = U_d + jU_q \quad (3.3)$$

$$\hat{I}_s(d,q) = I_d + jI_q \quad (3.4)$$

where:

$R_S$ is stator resistance, $L_S$ is stator inductance, $U_S$ is stator voltage, e is excited voltage, $i_d$ is Instantaneous real power current, $i_q$ is Instantaneous reactive power current, $i_s$ is the whole current, and γ is Angular velocity.

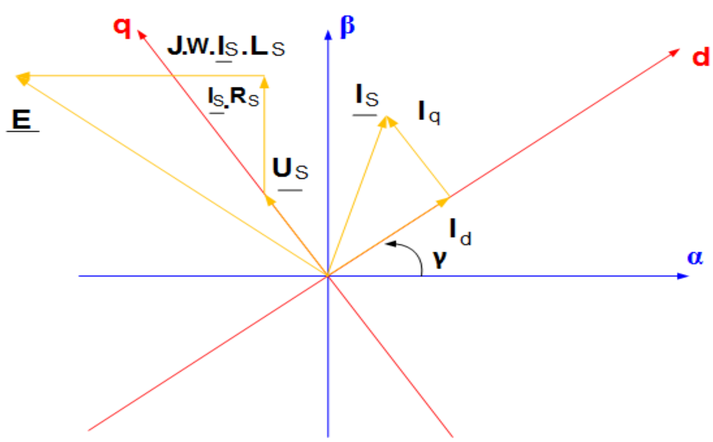


*Fig 3.5 The phasor diagram of a permanent magnet synchronous generator model*

The equations of the synchronous generator are:

$$\frac{d\Psi_d}{dt} = U_d - R_1.I_d + \Omega_L.\Psi_q \tag{3.5}$$

$$\frac{d\Psi_q}{dt} = U_q - R_1.I_q - \Omega_L.\Psi_q \tag{3.6}$$

Where:

$\Psi_d$ and $\Psi_q$ are the components of the magnetic field, and $\Omega_L$ is the electrical angular velocity.

So the equations of the magnetic field in are:

$$\Psi_d = \Psi_{pm} + L_d.I_d \tag{3.7}$$

$$\Psi_q = L_q.I_q \tag{3.8}$$

Where:

$\Psi_{pm}$ is the synaptic magnetic field with the rotor.

So the equation of the torque is:

$$M_{MI} = \frac{3}{2}P_P(\Psi_d.I_q - \Psi_q.I_d) \tag{3.9}$$

Where:

$M_{MI}$ is the torque of the machine.

We have the mechanical velocity:

$$J.\frac{d\Omega_m}{dt} = (M_{MI} - M_W) \tag{3.10}$$

So we can calculate the velocity without using measurements by using the following equation:

$$\Omega_m = \frac{1}{J}\int(M_{MI} - M_W)dt \tag{3.11}$$

Where:

$M_W$ is the load torque, and J is the whole Torque inertia.

These principles is used in the mathematical modeling of a permanent magnet synchronous generator rotor as shown in fig 3.6, which illustrates the schematic diagram of a PMSG rotor.

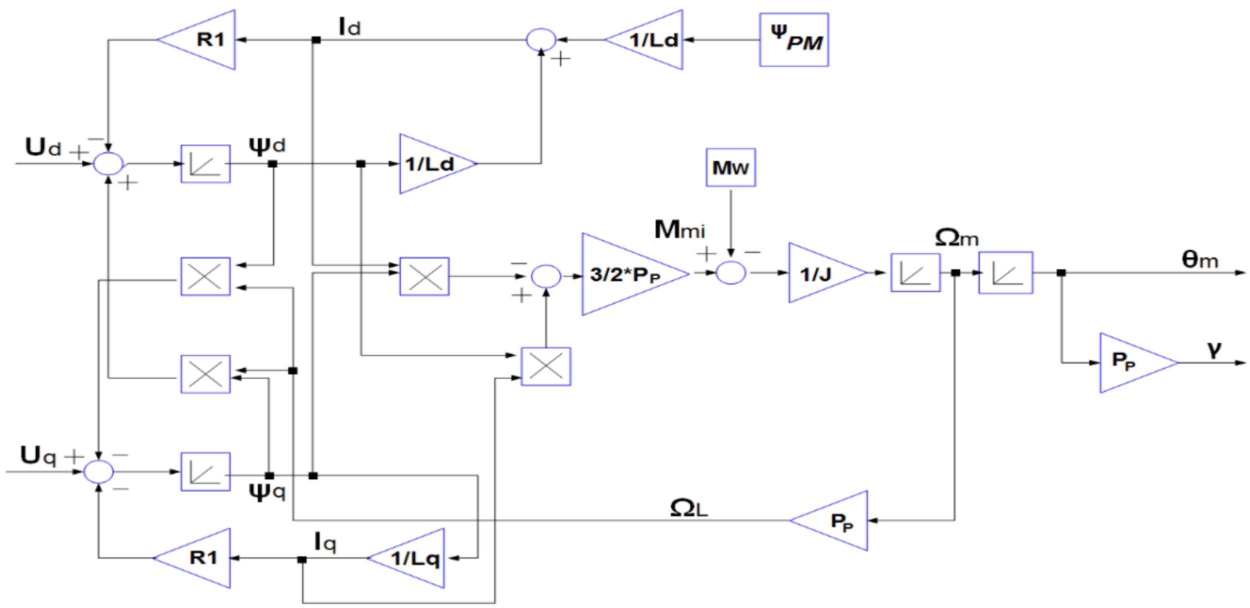


*Fig 3.6 Schematic diagram of a permanent magnet synchronous generator rotor*

## 3.5.2 Wind Power Generation System with Gearbox

From its origination the modern wind industry has encountered high gearbox breakdown rates owing to design deficiencies and underestimation of functioning loads. Observing of wind turbine gearboxes has gained significance interest among manufacturers as wind turbines become larger and move to more unreachable places like offshore applications. Worries among wind turbine manufacturers about gearbox dependability results from complicated repair processes, high replacement costs and long downtimes which can lead to revenue losses for utility authorithies. A gearbox is typically used in a wind turbine to improve rotational speed from low-speed rotors to higher speed electrical generator. The design of a wind turbine gearbox is demanding owing to the loading and environmental situations in which the gearbox must function. Torque from the rotor produces power, but the turbine rotor is equally put in huge moments and forces to the wind turbine drivetrain. It is significant to make sure that the drivetrain convincingly separates the gearbox, or to make sure that the gearbox is designed to sustain loads, or else internal gearbox constituents can become seriously misaligned. This can bring about stress concentrations and failures. Wind turbine drivetrains experiences serious transient loading in the course of start-ups, shut-downs, emergency stops, and throughout the time of grid connections. Electrical load cases that result in torque reversals might be specifically harmful to bearings, as rollers might be skidding in the course of sudden relocation of loaded area. Seals and lubrication schemes must work steadily over a broad temperature variation to stop the ingress of dirt and moisture, and carry out work successfully at all rotational speeds in the gearbox. Additional reasons of failures in gearboxes are inclusive of manufacturing errors such as grind temper or material inclusions, surface related problems, such as scuffing or micropitting, and fretting problems from small vibratory motions, such as might take place when a machine is parked. Several wind-turbine gearboxes have equally gone through basic design problems such as unproductive interference fits that brings about unintended motion and wear, inefficiency of the internal lubrication paths and problems with sealing. Improving the resistance of future gearbox designs to all these problems is a major factor for the future cost of power produced by wind turbines. Hence, the need for a gearless wind turbine system [107], - [110]. A typical wind turbine with gearbox is shown in fig 3.7.

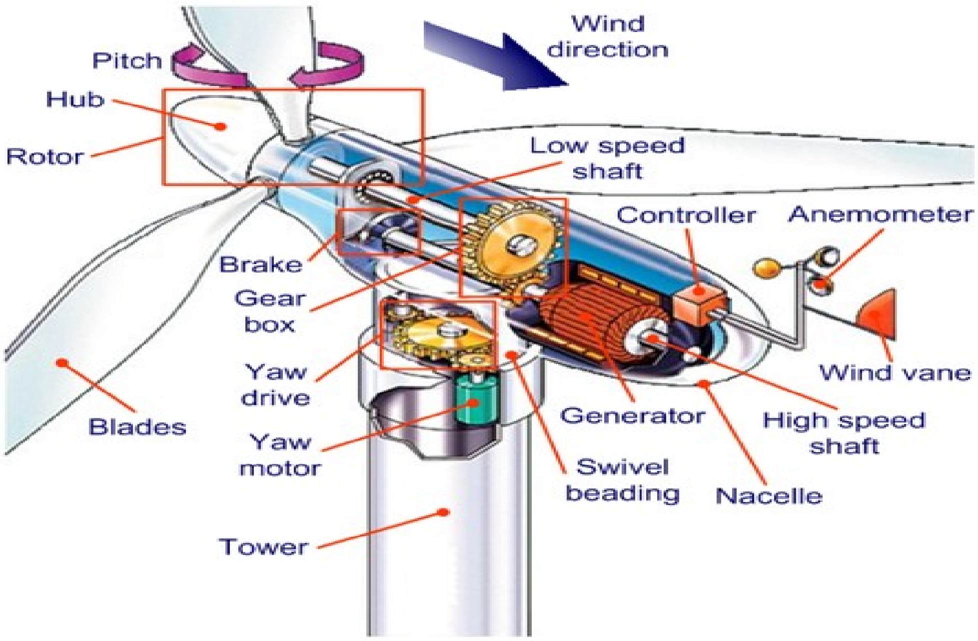


*Fig 3.7 A wind turbine with gearbox [111]*

### 3.5.3 Gearless Wind Power Generation System

As an alternative to gearboxes, a novel gearless generator technology can be used. This makes the turbines more dependable, by cutting downtime and repair costs, a special significant consideration for offshore wind turbine applications, where it is extremely more expensive to carry out maintenance. Doing away with the gearbox from the wind turbine detaches the technically most complicated component of the wind turbine, essentially enhancing reliability. Besides, if a permanent magnet is utilized in the generator, as is the case with modern turbines, the efficiency of the turbine goes up even more. Gearless wind turbine with Permanent Magnet Generator (PMG) technology get rid of losses owing to its external excitation power. The direct drive or gearless wind turbine is a low-speed generator that do away with the need for a gearbox from the wind turbine’s drive train. The gearless wind turbines have the following benefits; they are lighter as likened to traditional turbines, they have significantly lower maintenance costs, and it is not required to replace gearbox as they are gearless wind turbines. The commonly chosen gearless wind turbine generator is the permanent magnet type generator, as it is lighter in weight and has high reliability for offshore applications [112], [113], [114], [115]. The diagram of a gearless wind turbine is shown in fig 3.8.

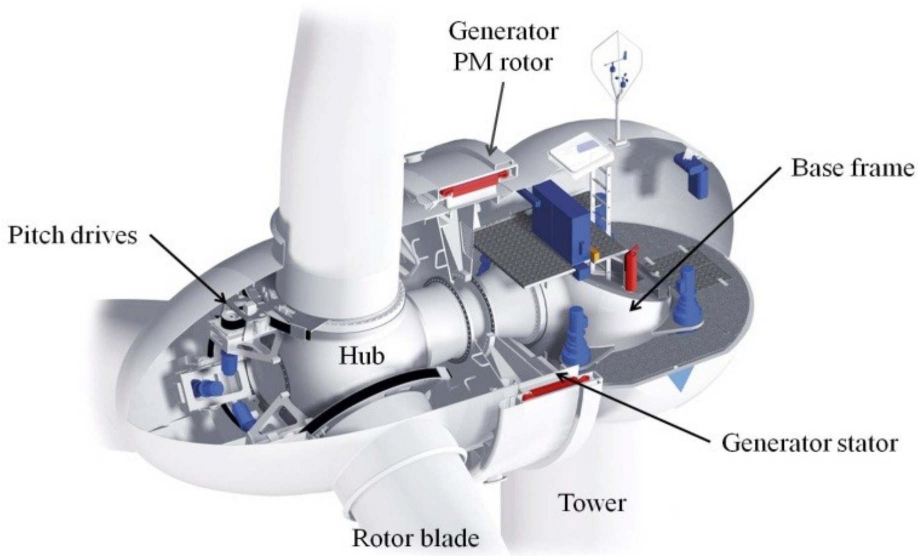


*Fig 3.8 A gearless wind turbine [116].*

# 3.6 Power Electronics for Wind Power Generation Systems

The global electric-power consumption is still rising and there is constant demand to increase electricity production. The generation, distribution and utilization of power should be as technologically well organized as possible and incentives to save energy at the consumer's end should be layout. The deregulation of power has reduced investment in larger electric-power plants, which imply that the requirement for new electric-power sources might be increased in the near future. Two main technologies will play significant part in solving this future issues. One is to convert the electric-power generation sources from the traditional, fossil and short term founded power sources to renewable power resources. The other option is to utilize highly efficient power electronics converters in electricity systems, electricity generation and power consumer's application. There is a widespread utilization of wind turbines in the electricity distribution networks and more and more wind power stations, being used as electric-power plants, are joined directly to the electric-power transmission networks. As the electricity grid spread and power level of wind turbine generators rises steadily, wind energy began to have significant effects on the electric-power grid. Therefore, more advanced generators, power electronic converter schemes, and control solutions have to be initiated in order to improve the features of the wind power plant and make it more fitted to be merged into the electric-power grid. The wind is a non-storable power source, whose electric-power requires priming into interchangeable power in order for it to be competitive for large-scale electric-power production. A crucial mission is then to make wind power as commercially important and fungible as electricity generated by conventionally, executed power plants such as fossil fuel, hydroelectric, nuclear power plants and so on. Power electronics converters is a vital prospect when priming wind power. As the power variation of wind turbines rises the control conditions become more significant and it is obligatory to initiate power electronics converters as an interface between wind turbines and electricity grid networks. Power electronics converters is transforming the principal features of the wind turbine from being an energy source to an active power source device. Presently, the cost per production of kWh of wind power is so low, which makes solutions with power electronics technology more appealing [76], [95], [117], [118], [119], [120], and [121].

Depending on the kind of generator, power electronics converters, speed controllability, and the manner in which the aerodynamic power restricts wind turbine designs normally into various classification ideas. In these wind turbine conceptions, power electronics converters play quite distinct tasks in the wind turbine system and has diverse power rating considerations. Until now, the configuration of the doubly-fed induction generator (DFIG) provided with partial-scale power electronics converter is influencing the market, but it is hope that in the very near future the configuration having synchronous generator (SG) with full-scale power electronics converters is expected to take over. In actual fact, the solutions with full-scale power electronics converter are attractively preferred technology options in the best-selling power variation of wind turbine generators [71], [76], [96], [99], and [121]. The largely embraced solution in power electronics converters for wind turbine systems in the best seller range 1.5–3 MW, is the utilization of the 2-two-level voltage source power electronics converters in a back-to-back configuration. At lower and higher powers, it is feasible to find other solutions such as a diode bridge for the generator in the case of a synchronous generator and equally the utilization of multilevel converters to penetrate medium voltage for high-power implementations [76], [97]. The requirements presented on power electronic converters for wind turbine systems are shown in fig 3.9.

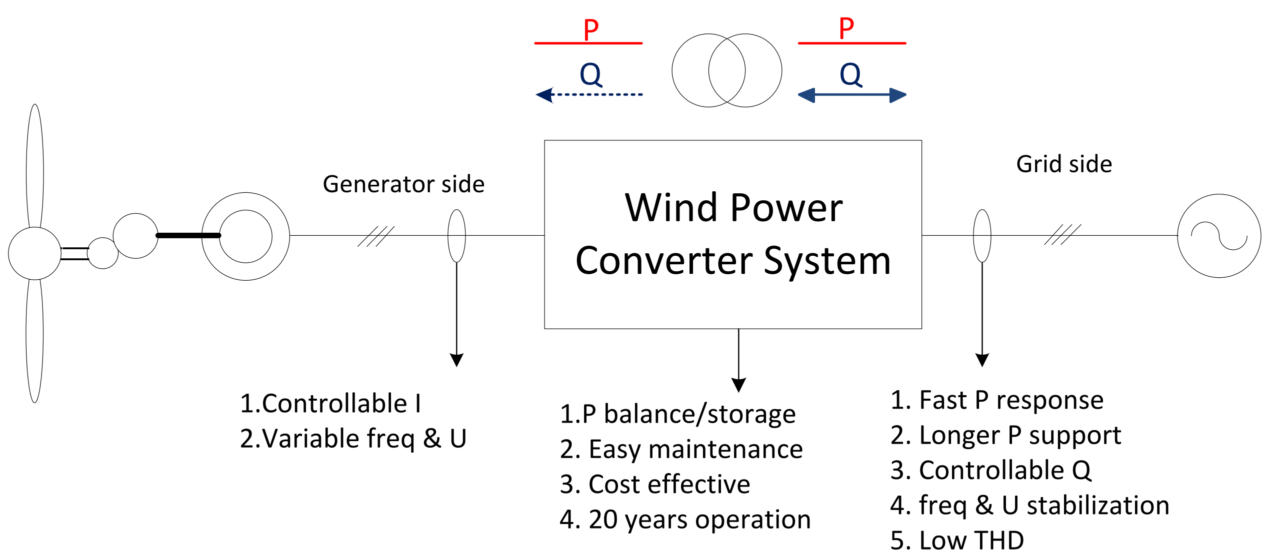


Fig 3.9 Wind power conversion and demands to power electronics converters [76].

As the interface between the wind turbine generator and power grid, the wind power electronics converter has to satisfy the requirements of both sides. For the generator side: the current flowing in the generator stator should be controlled to adjust torque and as a consequence of the rotating speed. This will contribute to the active power balance in normal operation when extracting the maximum power from the wind turbine but equally in case grid faults appear. Moreover, the converter should have the ability to handle variable fundamental frequency and voltage amplitude of the generator output to control the speed. As for the grid side: the converter must comply with the grid codes regardless of the wind speed. This means it should have the ability to control the inductive/capacitive reactive power (Q) and perform a fast-active power (P) response. The fundamental frequency as well as voltage amplitude on the grid side should be almost fixed under normal operation, and the total harmonic distortion (THD) of the current must be maintained at a low level. Inherently, the converter needs to satisfy both the generator side and grid side requirements with a cost-effective and easy maintenance solution. This requires a high-power density, reliability, and modularity of the entire converter system. Moreover, the wind power converter may need the ability to store the active power and boost up the voltage from the generator side to the grid side. extracting the maximum power from the wind turbine but also in case grid faults appear. Moreover, the power electronics converter should have the ability to handle variable fundamental frequency and voltage amplitude of the generator output in order to control the speed. [71], [76], [121], [122], and [123].

The aerodynamic rotor of the wind power arrangement is precisely matched with a gearless generator. The synchronous generator is linked to the electric-power grid by means of a full-scale frequency converter scheme, which is utilized to control the speed of the generator and power flow to the grid side of the wind turbine generator arrangement. The permanent magnets are installed on the generator rotor, making provision for fixed excitation of the generator. The power gotten from the generator is fed via the stator windings into the full-scale frequency converter, which changes the varied generator frequency to constant grid frequency. The full-scale frequency converter structure is made up of a back-to-back voltage source converter, that is the generator-side converter and the grid-side converter joined by means of a DC-link, which is then controlled by IGBT switches. In a variable-speed wind turbine generator, a permanent magnet synchronous generator is installed to the electricity grid with the aid of a back-to-back arrangement of power electronics converters. The first converter, which is the generator-side converter, is joined to the stator windings of the permanent magnet synchronous generator. While the second converter, which is the grid side converter is linked to the electricity grid at the Point of Common Coupling (PCC) with the aid of Alternating Current (AC) filter. The Direct Current (DC) terminals of the two power electronics converters are joined together by means of DC shunt capacitor. The power strategy of the converters contains a three-leg voltage source inverter. Nevertheless, diverse control strategies hinged on the systems control function can be applied to the inverter switches [72], [124] – [130].

### 3.6.1 Filters and Transformers in Wind Power Conversion Systems

Transformers and filters have a pivotal role for volume and losses in wind power conversion schemes. All wind turbine manufacturers are using step-up transformer for connecting generators to the electricity grid. Research is ongoing in order to replace it with a transformer of unity transformer ratio or even maybe to avoid it, this will lead to high power and high voltage transformer-less solutions which is now a technological challenge. Regarding filters, typically LCL filter is the embraced solution to attenuate Pulse-Width Modulation (PWM) harmonics, but in case a diode bridge is utilized on the generator side and in case of higher power wind turbine generator systems that equally have strict demands to grid voltage harmonics, trap filters may equally be used in the final solution. Damping of resonances, associated to the LCL filter, is equally important and the utilization of passive damping can bring about high losses and thus lower power generation and compromise the attenuation of PWM harmonics that is provided by the filter. This might lead to the utilization of active damping, acting on the controller structure or the utilizing of more complex passive damping solutions [76], [131], [132] and [133].

The traditional power electronics converter voltage level is in the range of 380–690V, this is owing to the low generator voltage rating and the usage of two-level power converter topology. To bring about decrease in the electrical losses, a power frequency of about 50/60 Hz electric-power transformer is usually utilized in wind power production systems installed inside the turbine nacelle, this is to step-up the voltage to medium voltage level normally between 11–33 kV as shown in fig 3.10. This heavy and bulky transformer to a very large extent increases the weight and volume of the nacelle as well as mechanical stress of the tower. Nowadays components can handle higher current and voltage ratings, the electric-power losses have decreased and devices is becoming more reliable for the control of megawatt scale power owing to the power electronics converters as a fast advancing technology [134], [135].

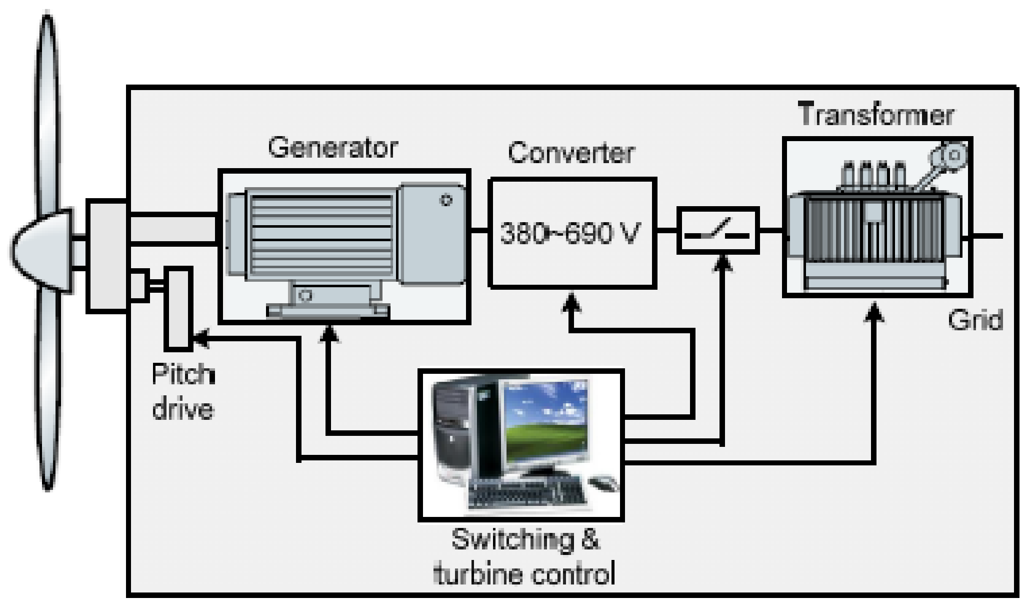


*Fig 3.10 Fully-rated power converter based wind turbine generator system [135].*

The Solid-State Transformer (SST) interfaced with PMSG is being considered as an emerging technology where emphasis is mostly on the design of the equipment. The solid-state transformer interfaced PMSG for wind power conversion scheme allows a direct interface to PCC with solid-state transformer and do away with the bulky AC line frequency transformer utilized in the conventional PMSG wind power schemes [136].

The Insulated Gate Bipolar Transistor (IGBT) is the most generally utilized power semiconductor switch covering an extensive area of applications such as domestic, industrial motor control, traction, renewable power sources, and so on. Insulated gate bipolar transistors (IGBT), Integrated Gate Commutated Thyristor (IGCT) and MOS-Controlled Thyristor (MCT) are the three new designs of power devices. IGBT is the most widespread utilized power electronic equipment at present. An IGBT is fundamentally a hybrid MOS-gated turn on/off bipolar transistor that combines the characteristics of the Metal Oxide Semiconductor Field Effect Transistors (MOSFET), Bipolar Junction Transistor (BJT) and thyristor [137] – [140].

[137], [141], [143]. [137], [142] – [143]. The latest advancement in switching devices is playing a significant part in the evolution of higher power electronics converters for wind power turbines with increased reliability and efficiency. The principal selections are IGBT modules, IGBT press pack, and IGCT press pack as shown in table 3.1 [76]

*Table 3.1 Main switching devices for wind power converters [76].*

| | IGBT module | IGBT Press-pack | IGCT press-pack |
|---|---|---|---|
| Power Density | Moderate | High | High |
| Reliability | Moderate | High | High |
| Cost | Moderate | High | High |
| Failure mode | Open circuit | Short circuit | Short circuit |
| Easy maintenance | + | - | - |
| Insulation of heat sink | + | - | - |
| Snubber requirement | - | - | + |
| Thermal resistance | Moderate | Small | Small |
| Switching loss | Low | Low | High |
| Conduction loss | High | High | Low |
| Gate driver | Small | Small | Large |
| Major manufacturers | Infineon, Mitsubishi, ABB, Semikron, Fuji | Westcode, ABB | ABB |
| Medium voltage ratings | 3.3 kV / 4.5 kV /6.5 kV | 2.5 kV / 4.5 kV | 4.5 kV / 6.5 kV |
| Max. Current ratings | 1.5 kA / 1.2 kA / 750 A | 2.2 kA / 2.4 kA | 2.1 kA /1.3 kA |

The press-pack technology brings about an increase in reliability, still to be scientifically demonstrated but known from industrial practice, higher power density, that is easier stacking for series connection, and better cooling ability at the price of a higher cost in contrast to power modules. Press-pack IGCT is known to support the advancement of MV power converters and are already state of the art technology in high-power electric drives such as utilized in oil and gas applications, but not yet universally adopted in the wind turbine industry owing to cost issues. Nevertheless, the module technology has longer record of practical applications and less mounting issues. Furthermore, themost critical point for reliability, the lift-off as a result of thermal cycling of the bond wires that is used to connect the dies in the module, is an area of ongoing advancement both in materials and its solution in the utilization of flexible foils rather than bond wires that can lead to 35% reduction in volume [76], [144], [145], [146], and [147].

## 3.7 Active and Reactive Power Control in Wind Energy Systems

Variable speed operation of Doubly-Fed Induction Generator (DFIG) wind turbine system founded on active and reactive power capabilities, lower cost of power electronics converter and decreases power losses in contrast to wind turbine generators utilizing fixed speed generator technology. Variable speed wind turbine systems with new standards are more effective owing to their improved efficiency in being able to capture more wind energy and their capability to attain higher power quality. Furthermore, wind turbine systems of variable speed can control the speed of the turbine output power and thus reduces the load stress on various parts of the turbine structure, including the blades and tower. This brings about, higher power efficiency, longer life time, and improved power quality, thereby making these wind turbines affordable in the market place, in spite of its high initial costs [148] – [153]. As more and more power electronics converters are being incorporated into the wind energy conversion system, so as to improve its control and interconnection to the electricity grid system. Emphasis is now mainly on the power schemes where total control of active and reactive power can be acquired at all operating points by utilizing the partial-scale power electronics converter or full-scale power electronics converter [76].

## 3.7.1 Variable Speed Wind Conversion Systems with Partial-Scale Power Converter

The most embraced partial scale frequency converter is chosen together with the DFIG concept, which gives a variable speed controlled wind turbine system with a wound rotor induction generator and partial scale power electronics converter rated to about 30% of nominal generator power on the rotor circuit. The arrangement is shown in fig 3.11 [76].

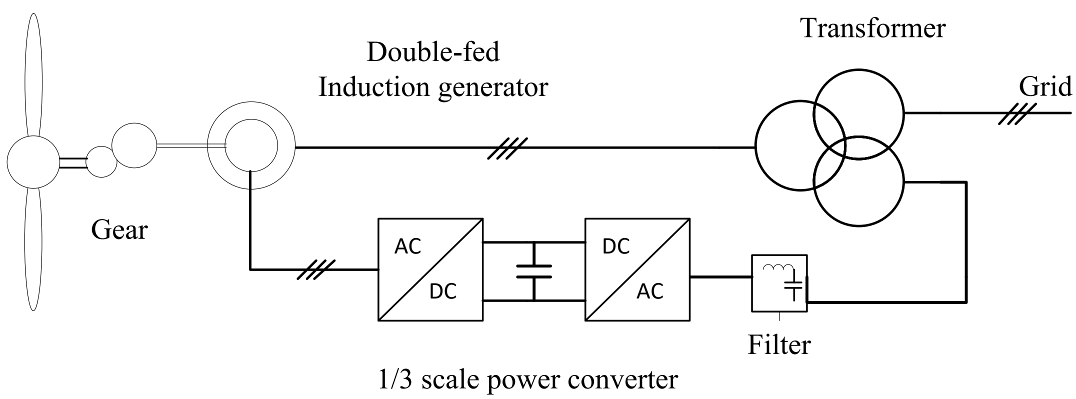


*Fig 3.11 Variable speed wind turbine with partial-scale power converter [76].*

The stator is directly joined to the electricity grid, while a partial scale power electronics converter controls the rotor frequency and consequently the rotor speed. The power rating of the partial-scale frequency converter determines the speed range, which is typically ±30% around synchronous speed. Also, this converter carry out reactive power compensation and smoothens the electricity grid interconnection. The smaller frequency converter makes this concept appealing from a cost-effective point of view. In this case, the power electronics allows the wind turbine to take action as a dynamic power source to the electricity grid. Nevertheless, its major disadvantages are the usage of slip rings and the protection schemes/controllability just in case of power grid faults. The utilization of a reduced size power converter is equally practicable with Permanent Magnet Synchronous Generator (PMSG), such as in an instance where a 20% power electronics converter is positioned in series with the stator winding to actively damp the generator [76], [154], [155], and [156].

### 3.7.2 Variable Speed Wind Conversion Systems with Full-Scale Power Converter

A variable speed wind turbine generator arrangement with full-scale power conversion is equal to the full variable speed controlled wind turbine generator, with the generator joined to the electricity grid via a power electronics converter as shown in fig 3.12.

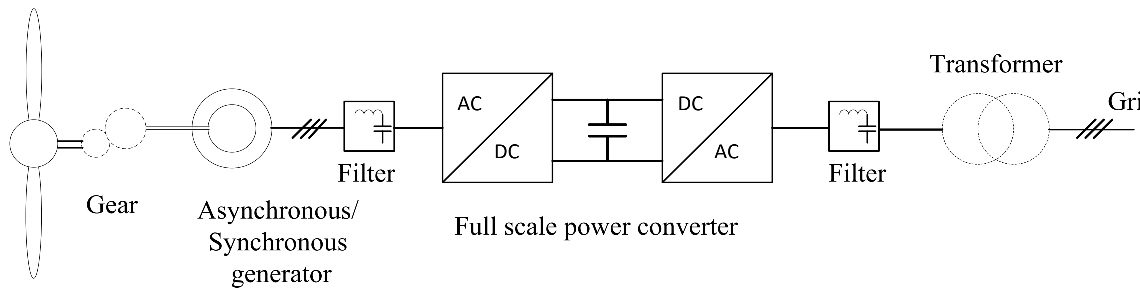


*Fig 3.12 Variable speed wind turbine with full-scale power converter [76].*

The frequency converter carry's out reactive power compensation and a smooth electricity grid linkage for the whole speed variation. The generator can either be asynchronous generator, electrically excited synchronous generator, or permanent magnet excited synchronous generator such as the PMSG. The stator windings are joined to the electricity grid via a full-scale power electronics converter. Some variable speed Wind Turbine Systems (WTSs) are gearless as can be seen in the dotted gearbox in fig 3.12. In these circumstances, a heavier direct driven multipole generator is utilized. Wind turbine manufacturers uses more direct driven type systems. The voltage level of the full-scale power conversion schemes can be from low-voltage, that is below 1 kV to medium-voltage (MV) level and, in the near future, the voltage level might be more suitable for connecting directly to the electricity grid system and to avoid using any transformer [76], [131].

## 3.8 Promising Power Converter Topologies for Wind Energy Systems

Before now, there has not been much varieties for converter topology utilized in wind energy applications. Two-Level Pulse-Width-Modulation Voltage Source Converters (2L-PWM-VSC) or simpler circuits were usually utilized in the low voltage level and are effectively used to fulfil most of the conditions. Nonetheless, owing to the significant increase in the demand for power capacity, economy, reliability, and controllability, the effectiveness of single 2L-PWM-VSC converter appears not to be sufficient for the future wind turbine system. As a result, a number of more-powerful and developed power electronics converter solutions for the succeeding generation of wind turbines are being suggested. The multilevel converter arrangements or topologies are becoming more appealing and widespread choice for wind turbines applications. Some of the promising arrangements are either still in the academics or already in the industry [76], [157], [158].

## 3.8.1 Single Cell Power Electronics Converters for Wind Energy Systems

Wind turbine power electronics converter plays a very significant part in assisting end-users to establish an ideal wind economy. The choice of the correct power electronics converter is essential in the turbine design and for more profitable return on investment. Manufacturers in the industry make available power electronics converters for small-scale and utility-scale wind turbine technologies. Wind turbine power electronics converters, that are appropriate for any of today's turbine concepts, provides durable, reliable performance and are supported by an entire set of life-cycle services. In the past, there has not been much varieties of power electronics converter topology utilized in wind power applications. The 2L-PWM-VSC or simpler circuits were generally utilized in the low voltage level and have the ability to fulfil nearly all of the demand. However, due to the significant increase in the requirement for power efficiency, cost-effectiveness, reliability, and controllability, the capabilities of the single 2L-PWM-VSC power electronics converter seems not to be adequate for the future wind turbine scheme. [157], [158].

### 3.8.1.1 Unidirectional Power Converter Used in Wind Power Systems

Nowadays, it is a trend to use permanent magnet synchronous generator in the full-rated power electronics converter wind turbine systems. As there is no reactive power required in such a generator and active power flows unidirectionally from the permanent magnet synchronous generator to the electricity grid via the power converter, only a simple diode rectifier can be applied to the generator side power electronics converter in order to acquire a cost-efficient solution. Nevertheless, diode rectifier even if multiphase or 12-pulses brings about low frequency pulsations that can trigger off shaft resonance. Semi controlled rectifier solutions are equally feasible. In order to get variable speed functioning and stable DC bus voltage, a boost DC-DC power converter can be installed in the DC link or the DC voltage can be controlled or regulated by utilizing rotor excitation, as shown in fig 3.13, it is a Two-level unidirectional voltage source converter (2L-UNI) for wind turbine systems. It is a full-rated power electronics converter wind turbine system with permanent magnet generator [76], [159], [160].

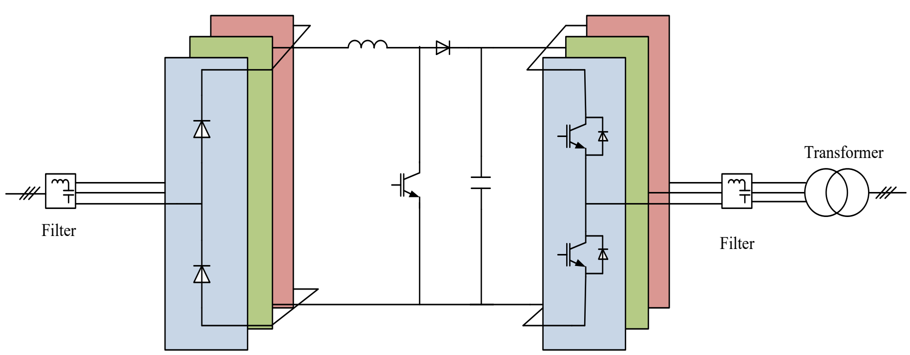


*Fig 3.13 Two-level unidirectional voltage source converter (2L-UNI). [76].*

It is known that for power levels in the range of Mega Watts (MWs), the DC/DC converter needs to be made of a number of interleaved components or by a three-level solution. Fig 3.14, displays the usage of two current source converters in a back-to-back linkage. The benefit of the suggested solution can be to utilize the inductance of the long cables which is used in the wind parks, if a DC distribution is chosen or utilized in case the generator converter is installed in the nacelle while the electricity grid power electronics converter is positioned at the bottom of the wind turbine. The utilization of a voltage source inverter on the electricity grid side is obligatory in the case of fig 3.13, topology due to the fact that capacitive DC storage is utilized. In a similar manner, the utilization of current source inverter on the electricity grid side is required when considering fig 3.14, topology as a result of the fact that the DC storage is inductive [76], [161], [162], and [163].

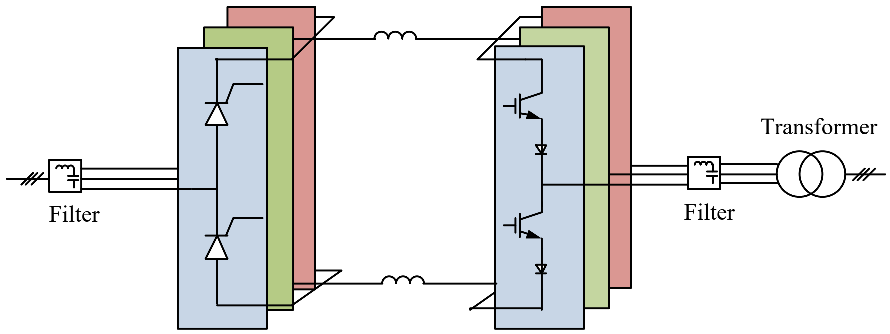


*Fig 3.14 Full-rated power converter wind turbine with permanent magnet generator (Current source version) [76].*

### 3.8.1.2 Two-Level Power Converter (2L-BTB) Used in Wind Power Systems

The 2L-PWM-VSC is the most regularly used three-phase (3ϕ) power electronics converter topology in wind turbine schemes. The mastery obtainable in this field of study is immense, and it is a well-known technology. Two 2L-PWM-VSCs are normally arranged as a back-to-back design (2L-BTB) with a transformer on the electricity grid side, these act as contact between the generator and the electricity grid in the wind turbine systems, as displayed in fig 3.15. The technical benefit of the 2L-BTB solution is the comparatively simple design and usage of fewer components, which to a large extent is partly responsible for the well-proven resilient and reliable performance of the device [76], [158].

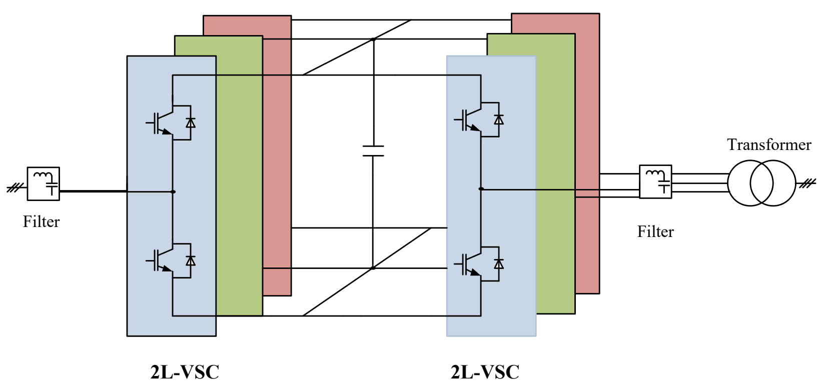


*Fig 3.15 Two-level back-to-back voltage source converter for wind turbines.*

Nevertheless, as the power and voltage range of the wind turbine system increases, the 2L-BTB converter might be affected by large switching losses and lower efficiency at megawatts (MW) and medium voltage (MV) power levels. The obtainable switching devices equally need to be connected in parallel or in series in order to get the essential power and voltage of wind turbines, this might result in reduced simplicity and reliability of the power electronics converter. Other difficulty in the 2L-BTB solution is the two-level output voltage. The exclusively two voltage stages brings about relatively higher *dv/dt* stresses to the generator and transformer of the entire scheme. Bulky output filters might be required to place a limit on the voltage gradient and lessen the Total Harmonic Distortion (THD). The 2L-BTB topology is state of the art in DFIG-based wind turbine technologies. A number of wind turbine manufacturers are equally utilizing this topology for the full-rated power electronics converter wind turbine systems with squirrel-cage induction generator [76], [98], [99], [158], [164], [165], and [166].

## 3.8.2 Multilevel Power Converter Used in Wind Power Systems

As the power capacity of wind turbine systems keeps increasing, even to the extent of 10 MW, it becomes more and more problematic for the conventional 2L-BTB solution to attain satisfactory performance with the obtainable switching devices. Having the capability of more output voltage levels, larger output power and higher voltage amplitude, multilevel power electronics converter topologies are becoming more appealing and a widespread prospect in wind turbine applications. Normally, multilevel converters can be classified into three types: these are including of, neutral-point diode clamped design, flying capacitor clamped design, and the cascaded converter cells design. In order to obtain a cost-effective solution, multilevel converters are mostly utilized in the 3 MW to 7 MW variable speed full-scale power electronics converter wind turbine schemes. [76], [158], [167], [168], [169], [170], and [171].

### 3.8.2.1 Three-Level Neutral-Point Diode Clamped Back-To-Back Topology (3L-NPC BTB)

The Three-level neutral-point diode clamped topology is one of the main commercialized multilevel power converters in the market place. Like the 2L-BTB technology, it is normally arranged as a back-to-back design in wind turbine systems, as depicted in fig 3.16, which is called the Three-level neutral-point clamped back-to-back (3L-NPC BTB) converter for ease of use [76], [158].

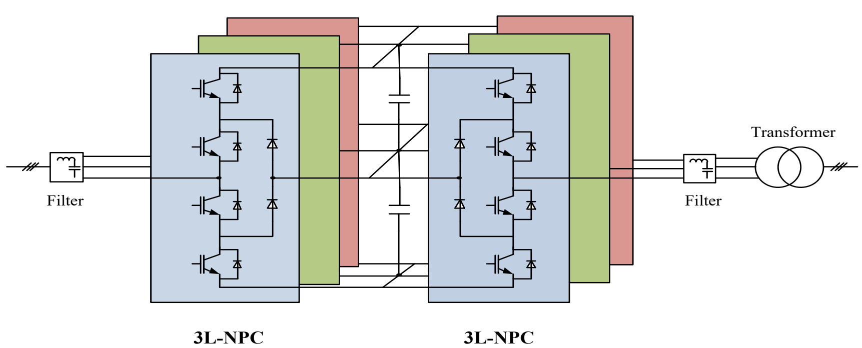


*Fig 3.16 Three-level neutral-point clamped back-to-back converter for wind turbines. (3L-NPC BTB).*

This technology though still in its research stage is able to realize one more output voltage level and less *dv/dt* stress as in contrast to the 2L-BTB, hence the filter size is smaller. The 3L-NPC

BTB is equally capable of outputting the double voltage amplitude when compared to the two-level topology as regards to the switching devices of the same voltage rating. The midpoint voltage variation of the DC bus utilized in the design is a disadvantage of the 3L-NPC BTB technology. Even so, this issue can be ameliorated by the control of the redundant switching status. Nevertheless, it is established that the loss distribution is unequal between the outer and inner switching devices in the switching arm, and this issue may result in derated converter power capacity when it is eventually practically designed and put to use [76], [158], [168], [171], [172].

### 3.8.2.2 Three-Level H-Bridge Back-to-Back Topology (3L-HB BTB)

The 3L-HB BTB solution is made up of two H-bridge converters which are arranged in a back-to-back structure, as unveil in fig 3.17. It can realize output performance as similar to the 3L-NPC BTB solution, but here, the unequal loss distribution and clamped diodes are gotten rid of. It is expected to be more efficient than the 3L-NPC BTB solution, when it is eventually put to practical use and it also has the potential of equal usage of switching devices as well as having higher design power capacity [158], [167], [168], [173].

Furthermore, as only half of the DC bus voltage is required in the 3L-HB BTB design as compared to the 3L-NPC BTB structure. Therefore, there are less series linkage of capacitors and no midpoint in the DC bus, hence the size of the DC link capacitors can be further reduced. Nonetheless, a 3L-HB BTB solution requires an open-winding structure in the generator and transformer in order to establish isolation between each phase. This attribute has both merits and demerits: on one hand, an open-winding design allows comparatively isolated operation of each phase, and a possible fault-tolerant capability is as a result gotten if one or even two phases of the generator or the generator side power converter are in any way out of operation. On the other hand, an open-winding design needs double cable length and weight in order to be able to connect with the generator and the transformer. Extra cost, losses, and inductance by the cables can equally be major hindrance. The open-windings influence on the losses/weight of the generator and the transformer are issues that need to be further investigated [76], [158].

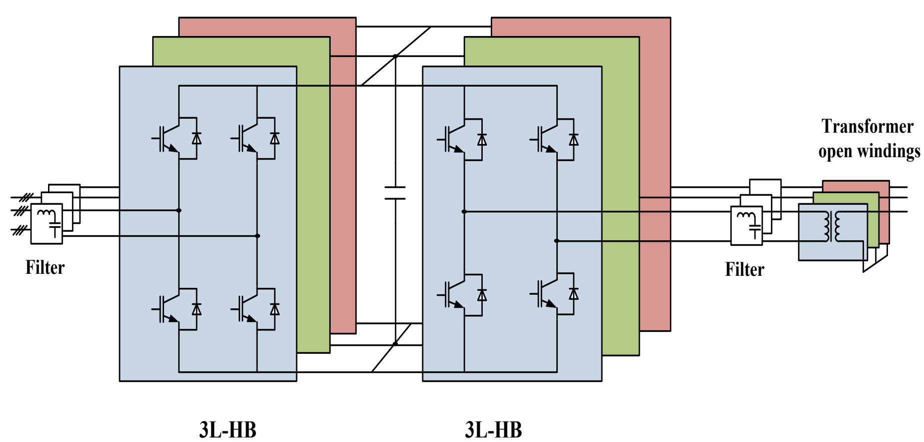


*Fig 3.17 Three-level H-bridge back-to-back converter for wind turbines. (3L-HB BTB).*

### 3.8.2.3 Five-Level H-Bridge Back-to-Back Topology (5L-HB BTB)

The Five-Level H-Bridge Back-to-Back (5L-HB BTB) converter is made up of two back-to-back H-bridge converters utilizing the 3L-NPC switching arms, as presented in fig 3.18. It is an extension of the 3L-HB BTB technology and shares the same special demands for open-winding generator and transformer. With the 5L-HB BTB having the same voltage rating as the switching device, this technology can achieve five level output voltage, and double voltage amplitude as compared to the 3L-HB BTB technology. These qualities allow smaller output filter and less current rating in the switching devices as well as the cables used in realizing the design. But, when compared to the 3L-HB BTB, the 5L-HB BTB power converter technology introduces more switching devices, which could reduce the reliability of the whole system design. The issues of unequal loss distribution as well as that of larger DC link capacitors will regrettably reoccur [76], [158], [165], [174].

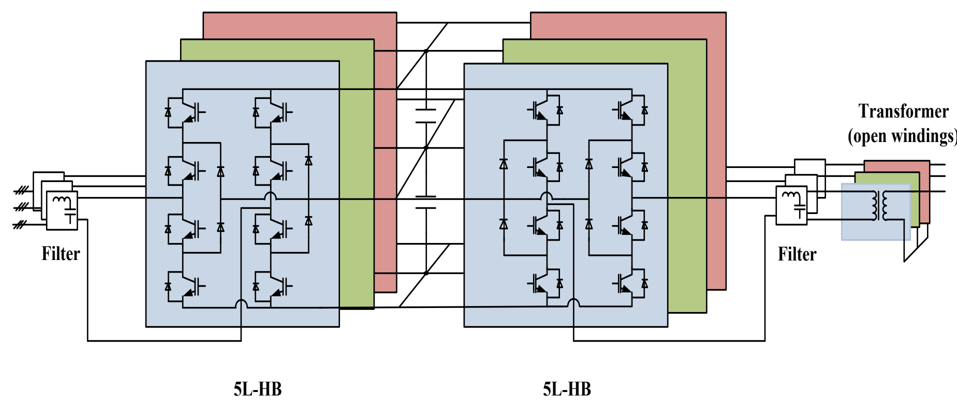


*Fig 3.18 Five-level H-bridge back-to-back converter for wind turbines. (5L-HB BTB).*

### 3.8.2.4 Three-Level Neutral-Point Diode Clamped Topology for Generator Side and Five-Level H-Bridge Topology for Grid Side (3L-NPC + 5L-HB)

Normally in wind power converters, the output quality prerequisites of the electricity grid side are much stricter than those of the generator side. In order to adjust to this unsymmetrical need of the wind power converters, a compound arrangement utilizing the 3L-NPC topology on the generator side and 5L-HB topology on the electricity grid side can be chosen, as illustrated in fig 3.19. On the generator side, this arrangement has a performance comparable to the 3L-NPC BTB technology. Considering the electricity grid side, it has the same performance just as the 5L-HB BTB. The voltage levels and amplitude of the electricity grid side are higher than those on the generator side. Here, an open-winding design in the generator is avoided; thus, the cable length on the generator side is reduced to half, but the potential fault-tolerant capability is equally gotten rid of. This option has less switching devices as compared to the 5L-HB BTB, but unequal loss distribution in the switching devices do exist. In general, large quantity of power semiconductors as well as their auxiliary constituents could reduce power converter reliability and increase the cost. The entire system weight and volume reduction in the wind turbine application all the same needs to be further probed [76], [158], [175].

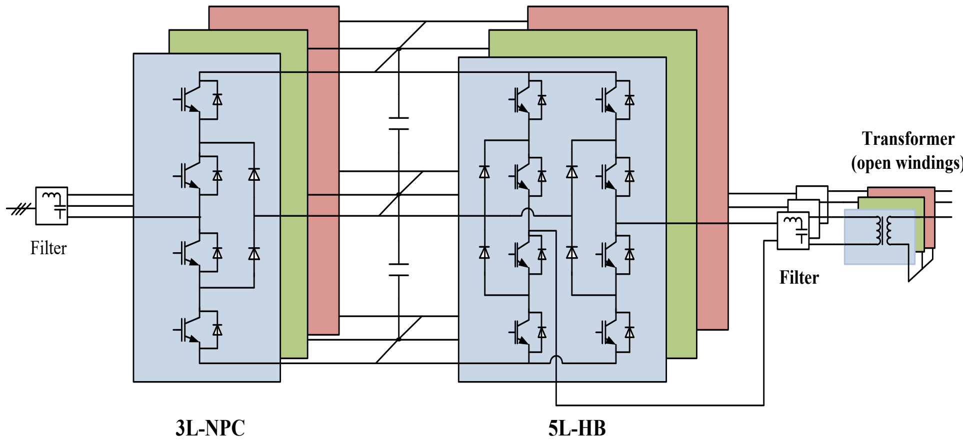


*Fig 3.19 Three-level neutral-point clamped and five-level H-bridge converter for wind turbines. (3L-NPC + 5L-HB).*

The comparison between the various technologies for single-cell full-scale power converter wind turbine systems is tabulated in table 3.2, this is in relation to power semiconductor numbers, output voltage ability, fault-tolerant ability, as well as their main advantages and disadvantages.

*Table 3.2 Comparison of the One-Cell Power Electronic Converter Solutions for Wind Turbines.*

| | 3L-NPC | 3L-HB | 5L-HB | 3L+5L |
|---|---|---|---|---|
| IGBT numbers | 24 | 24 | 48 | 36 |
| Diode numbers(1) | 36 | 24 | 72 | 54 |
| Switch current | $I_{ph}$ | $I_{ph}$ | $I_{ph}$ | $I_{ph}$ |
| Switch voltage | $0.5V_{dc}$ | $V_{dc}$ | $0.5V_{dc}$ | $0.5V_{dc}$ |
| Max. output voltage (2) | $0.5V_{dc}$ | $V_{dc}$ | $V_{dc}$ | $0.5V_{dc} + V_{dc}$ |
| Output-switch voltage ratio | 1 | 1 | 2 | 1+2 |
| Voltage WTHD(3) | 0.84% | 1.15% | 0.73% | 0.73% |
| Output connection | Standard | Open winding | Open winding | Open winding |
| Fault tolerant ability(4) | No | Yes | Yes | No |
| Advantages | Matured technology | Less DC link capacitors, Equal loss distribution | More output voltage levels, Higher voltage utilization of devices(5) | Higher performances on grid side than generator side |
| Disadvantages | Unequal loss distribution,DC bus midpoint | Zero-sequence current path, More cables | Zero- sequence current path, More cables and devices | Unequal loss distribution, DC bus midpoint |

Notes:

1. Include both freewheeling diodes and clamping diodes.

2. Theoretical maximum amplitude of output phase voltage.
3. Simulation results of grid inverter $f_s/f_0 = 21$, $M = 1$, $80^{th}$ harmonics, modulation methods in [56], voltage of $V_a - V_b$.
4. If one or two phase of generator side converter fails, still keep working.
5. Large output-switch voltage ratio (higher output voltage using the same voltage rating devices).

### 3.8.3 Multiples Cells Power Converters for Wind Turbines

The most commercialized cascaded power converter cells multilevel topologies are the Cascaded H-Bridge (CHB) converter as displayed in fig 3.20. Regrettably, the Cascaded H-Bridge requires isolated DC link for each converter cell. This feature might involve a complex multi-pulse transformer on the generator side, causing larger weight and volume. An arrangement which shares much the same idea with some of the succeeding generation traction power converters is vividly shown in fig 3.20. It is founded on a back-to-back Cascaded H-Bridge converter design, with galvanic insulated DC/DC converters as interface. The DC/DC power converters with medium-frequency transformer function at a number of kHz to dozens of kHz, the transformer size is as a result of this reduced. Due to the cascaded design, this arrangement can be directly joined to the electricity transmission grid of rating between 10 kV to 20 kV with high output voltage quality, filter-less design, and redundancy capability [165], [176] – [179].

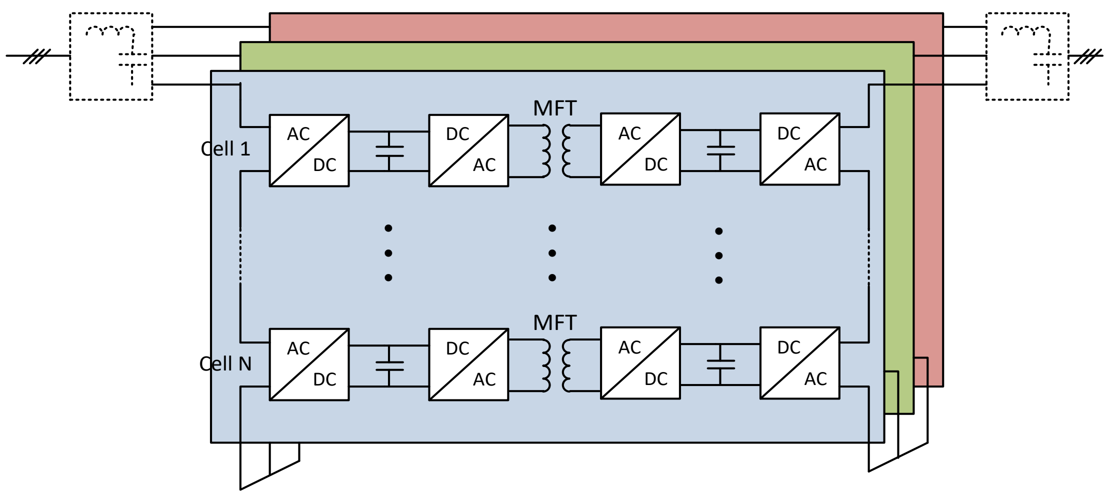


*Fig 3.20 Cascaded H-bridge back-to-back converter for wind turbines with medium-frequency transformer (**S**−**S**).*

Fig 3.21 presents a different approach, the power is increased by using a multicell design, such as, connecting the cells in series on a Medium Voltage Direct Current (MVDC) bus, while the electricity grid power converters are joined in parallel. The main merit of this approach is that standard low voltage modules might be utilized in MVDC applications [180].

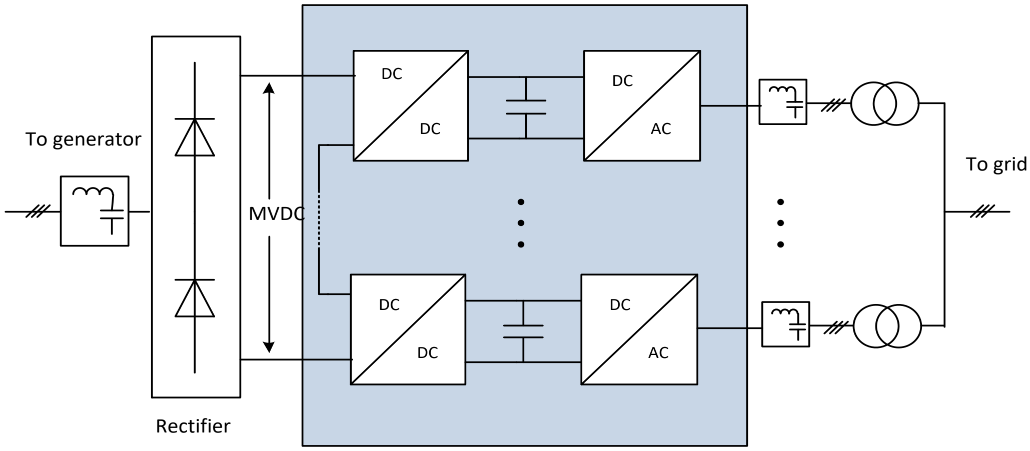


*Fig 3.21 Series connection of power converter cells using a common grid converter diode bridge, an MVDC link, and boost converters with two-level inverters parallel connected to the grid (**S−P**).*

Fig 3.22 illustrates the solution adopted in a 4.5-MW wind turbine system with parallel connection of the cells both on the generator side and on the electricity grid side. Some wind turbine manufacturers have introduced this kind of solution in several of their multi-megawatt wind turbine systems [181], [182].

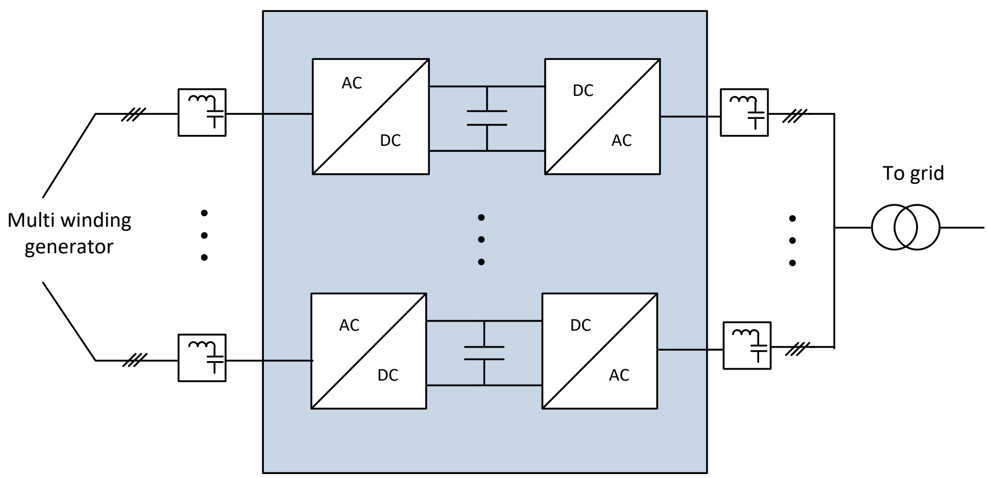


*Fig 3.22 Parallel connection of power converters in which PWM signals are interleaved to achieve harmonic cancellation (**P−P**).*

Fig 3.23 depicts a solution for a high-power high-voltage transformer-less wind turbine system, where the coils of the generator are joined to the AC/AC power converter that are joined in series on the electricity grid side. Here, the coil windings have to be isolated [131].

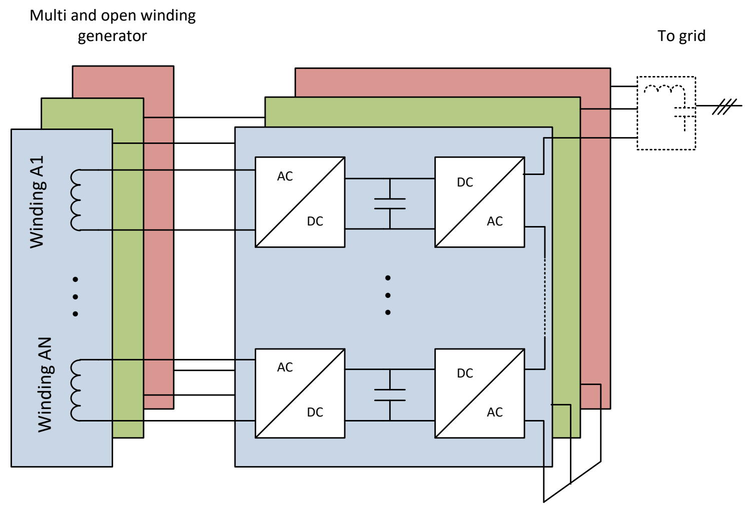


*Fig 3.23 Magnetic parallel connection of power converters on the generator side and series connection on the grid side (**MP−S**).*

Fig 3.24, vividly shows a power electronics converter established based on series connection of matrix converters in which the output of the device feeds several windings of a transformer leading to a magnetic parallel arrangement [183].

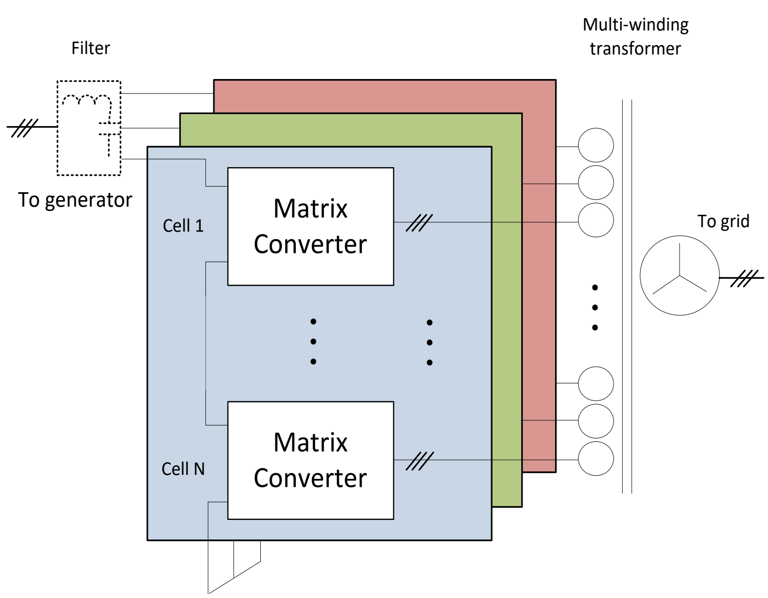


*Fig 3.24 Series connection of matrix converters with magnetic paralleling on the grid side (**S−MP**).*

All the discussed topologies have fault-tolerant abilities, and higher number of components are equally being used in their designs. The major differences between them is in their requirement with respect to the generator and the transformer as summarized in table 3.3. (the more + the better, 0 means moderate, − means no such ability).

*Table 3.3 Comparisons of the Multicell Solutions for Wind Turbines.*

| Configurations | S-S | S-P | P-P | S-MP | MP-S |
|---|---|---|---|---|---|
| Generator | Standard | Standard | Open winding | Standard | Open winding |
| Transformer | 0 | - - | - | - - - | 0 |

# 3.9 Control Structure of Wind Power Systems

The control structure of a wind turbine system requires both fast and slow control dynamics, as shown in fig 3.25, where a general control design for a wind turbine system, including the turbine, generator, filter, and power converter, is presented. The wind turbine notion can either be the variable-speed wind turbine concept with partial-scale power electronics converter and a doubly-fed induction generator type or the variable-speed wind turbine concept with full-scale power electronics converter type. In general, the power flowing in and out of the wind power generation system has to be carefully controlled. The power produced by the turbines should be controlled with the aid of mechanical parts such as, pitch angle of the blades, the yawing system, and so on. For the time being, the whole control scheme has to follow the power generation commands given by the electricity distribution system operator (DSO) and/or the electricity transmission system operator (TSO) [95], [132], [162], [184], [185], [186], [187] [188].

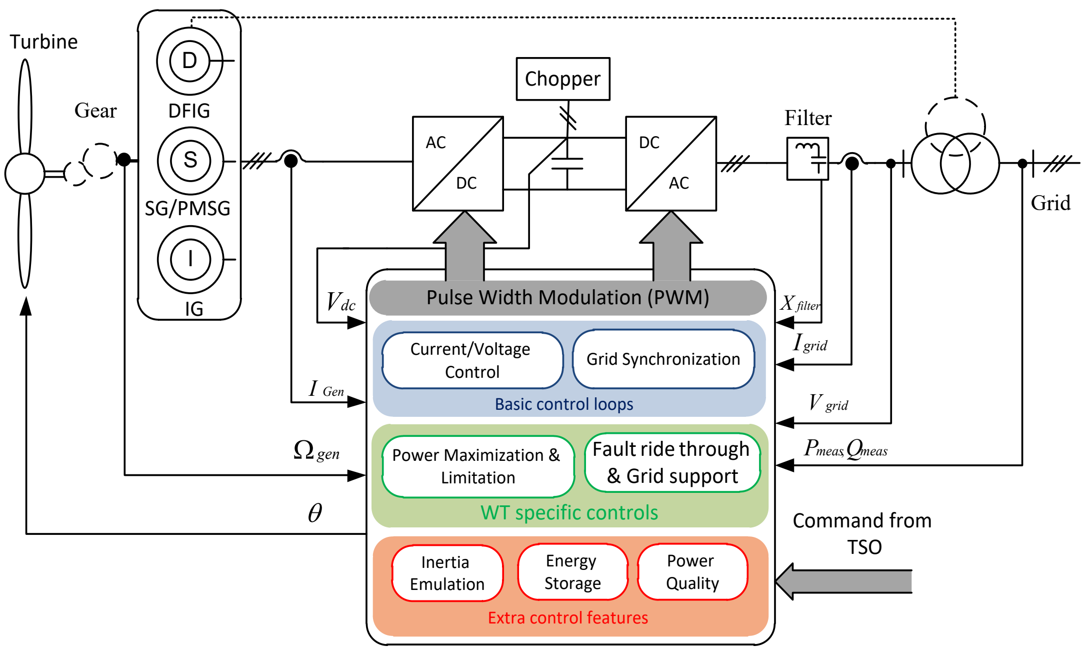


*Fig 3.25 General control structure for modern wind turbines [95].*

The advanced attributes of the wind turbine system control procedure that might be of interest and should be put into consideration are including of the maximization of the generated power, ride through operation of the electricity grid faults, and provision of electricity grid supporting functions in both normal and abnormal operations, and so on. In the variable-speed wind turbine idea, the current in the generator side will normally be transformed by controlling the generator side converter, and as a result the rotational speed of the wind turbine can be modified to actualize maximum power generation based on the obtainable wind power. With respect to operations under electricity grid fault, synchronized control of a number of subsystems in the wind turbine scheme such as the generator and/or the electricity grid side converters, braking chopper/crowbar, and pitch angle controller are obligatory. Ultimately, the fundamental controls such as current regulation, DC bus stabilization, and the electricity grid synchronization have to be performed fast by the wind power electronics converter, where the proportional-integral controller and proportional-resonant controllers are normally utilized [122], [123], [188].

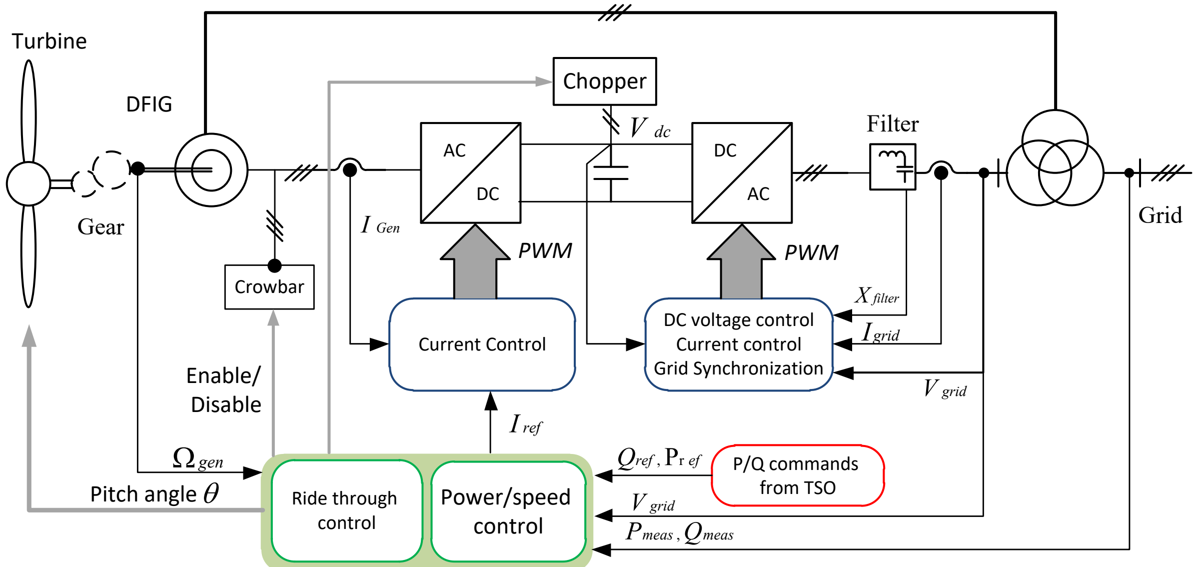


*Fig 3.26 Control of a wind turbine with doubly-fed induction generator [95].*

An illustration of the control techniques for a doubly-fed induction generator based wind turbine system are visible in fig 3.26. In the lower part of the diagram, the maximum power generated by the wind turbine will normally vary the rotational speed, which is proportional with the wind speed, thereby keeping the pitch angle $\theta$ fixed. At usually very low wind speed, the rotational speed will be fixed at the maximal permissible slip to avert over voltage of the generator output. A pitch angle controller is utilized to limit the power when the wind turbine output is higher than the nominal power. The sum total electrical power of the wind turbine system is regulated by controlling the doubly-fed induction generator through the rotor side converter. The control scheme of the electricity grid side converter is merely just to keep the DC-link voltage fixed. It is of note that a trend is to utilize a crowbar joined to the rotor of the doubly-fed induction generator in order to ameliorate the control performance under electricity grid faults [189], [190].

A different instance for the control method utilized for full-scale converter-based wind turbine idea can be seen in fig 3.27. One benefit of this wind turbine system is that the DC-link carry out some sorts of control decoupling between the wind turbine and the electricity grid. The DC-link will equally give a choice for the wind turbines to be joined with the energy storage units, which can more advantageously control the active power flow into the electricity grid network, this characteristic will furthermore ameliorate the electricity grid supporting capabilities of the wind turbine systems. The produced active power of the wind turbine system is controlled by the generator side converter, in contrast with the fact that the reactive power is controlled by the electricity grid side converter. Here, a DC chopper is usually introduced to avert overvoltage of

DC-link in situations of electricity grid faults, when the additional turbine power requires to be dissipated as the sudden drop of electricity grid voltage [95].

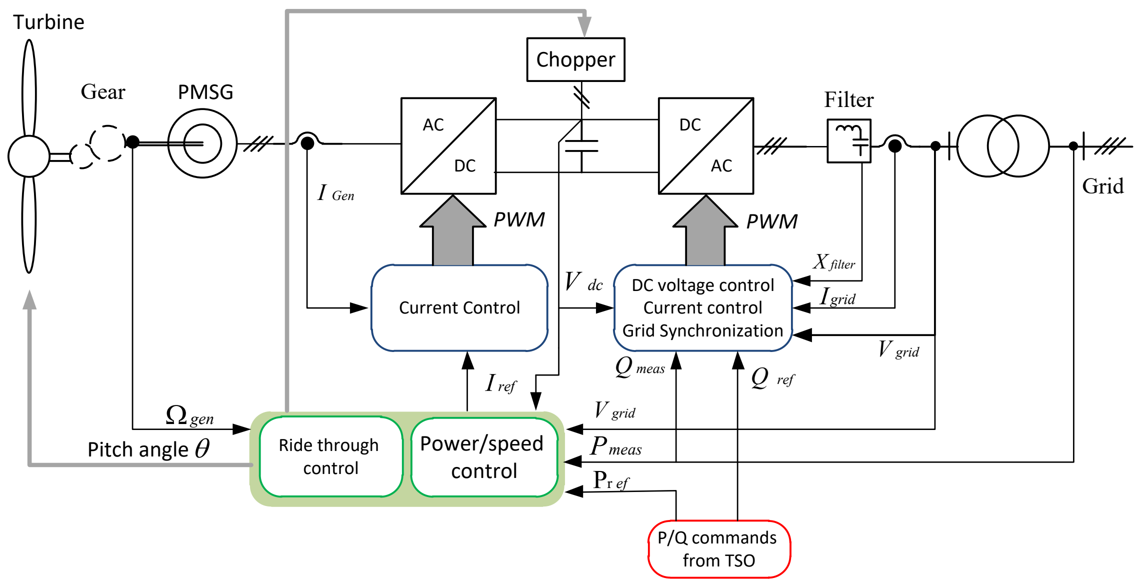


*Fig 3.27 Control of active and reactive power in a wind turbine with multipole PMSG.*

# 3.10 Grid Integration of Wind Power Systems

The fluctuation and unpredictable characteristics of wind power are not favorable for the electricity grid operation. Most nations have strict requirements for the functioning of wind turbine systems, known as electricity grid codes, which are updated on regular basis. Essentially, the electricity grid codes are always trying to make the wind turbine system to act as a traditional power plant from the electrical utility view point. Meaning that wind turbine systems should not only be a passive power source merely administering obtainable power from the wind, but equally acting like an active production unit, which can effectively control the supplied active/reactive power based on demands, and supply of frequency/voltage support for the electric-power grid. [95], [175], [191] – [194].

In accordance with most grid codes, the individual wind turbine must be able to control active power at the Point of Common Coupling (PCC). Usually, active power is regulated based on electricity grid frequency, this is done so that the grid frequency can be no matter how sustained. In some countries, active power is reduced when frequency rises greater than 48.7 or 50.15 Hz depending on the power reserving scheme. In the same vein, the reactive power administered by the wind turbine system equally has to be regulated in a certain range. Some grid codes give a range of the reactive power administered by the wind turbine system to the active power output, which leads to larger MVA capacity when designing the whole converter scheme. Furthermore, the transmission system operators will usually stipulate the reactive power range of wind turbine systems based on the grid voltage levels. This reactive power control should be achieved at a slow speed under the time constant of minutes in steady-state operation [175], [193], [194]. The organization of the control plan of a typical frequency inverter for the electricity grid side is displayed in fig 3.28,

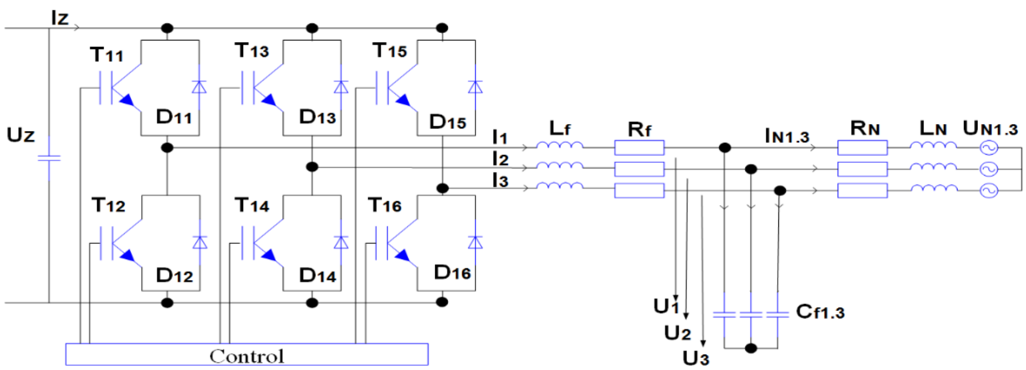


*Fig 3.28 Control structure of a typical grid-side frequency inverter.*

The aim of the driving converter in a wind turbine generator scheme is to determine the moment and the time of contact for each switch. The technique of driving is Pulse Width Modulation (PWM), which utilizes digital signals to control power applications, as well as being sufficiently uncomplicated to change back to analog with the least possible hardware. Fig 3.29 gives an idea on how to drive this converter [126], [127]. From fig 3.29. the equations given below in equation (3.12), (3.13) and (3.14) is generated.

$$I_{ctr1} = \underline{V_1}(t) = 0{,}5 \times AF.\sin(\omega.t) \tag{3.12}$$

$$I_{ctr2} = \underline{V_2}(t) = 0{,}5 \times AF.\sin(\omega.t + \frac{2.\pi}{3}) \tag{3.13}$$

$$I_{ctr3} = \underline{V_3}(t) = 0{,}5 \times AF.\sin(\omega.t - \frac{2.\pi}{3}) \tag{3.14}$$

Where:

$I_{ctr1}$, $I_{ctr2}$, and $I_{ctr3}$ are outputs of the control circuit, and AF is the amplitude function.

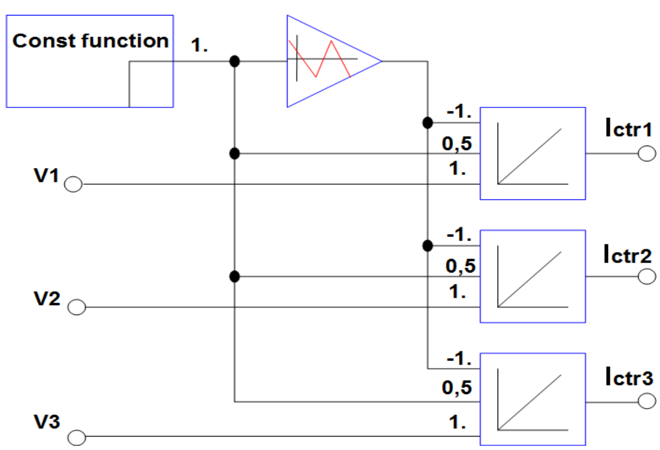


*Fig 3.29 Control structure for electricity grid-side frequency inverter.*

In addition to their usual operation, Transmission System Operators (TSOs) in different countries do issue strict electricity grid supporting requirements for wind turbine systems under electricity grid faults. These electricity grid requirements entail that the boundaries with various grid voltage dip amplitudes as well as the permissible disturbing time are defined for wind farm schemes. It is equally becoming a need that the wind turbine systems should also provide reactive power up to 100% of current capacity, in order to play a part in voltage recovery process when voltage sag is present on the grid or power line. This grid codes demand is relatively difficult to be met by most wind turbine concepts. Therefore, other power quality units like STATCOMs might in all likelihood be introduced to assist wind turbine systems in attaining these tough requirements [175], [191], [193], [194].

*Table 3.4 Comparison of grid integration performances between traditional power plant and wind turbine plant, the more + the better, 0 means moderate, − means no such ability*

| Grid Integration Features | Conventional Power Plant | WTG in the past (without/few PEC) | WTG nowadays/future (with PEC) |
|---|---|---|---|
| Active power control | + | 0 | + |
| Reactive power control | + | 0 / - | ++ |
| Short circuit capability | ++ | + | ++ |
| Voltage backup | ++ | - | + |
| Power output inertia | ++ | - | + |
| Frequency control | ++ | - | ++ |
| Black start capability | + | - | + |

The requirements for additional grid supports by wind turbine systems has raised the cost per generated kilowatt hour, it has also made wind power more appropriate to be largely utilized and integrated into the electric-power grid. It is anticipated that there will be stricter electricity grid codes in the future, this will result in continuous challenges in wind turbine systems and will equally continue to bring about advancement in power electronic technologies. Table 3.4 compares the characteristics of traditional power plant, wind turbine generation (WTG) systems in the past and nowadays/future. Here, grid integration performances have been focused on. Introduction of more advanced power electronics, controls, and electricity grid regulations, the start-of-the-art wind turbine system furnished with synchronous generator and full-scale power electronics converter can more or less equal the performance of traditional power plants, making wind power technology to be more suitably integrated into the electric-power grid [95].

The constant stator voltage control system is considered to be of utmost advantage in gearless wind turbine applications. The DC-link voltage is kept constant to ensure that the generated active power is fed via the DC-link to the electricity grid, all this is done to make sure that no energy is dissipated in the DC-link [32]. Fig 3.30, illustrates the control circuit of a synchronous generator. It controls the currents of the synchronous generator in the rotor coordinate order and the input quantities which are stator currents ($I_{L1}$, $I_{L2}$, $I_{L3}$) changed into the stator coordinate system ($\alpha$, $\beta$). These currents ($I_\alpha$, $I_\beta$) are rotated from the stator coordinate system to the rotor coordinate system (d, q) by utilizing the vector negative adapter (-VD) technique [126], [195], the electric angle is gotten from the model of the synchronous generator utilized in the wind conversion system.

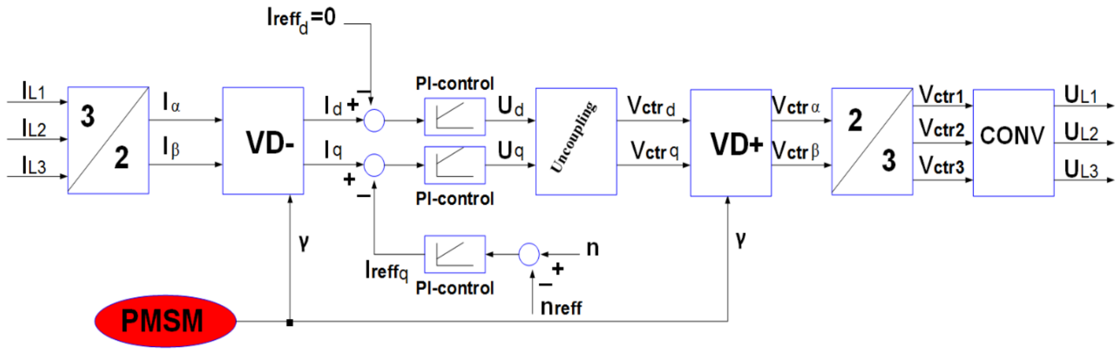


*Fig 3.30 The control circuit of a synchronous generator.*

This then makes the stator currents in the rotor to be in the coordinate system ($I_d$, $I_q$ ) and both the constant and fixed currents are stabilized, this brings about a good assumption for the control system $I_d$, which is utilized to control the reactive power and $I_q$ is utilized to control the synchronous generator torque [196]. Equally, ($I_d$, $I_q$) are compared with reference values ($I_{d.ref}$, $I_{q.ref}$) and the product of the deviation is sent to the PI controller. The output is a continuous disengagement process to get driving vectors in the rotor coordinate system ($V_{d.ctr}$,$V_{d.ctr}$). These are then transformed to the stator coordinate system ($V_{\alpha.ctr}$,$V_{\beta.ctr}$) [195] and afterwards it is changed to vectors ($V_{ctr1}$,$V_{ctr2}$,$V_{ctr3}$). in the 3-$\phi$ system. This process provides switch-off and switch-on for the rectifier IGBT switches.

If the DC-link voltage remain constant by utilizing the generator-side converter control, the active power of the generator is conveyed through the DC-link to the electricity grid-side converter. Consequently, the active power generated by the wind turbine can be controlled using the elecricity grid side converter. Owing to the converter mechanism used, the reactive power operational point of the generator side and the grid side converter are fully decoupled. This means that the reactive power, which is finally supplied to the electricity grid network, can be independently controlled by the electricity grid side converter. Hence, the same control system is utilized on both the generator and the electricity grid network. The control circuit of the grid network is vividly shown in fig 3.31 [32], [126], [195].

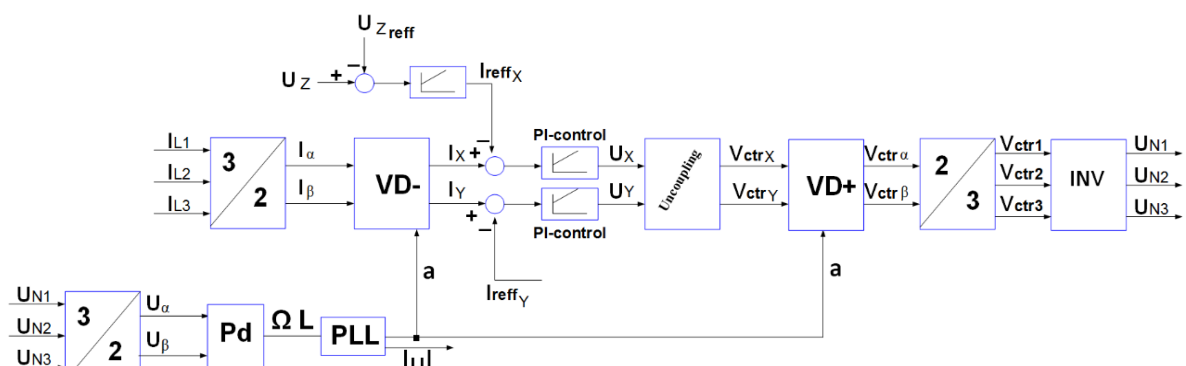


*Fig 3.31 The control circuit of an electricity grid network.*

# 3.11 Types of Wind Turbine Technologies Utilized in Wind Energy Conversion Systems

Apart from mechanical power regulation, wind turbines are further classified into fixed speed (Type-1), limited variable speed (Type-2), or variable speed with either partial (Type-3) or full (Type-4) power electronic conversion. Distinct kinds of speed control mechanism are implemented by means of different rotating Alternating Current (AC) machines and power electronics devices. There is another kind of machine referred to as Type-5 wind turbine, in which the mechanical torque converter between the rotor's low-speed shaft and the generator's high-speed shaft controls the generator speed as well as the electrical synchronous speed, this kind of machine make use of a synchronous machine directly joined to a medium voltage electricity grid [197], [198], [199], [200].

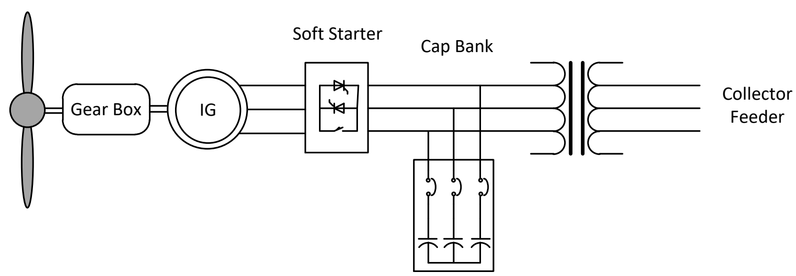


*Fig 3.32 A Typical Configuration of Type-1 Wind Turbine Generator [197].*

The Type-1 wind turbine generator is implemented with a squirrel-cage induction generator and joined to the step-up transformer directly as can be seen in fig 3.32. The wind turbine speed is fixed or nearly fixed to the electric-power grid's frequency, and produces real power (P) when the wind turbine shaft rotates. Despite the possibility that there is a bit of variability in the output with the slip of the machine, Type-1 wind turbines normally operate at or very close to a rated speed. The main disadvantage of the induction machine is that as its excitation field consumes reactive power, then the larger currents the machine can draw when started across-the-line. To make better these effects the wind turbine usually make use of a soft starter and discrete steps of capacitor banks within the wind turbine [197], [198], [199], [200].

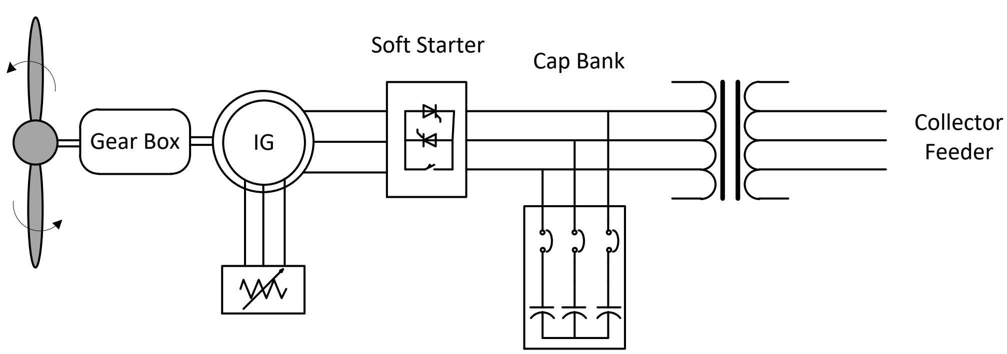


*Fig 3.33 A Typical Configuration of a Type-2 Wind Turbine Generator [197]*

In the Type-2 wind turbines, wound rotor induction generators are joined directly to the wind turbine generator step-up transformer in a manner much the same as the Type-1 wind turbine with regards to the machines stator circuit, but it equally includes a variable resistor in the rotor circuit as shown in fig 3.33. This can be accomplished with a set of resistors and power electronics devices external to the rotor with electrical currents flowing between the resistors and rotor via slip rings. As an alternative, the resistors and power electronics can be installed or mounted on the rotor, thereby doing away with the slip rings, this is known as the Weier design. The variable resistors are joined into the rotor circuit gently and can be used to control the rotor currents quite quickly so as to keep the power constant even during gusting circumstances, and this can influence the machine's dynamic response during electricity grid disturbances. By connecting resistance to the rotor circuit, the real power curve, can be stretched to higher slip and higher speed ranges. This is meaning that the wind turbine would have to spin quicker in order to produce the same output power, for any added rotor resistance. This will allow the blades pitching mechanisms some capability to control the speed and move the wind turbines operation to tip speed ratio, that is the ratio of the tip speed to the ambient wind speed, so as to actualize the best energy catch. It is normal that speed variations of up to 10% is feasible, permitting for some degree of freedom in energy catch and self-protective torque control [197], [198], [200]

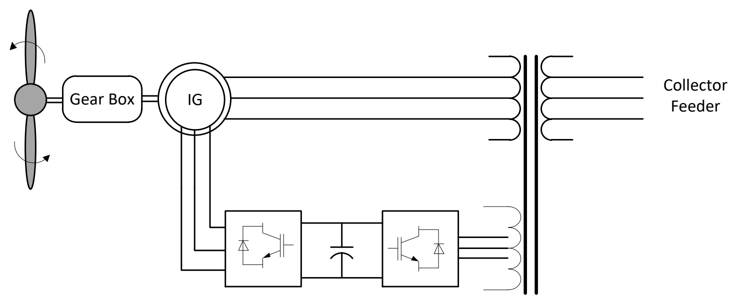


*Fig 3.34 A Typical Configuration of a Type-3 Wind Turbine Generator [197]*

The Type-3 wind turbine, which is commonly known as the Doubly Fed Induction Generator (DFIG) or Doubly Fed Asynchronous Generator (DFAG), takes the Type-2 wind turbine design to the succeeding level, by joining variable frequency AC excitation, instead of just a simple resistance to the rotor circuit. The extra rotor excitation is provided by means of slip rings which are current regulated, voltage-source converters, this can modify the rotor currents' magnitude and phase almost instantaneously. The rotor-side power converter is linked back-to-back with the electricity grid side power converter, which interchanges power directly with the electric-power grid. This is vividly shown in fig 3.34. A small quantity of power injected into the rotor circuit can effect a large control of power in the stator circuit of the conversion system. This is one main merit of the doubly fed induction generator, a reasonable control of the output is obtainable with the attendance of a set of converters that are usually only 30% of the rating of the machine. In addition to the real power that is supplied to the electricity grid from the generator's stator circuit, power is equally supplied to the electricity grid via the grid-connected inverter when the generator is moving faster than the synchronous speed. But when the generator is moving slower than the synchronous speed, real power will flow from the electricity grid, via both converters, and from the rotor to the stator. These two modes of operation are made possible by the four-quadrant nature of the two converters used in the system, which do allow much wider speed range, for both above and below synchronous speed by up to fifty percent (50%), despite the fact that narrower ranges are more common [197], [198], [200].

The remarkable merit of the doubly fed induction generator, is that it offers the advantages of separate real and reactive power control, much like the conventional synchronous generator, while being capable of running asynchronously. The field of industrial drives has produced and matured the conceptualization of vector or field oriented control of induction machines. Utilizing these control systems, the torque producing constituents of the rotor flux can be made to react quick enough that the machine remains under considerable control, even during important electricity grid disturbances. Although, the Type-3 wind turbine is more expensive than the Type-1 or Type-2 machines, the Type-3 machine is becoming popular owing to the numerous benefits derive from this machine [197], [198], [200].

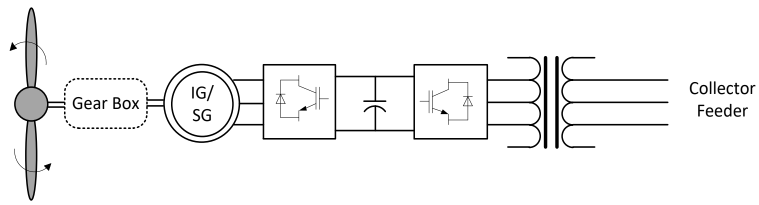


*Fig 3.35 A Typical Configuration of a Type-4 Wind Turbine Generator*

The Type-4 wind turbine as depicted in fig 3.35 offers a great deal of flexibility in its design and operation as the output of the rotating machine is sent to the electricity grid via a full-scale back-to-back frequency converter. The wind turbine is permitted to rotate at its optimal aerodynamic speed, which results in a wild alternating current output from the machine. Furthermore, the gearbox might be completely remove or gotten rid of such that the machine spins at a slow wind turbine speed and produces an electrical frequency that is well below that of the electricity grid. This is no issue for a Type-4 wind turbine, as the inverters changes the power, and offer the potentiality of reactive power provision to the electricity grid, much like the Static Synchronous Compensator (STATCOM). The rotating machines of the Type-4 machine illustrated here have been built as wound rotor synchronous machines, which is comparable to traditional generators found in hydroelectric power plants with control of the field current and high pole numbers, as permanent magnet synchronous machines or as squirrel cage induction machines. Nonetheless, based on the capability of the machine side inverter to control real and reactive power flow, whichever kind of machine could be utilized. Progress in power electronic devices and controls in the last years have made the converter technologies both responsive and efficient. It is important to mention here that, even so, that the power electronic converters have to be sized to pass the full rating of the rotating machine in question, in addition to any of its capacity to be utilized for reactive power compensation [197], [198], [200].

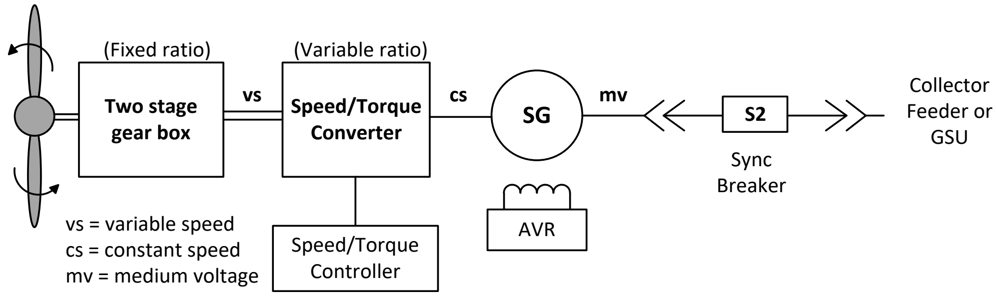


*Fig 3.36 A Typical Configuration of a Type-5 Wind Turbine Generator*

The Type-5 wind turbines as unveiled in fig 3.36, is made up of a normal wind turbine generator variable-speed drive train joined to a torque/speed converter coupled with a synchronous generator. The torque/speed converter converts the variable speed of the rotor shaft to a constant output shaft speed. The closely coupled synchronous generator, which is functioning at a fixed speed comparable to the electricity grid frequency, can afterwards be directly joined to the electricity grid via a synchronizing circuit breaker. The synchronous generator can be designed suitably for whichever required speed normally 6 pole or 4 pole and voltage normally medium voltage for higher efficiency. This approach necessitates speed and torque control of the torque/speed converter along with the normal voltage regulator, that is the Automatic Voltage Regulator (AVR), the synchronizing scheme, and the generator protection scheme inherent with a grid-linked synchronous generator [197].

## 3.12 Reactive Power Compensation of Wind Connected Power Systems

The conventional wind turbine is normally a mere induction generator with little ability for voltage ride through or power factor control. During networks disturbances, the power plant would most likely trip off-line. Furthermore, the wind power plant did not have to provide any additional or auxiliary services such as voltage control, variable power factor, dynamic system support, and so on. Generally, older wind power plants did not need reactive compensation systems. The new generation of wind turbines has far greater ability. Wind power plant centralized control schemes can supply the additional services needed by interconnection agreements. Besides, more conditions are being applied to enable wind power plants respond like conventional synchronous machine generation power plants during fault situations, and to have dynamic response and control ability. All of these factors require that wind power plant should have a collector scheme structure that can adapt to these conditions. There are numerous areas of consideration when determining the reactive power compensation scheme within wind power plants collector design. Nearly all wind power plants have an interconnection agreement that might define the parameters of what is needed. In defining the minimal power factor and voltage-ride-through demands for the interconnection of wind power plants to transmission service providers, a wind power plant designer or engineer should be well informed that reactive power compensation alone might not ensure low voltage-ride-through for the wind power plant. By preference, it is the interaction with the electricity grid of the reactive power compensator mechanism with the specific wind turbine generators in the wind power plant as a scheme that impacts compliance with these conditions. Once the principal preconditions are known there is a secondary listing that might as well define items such as the response time, voltage control requirements, constant susceptance (that is imaginary part of admittance) requirements, power factor control requirements, low voltage ride-through, high voltage ride-through, voltage recovery requirements and post fault contingency requirements, as an integral part of the wind power plant and reactive compensation scheme [198], [199], [201], [202], [203], [204].

The reactive power flow from the electricity grid to the wind power plant at the Point-of-interconnection (POI) is given by the following expression [201]:

$$Q_{poi} = Q_{gen} + 3I^2X - V^2\omega C - Q_{comp} \quad (3.15)$$

where $Q_{gen}$ is the leading or inductive reactive power consumption of the wind turbines, which is negative when the wind turbine generator is operating at a lagging or capacitive power factor, $X$ is the equivalent series reactance of the cables, lines and transformers, $C$ is the equivalent shunt reactance of especially the cables, and $Q_{comp}$ is the reactive-power administered by any centralized reactive power compensation scheme. With regards to the simple induction generators, the reactive power consumption relies on the loading and terminal voltage in accordance with the following approximation [201]:

$$Q_{gen} = V^2/X_m + 3I^2X_l \tag{3.16}$$

Where $X_m$ and $X_l$ stands for the magnetizing and leakage reactance. For the doubly-fed induction generator and full-power-converter machines, the reactive power can be controlled on the terminating ends of the machine or at the electricity grid side of the wind turbine transformer within the wind turbine generating system. Without reactive power compensation, the reactive power exchange is made up of a term which is proportional to the square of the voltage and another term that is proportional to the square of the current. Since the voltage variations are considerably less than the current variations, it is the second-mentioned term that needs the main compensation. Wind turbine generators can supply or consume reactive power, based on the kind utilized in a system. Simple induction generators normally make use of Power Factor Correction Capacitors (PFCCs) to correct the power factor at the terminals of machines to unity or near unity. The doubly-fed induction generator and full converter-based wind turbine generators can operate dynamically over a defined power factor variation, such as 0.95 inductive to 0.95 capacitive. A specific wind turbine might have different steady state versus dynamic ability [198], [199], [201].

### 3.12.1 Reactive Power Compensation Using Type 1, 2, 3, 4 and 5 Wind Turbine Technologies in Wind Farms

Large-scale wind power integration entails that wind power should be pliable and controllable much comparable to traditional production. This equally imply that with rising wind power penetration into the electric-power grid, auxiliary support services which is presently offered majorly by traditional generation should equally be satisfactorily provided by wind power generation in a reliable way. Intermittent nature and lack of suitable controllability of wind power constitutes severe challenges to secure stable operation of large-scale wind penetrated power networks. The continual displacement of traditional power plants by wind turbine systems is already being adopted in many countries. Dynamic voltage control service at electricity transmission network level which is presently being administered via traditional power plants in conventional electric-power systems, is constituting notable challenge in large-scale wind integrated electric-power networks. The issue of dynamic voltage security is anticipated as one of the main worry for secure and stable functioning of future large-scale wind integrated electric-power networks [198], [205], [206], [207]. The voltage control abilities of a wind turbine generator are dependent on the kind of wind turbine utilized in a system. Type-1 and Type-2 wind turbine generators cannot normally control voltage. Rather, these wind turbine generators normally make use of power factor correction capacitors to sustain the power factor or reactive power output on the low-voltage terminal ends of a machine to a set-point [197], [198].

Rising wind power penetration specifically the Type-1 and Type-2 wind turbine technology, that do need reactive power from the electricity grid rather than generating reactive power unfavorably influence voltage stability that has long since been the cause of several major electricity blackouts observed across the universe. Wind turbine systems specifically the fixed speed type with traditional induction generators, display strong coupling between active power production and reactive power assimilation. Therefore, in such kind of wind turbine systems, any fluctuation in active power production brings about comparable behavior in reactive power assimilation. In such situation, lack of adequate dynamic reactive power can affect the electric-power system voltage seriously, most critical being close to the point of common coupling. Moreover, lack of suitable dynamic reactive power support from wind power generators coupled with displaced traditional generation worsens the problem of dynamic voltage security in large-scale wind integrated electric-power networks. Consequently, in order to ensure stable and secure functioning of high wind penetrated electric-power networks, alternative measures to strengthen or make stronger the voltage security of power systems need to be investigated [198], [200].

Grid code requirements at the generator unit level have raised issues in the past years mainly due to the exploration of the reactive power ability of wind turbine technology. The coordinated control scheme for doubly-fed induction generator wind farm to achieve reliable voltage control have since been considered. Improved reactive power ability of the doubly-fed induction generator have been shown by embracing a combination of both the electricity grid side and rotor side control of wind conversion systems. Different reactive power control strategies have been suggested in wind integrated electric-power systems. These control schemes are mainly localized wind farm control schemes that optimize reactive power sent in order to minimize power system losses. Also, dynamic optimization based method for optimal allocation of dynamic reactive power sources in large-scale wind integrated electric-power systems have equally been suggested. It is necessary to mention at this point that in highly penetrated wind power systems, primary/dynamic voltage control is one of the major problem owing to the combined unfavorable effect of displaced traditional generation power plants and less or even negative dynamic reactive power support by wind generation power plants. Thus, to attain realistic optimal allocation of dynamic reactive power resources, electric-power system dynamics must be put into consideration. Research have revealed that dynamic optimization based method shows that consideration of available local alternatives in optimal allocation of dynamic reactive power sources for large-scale wind integrated electric-power system can address the dynamic voltage security problem in an economic and reliable manner [198], [208], [209], [210], [211].

Moreover, effective usage of wind turbine systems specifically the Type-3 and Type-4 based wind power plants, can be one easy way to implement a cost-effective approach to solve the problem of dynamic voltage control. This approach can minimize or even avoid the installation of new infrastructure that otherwise would be needed to sustain secure and stable functioning of large-scale wind integrated electric-power systems. Besides, existing wind turbine systems specifically those joined at transmission system voltage level equally offer an appealing alternative for dynamic reactive power support, with the Type-3 and Type-4 wind turbine systems being the major contenders. The Type-4 wind turbines are usually preferred owing to their higher control flexibility and their ability to offer reactive power support even during shutdown time. With suitable up-grading of existing wind power plants located at potential locations that are critical for dynamic voltage control, a substantial cost might be saved by avoiding the installation of new infrastructure that is otherwise needed. Upgrading of potential wind power plants will generally include upgrading the electricity grid side converter and its related control firmware. Additionally, with the current infrastructure of functional wind power plants, the sum total reactive power margin obtainable for most of the active power operating points surpasses the reactive power needed by grid code requirements. Under such situations, extra dynamic reactive power reserve can be offered by wind turbine systems. This implying that for large-scale wind integrated electric-power systems, efficient utilization of existing resources like refurbishment of traditional electric-power plants and up-grading of existing wind farms specifically the Type-4 wind turbine based wind farms and efficient management of reactive power in wind turbines specifically in wind parks can lower the cost of operation and prolong the life of dedicated dynamic reactive power sources [198], [200].

The Types-3, 4 and 5 wind turbine generators can be used to control voltage. These wind turbine generators are able to vary reactive power at a given active power and terminal voltage, which allows the control of voltage. In a Type-3 wind turbine generator, voltage is controlled by converting the direct constituent of the rotor current, that is the part of the current that is in-line with the stator flux. In a Type-4 wind turbine generator voltage control is actualized by varying the quadrature reactive part of current at the electricity grid-side converter. To permit voltage control ability, the electricity grid-side converter must be rated above the rated megawatt of the machine. Owing to the fact that a synchronous generator is utilized in a Type-5 wind turbine system, an automatic voltage regulator is normally needed. Modern automatic voltage regulators can be programmed to control reactive power, power factor and voltage in electric-power networks [197], [212].

# 3.13 Voltage Stability in Wind Power Conversion Systems

Voltage stability is referred to as the capability of an electric-power system to maintain steady voltages at all the buses in a power system after being subjected to disturbance from a given initial functioning condition. Voltage stability relies on power systems capability to sustain and/or restore equilibrium between electrical load demand and supply. Instability that might result in such system can occur in the form of progressive fall or rise of voltages at several buses. Potential consequence of voltage instability is the loss of load in an area/zone or tripped electricity transmission lines and other components by their protective systems, this can lead to cascading outages. A loss of synchronism of some generators can result from these outages or from operating conditions that violate field current limit of synchronous generator; or when considering the variable speed wind turbine generator, the current limits of power switches. Voltage stability can vary during the event; it can be short term (< 1 minute), or it might evolve during several hours [213], [214], [215].

Reactive power losses in an electric-power transmission line can be provided from either individual buses, or can be shared by the buses in question on power lines. Parallel compensation can be implemented on both sides for any two busses used. Reactive power compensation can be performed by controlling the generator itself, or can be supplied from external compensation, such as synchronous condensers, adjustable capacitor banks, and static power compensation such as static VAR compensator or static compensation which is the static synchronous compensator.

Two possible compensations are usually implemented in a wind turbine system: first is reactive power compensation at the wind turbine level, which is mostly in Type-1 and Type-2 wind turbine generators; the second is at the electrical plant level, which is normally at the lower side of the substation transformer. Plant-level compensation is usually added when a wind power plant is joined to a weak electricity grid. The Type-3 and Type-4 wind turbines are furnished with power electronics converters that can provide controllable reactive power compensation to an electric-power network [215], [216], [217], [218]. Reactive power compensation can equally be achieved by making use of series compensation. The merit of this is that the voltage and current rating of the series compensation is comparatively small bearing in mind that it is pre-arranged to compensate for the voltage drop of the electric-power line impedance. Series compensation is generally utilized to compensate long electricity transmission lines; even so, care should be taken not to make it susceptible bringing about sub-synchronous resonance [215].

# 3.14 Reactive Power Compensation Inside a Wind Farm

Voltage stability issues might arise as a result of the need for reactive power by some wind turbines. This factuality becomes more consequential when a wind turbine conversion system experiences a voltage dip, which leads to the problem of how to generate enough reactive power for the wind turbine generators. Several confirmed ways out for transient and steady-state voltage control issues are including of; Mechanical Switched Capacitors (MSCs), Static VAR Compensators (SVCs), and Static Synchronous Compensator (STATCOM) [40], [41], [98], [216], [219].

## 3.14.1 Mechanical Switched Capacitors (MSCs)

The Mechanically Switched Capacitors (MSCs) are high and medium voltage devices installed in an electric-power system to provide the needed capacitive reactive compensation and power factor correction. The usage of mechanical switched capacitors has increased owing to the fact that they are relatively inexpensive in contrast with other devices and techniques, they are easy and quick to install, and can be installed practically anywhere in the electric-power transmission and distribution systems. The Mechanical Switched Capacitors are utilized to stabilize electric-power system voltage, keeping voltage fluctuations brought about by load variations and changes in power system situations within the confines of acceptable limits. In effect, it supplies direct compensation of changes in the reactive power specification of installed loads and keeps the electricity transmission lines free from auxiliary reactive power flow, thereby lowering electricity transmission losses. Suitably designed mechanical switched capacitors equally ameliorate network voltage stability under fault circumstances. Large voltage dips which is caused by network disturbances, that is short circuit followed by changes in power system conditions, can be lowered in this manner. Even so, the successfulness of voltage stabilization is hinged on the distance from fault location on the line. The mechanically switched capacitors incorporate only static elements like capacitors, reactors and surge arresters, and can be joined directly to the high voltage bus-bar network or via a transformer. It offers several advantages and benefits for the electricity transmission networks. These advantages are including of: Enhancement of system performance, quality and efficiency of electric-power systems; Power losses minimization; Helping the joining of renewable power sources into the electric-power systems; Lowering of environmental load such as $CO_2$ emission; and Making electric-power systems more cost effective [220], [221].

The mechanically switched devices are the most cost effective reactive power compensation devices. They are a simple and low-cost solution, but low-speed solution for voltage control and system stabilization under heavy load situations. Their uses have practically no impact on short-circuit power but it sustains voltage at the point of connection. An advanced type of the mechanically switched capacitor is the Mechanically Switched Capacitor with Damping Network (MSCDN) for prevention of network resonances [222].

The purpose for using mechanically switched devices is to achieve a capacitor bank with if possible high reactive power. Two kinds of capacitor switching are feasible: These are single bank switching and back to back switching. In the single bank switching scenario only one capacitor is joined to the electricity grid. The inrush current is principally affected by the inductances on the path from the source to the capacitor. But in the back-to-back switching scenarios, where one capacitor is already joined to the electricity grid, and another one is joined afterwards, the inrush currents are principally impacted by the inductances in the path from the first to the second capacitor. Therefore, current limiting reactors should be designated in order to lower the currents in case of back-to-back switching. It should be stated that both the transformer and the current limiting reactors utilizes some parts of the capacitive reactive power. This is usually incorporated when the capacitor ratings are allocated [223], [224].

The diagram depicted in fig 3.37, is composed of a bank of shunt capacitors switched mechanically to supply reactive power compensation. The size of individual capacitor might be restricted so as to avert large voltage transients in a network. The major issues usually encountered by wind farms using this technology includes excessive switching of capacitor bank that does lead to failures, application of inherent voltage steps stress on the wind turbines, and increases in the needed maintenance of wind conversion system [98].

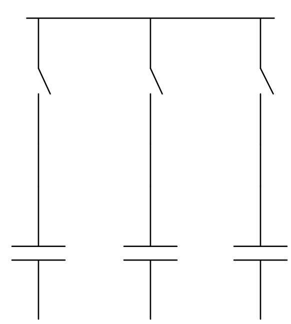

*Fig 3.37 A Mechanical Switched Capacitor bank [98].*

## 3.14.2 Static VAR Compensators (SVCs)

A Static Var Compensator (SVC) is a thyristor-controlled (since it is thyristor controlled, thus it is called static) generator of reactive power, either lagging or leading, or both. This piece of equipment is also called a static reactive compensator. An SVC is a high voltage device that regulates effectively the network voltage at its coupling end. Its major function is to keep the network voltage constantly at a set reference point. Some other control characteristics of SVC are: voltage control, reactive power control, damping of power oscillations, and unbalance control. The design and configuration of an SVC device is all the time modified to the particular project specifications. An SVC is one of the regulators founded on Power Electronics and other static devices known as Flexible Alternating Current Transmission Systems (FACTS) regulator, which is used to improve the ability and the flexibility of a transmission network. [216],[225], [226], [227]. Static Var Compensator is a shunt-linked static VAR producer or assimilator whose output is regulated to exchange capacitive or inductive current so as to keep in good condition or regulate specific parameters of an electrical power system, typically bus voltage. SVC is founded on thyristors without gate turn-off ability. The operating concept and features of thyristors achieved variable reactive impedance SVC includes two main parts and their fusion: Thyristor-controlled Reactor (TCR) and Thyristor-switched Reactor (TSR); and Thyristor switched capacitor. The objectives of SVC design are reactive and load imbalance compensation, and with the use of traditional quantities in its regulator, it may be utilized in collaborative compensation methods for smart grids [216], [228], [229].

The Static VAR Compensation (SVC) systems uses thyristor-controlled elements, that is normally Thyristor-Controlled Reactors (TCRs) and Thyristor-Switched Capacitor (TSCs), this is equally in addition to mechanical switched capacitors in order to obtain dynamic control of reactive power. Usually, static VAR compensators are joined to the collector bus that links a wind farm to the point of common coupling so as to provide the required power factor or voltage level. The static VAR compensator can be used to adjust reactive power, which basically solve the issues of steady-state voltage [98], [216].

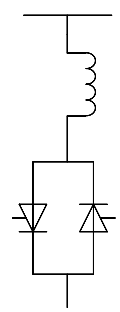

*Fig 3.38 SVC basic components of a Thyristor-Controlled Reactor [98].*

Fig 3.38, represents a thyristor-controlled reactor, which is a device made up of three legs, each of the leg having an inductor and a static switch. The static switch is composed of two anti-parallel joined thyristors. The power is controlled by transforming the current flow via the inductor by means of the switch. The ON-state of the thyristors can be modified by the firing angle. But, this device does produces current harmonics owing to its current waveform [98].

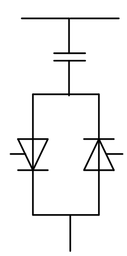

*Fig 3.39 SVC basic components of a Thyristor-Switched Capacitor [98].*

A thyristor-switched capacitor is depicted in fig 3.39, which is consisting of a bank of switched capacitors. Each capacitor has its own static switch, which is comparable to a thyristor-controlled reactor device, but in this scenario or situation, the switching takes place when the voltage across the thyristor is zero. As a result, this device does not generate current harmonics. Nevertheless, owing to the utilization of switching capacitors, thyristor-switched capacitor might generate voltage transients. The combination of these elements can provide good reactive power compensation performances. Thyristor-controlled reactor can be combined with fixed capacitors or with thyristor-switched capacitor. Fig 3.40, shows a thyristor-controlled reactor used in combination with a fixed capacitor bank. This solution is frequently utilized for electric-power sub-transmission and distribution systems. The current harmonics might be eliminated or gotten rid of by tuning the fixed capacitors as passive filters. While fig 3.41, combines TCR and TSCs in one reactive power compensation scheme. Thus, a continuous variable reactive power is gotten across the whole control range in addition to the full control of both inductive and capacitive components of compensation [98].

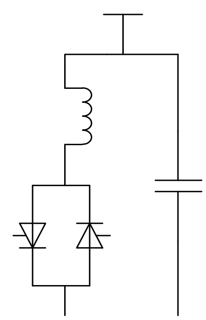

*Fig 3.40 A Thyristor-Controlled Reactor with a fixed capacitor [98].*

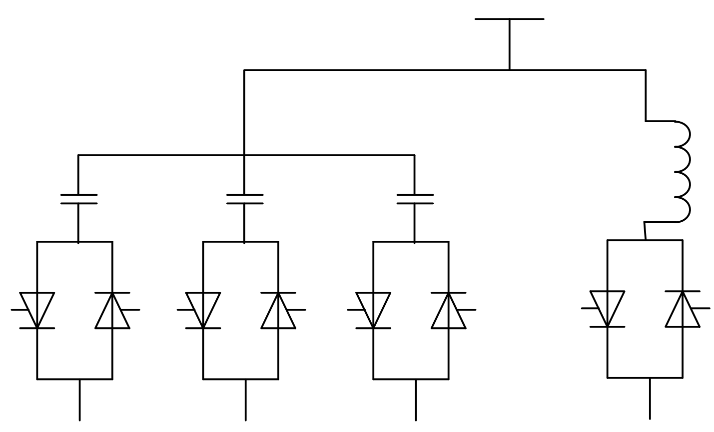


*Fig 3.41 A Thyristor-Controlled Reactor with Thyristor-Switched Capacitor [98].*

### 3.14.3 Static Synchronous Compensator (STATCOM)

Static synchronous compensators (STATCOMs) are part of FACTS device lineage. Their primary aim is to provide a fast acting, precise, and adjustable quantity of reactive power to an AC power system network to which they are linked. STATCOMs accomplish this by modifying the magnitude and polarity (phase) of the reactive constituent of the current flowing into and out-of their AC side. This allows STATCOMs to regulate the quantity and direction of movement of the reactive power swapped with the AC power systems. They are frequently applied for dynamic power factor correction, such as dynamic reactive power compensation, in industrial machinery working with large arbitrary peaks of reactive power needed. STATCOMs multiply the power factor of machinery, reduces voltage variations at machinery input, which prevents harm to the power plant, and minimizes equipment's operating costs. A back-to-back Voltage-Source Converter (VSC) is usually utilized in order to realize full control of active and reactive power. A STATCOM system based on a voltage-source converter is used to produce reactive power. Voltage-source converter uses power electronic devices such as IGBTs, IGCTs, or gate turn-off thyristors (GTOs), and they can equally be arranged as a multilevel bidirectional converter. As can be seen in fig 3.42, a voltage-source converter is joined to the electricity grid to inject or absorb reactive power via an inductor X. This scheme is appropriate for mitigating both steady-state and transient situations. Comparing this technology with SVCs, STATCOMs do provide less disturbances, faster response, and better performance at reduced or lowered voltage levels [98], [230].

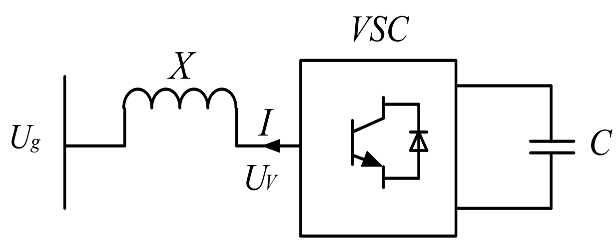


*Fig 3.42 STATCOM based on VSC connected to PCC via an Inductor [98].*

From fig 3.42, if the power angle remains zero (δ = 0), the active and reactive power injected to the electricity grid network by the STATCOM can be expressed as [98];

$$P = \frac{U_g\, U_V}{X} \sin\delta \; = 0 \qquad (3.17)$$

$$Q = \frac{U_g\, U_V}{X} \cos\delta - \frac{U_g^2}{X} = \frac{U_g}{X}\left(U_V - U_g\right) \qquad (3.18)$$

Hence, the voltage-source converter acts as a reactive power generator or producer (Q > 0, capacitive behavior) if $U_V > U_g$, and as a reactive power absorber or assimilator (Q < 0, inductive behavior) if $U_V < U_g$. In application, a small phase shift is utilized to compensate the voltage-source converter losses. The reactive power injected or infused onto the electricity grid can be controlled faster by using the other systems. The response time of the system is limited by the switching frequency and the size of the inductor [98].

# 3.15 Reactive Power Compensation Outside a Wind Farm

So as to send the active power produced by a wind farm into the electricity grid, the power transmission control has to be put into consideration. Power oscillations and voltage collapses should be prevented. Fig 3.43 illustrates a feasible solution to prevent these disadvantages, which utilizes a Thyristor-Controlled Series Compensation (TCSC) outside a wind farm. The thyristor-controlled series compensation changes the equivalent capacitor value by switching the parallel-connected inductor. Hence, a variable capacitor can be gotten and adjusted to increase the dynamic stability of power transmission, improve or enhance voltage regulation and reactive power balance, and to also control power flow of electricity grid lines [98], [231]. Fig 3.44 shows the detailed diagram of the thyristor-controlled series compensator used in the wind farm shown in fig 3.43.

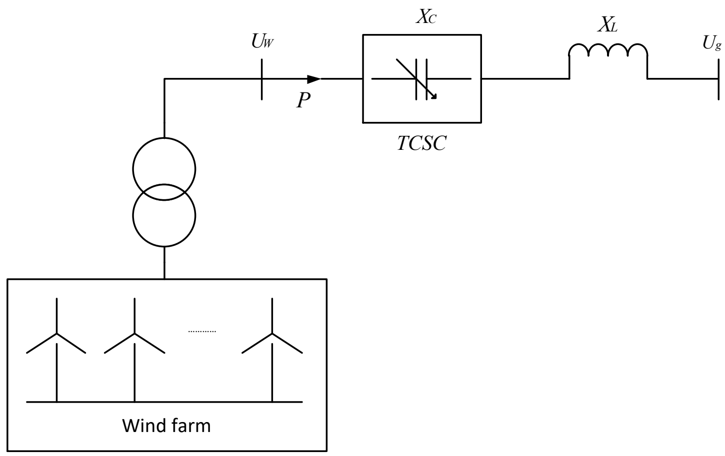


*Fig 3.43 A Thyristor-Controlled Series Compensation Wind Farm Connection [98].*

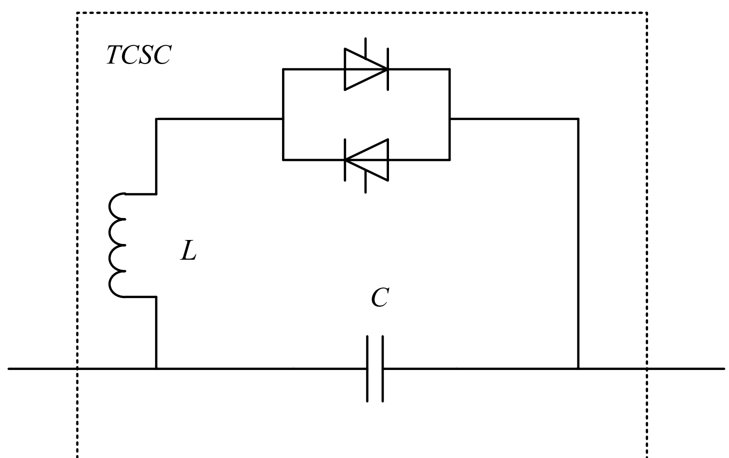


*Fig 3.44 A Thyristor-Controlled Series Compensator [98].*

From fig 3.43, it can be seen that the active power transmitted from the wind farm network to the electricity grid can be expressed as:

$$P = \frac{U_g U_W}{X_L - X_C} \sin\delta \tag{3.19}$$

Where $X_L$ is the reactance of the electric-power line, $X_C$ is the admittance of the thyristor-controlled series compensator, Ug is the voltage of the electricity grid, $U_W$ is the voltage of the wind farm, and δ is the angle between Ug and $U_W$.

Given equation (3.19), the relationship between P and δ can be plotted graphically, as depicted in fig 3.45. It is noticed that the reactance value limits the maximum power to be transmitted, and imposes a larger power angle that can results in instabilities and oscillations. But, if a thyristor-controlled series compensator is added to the system, both the total equivalent impedance of the electric-power line and the power angle can be reduced, thereby ameliorating the steady-state and the transient system behavior. This scheme might be of benefit for wind farms situated far away from the point of common coupling, such as offshore wind farms [98].

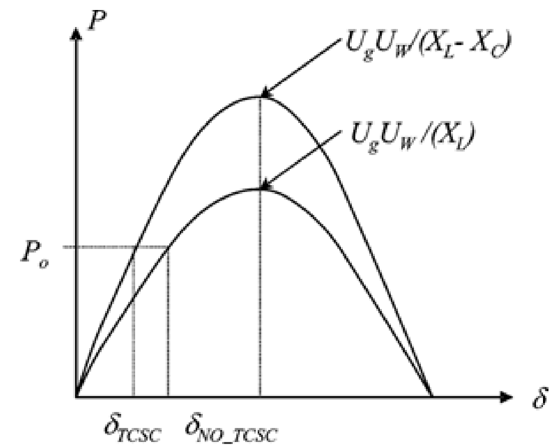


*Fig 3.45 Active power injected from the wind farm to the electricity grid [98].*

# 3.16 Economics of Wind Energy Conversion Systems

Clean and renewable power gotten from sunlight, water or wind around planet earth do not make a net contribution of carbon dioxide emission to the air. Thus, these power sources should be utilized to preserve our planet, due to global warming and the harmful consequences of carbon emissions to the environment. Hence, it would be nice to have an estimated idea of the windy and sunny fields in different places on the planet, in order to ascertain the unit cost of power output of diverse wind and solar power conversion schemes. Presently, wind power appears to be a sensible choice owing to the fact that wind power producing costs are lower than solar power costs. Besides, wind power has been experiencing extraordinary fast development for some years now due to the reason that its power producing cost has reduced. One of the very significant economic advantages of wind energy is that it reduces the subjection of our economies to fuel price volatility. This advantage is so substantial that it could effortlessly give reasons for a larger share of wind power in many countries, even though wind energy is more expensive per kWh as compared to other kinds of electric-power production methods [232], [233].

The intention of choosing any kind of power production techniques ultimately depends on its economics. Renewable energy in general and wind power in particular have experienced its production costs falling in recent years. It is estimated that wind energy in most nations is hitherto competitive with fossil fuel and nuclear energy if the social/environmental costs are being put into consideration. The total installed cost of wind power scheme includes the cost of the wind turbine, land, tower, and its accessories. The maintenance cost of wind schemes is usually very small and annual maintenance cost might be about 2% of the overall system cost. The cost of financing to acquisition of wind power system can add significantly to the total cost of wind power scheme. Additionally, there might be some hidden costs like property tax, insurance of the wind power system and any accident that might arise from the wind power system, and so on. Looking at this issue from another perspective, income from wind power system is the product of the annual power output and the per unit cost of electricity. One of the main merits of producing electricity from wind power system over traditional means is that wind is free. The bulk cost of wind power system happens once. While traditional production utilizes non-renewable fuels whose price continues to increase rapidly. Attempts are being made to reduce the cost implication of wind power by its design improvement, utilizing better technology for its manufacture, finding new suitable sites for wind power systems installation, and development of better control schemes for wind conversion systems [233], [234], [235].

# 3.17 Environmental Concerns of Wind Energy Development

The functioning of wind energy systems has zero emissions of noxious substances. It does not add-up to the cause of global warming, the fuel for wind power which is the wind is free, and is quite evenly distributed around the globe. The estimated period required to produce and install wind turbine amounts to three months. But, as with all other sources of energy, wind power also does have environmental impact. Its effect on wildlife is low as compared to both human domestic and industrial activities. Nevertheless, there is likely negative effects on certain populations of sensitive species, and attempts to mitigate these effects should be put into consideration in the planning phase. Wind power production, like any other industrial activity of human, might cause impacts on the environment which need to be analyzed and mitigated. Despite the fact that wind power plants have relatively little impact on the environment when compared to fossil fuel power plants, there is apprehension over the noise produced by the rotor blades, its visual impacts, and deaths of birds and bats that fly into the rotors during avian/bat mortality. Unlike many other power production technologies, wind power turbines do not utilize combustion to produce electricity, and therefore do not produce air emissions. The only possible toxic or hazardous materials are relatively small quantity of lubricating oils and hydraulic and insulating fluids. Hence, the pollution of surface or ground water or soils is highly unlikely. The principal health and safety concerns are connected to blade movement and the presence or existence of industrial machinery in places possibly accessible to the public. Another worry related with wind turbine systems is its possible interference with radar and telecommunication facilities. Just like all other electric-power generating amenities, wind generators do produce both electric and magnetic fields [235], [236].

When compared to the environmental impacts of conventional power sources, the environmental effects of wind energy plants are relatively minor. Wind energy utilizes no fuel, and does not emits air pollution, as do fossil fuel energy sources. The power utilized to manufacture and transport the materials utilized to build a wind energy plant is equal to the new power generated by the power plant within a few months of its operation. Hazard to birds is oftentimes the major criticism against the installation of wind turbine systems. Nonetheless, analysis have shown that the number of birds killed by wind turbines is negligible as compared to the number of birds that died as a result of other human being activities, and most especially the environmental effects of utilizing non-clean energy sources. While a wind farm might cover a large expanse of land, most land uses such as agricultural practices are compatible, with only small portions of land for turbine foundations and infrastructure is made unavailable for use. Wind power make use of no fuel for continuing functioning, and has no emissions directly linked to electricity generation. Its functioning does not produce carbon-dioxide, sulfur-dioxide, mercury, particulates, or any other kind of air pollution, as does fossil fuel energy sources. As the total number of offshore wind power farms increases and move far-away into deeper water, there comes the question if the ocean noise that is produced as a result of mechanical motion of the turbines and other vibrations which can be transmitted through the tower arrangement to the sea, will be significant enough to harm sea mammals. Tests carried out for shallow installations showed that the levels were only significant for up to a few hundred meters [237]. There is also the issue of water use, since wind power turbines do not involve thermal power generation where cooling is required, water supplies are not mandatory for their operation. Very small quantity of water might be needful in arid locations for cleaning the blades. This is negligible when compared to the water needed for cooling of traditional power plants. Landscape and Visual Impact are also environmental effects of wind energy development, they are the most usually cited impact that wind turbines have on our landscape. This visual impact can either be positive or negative, depending on the perception one viewed it. The visual impact of a wind farm is a function of the number of turbines, turbine size and design, color, and the layout of the wind conversion system or wind farm. Wind turbines can be comparable to the sizes of other human-made constructions. But, the technology is relatively new to the general public and most people are unfamiliar with its functioning. There is also the issue of Shadow Flicker. In many countries, where turbines are oftentimes situated close to communities and households, the shadow of the moving blades might be bothersome. There is the worry in some areas that the flickering of the shadow of the moving blades of wind turbines can trigger epileptic seizures. Nonetheless, photosensitivity epilepsy is very uncommon [238].

# Chapter 4

# 4 Design Basis and Models Development in this Thesis

This chapter summarizes the input data developed and used in the simulation code verification and in the integrated loads analyses presented in subsequent chapters. A large collection of input data is needed, including detailed specifications of the wind turbine and support platform, along with a design basis. Reducing the power losses and drop voltage in addition to increasing the power factor in transmission lines and distribution system is a very important issue in electrical power grid. The goals for the former could be achieved by several methods some of which is traditional like capacitors bank or synchronous condensers connected to the substation. Also, this can be achieved using new technologies which depends on renewable energy sources and power electronics.

The function for the new methodology is defined by:

$$f(losses) \vdots A_{ka}, L_{kl}, D_{kd}$$

Where:

$f(losses)$: Power losses.

$A_{ka}$: Position of sources, active and reactive power, renewable sources where $ka$ refers to the position of reactive power injection in the S.S.

$L_{kl}$: Parameters of lines and loads where $kl$ refers to the load power and line length.

$D_{kd}$: Compensation device where $kd$ refers to the type of generator and mechanism which will decrease the power losses.

This research and methodology depends on using wind farm to achieve the required goals. The background research ideas is designed as follows:

1- **Model:** Creating mathematical and simulation model for a substation system and wind farm and using different lengths for lines and loads and different positions of placement of the wind farm to study the effect of each change.
2- **Regulator:** Design a regulator depends on the parameters of the substation system to generate the required suitable reactive power from the wind farm.
3- **Results:** Applying the methodology on the model and obtaining results for voltage, active power, reactive power, voltages drop, power losses, etc for all scenarios, lengths and loads.
4- **Results after Regulation:** obtaining results for all scenarios and comparing these results with results gotten from 3.

# 4.1 Wind Farm Model

The used wind farm consists of synchronous generator which can generate reactive power and also full scale IGBT back-to-back voltage source converter so it can generate reactive power separately of active power and this allow to control the injected reactive power and voltage in wide range and easily. Fig 4.1 shows an electrical model of the wind turbine.

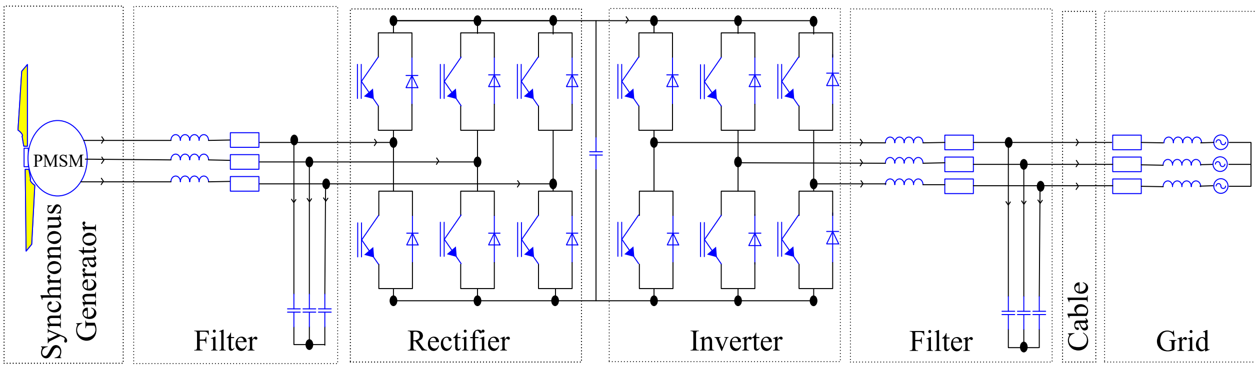


*Fig 4.1 An electrical model of the wind turbine.*

The active power is a function of the wind speed as shown in fig 4.2. The relationship between reactive power and $Q_{ref}$ is linear, where the generated reactive power is the nominal power after multiplying it by the value of $Q_{ref}$. Hence, the reactive power is a function to the value of $Q_{ref}$ as can be seen in fig 4.3.

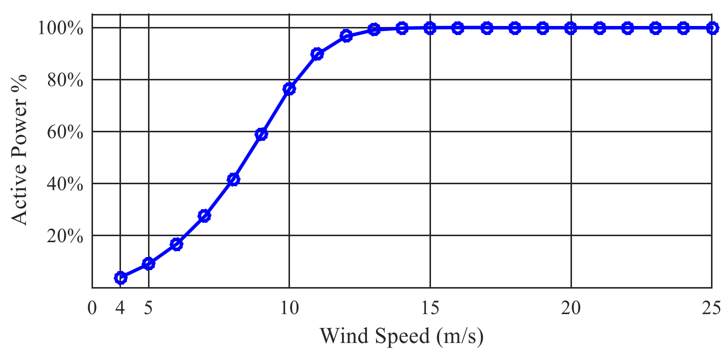


*Fig 4.2 A plot of active power against the wind speed.*

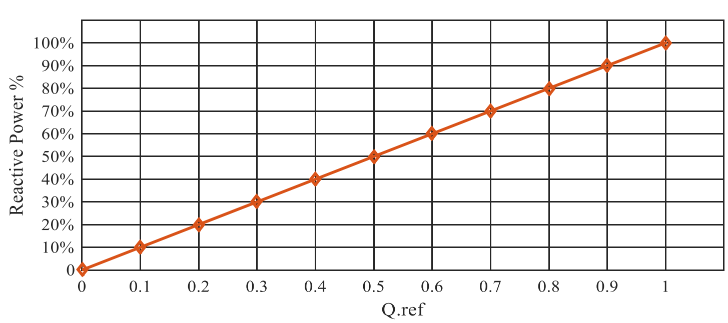


*Fig 4.3 A plot of reactive power against $Q_{ref}$*

### 4.2 Electrical Model:

Here, a simulation model and methodology for the substation system (S. $S_1$) and wind farm where an electrical system (E. S) supplies power to k distribution systems (D. S) is established and the case study will be applied on each one of them. The chosen distribution system (D. $S_1$) is a substation system (S. $S_1$) which has n loads and this research concentrate on studying the effect of using the former wind form to reduce power losses in each of the following scenarios:

1- Scenario A: wind farm OFF
2- Scenario B: wind farm connected to the bus bar which supply all transmission lines.
3- Scenario C: wind farm connected to the end of one line.
4- Scenario D: wind farm connected to the end of each transmission line.

The pictorial and schematic description of the methodology is illustrated in fig 4.4 and fig 4.5 respectively.

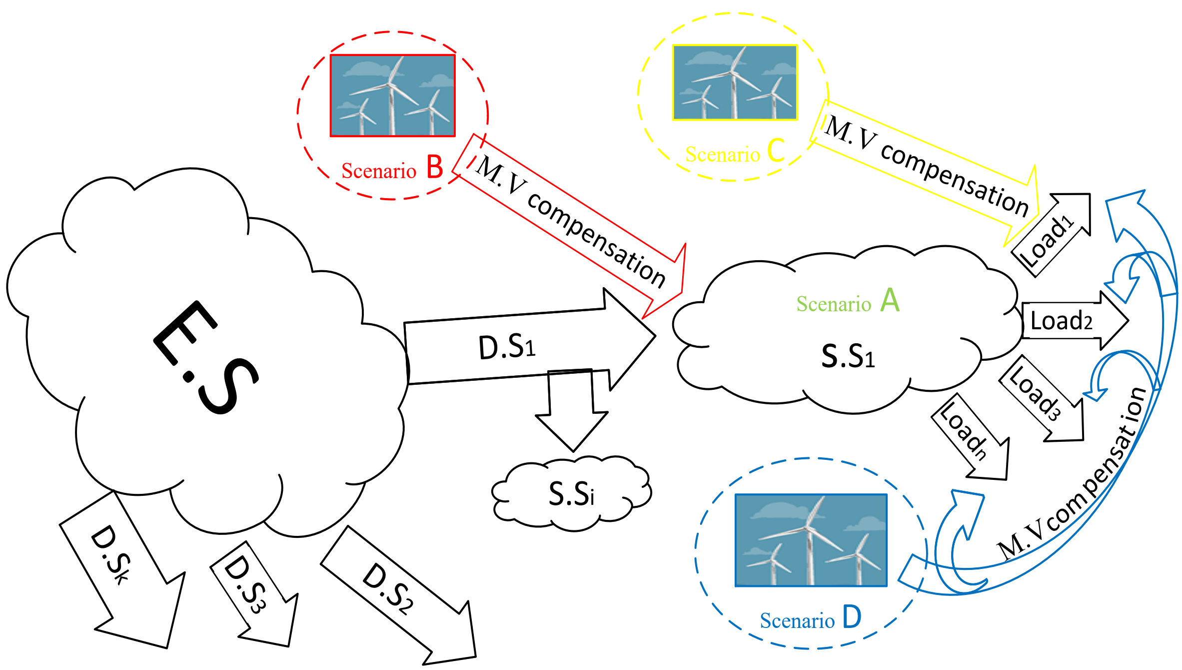


*Fig 4.4 A pictorial description of the scenarios.*

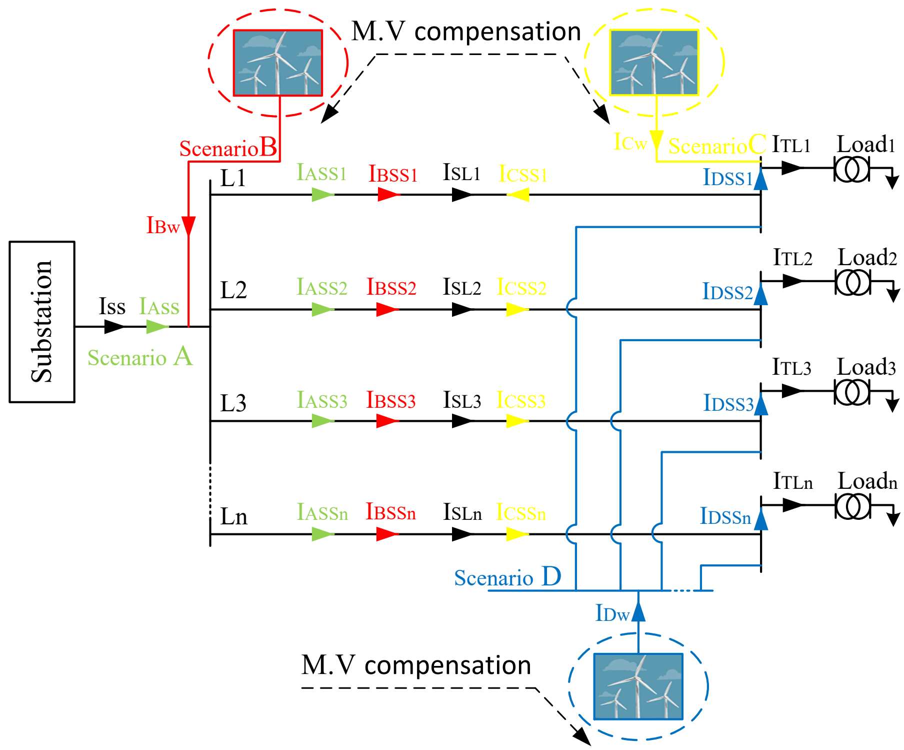


*Fig 4.5 A schematic description of the various scenarios.*

# 4.3 Mathematical Model

Considering the MV substation system (S. S1) and its vector components:

$$S_{SS} = \sum_{i=1}^{n} S_{SLi} \tag{4.1}$$

$$I_{SS} = \sum_{i=1}^{n} I_{SLi} \tag{4.2}$$

Where:

$S_{SS}$ is apparent power of the substation system.

$I_{SS}$ is total line current of the substation system.

$I_{SLi}$ is line current supplied to the n$^{th}$ number of power lines from the substation.

$S_{SLi}$ is apparent power supplied to the n$^{th}$ number of power lines from the substation.

$i = 1,2,3, \dots \dots, n.$ i.e. n$^{th}$ number of Lines

Hence, for n[th] lines that supply n[th] loads on the end of line from the MV substation, the set of transformer and load is equal to total load. Thus, the total apparent power of each n[th] number of set is $S_{TLi}$ ,where:

*i=1,2,3,……,n.* i.e. number of Loads. Therefore, Line number = each load number.

In fig 4.5:

$$P_{SLi} = \Delta P_{LLi} + P_{LTi} \tag{4.3}$$

Where:

$P_{SLi}$ is active power supplied to the n[th] number of lines.

$\Delta P_{LLi}$ is active power losses of the n[th] number of lines.

$P_{LTi}$ is active power of the n[th] number of lines.

From equation (4.3):

$$\Delta P_{LLi} = P_{SLi} - P_{LTi} \tag{4.4}$$

The power losses on the line is given by:

$$\Delta P = 3{I_L}^2 \cdot R_{1L} \tag{4.5}$$

And the difference in voltage (voltage drop) of each phase is given by:

$$\Delta V = I_L \cdot Z_L \tag{4.6}$$

considering only Scenario A, and from equation (4.5), and fig 4.5:

$$\Delta P_{LLi} = 3(I^2{}_{SLi} \cdot R_{1LLi}) \tag{4.7}$$

Therefore, power losses for n[th] number of lines for Scenario A will be:

$$\Delta P_{ALLi} = 3(I^2{}_{ASSi} \cdot R_{1LLi}) \tag{4.8}$$

Where:

$$I_{SLi} = I_{ASSi} \tag{4.9}$$

$I_{ASSi}$ is the line current for n[th] number of power lines and it is equal to $I_{SLi}$ for Scenario A.

$\Delta P_{ALLi}$ is power losses of n^th number of lines for Scenario A.

Therefore, the total losses of S. $S_1$ for Scenario A will be:

$$\Delta P_{AT} = \sum_{i=1}^{n} \Delta P_{ALLi} \tag{4.10}$$

Similarity, from equations (4.6), and (4.9), and fig 4.5:

$$\Delta V_{ALLi} = I_{ASSn} \cdot Z_{LLi} \tag{4.11}$$

Where:

$\Delta V_{ALLi}$ is the voltage drop on n^th number of lines of Scenario A.

$Z_{LLi}$ is longitudinal impedance of n^th number of lines.

considering scenario B:

The wind energy compensation strategy is connected to the bus bar which supply all transmission lines as shown in fig 4.5, applying Kirchhoff's current law:

$$I_{BSS} = I_{SS} + I_{BW} \tag{4.12}$$

Where:

$I_{BW}$ : wind farm line current

$I_{BSS}$ : total substation line current of Scenario B.

From equation (4.12) and the vector directions of the wind farm parameters in fig 4.5:

$$I_{BSSi} = I_{Sli} + I_{BWi} \tag{4.13}$$

Where:

$I_{BWi}$ is a constituent of the of wind farm line current going through n^th number of lines.

$I_{BSSi}$ is the new line current supplied to n^th number of power lines of Scenario B.

From equation (4.5), (4.12) and (4.13), the power losses for n^th number of lines of Scenario B is written as:

$$\Delta P_{BLLi} = 3({I^2}_{BSSi} \cdot R_{1LLi}) \tag{4.14}$$

$$\Delta P_{BLLi} = 3 \cdot R_{1LLi}(I^2{}_{SLi} + I^2{}_{BWi} + 2.I_{Sli}.I_{BWi}) \tag{4.15}$$

Where:

$\Delta P_{BLLi}$ is power losses for n$^{th}$ number of lines of Scenario B.

Therefore, the total losses of S. $S_1$ for Scenario B will be:

$$\Delta P_{BT} = \sum_{i=1}^{n} \Delta P_{BLLi} \tag{4.16}$$

Similarity, from equations (4.6), (4.12), and (4.13), and fig 4.5:

$$\Delta V_{BLLi} = I_{BSSi} \cdot Z_{LLi} \tag{4.17}$$

$$\Delta V_{BLLi} = (I_{SLi} + I_{BWi}) \cdot Z_{LLi} \tag{4.18}$$

Where:

$\Delta V_{BLLi}$ is the voltage drop of n$^{th}$ number of lines of Scenario B.

considering scenario C:

The wind energy compensation strategy is connected to the to the end of line number 1 where the direction of power flow will change in line number 1 as shown in fig 4.5, applying Kirchhoff's current law:

$$I_{CSS1} = I_{CW1} = I_{CW} - I_{TL1} \tag{4.19}$$

Where:

$I_{CW}$ : the total current of wind farm

$I_{CW1}, I_{CSS1}$ : the new current for the transmission line number 1 in scenario C

From equation (4.9) and (4.19):

$$I_{CSS1} = I_{CW1} = I_{CW} - I_{SL1} \tag{4.20}$$

Also, applying Kirchhoff's current law for n line:

$$I_{CSSi} = I_{Sli} + I_{CWi} \tag{4.21}$$

Where:

$i = 2,3, \dots \dots , n.$ : Line number.

$I_{CSSi}$ : the new current for the transmission line number n in scenario C

$I_{CWi}$ : is a constituent of the of wind farm line current going through line number n.

From equation (4.19), (4.20) and (4.21), the power losses for line number 1 and n[th] number of lines of Scenario C is written as:

$$\Delta P_{CLL1} = 3((I_{CW} - I_{SL1})^2 \cdot R_{LL1}) \tag{4.22}$$

$$\Delta P_{CLL1} = 3(I^2{}_{CSS1} \cdot R_{LL1}) \tag{4.23}$$

$$\Delta P_{CLLi} = 3((I_{Sli} + I_{CWi})^2 \cdot R_{LLi}) \tag{4.24}$$

$$\Delta P_{CLLi} = 3(I^2{}_{CSSi} \cdot R_{LLi}) \tag{4.25}$$

Where:

$\Delta P_{CLL1}$: the power losses for line number 1 in Case C.

$\Delta P_{CLLi}$ : the power losses for power losses for n$^{th}$ number of lines of Scenario C.

Therefore, the total losses of S. $S_1$ for Scenario C will be:

$$\Delta P_{CT} = \sum_{i=1}^{n} \Delta P_{CLLi} \tag{4.26}$$

Similarity, from equations (4.6), (4.20) and (4.21), and fig 4.5:

$$\Delta V_{CLL1} = I_{CSS1} \cdot Z_{LL1} \tag{4.27}$$

$$\Delta V_{CLLi} = I_{CSSi} \cdot Z_{LLi} \tag{4.28}$$

Where:

$\Delta V_{CLL1}$ is the difference in voltage drop of line number 1 of Scenario C.

$\Delta V_{CLLi}$ : is the voltage drop of n$^{th}$ number of lines of Scenario C.

$i = 2,3, \dots \dots , n.$ : Line number.

considering scenario D:
The wind energy compensation strategy is connected to the to the end of each line as shown in fig 4.5, applying Kirchhoff's current law:

$$I_{TLi} = I_{DWi} + I_{DSSi} \tag{4.29}$$

From equations (4.9) and (4.29):

$$I_{SLi} = I_{DWi} + I_{DSSi} \tag{4.30}$$

Therefore:

$$I_{DSSi} = I_{SLi} - I_{DWi} \tag{4.31}$$

Where:

$i = 1,2,3, \dots \dots, n.$ : Line number.

$I_{DSSi}$ : the new current for the transmission line number n in scenario D

$I_{DWi}$ : is a constituent of the of wind farm line current going through line number n in scenario D

From equations (4.5) and (4.31) the power losses for $n^{th}$ number of lines of Scenario D is written as:

$$\Delta P_{DLLi} = 3((I_{SLi} - I_{DWi})^2 \cdot R_{LLi}) \tag{4.32}$$

$$\Delta P_{DLLi} = 3(I^2{}_{DSSi} \cdot R_{LLi}) \tag{4.33}$$

Where:

$\Delta P_{DLLi}$ : the power losses for $n^{th}$ number of lines of Scenario D.

Therefore, the total losses of S. $S_1$ for Scenario D will be:

$$\Delta P_{DT} = \sum_{i=1}^{n} \Delta P_{DLLi} \tag{4.34}$$

Similarity, from equations (4.6) and (4.31), and fig 4.5:

$$\Delta V_{DLLi} = I_{DSSi} \cdot Z_{LLi} \tag{4.35}$$

Where: $\Delta V_{DLLi}$ : is the voltage drop of $n^{th}$ number of lines of Scenario D.

$i = 1,2,3, \dots \dots, n.$ : Line number.

# 4.4 Scenarios, Cases and Lengths

Changing the position of reactive power injection, reactive power of loads and transmission lines lengths is very important to analyze wind farm effects and its ability to supply the required reactive power and reducing losses and voltage drop in addition to maintain the voltage in the allowed limits. Increasing the reactive power of loads must coincides with increasing the $Q_{ref}$ of wind farm to condense the reactive power and the value of $Q_{ref}$ can be calculated by the following equation which convert the increase of reactive power of loads. The increase calculated comparable to basic state of each load:

$$Q_{ref} = \frac{Q_{L1}\,\% * Q_{L1} + Q_{L1}\,\% * Q_{L1} + \cdots + Q_{Li}\,\% * Q_{Li}}{Q_{Twind}} = Q_L\,\% * K \tag{4.36}$$

Where:

$Q_{Li}\,\%$ : increase percentage of reactive power of load number i.

$Q_{Li}$ : basic reactive power of load number i.

$i = 1,2,3, \dots \dots, n.$ : Line number.

$Q_{Twind}$ : total reactive power of wind farm.

$K$ : wind farm constant

Therefore, the scenarios which had been mentioned will apply in different cases of reactive power as illustrated in table 4.1 and 4.2:

*Table 4.1 Cases for scenario A*

| Step | Rate increase $Q_L$ % | Wind Farm Mode |
|---|---|---|
| 1 | 0% | OFF |
| 2 | 33.33% | OFF |
| 3 | 66.66% | OFF |
| 4 | 100% | OFF |
| 5 | 133.33% | OFF |

*Table 4.2 Cases for scenario B, C and D*

| Step | Rate increase $Q_L$ % | Wind Farm Mode | $Q_{ref}$ (p.u.) |
|---|---|---|---|
| 1 | 0% | ON | $0\% * K$ |
| 2 | 33.33% | ON | $33.33\% * K$ |
| 3 | 66.66% | ON | $66.66\% * K$ |
| 4 | 100% | ON | $100\% * K$ |
| 5 | 133.33% | ON | $133.33\% * K$ |

# 4.5 Regulator Model

The regulator can depend on different methods and parameters from the substation system. It can depend on reactive power values for example or the daily energy demand curve. In this research the regulator will depend or sending and receiving voltage in addition to voltage drop for the transmission lines. In the regulator following equations will be used for all scenarios:

1- Voltage drop:

A- Positive voltage drop: that means the sending voltage is higher than receiving voltage. the maximum allowable drop in voltage for MV transmission lines is limited to 10% of the sending end bus voltage therefore:

$$\text{If } \Delta V_{allowed} \geq \Delta V \geq 0 \Longrightarrow$$

$$1 \geq \frac{\Delta V}{\Delta V_{allowed}} \geq 0 \Rightarrow$$

$$1 \geq Value_{i1} \geq 0$$

$$\text{Else } \Delta V > \Delta V_{allowed} \Longrightarrow$$

$$Value_{i1} > 1$$

When $Value_{i1} > 1$ that means voltage drop exceed the limits so this value will increase the total value to increase the generated reactive power.
Where:

$\Delta V_{allowed}$ : allowed voltage drop for the transmission line.

$\Delta V$ : measured voltage drop.

$Value_{i1}$ : the generated value number 1 from this part of regulator for line i.

B- Negative voltage drop: that means the sending voltage is lower than receiving voltage. therefore:

$$\text{If } \Delta V_{allowed} \geq |\Delta V| \geq 0 \Longrightarrow$$

$$0 \geq |\Delta V| - \Delta V_{allowed} \geq -\Delta V_{allowed} \Rightarrow$$

$$0 \leq \frac{\Delta V_{allowed} - |\Delta V|}{\Delta V_{allowed}} \leq 1$$

$$1 \geq Value_{i1} \geq 0$$

$$\text{Else } |\Delta V| > \Delta V_{allowed} \Longrightarrow$$

$$Value_{i1} < 0$$

When $Value_{i1} < 0$ that means, voltage drop exceed the limits but in reserve position (receiving voltage bigger than sending voltage) so this value will decrease the total value to decrease the generated reactive power.

2- Sending voltage: the changes in sending voltage should not exceed $\pm 10\%$ therefore:

$$\text{If} \quad 0.9V_{system} \leq V_{Sm} \leq 1.1V_{system} \Longrightarrow$$

$$-0.9V_{system} \geq -V_{Sm} \geq -1.1V_{system} \Longrightarrow$$

$$0.2V_{system} \geq 1.1V_{system} - V_{Sm} \geq 0 \Longrightarrow$$

$$1 \geq \frac{1.1V_{system} - V_{Sm}}{0.2V_{system}} \geq 0 \Longrightarrow$$

$$1 \geq Value_{i2} \geq 0$$

$$\text{Else if} \quad V_{Sm} > 1.1V_{system} \Longrightarrow$$

$$Value_{i2} < 0$$

When $Value_{i2} < 0$ that means sending voltage is very high and exceed the limits so this value will decrease the total value to decrease the generated reactive power.

$$\text{Else} \quad V_{Sm} < 0.9V_{system} \Longrightarrow$$

$$Value_{i2} > 1$$

When $Value_{i2} > 1$ that means sending voltage is very low so this value will increase the total value to increase the generated reactive power.

Where:

$V_{system}$ : nominal voltage of the MV substation system.

$V_{Sm}$ : measured value of sending voltage.

$Value_{i2}$: the generated value number 2 from this part of regulator for line i.

3- Receiving voltage: the changes in receiving voltages should not exceed $\pm 10\%$ therefore:

$$\text{If} \quad 0.9V_{system} \leq V_{Rm} \leq 1.1V_{system} \Longrightarrow$$

$$-0.9V_{system} \geq -V_{Rm} \geq -1.1V_{system} \Longrightarrow$$

$$0.2V_{system} \geq 1.1V_{system} - V_{Rm} \geq 0 \Longrightarrow$$

$$1 \geq \frac{1.1V_{system} - V_{Rm}}{0.2V_{system}} \geq 0 \Longrightarrow$$

$$1 \geq Value_{i3} \geq 0$$

$$\text{Else if} \quad V_{Rm} > 1.1V_{system} \Longrightarrow$$

$$Value_{i3} < 0$$

When $Value_{i3} < 0$ that means receiving voltage is very high and exceed the limits so this value will decrease the total value to decrease the generated reactive power.

$$\text{Else} \quad V_{Rm} < 0.9V_{system} \Longrightarrow$$

$$Value_{i3} > 1$$

When $Value_{i3} > 1$ that means receiving voltage is very low so this value will increase the total value to increase the generated reactive power.

Where:

$V_{system}$ : nominal voltage of the MV substation system.

$V_{Rm}$ : measured value of receiving voltage.

$Value_{i3}$ : the generated value number 3 from this part of regulator for line i.

4- Generated value of the regulator: this value is the $Q_{ref}$ value which will cause to generate the suitable reactive power for the MV substation system therefore the generated value for each line is:

$$Q_i = \frac{(Value_{i1} + Value_{i2} + Value_{i3})}{3} \tag{4.37}$$

And total value will be:

$$Q_{ref} = \frac{Q_1 + Q_2 + \cdots + Q_n}{n} \tag{4.38}$$

Where:

$Q_i$ : generated value of line i.

$i = 1,2,3, \dots \dots, n.$: Line number.

And the following algorithm describe the regulator for 1 line as shown in fig 4.6.

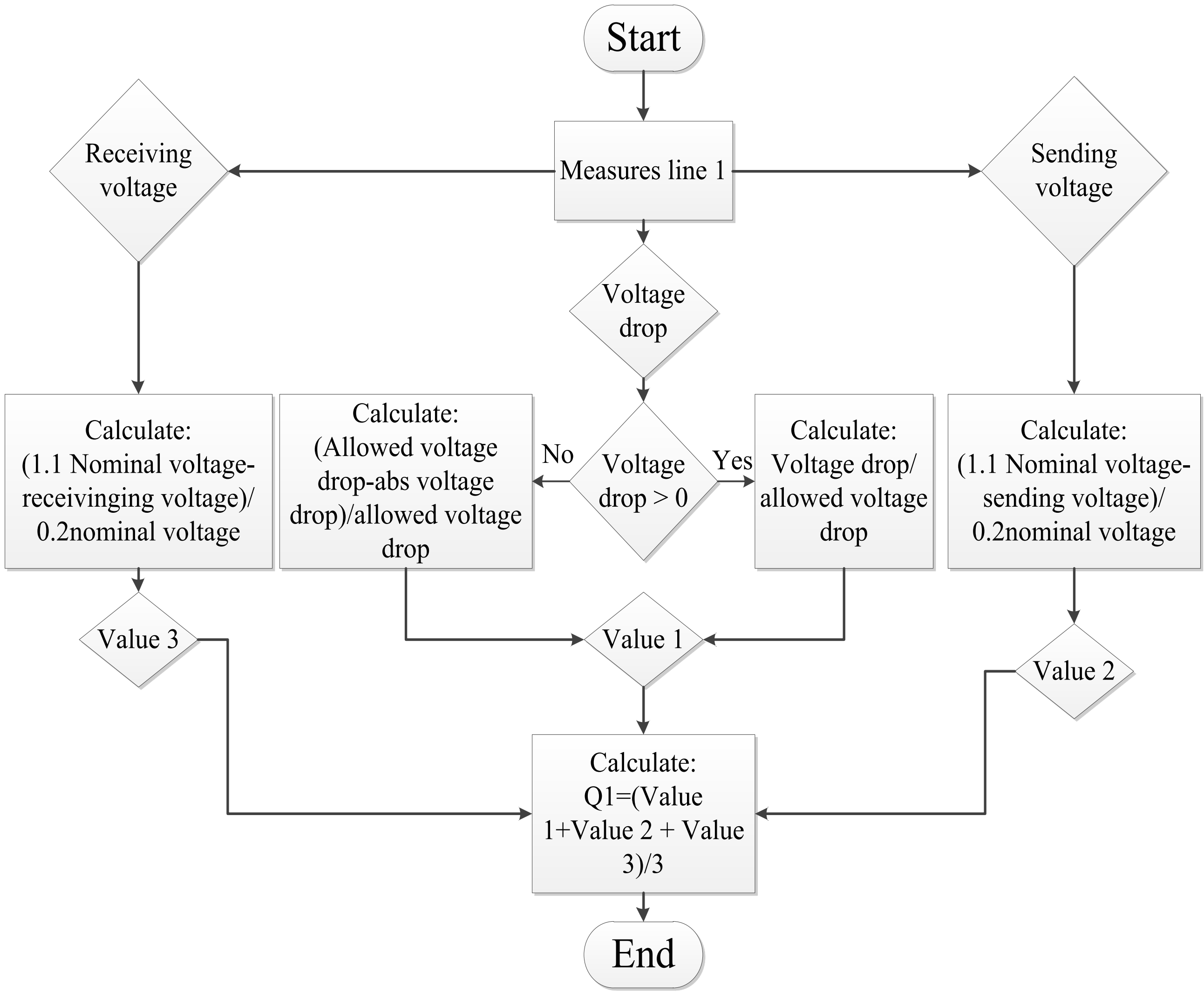


*Fig 4.6 The algorithm developed for the regulator considering 1 line*

And the following algorithm for n lines is developed as represented in fig 4.7.

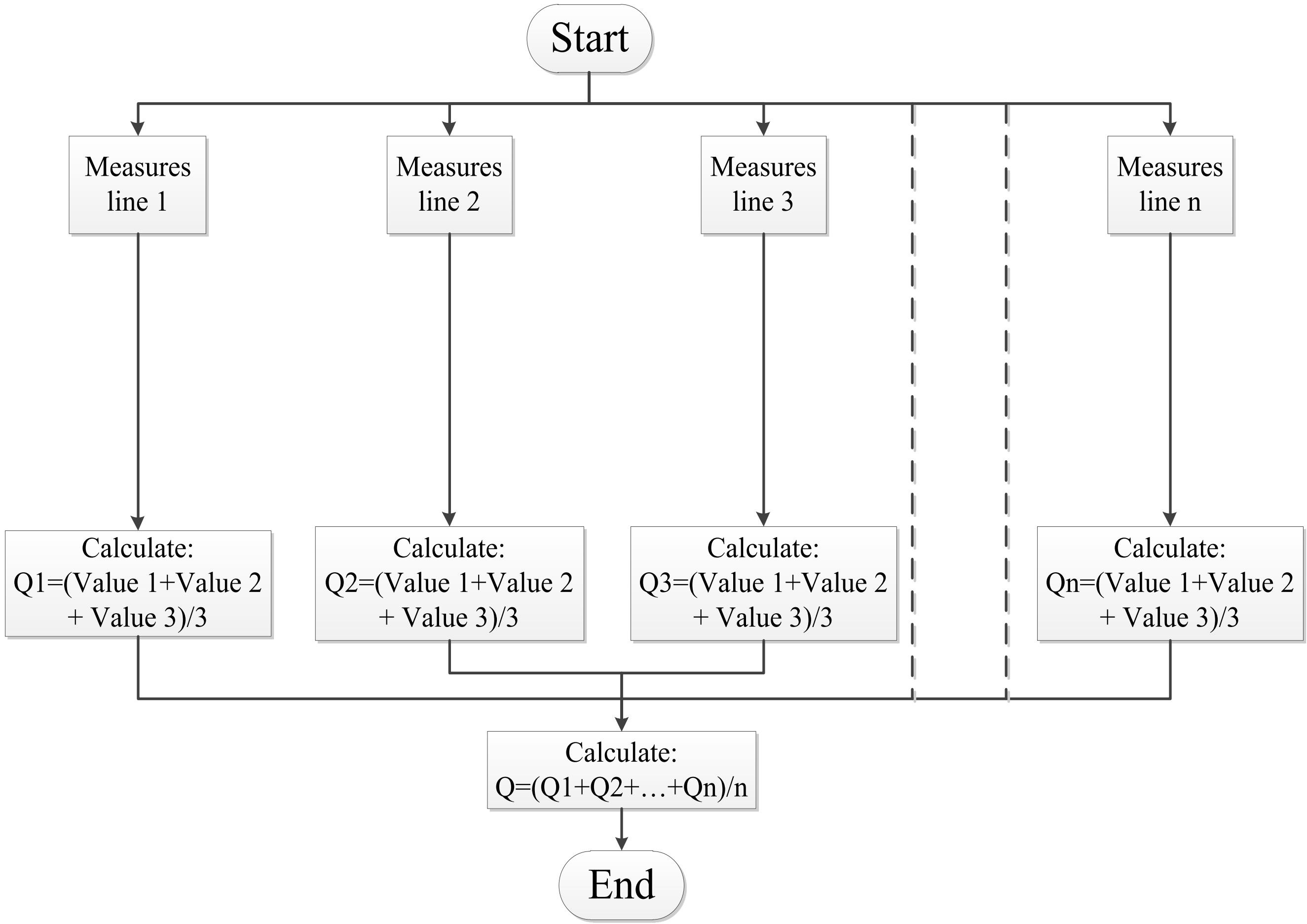


*Fig 4.7 The algorithm developed for the regulator considering nth number of lines.*

# Chapter 5

# 5 Case Studies and Simulations: Loads Analysis Overview, Description, Results and Discussion

## 5.1 The Benchmark Commercial Electric-Power Generation System

This part discusses a typical scheme of the commercial electric-power generation system. this is chosen as a benchmark system against which to generate a simulation scheme of the commercial electric-power system. Fig 5.1 illustrates the electrical installation network of the electric-power generation system showing the major system components. The network consists of a 90 MVA sub-transmission station connected with a 3-phase 3-line 66 kV power line, each of the line is a 3-phase system of varying lengths on which the same installed load capacity of 20.88 MVA is powered via a 66/20 kV transformer. The length of each of the MV power lines,$L_1$, $L_2$ and $L_3$ are 50km, 55km and 60km respectively. The benchmark electrical network is shown in fig 5.1.

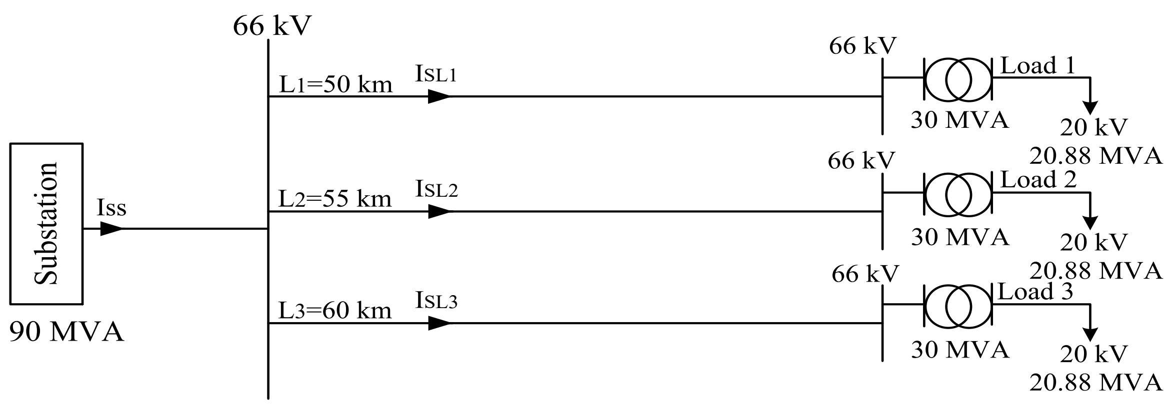


*Fig 5.1 The benchmark commercial electrical network*

*Table 5.1 Parameters of the MV commercial electrical power lines*

| Line number | 1 | 2 | 3 |
|---|---|---|---|
| Positive resistances $r_1$(Ω/km) | 0.1153 | 0.1153 | 0.1153 |
| Zero-sequence resistances $r_0$ (Ω/km) | 0.413 | 0.413 | 0.413 |
| Positive inductances $l_1$ (mH/km) | 1.05 | 1.05 | 1.05 |
| zero-sequence inductances $l_0$(mH/km) | 3.32 | 3.32 | 3.32 |
| Positive capacitances $c_1$ (nF/km) | 11.33 | 11.33 | 11.33 |
| zero-sequence capacitances $c_0$ (nF/km) | 5.01 | 5.01 | 5.01 |

| | | | |
|---|---|---|---|
| Frequency $f_n$ (Hz) | 50 | 50 | 50 |
| Length (km) | 50 | 55 | 60 |
| Phase resistance $R_1$ (Ω) | 5.7650 | 6.3415 | 6.9180 |
| Phase Inductive reactance $X_1$ (Ω) | 16.493 | 18.143 | 19.720 |
| Phase susceptance $B$ (μS) | 1.7798 | 1.9576 | 2.1356 |

*Table 5.2 Parameters of the three-phase 66/20 kV transformers*

| TRANSFORMER 1,2,3 | Low voltage winding | high voltage winding |
|---|---|---|
| Connection type | D11 | Yg |
| $V_{rms}$(kV) | 66 | 20 |
| $R$ (Ω) | 0.6534 | 0.0200 |
| $L$ (H) | 0.0831930 | 0.0025465 |
| Frequency $f_n$ (Hz) | 50 | |
| Nominal Power $S_n$ (MVA) | 30 | |
| Magnetization resistance $R_m$ (MΩ) | 0.2178 | |
| Magnetization inductance $L_m$ (H) | 693.28 | |

Table 5.1 and 5.2 shows the parameters of the MV commercial electrical power lines and parameters of the three-phase 66/20 kV transformers respectively. The load parameters of each three phase series loads were measured and tabulated in Table 5.3. Also, measurements of sending and receiving power (i.e. power losses) and voltage (i.e. voltage drops) for line 1, 2, and 3, are taken, this is shown in Table 5.4.

*Table 5.3 Measured values of the three-phase series loads*

| parameters Load 1,2,3 | |
|---|---|
| Active Power $P_L$ (MW) | 20 |
| Reactive Power $Q_L$ (MVAr) | 6 |
| Apparent Power $S_L$ (MVA) | 20.88 |
| P.F $\cos(\varphi_L)$ | 0.957 |
| Frequency $f_n$ (Hz) | 50 |
| consumer's voltage (kV) | 18.98 |

*Table 5.4 Measured parameters of the benchmark commercial three-phase lines*

| Line | $P_s$ (MW) | $P_r$ (MW) | $Q_s$ (MVAr) | $Q_r$ (MVAr) | $U_s$ (kV) | $U_r$ (kV) | $\Delta P$ (MW) |
|---|---|---|---|---|---|---|---|
| 1 | 16.89 | 16.45 | 7.11 | 6.41 | 64.67 | 61.38 | 0.44 |
| 2 | 16.78 | 16.26 | 7.08 | 6.33 | 64.67 | 61.09 | 0.52 |
| 3 | 16.66 | 16.09 | 7.02 | 6.27 | 64.67 | 60.87 | 0.57 |

## 5.2 Simulation Scheme of the Commercial System Without Wind Farm (Case A) and With Wind Farm (Cases B, C, D)

To create a simulation scheme with the proposed methodology, we carried out simulation of the commercial system without wind farm (Case A) and with wind farm (Cases B, C, D) as can be seen in fig 5.2. The wind farm is made up of three wind turbines, rated at 3 ×10=30 MW, 3×10/0.9 = 33.33 MVA, 66 kV. In creating Case A from Scenario A, the reactive loads were increased (i.e. apparent power is increased) in steps of 5, step 1 is when the commercial Case is switched off, while for steps 1 to 5 the wind farm was switched off as depicted in Table 5.5 And Cases B , C, D are created from scenarios B,C and D with the reactive load being increased in % values as presented in Table 5.6 Cases B, C and D can be likened to case A, only that the wind farm is switched ON from step 1 to step 5, also the values of $Q_{ref}$ is varied from step 1 to step 5 in order to produce reactive power from the wind farm according to the usage of reactive power by the load. For Cases B, C, D the reactive power is produced according to $Q_{ref}$ and the wind speed with relation to the active power was measured and presented in table 5.6. Note that before making use of the regulator, the various cases are designated as Case B, C and D. But after making use of the regulator, it is then designated as Case B Reg., C Reg. and D Reg. respectively. The MATLAB/Simulink graphics screen layout blocks on PC monitor system with all parts including regulator is presented in fig 5.3 and for the regulator is shown in fig 9.1, an A3 page attachment in the appendix.

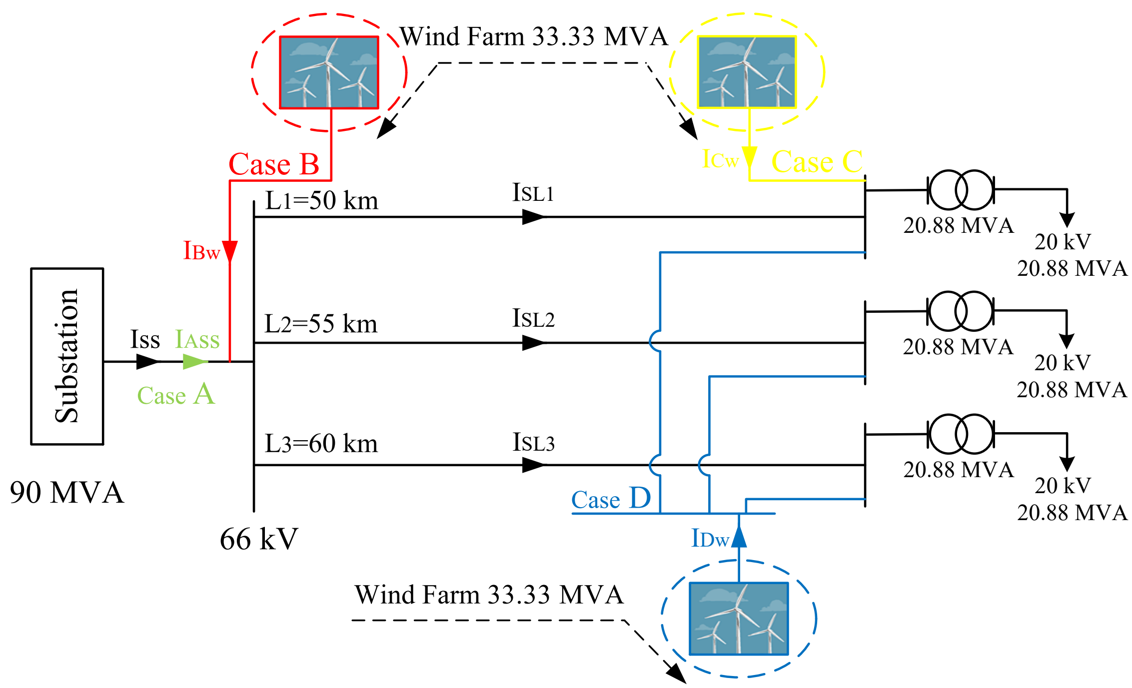


*Fig 5.2 Scheme of the proposed commercial (Case A) and wind farm (Cases B,C,D) simulation network*

*Table 5.5 Calculated values of reactive, active and apparent power for various steps of Case A*

| Step | Rate increase % $Q$ | Reactive Load $Q$ (MVAr) | Active Load $P$(MW) | Apparent Load$S$( MVA) | Rate increase % $S$ | Wind Farm Mode | Case |
|---|---|---|---|---|---|---|---|
| 1 | 0% | 6 | 20 | 20.880 | 0 % | OFF | A |
| 2 | 33% | 8 | 20 | 21.540 | 3 % | OFF | |
| 3 | 66% | 10 | 20 | 22.360 | 7% | OFF | |
| 4 | 100% | 12 | 20 | 23.324 | 12% | OFF | |
| 5 | 133% | 14 | 20 | 24.413 | 17% | OFF | |

*Table 5.6 Calculated values of reactive, active and apparent power for steps of Cases B,C,D*

| Step | Rate increase % $Q_L$ | Reactive Load $Q_L$(MVAr) | Active Load $P$(MW) | Apparent Load $S$(MVA) | Rate increase % $S$ | Wind Farm Mode | $Q_{ref}$ (p.u.) | Cases |
|---|---|---|---|---|---|---|---|---|
| 1 | 0% | 6 | 20 | 20.880 | 0 % | OFF | 0 | B |
| 2 | 33% | 8 | 20 | 21.540 | 3% | ON | 0.207 | C |
| 3 | 66% | 10 | 20 | 22.360 | 7% | ON | 0.387 | |
| 4 | 100% | 12 | 20 | 23.324 | 12% | ON | 0.567 | |
| 5 | 133% | 14 | 20 | 24.413 | 17% | ON | 0.747 | D |

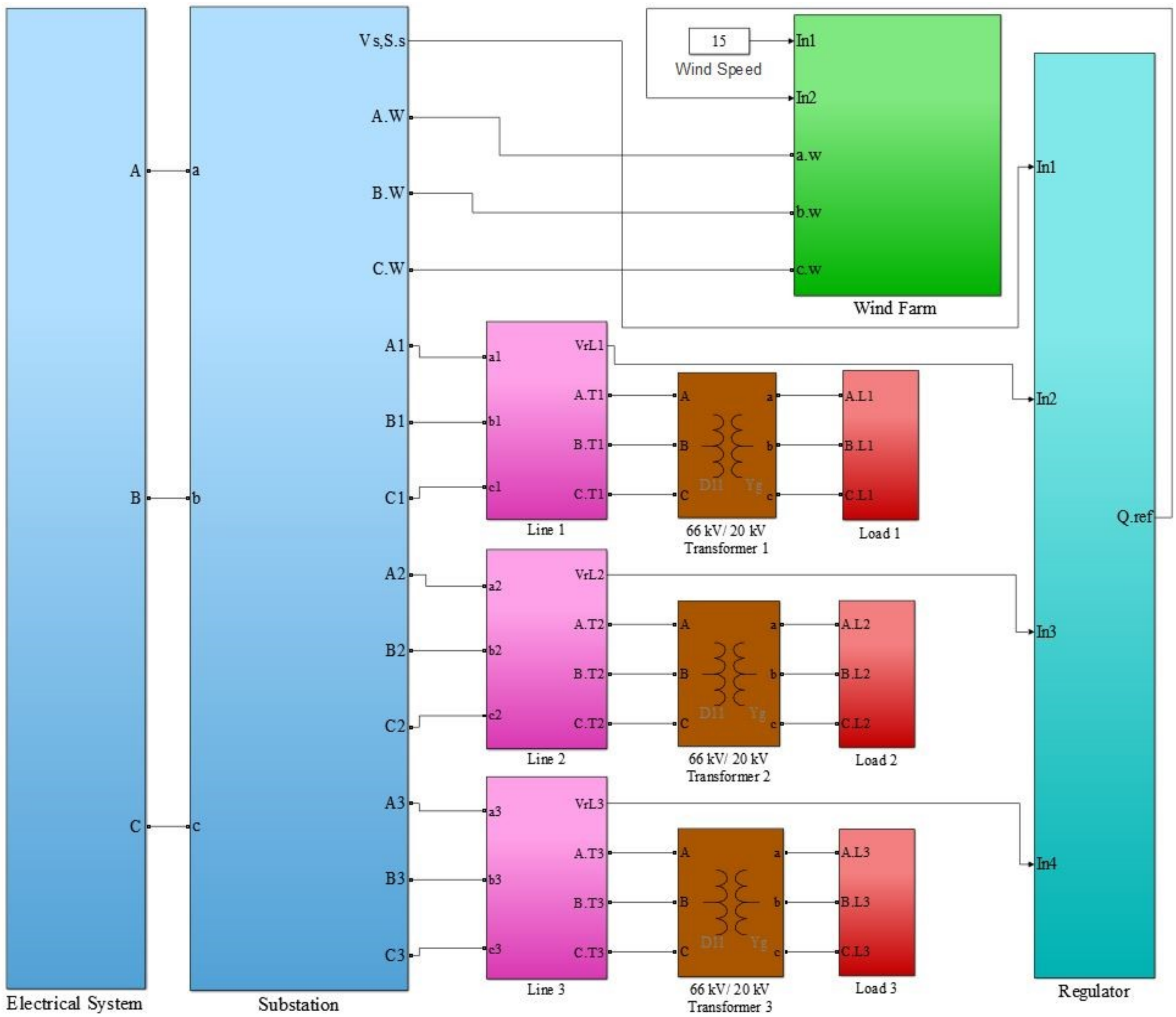


*Fig 5.3 MATLAB/Simulink graphics screen layout of the wind farm scheme on PC monitor system*

# 5.3 Case Study Without Regulator

## 5.3.1 The Wind Farm Without Regulator

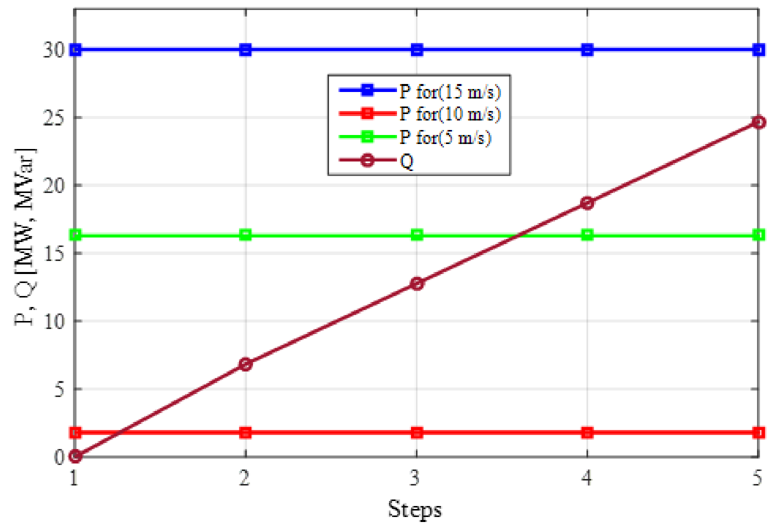


*Fig 5.4 Active and reactive power values of the wind farm for all steps and wind speeds (5, 10 and 15 m/s) without regulator.*

Fig 5.4 shows changes of active and reactive power in all cases. Here, the chosen wind farm can generate reactive power independently of the active power, when the wind speed is 5 m/s, the generated active power is 1.8 MW and for 10 m/s it is 16.3 MW and for 15 m/s it is 30 MW. These values are constant for all steps observed. The generated reactive power increased in linear gradients for each step from 0 MVar for step 1 to about 25 MVAr in step 5. Only active power is actually usable power, reactive power cannot be consumed and can therefore not power any electrical devices. It simply moves back and forth in the grid and thereby acts as an additional load. For this reason all cables, switches, transformers, and other parts of the simulation scheme of this thesis need to additionally consider reactive power. Hence, were designed for apparent power, the geometric sum of active and reactive power. The ohmic losses during energy conduction occur based on apparent power; additional reactive power therefore leads to greater conduction losses.

### 5.3.2 Sending and Receiving Voltage and Voltage Drop

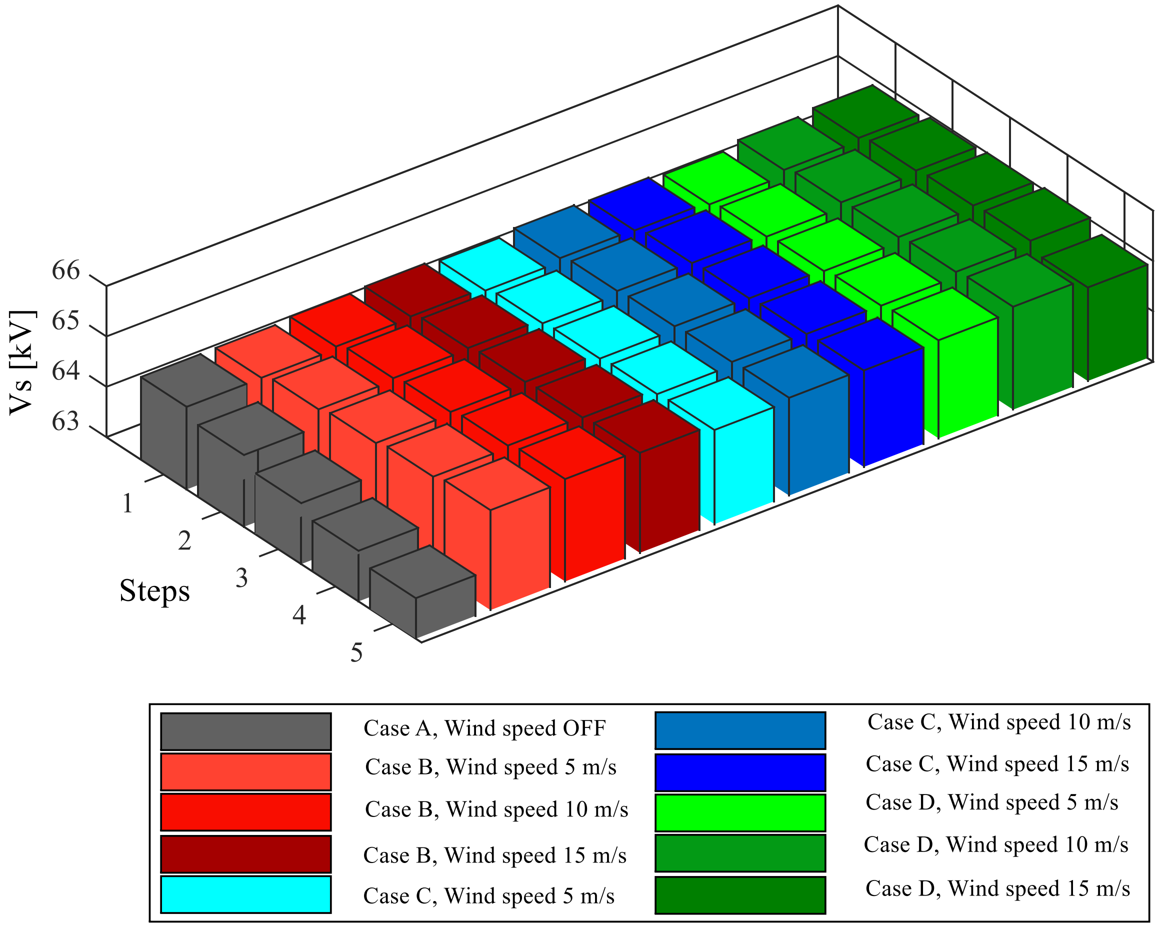


*Fig 5.5 Sending voltage in Cases A, B, C and D for wind speeds 5, 10, and 15 m/s without regulator.*

Fig 5.5 shows that sending voltage in cases B, C and D (with wind farm) is higher than observed in case A. In addition, the effects of increasing reactive power of loads (steps) is very little in Cases B, C and D as compared to case A. The figure also illustrates that the influence of increasing the wind speed is not remarkable. Wind turbines extract kinetic power from the air around them, and since less power makes for weaker winds, turbines do indeed make it less windy. Technically speaking, the climate zone right behind a turbine or rather behind all the turbines on a wind farm experiences what is called a "wind speed vacuum," or a "momentum deficit." This is to say that; the air slows down. The effect has implications for wind farm efficiency. Upwind turbines in a densely-packed farm may weaken the breeze before it reaches the downwind ones. It could even have a more general impact. If wind farms were constructed on a truly massive scale, their cumulative momentum deficit could conceivably alter wind speeds on a global scale, though how winds would change is complex, they do likely slow in places and speed up in others.

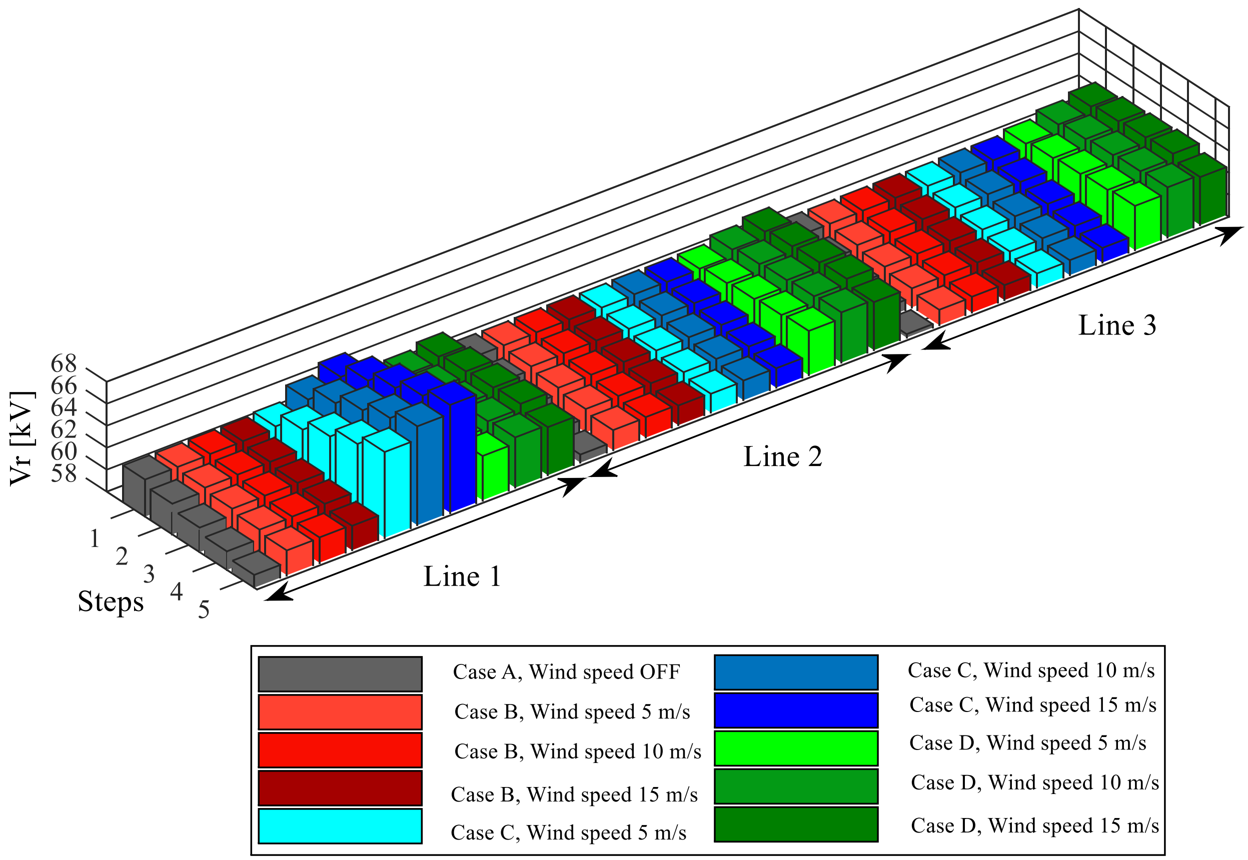


*Fig 5.6 Receiving Voltage in Cases A, B, C and D for wind speeds 5, 10, and 15 m/s without regulator for 3 different lengths lines.*

Also, fig 5.6 shows that the receiving voltage in cases B, C and D (with wind farm) is higher than it is in case A but with Case D (when the wind farm is connected to the end of all lines) is adjudged the best case since the voltage for all lines is more stable and it has the same value for all the lines and in general the voltage profile is higher when compared to other cases. In Case C the voltage of line 1 is extremely higher than other lines or cases because of the high reactive power injected to line 1. The influence of increasing wind speed is remarkable in case D and line 1 of case C where increasing the wind speed increase the voltage gradually. Also, the difference of lines lengths had effect on the voltage, increasing the lines length will increase the voltage drop for each line except for Case D, since the wind farm is connected to the end of all lines so the receiving voltage of all of them is the same. Any conducting wire has a resistance associated with it and the resistivity of the material is directly proportional to the length of the wire and inversely proportional to the area of the cross section of the wire. Although this does not have a greater impact, they do affect the voltage across it and thereby the current.

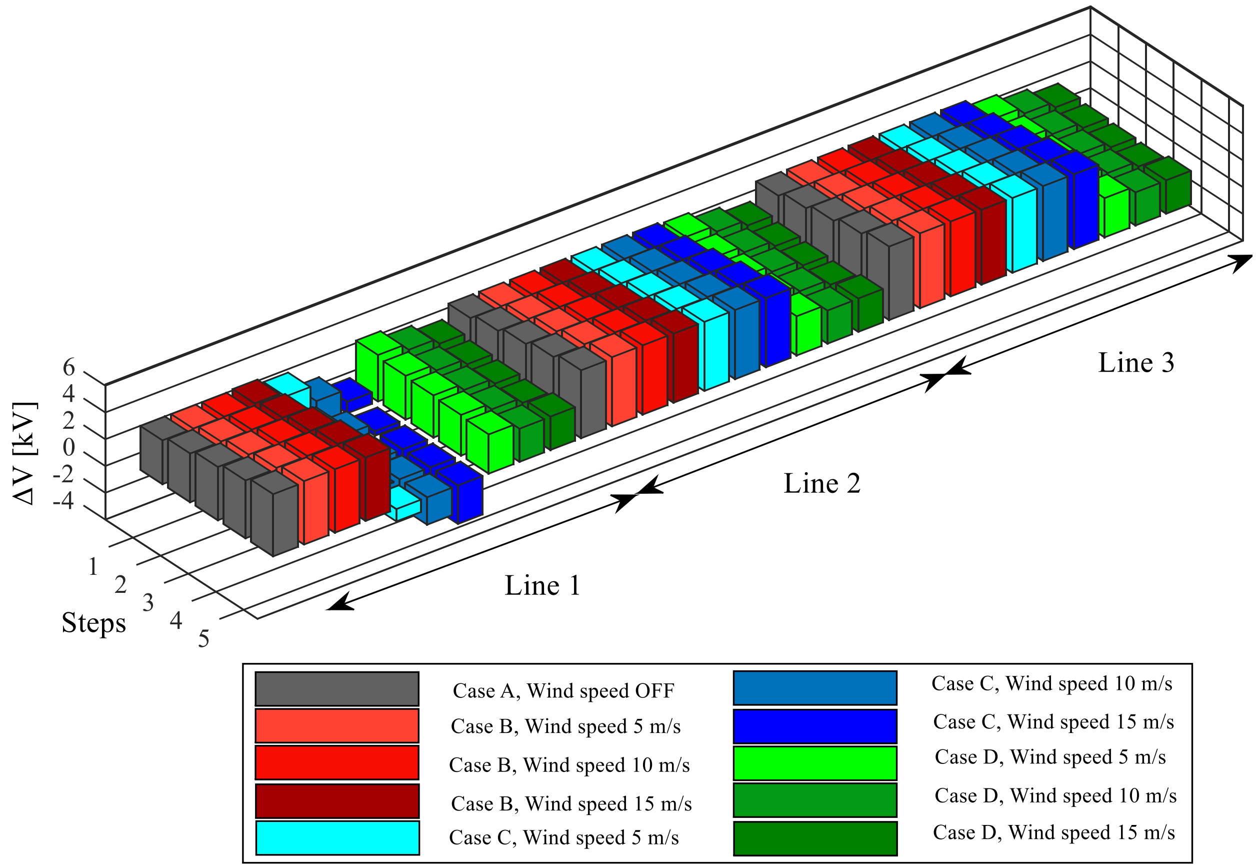


*Fig 5.7 Voltage drop in Cases A, B, C and D for wind speeds 5, 10, and 15 m/s without regulator for 3 different lengths lines.*

Fig 5.7 illustrates the changes in voltage drop, it could be noticed that voltage drop decrease only in case D and line 1 of case C. In other cases, the voltage drop increased in a little value because of increase in the sending voltage for these cases which brought about increase in power flow of all lines and slight increase in voltage drop. The small voltage value for speed 5 m/s and negative voltage value for speeds 10 and 15 m/s for line 1 of case C is as a result of the high reactive and active power injected on this line whose causes has been mentioned in fig 5.6 due to extreme increase in receiving voltage. The effect of increasing wind speed is remarkable only in case D and line 1 of case C, increasing the wind speed increases the generated active power. Therefore, as the power flow decreases on the lines, the voltage drop gradually decreases. Also, the difference of lines lengths affects the voltage drop, as increase in the length of line increases the impedance and hence the voltage drop increases except for Case D and line 1 of Case C as a result of the reasons already mentioned in fig 5.6.

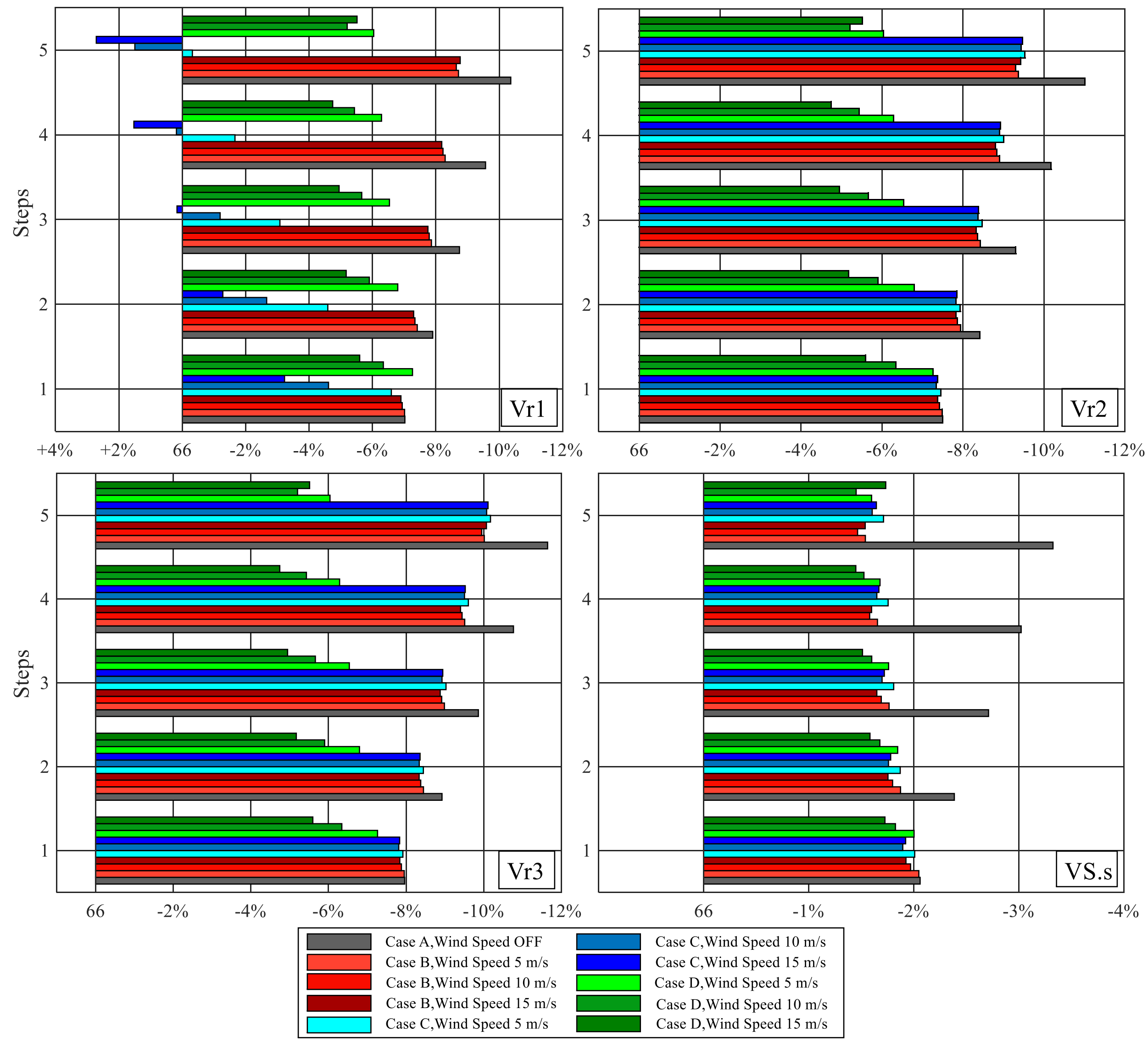


*Fig 5.8 Percentage of sending and receiving voltage in Cases A, B, C and D for wind speeds 5, 10, and 15 m/s without regulator to the nominal S.S voltage (66 kV).*

The values previously generated were converted to percent values by calculating the sending and receiving voltage as a percentage of the nominal voltage of S.S (66 kV) and by calculating the voltage drop as a percentage of the voltage drop of the first step of Case A which will be considered as a reference state for other values as shown in fig 5.8. Fig 5.8 depicts that sending and receiving voltage deviation from 66 kV become smaller in all Cases but that of Case D is the most stable Case. Here, it is seen that the voltage deviation is small and it has the same value (-6%) for all line lengths for receiving voltage and (-1.5 %) for sending voltage. In addition, Cases B and C is similar to each other when considering the sending voltage has a voltage deviation is -1.8 % and the receiving voltage of lines 2 and 3 has a deviation of -9 %. Case C is the best case for line 1, owing to the fact that higher power injection results in an increase of receiving voltage.

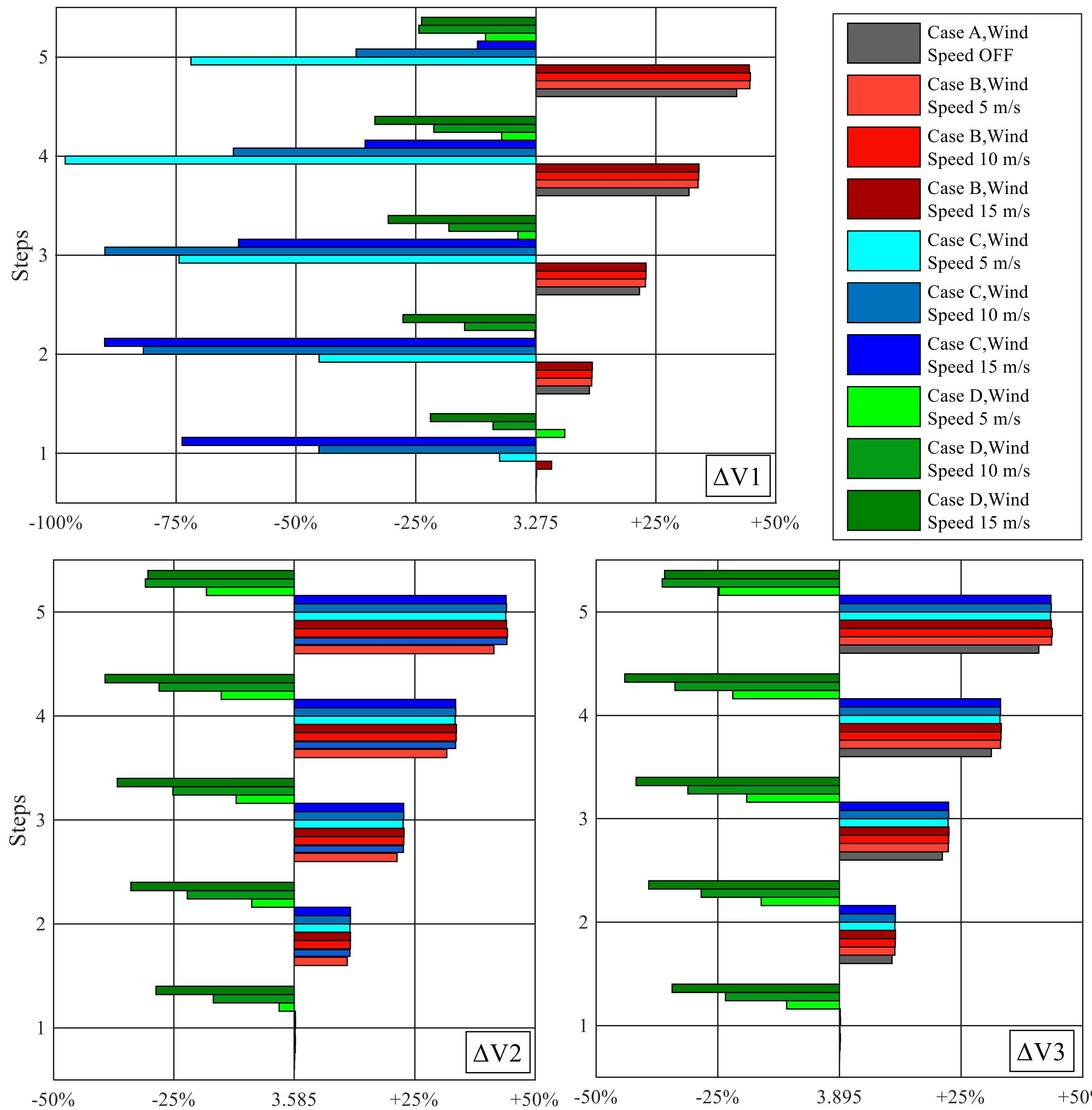


*Fig 5.9 Percentage of voltage drop in Cases A, B, C and D for wind speeds 5, 10, and 15 m/s without regulator to the reference voltage drop of case A.*

Fig 5.9 reveals that the voltage drop as a percentage to reference voltage drop increase gradually with the steps (increase in the load of reactive power) in all Cases except Case D and line 1 of Case C. Where the percentage of voltage drop increases from 0 % in step 1 to 40 % in step 5 in Cases A, B and C and for Case A and B for line 1, while the percentage of voltage drop decreases significantly in Case D, the decrease is about 20 % for line 1, 25 % for line 2 and 30 % for line 3. Also, the voltage drop decreases for line 1 of Case C in a considerable manner from 25 % to 100 % in step 4. In addition, the effect of wind speed is remarkable in Case D where high wind speed causes a considerable decrease in voltage drop. The more wind speed and force gotten, the greater is the amount of power the wind turbine generates.

### 5.3.3 Sending and Receiving Active Power and Power Losses:

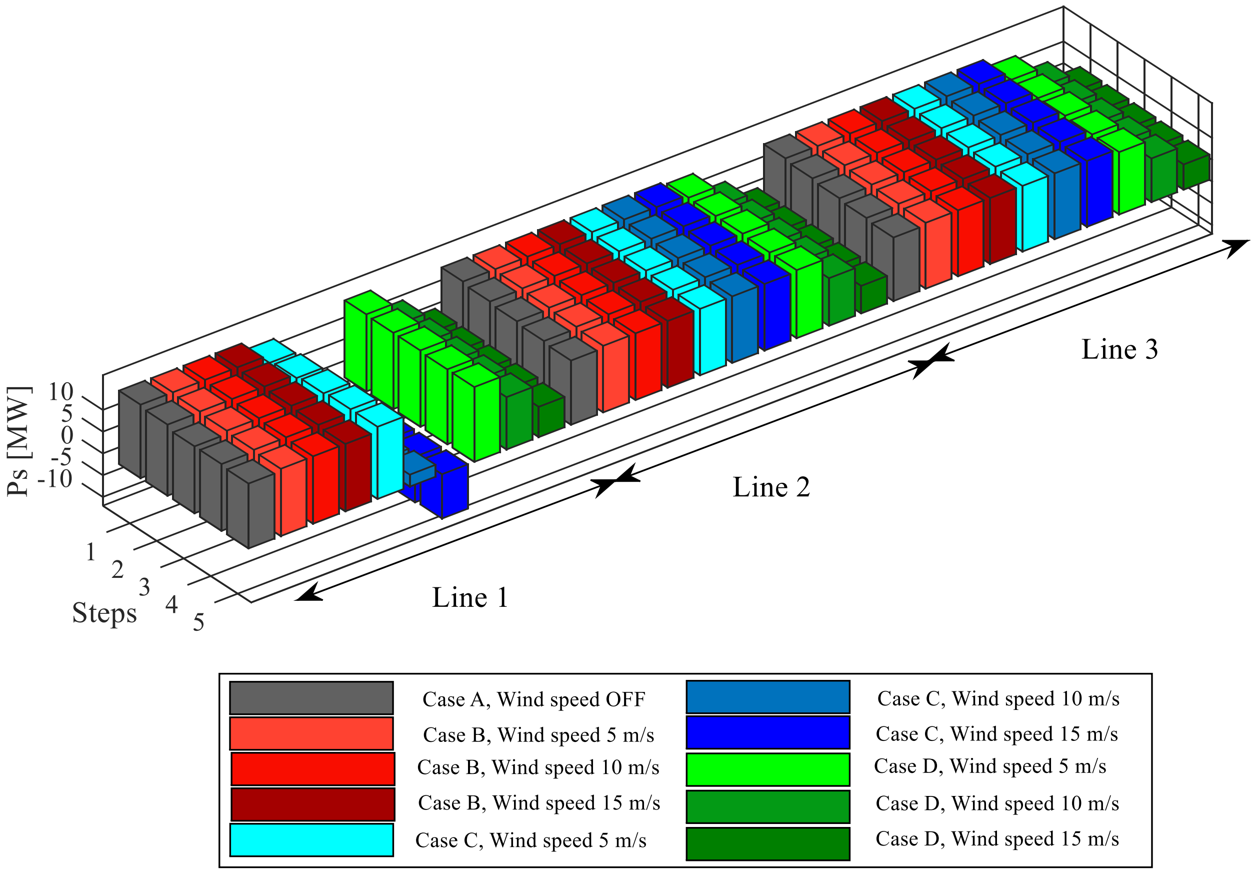


*Fig 5.10 Sending active power in Case A, B, C and D for wind speeds 5, 10, and 15 m/s without regulator for 3 different lengths lines.*

Fig 5.10 shows that the sending active power increases in Case B and C due to sending voltage increase in these Cases except for line 1 considering 10m/s and 15 m/s wind speed where the injected active power is very large. Therefore, the active power flow for this line will be small for wind speed 10 m/s or negative for wind speed 15 m/s. It is equally noticed that the active power in Case D is smaller than other Cases, since the active power is injected onto the ends of all the lines. The influence of wind speed is remarkable only in Case D and line 1 of Case 5, increasing the wind speed bring about a decrease in the active power flow through the lines, part of the required active power of loads comes from the wind farm. In addition, the differences of lines length affect the sending active power, increasing the length will increase the impedance bringing about a decrease in the power flow. In a similar manner, Fig 5.11 is very similar to fig 5.10. In fig 5.11, an increase in active power flow in Case B and C is experienced, while a decrease in active power flow is observed in Case D.

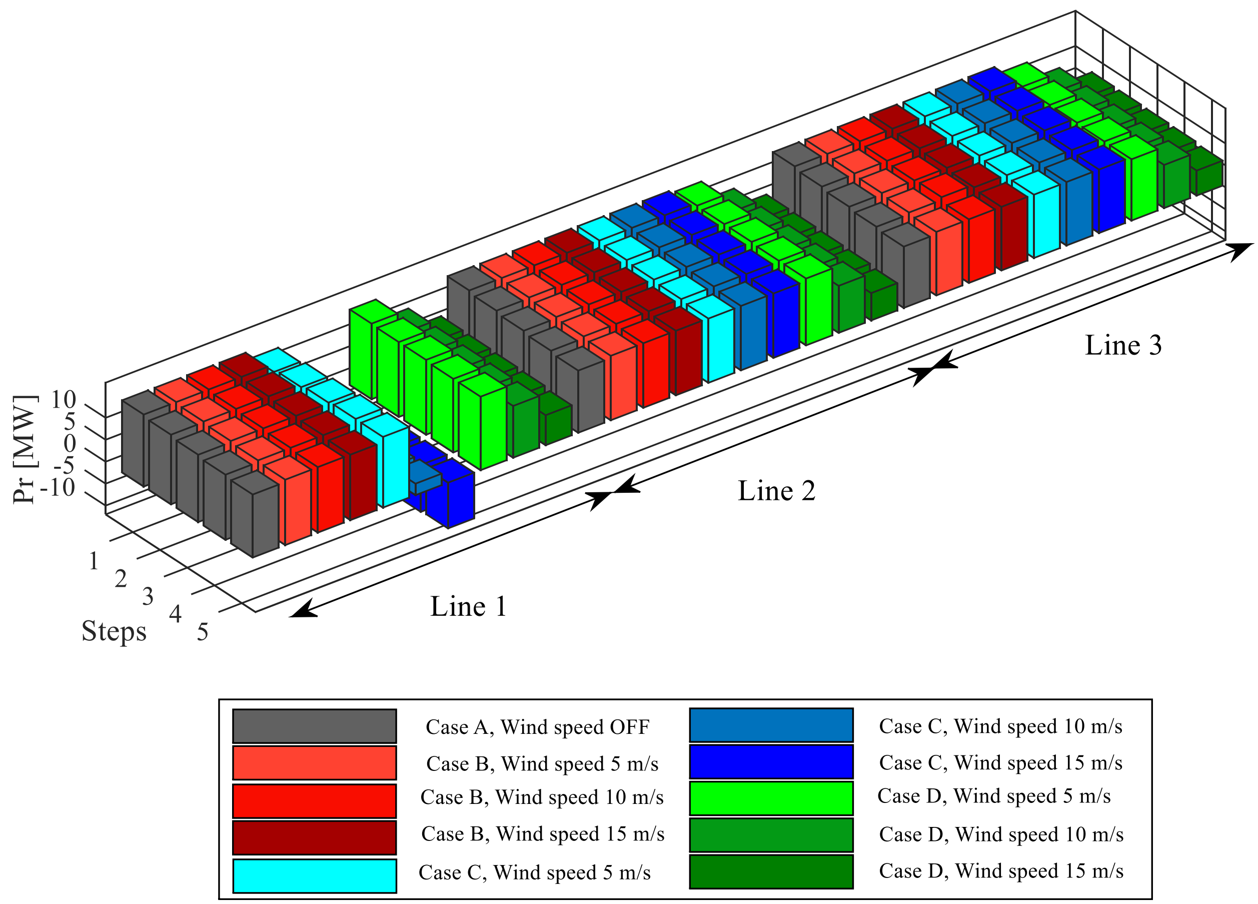


*Fig 5.11 Receiving active power in Case A, B, C and D for wind speeds 5, 10, and 15 m/s without regulator for the 3 different lengths lines.*

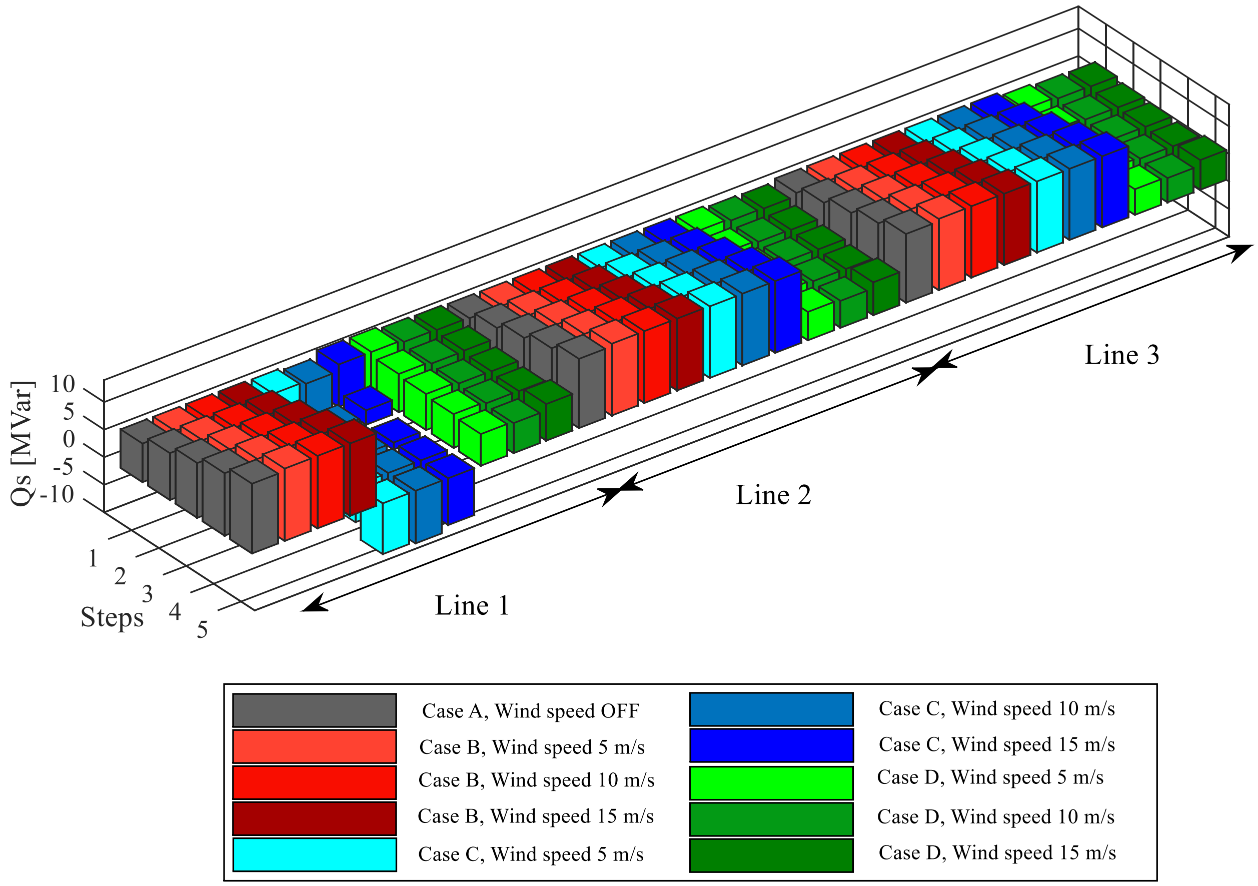


*Fig 5.12 Sending reactive power in Case A, B, C and D for wind speeds 5, 10, and 15 m/s without regulator for the 3 different lengths of lines.*

Fig 5.12, shows that the sending reactive power increases in Case B and Case C respectively. This is due to the sending voltage increase in these Cases except for line 1 where the injected reactive power is very large. Therefore, the reactive power flow for line 1 will be negative for all steps expect step 1 where the injected reactive power is zero. It is observed that the reactive power in Case D is smaller than other Cases owing to reactive power injected to the end of all lines. The influence of wind speed is not remarkable in all the Cases observed, this is so, since the generation of reactive power in the wind farm is independent of the wind speed and active power. In addition, the differences of the various line lengths affect the sending reactive power, implying that increasing the length of lines will increase the impedance causing the decrease in power flow. In the same vein, fig 5.13 is very similar to fig 5.12. Here, there is an increase in reactive power flow in Case B and C, while in case D a decrease in reactive power flow is experienced.

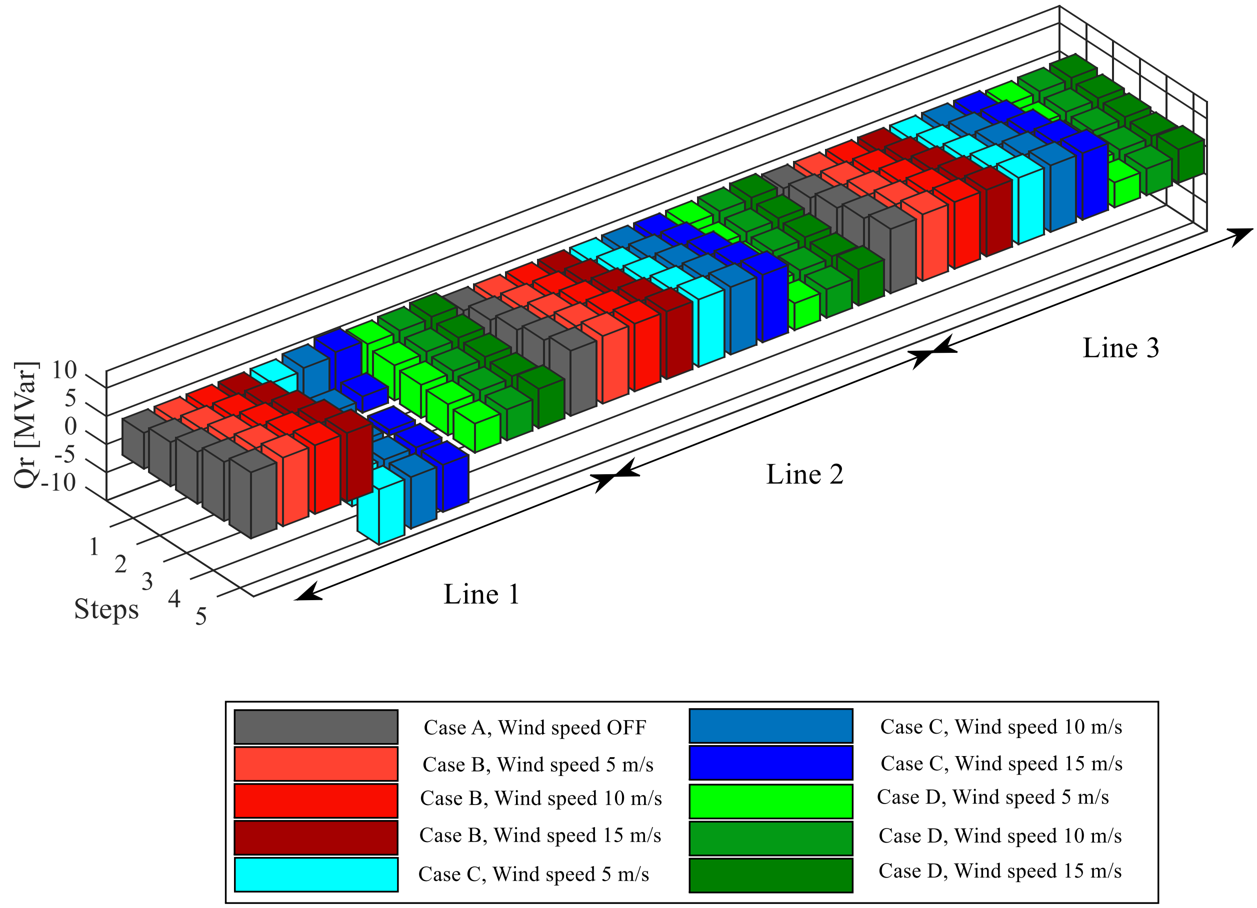


*Fig 5.13 Receiving reactive power in Case A, B, C and D for wind speeds 5, 10, and 15 m/s without regulator for the 3-different length of lines.*

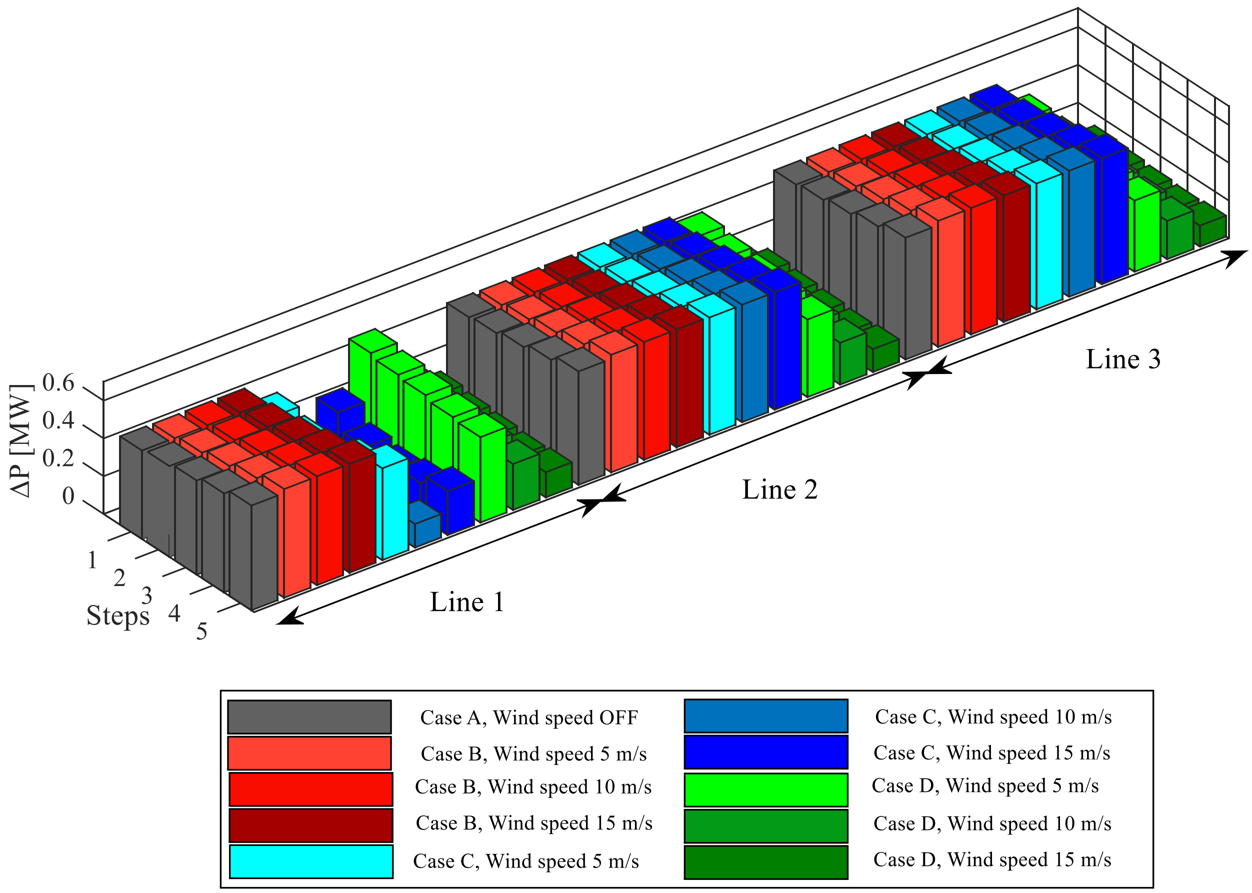


*Fig 5.14 active power losses in Case A, B, C and D for wind speeds 5, 10, and 15 m/s without regulator for 3 different lengths of lines.*

Fig 5.14, illustrates the changes in the active power losses. It is observed that these losses increased slightly in Case B and C except for line 1 of Case C. The power losses decrease due to the active power injected onto the end of line 1. It is vividly clear that Case D is the best, owing to the fact that the active power losses observed is lowest in this Case. The impact of wind speed is remarkable only in Case D and line 1 of Case C. It is observed that increasing the wind speed increases the generated active power, thereby reducing the power flow through the lines and the power losses monitored is of a small value. Increasing the power losses of line 1 for Case C at wind speed of 15 m/s increases the active power flow in reverse direction of line 1 which makes the active power losses to increase.

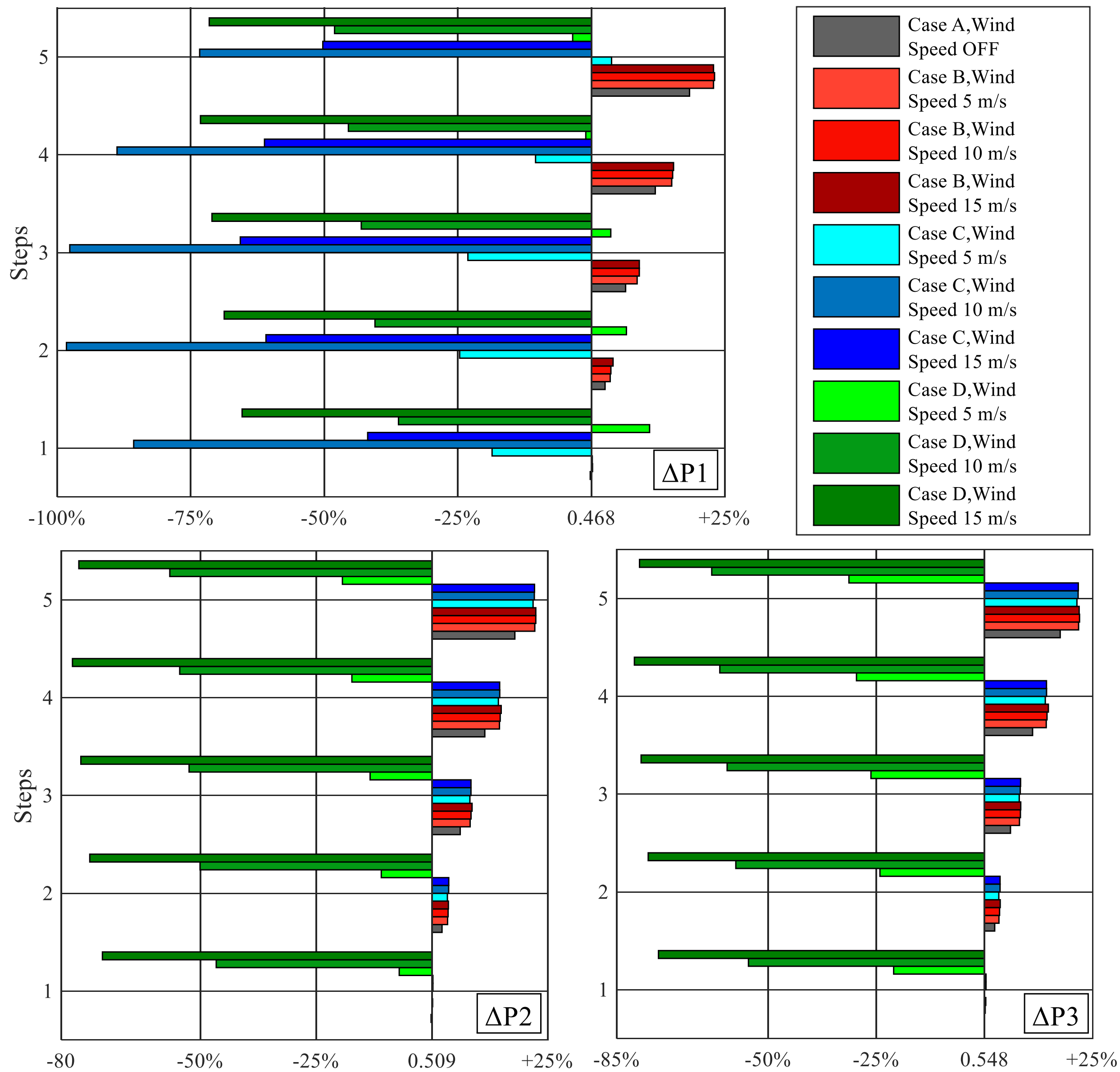


*Fig 5.15 Percentage of active power losses in Case A, B, C and D for wind speeds 5, 10, and 15 m/s without regulator to the reference active power losses of case A.*

Fig 5.15, shows that the active power losses as a percentage to reference active power losses increase gradually with the steps in all Cases except for Case D and line 1 of Case C. Where the percentage of active power losses increases from 0 % in step 1 to 20 % in step 5 in case A, B and C and for cases A and B for line 1. While the percentage of active power losses significantly decreases in Case D, the decrease is about 30 % for line 1, 35 % for line 2 and 40 % for line 3. Also, the active power losses decrease for line 1 of Case C in a considerable manner from 25 % to 100 % in steps of 2 and 3. In addition, the effect of wind speed is remarkable in Case D, higher wind speed brought about a considerable decrease in active power losses. The decrease in the active power is as a result of the substation capacity being increased by upgrading the transformers, that is lower active and reactive power losses, while the loads remain unchanged. This is also attributed to fact that 80 % of the simulated loads are voltage-dependent load, that is inductive loads.

### 5.3.4 Sending and Receiving Power Factor ( $\cos\varphi$ ):

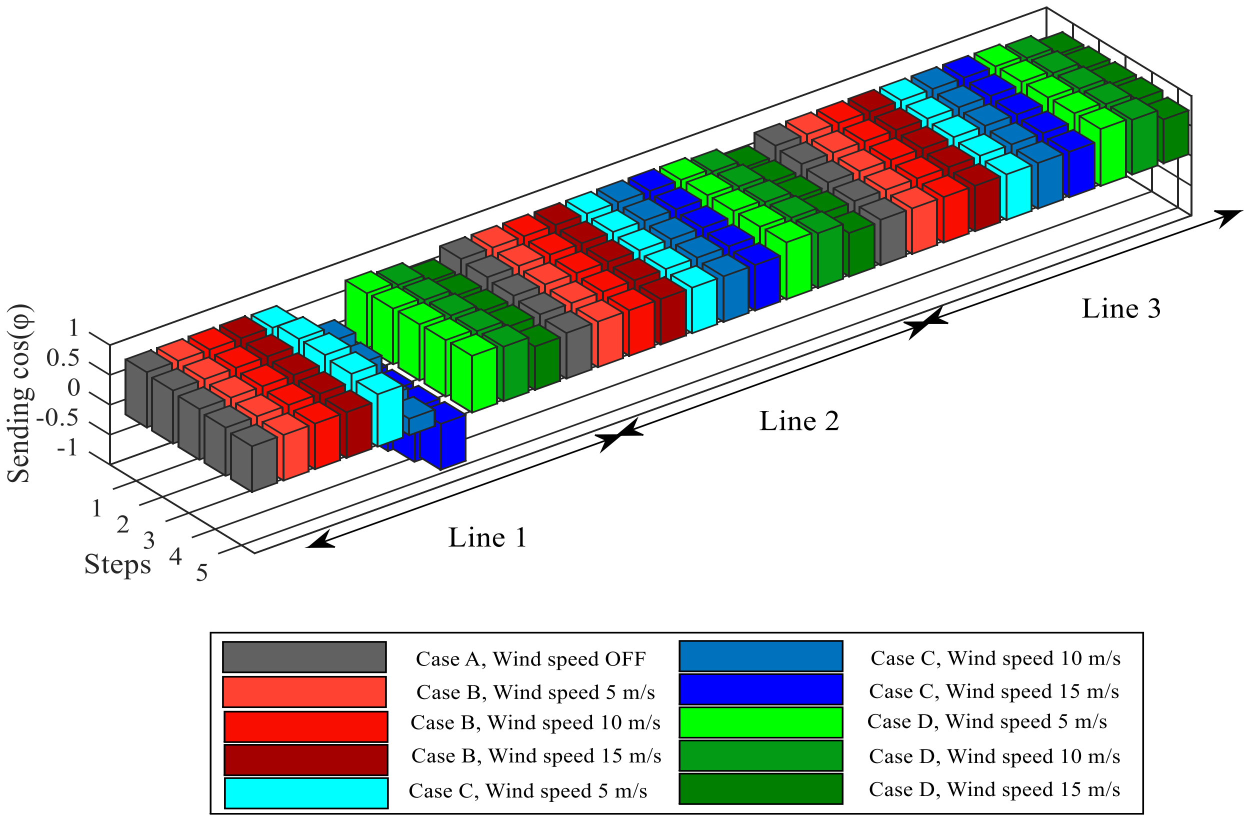


*Fig 5.16 Sending power factor in Case A, B, C and D for wind speeds 5, 10, and 15 m/s without regulator for the 3-different length of lines.*

Fig 5.16 depicts the power factor in case B and C and D, except for wind speed 10 and 15 m/s of line 1 (Case C) and 15 m/s (Case D) is higher than that of Case A owing to the increase in the active power flow through the lines where $\cos\varphi_S = \frac{P_S}{S_S}$ , this is as a result of the impact of the increase in the sending voltage. While the power factor of line 1 for Case C, considering wind speeds of 10 and 15 m/s is lower than that of Case A for 10 m/s and negative for 15 m/s owing to high active power injected onto the end of the line, which results in the power flowing in reverse direction. In Case D for wind speed 15 m/s the power factor is lower than power factor of case A for the same previous reason. The influence of the wind speed could be observed only in Case D and line 1 of Case C. In addition, the difference of the lines length slightly affects the sending power factor. The power factor of the longer line is lower than that of the shorter line since the active power losses recorded is higher. Minimum active power losses levels are reached with higher penetration levels if distributed generation is sufficiently dispersed; and reactive power generation capacity is enough. In variable power factor operation, active power losses decrease with higher penetration levels and low dispersion level, a contrary situation is observed when considering reactive power losses. Fig 5.17 is similar to fig 5.16. Here, the power factor in case B and C and D is higher than that of Case A, except for wind speed 10 and 15 m/s of line 1 as observed in Case C and 15 m/s for Case D with a contrary outcome.

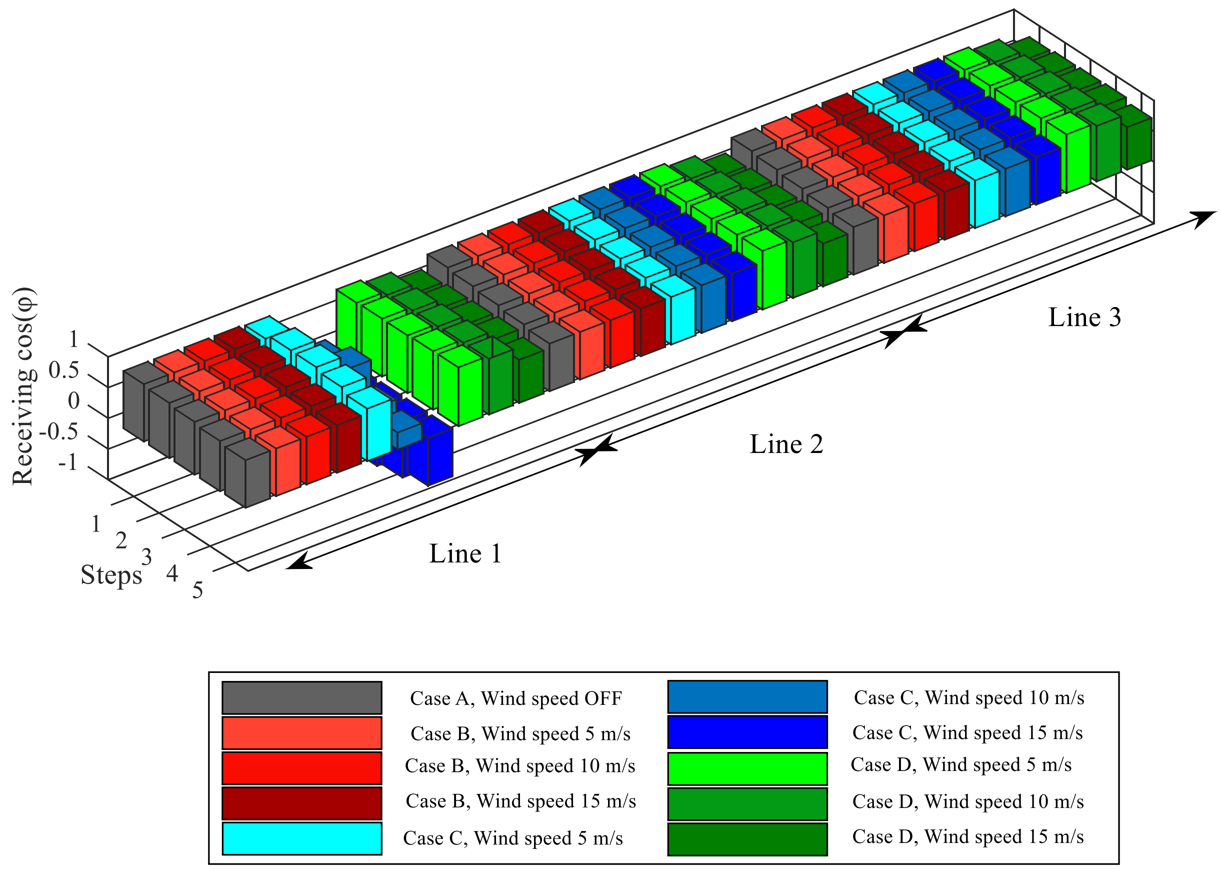


*Fig 5.17 Receiving power factor in Case A, B, C and D for wind speeds 5, 10, and 15 m/s without regulator for the 3-different length of lines.*

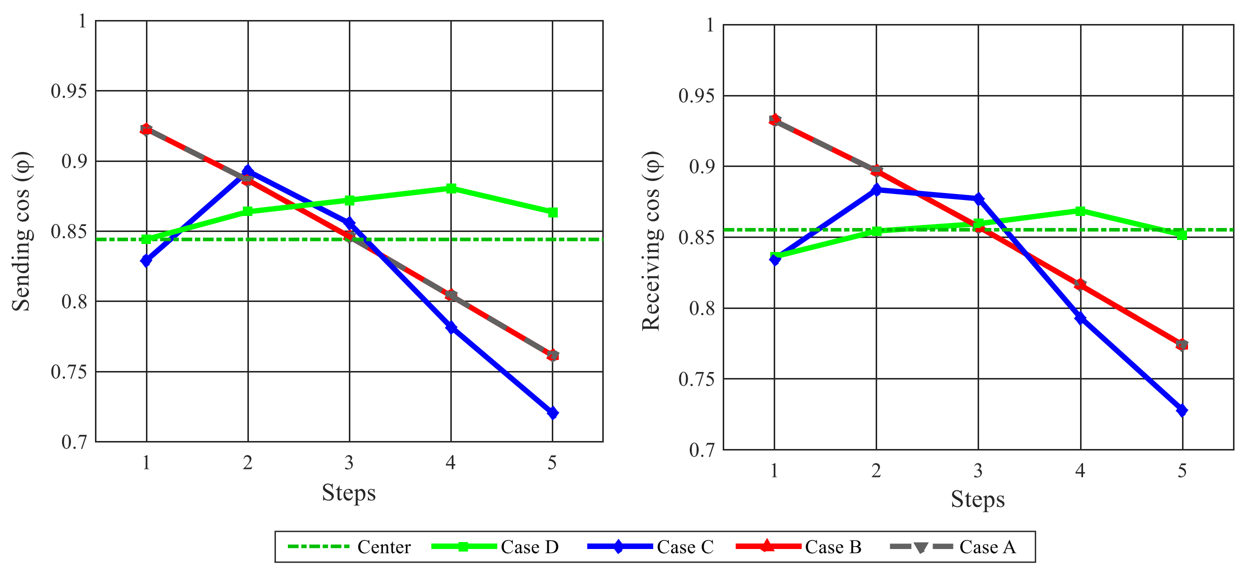


*Fig 5.18 Average value of sending and receiving power factor in Case A, B, C and D for wind speeds 5, 10, and 15 m/s without regulator*

The performance of power factor is vividly made clear in fig 5.18. A fast decrease of sending and receiving power factor for Case A and B is observed. The figure also illustrates that the power factor in observed in Case C is much better than that of Case A and B. Although, this power factor value is not stable for all lines and various steps observed. The best situation is that of Case D, the power factor is stable and close values were observed for all steps monitored. Electrical devices might exhibit electrical input current with a characteristic called "leading power factor". This situation may cause back-up power generation sources to become unstable and shut down.

# 5.4 Case Study With Regulator

Utilizsing the regulator is similer to the results without the regulator, but with some little differences.

## 5.4.1 Sending and Receiving Voltage and Voltage Drop

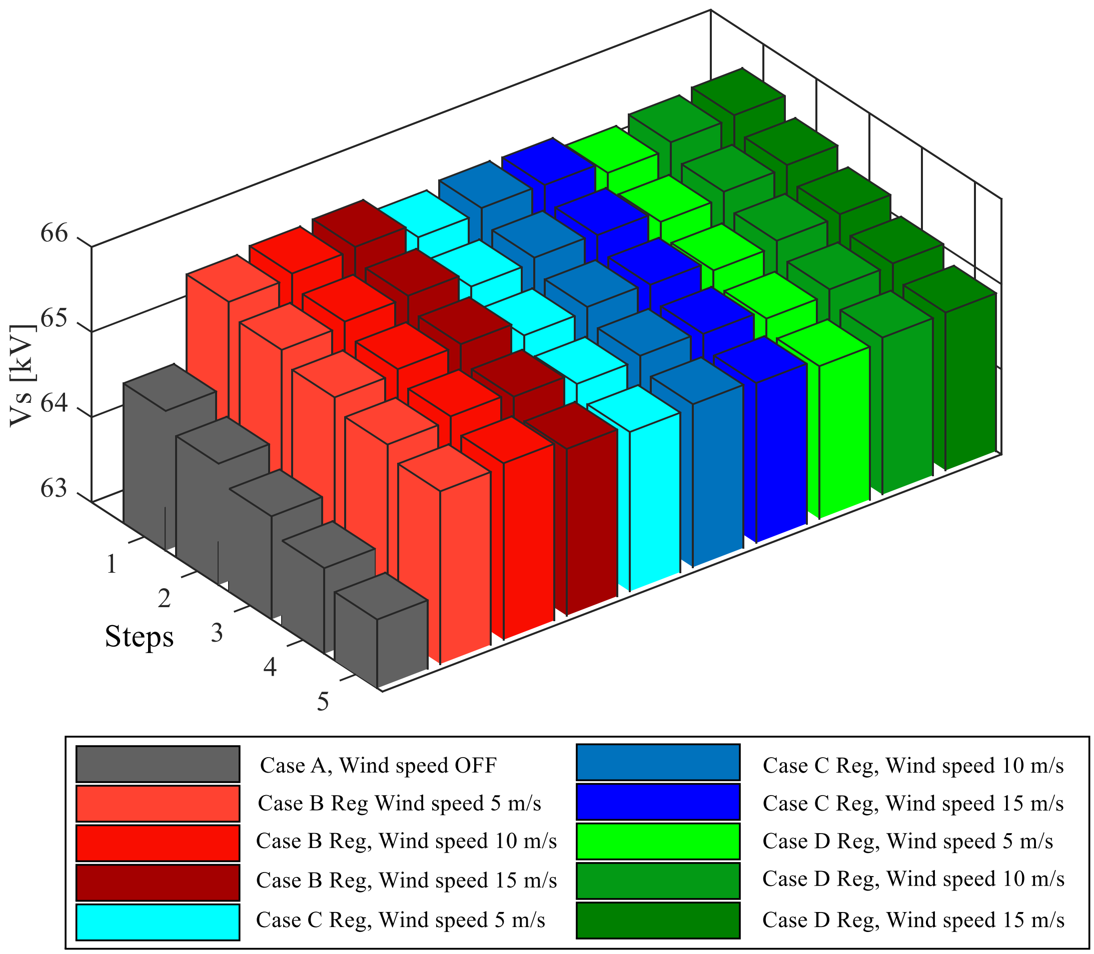


*Fig 5.19 Sending voltage in Case A, B, C and D for wind speeds 5, 10, and 15 m/s with regulator.*

Fig 5.19, reveals that the sending voltage in Case B, C and D with wind farm is higher than that of Case A. In addition, the effects of increasing reactive power of loads in steps is very little in

Case B, C and D as compared to that of Case A. This figure also shows that the effect of increasing the wind speed is not remarkable. Suppose the scheme in this thesis is a weak power system with a large reactive load. If the load is suddenly disconnected, a peak in the voltage is experienced.

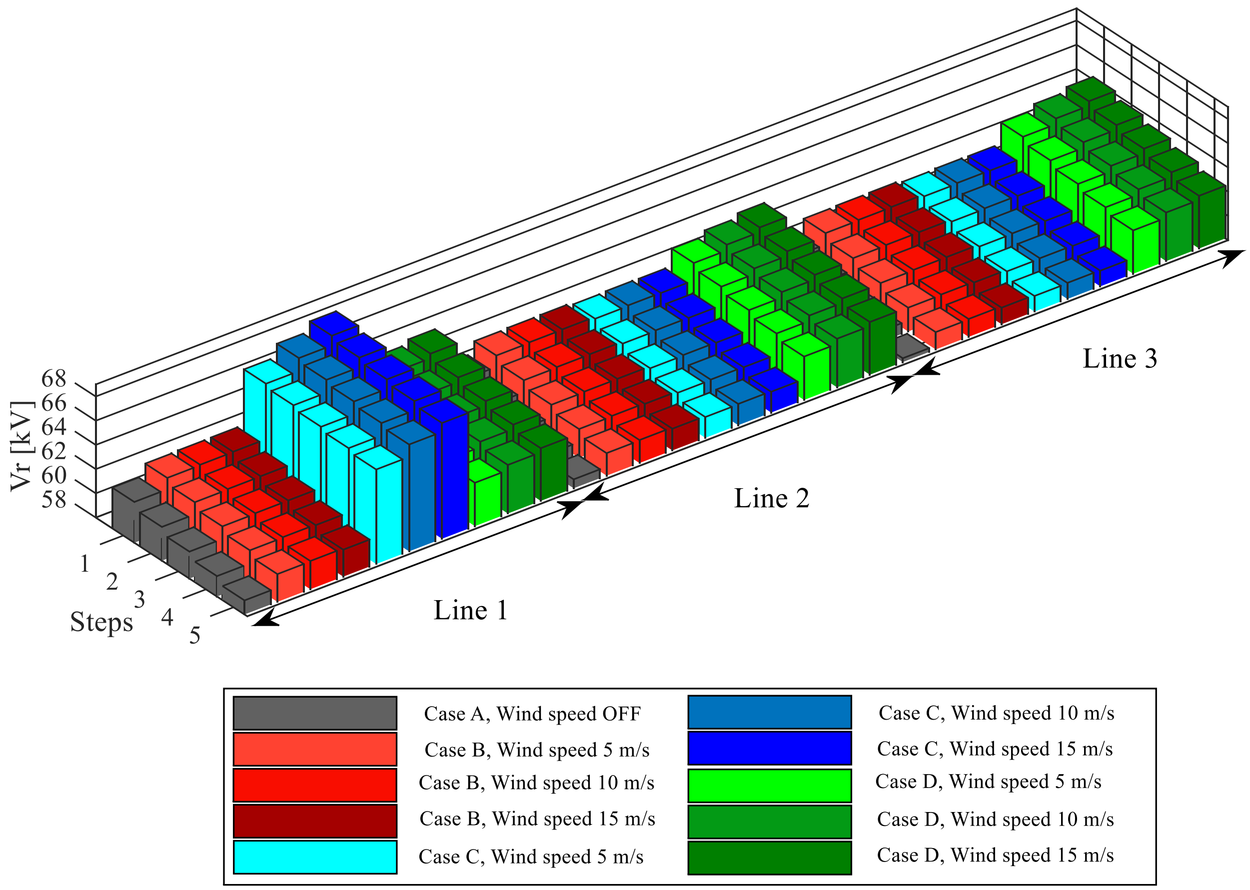


*Fig 5.20 Receiving Voltage in Case A, B, C and D for wind speeds 5, 10, and 15 m/s with regulator for the 3-different length of lines.*

Also, fig 5.20, shows that receiving voltage values in Case B, C and D with wind farm is larger than it is in Case A. But for Case D, when the wind farm is connected to the end of all the lines is the best Case situation observed, since the voltage for all lines is more stable and it has the same value for all lines and generally higher than all other Cases. Considering Case C, the voltage of line 1 is extremely higher than other lines or Cases owing to the high reactive power injected to line 1. The effect of increasing wind speed is remarkable in Case D and line 1 of Case C where increasing the wind speed, equally gradually increases the voltage. Also, the differences of the lines length affect the voltage, that is increasing the length of lines equally increases the voltage drop for each line except for Case D, since the wind farm is connected to the end of all the lines. Hence, the receiving voltage for all the lines is the same. Also, the effect of different steps is remarkable in all cases except for line 1 of Case C, the voltage decreases gradually by increasing the steps, but in line 1 of Case C it is stable owing to the regulators effect which takes sending and receiving voltage and drop voltage of all lines into account which give the sub-station better stability in critical situations. Reactive power, which is also called Vars is required to maintain the voltage to deliver active power (watts) through transmission lines. Loads require reactive power to convert the flow of electrons into useful work. When there is not enough reactive power, the voltage sags down and it is not possible to push the power demanded by loads through the length of power lines.

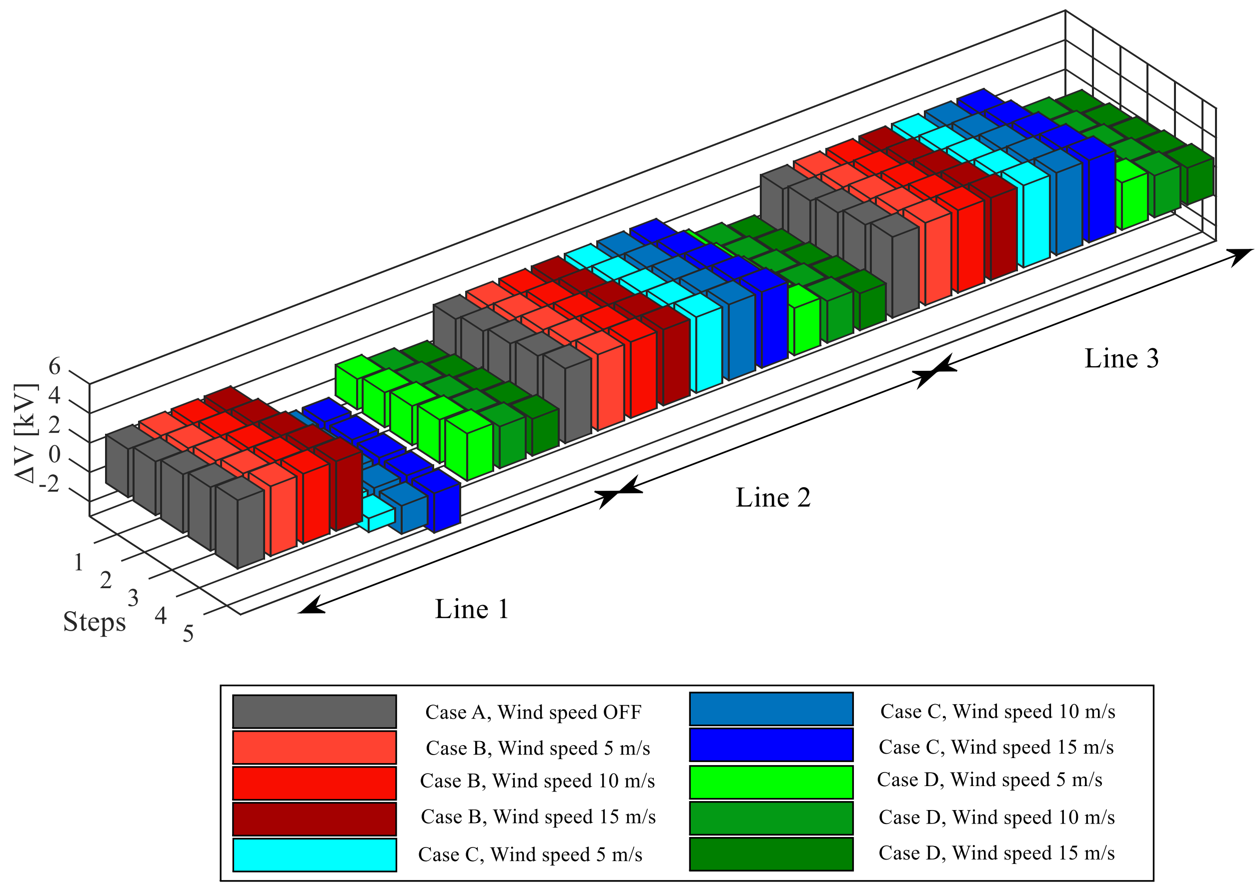


*Fig 5.21 Voltage drop in Case A, B, C and D for wind speeds 5, 10, and 15 m/s with regulator for the 3 different length of lines.*

Here, fig 5.21, illustrates the changes in voltage drop. It is observed that the voltage drop decreases only in Case D and line 1 of Case C. In all other Cases monitored, the voltage drop increases a little in value, increasing the sending voltage for these Cases bring about an increase in power flow of all the lines and a slight increase in the voltage drop. The small value of speed 5 m/s and negative value for speeds 10m/s and 15 m/s of voltage for line 1 of Case C due to the high reactive and active power injected onto this line causes as mentioned in fig 5.6 an extreme increase in receiving voltage. The effect of increasing the wind speed is remarkable only in Case D and line 1 of Case C, increasing the wind speed increases the generated active power. Therefore, the power flow decreases in the lines and the voltage drop equally decreases gradually. Consequently, the differences of the lines length affect the voltage drop, increasing the length equally increases the impedance of the lines. Therefore, the voltage drop increases except for Case D and line 1 of Case C, being for the obvious reason mentioned in fig 5.20. Also, the effect of different steps is not generally remarkable in all Cases.

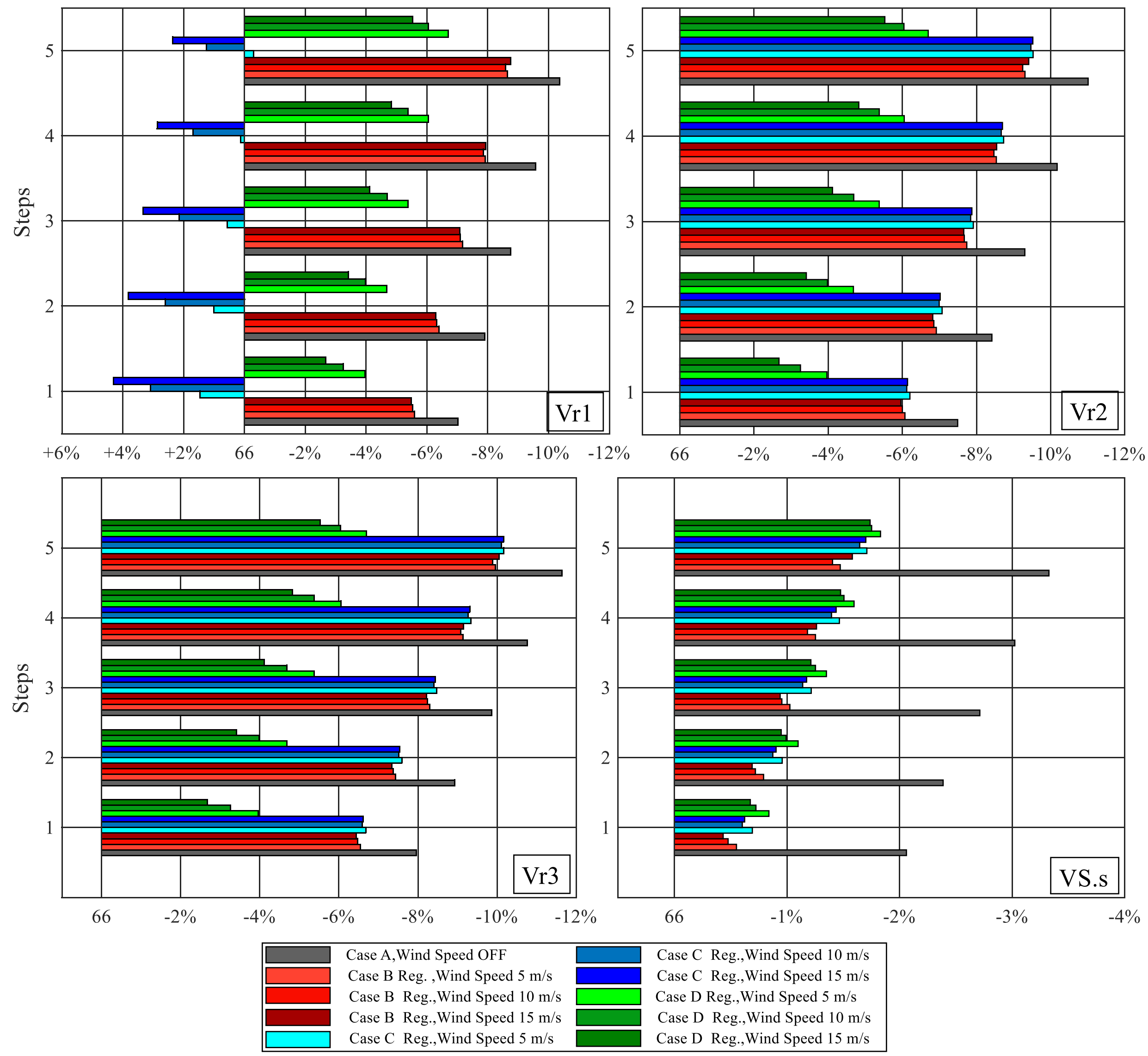


*Fig 5.22 Percentage of sending and receiving voltage in Case A, B, C and D for wind speeds 5, 10, and 15 m/s with regulator to the nominal sub-station voltage (66 kV).*

If the previous values were converted to percent values by calculating the sending and receiving voltage as a percentage of the nominal voltage of sub-station voltage (66 kV) and by calculating the voltage drop as a percentage of the voltage drop of the first step of Case A, which will be considered as a reference state for other values. Fig 5.22, shows that the sending and receiving voltage deviation from 66 kV become smaller in all the Cases observed, but Case D is the most stable, since the voltage deviation is small and it is about -4% to -6% in general for all lines for the receiving voltage values and -0.75 to -1.75 % in general for sending voltage values observed. In addition, Case B and C is similar to each other for sending voltage where voltage deviation is from -0.5 to -1.5 % and receiving voltage for lines 2 and 3, whose deviation is -6 % to -10%. Case C is the best Case for line 1 owing to the higher power injected onto the line, which results in an increase in its receiving voltage.

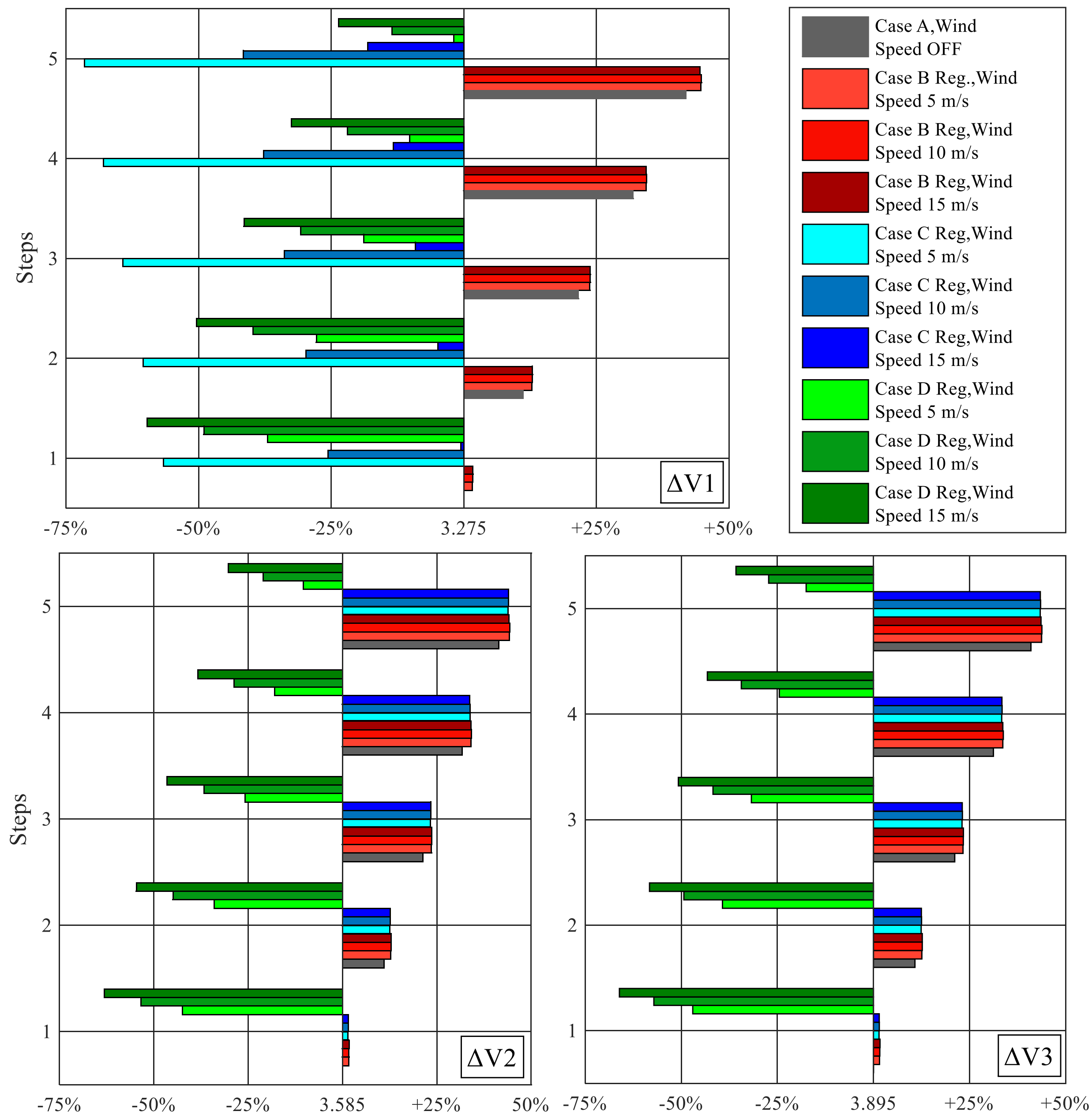


*Fig 5.23 Percentage of voltage drop in Cases A, B, C and D for wind speeds 5, 10, and 15 m/s with regulator to the reference voltage drop of Case A.*

It is illustrated in fig 5.23, that the voltage drop as a percentage of the reference voltage drop increases gradually with the steps, implying an increase in the load reactive power in all Cases except for Case D and line 1 of Case C, where the percentage of voltage drop increases from 0 % in step 1 to 40 % in step 5 in Case A, B and C respectively and for line 1 of Case A and B. While the percentage of voltage drop decreases significantly in Case D where the decrease in voltage is between 20 % to 50 % for line 1, 25 % to 55 % for line 2 and 30 % to 60% for line 3. Consequently, the voltage drop decreases for line 1 for Case C in a considerable manner, which is generally 25 % to 70 %. In addition, the effect of wind speed is remarkable in Case D, where high wind speed causes a significant decrease in voltage drop. Also, the wind speed has effect on line 1 of Case C. Where low speed brings about a decrease in the voltage drop, this results in a decrease in the power flow and line current through the power line.

### 5.4.2 Sending and Receiving Active Power and Power Losses

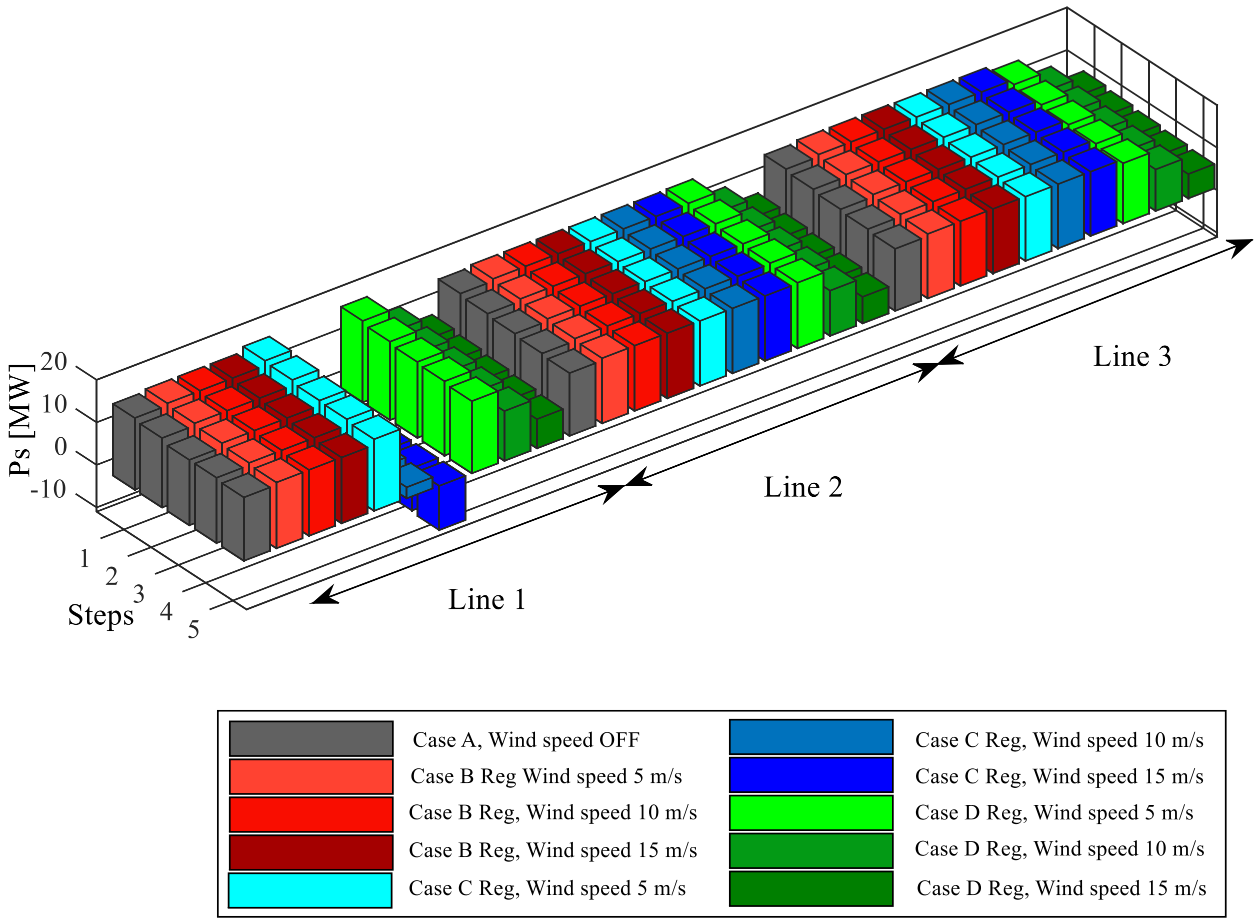


*Fig 5.24 Sending active power in Case A, B, C and D for wind speeds 5, 10, and 15 m/s with regulator for the 3 different length of lines.*

Fig 5.24 shows that the sending active power increases in Case B and Case C as a result of the sending voltage increasing in these Cases except for line 1 wind speed of 10m/s and 15 m/s. Here, the injected active power is very large. Hence, the active power flow for this line is small for observed wind speed of 10 m/s or negative for wind speed 15 m/s. Also, it could be noticed that the active power observed in Case D is smaller than other Cases, owing to the fact that active power is injected onto the ends of all the lines. The influence of wind speed is remarkable only in Case D and line 1 of Case C, whereby increasing the wind speed results in a decrease in the active power flow through the lines, where part of the required active power of loads comes from the wind farm. In addition, the differences of the lines length affect the sending active power where increase in the length bring about a corresponding increase in the impedance resulting in the decrease of power flow. It is worthy of note that the effect of different steps observed is generally not remarkable in all cases observed. Fig 5.25 is very similar to fig 5.24, an increase in active power flow is observed in Case B and C, while a decrease in active power flow is noticed in Case D.

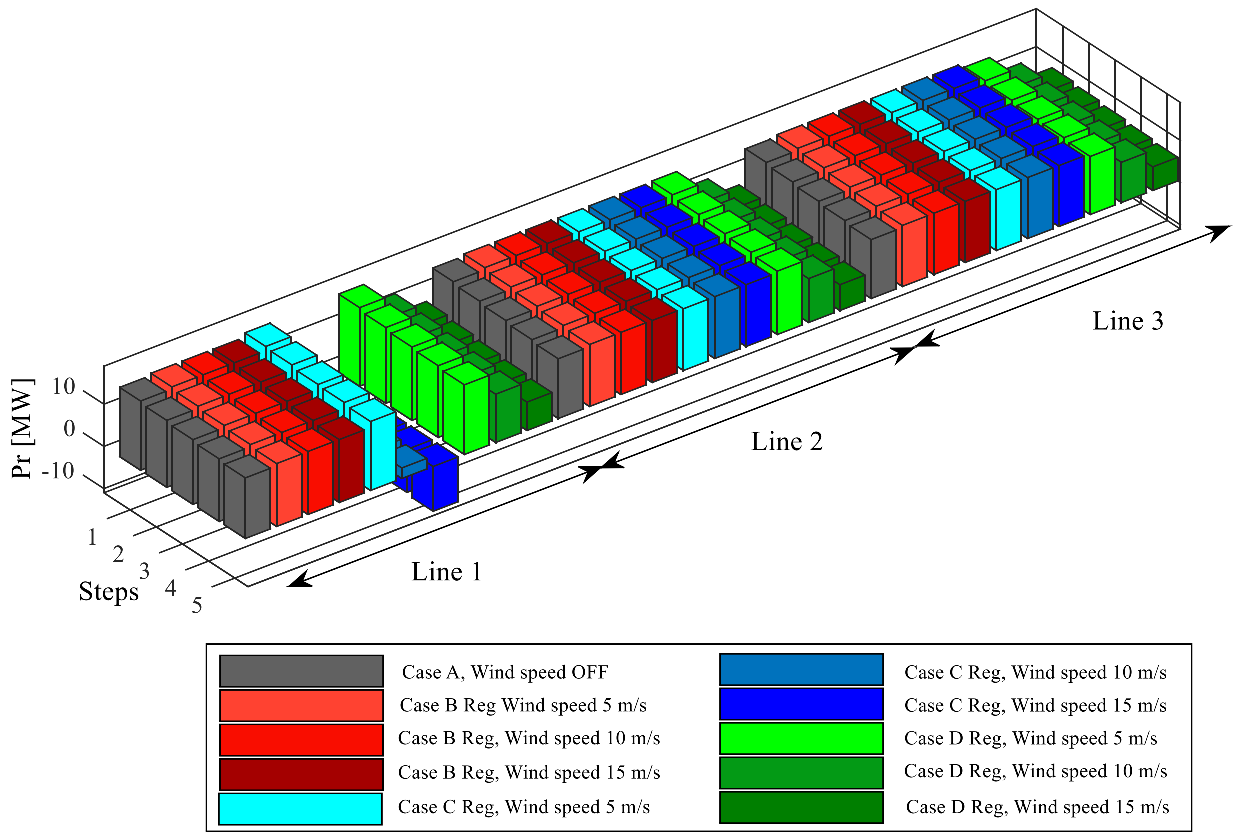


*Fig 5.25 Receiving active power in Case A, B, C and D for wind speeds 5, 10, and 15 m/s with regulator for the 3 different length of lines.*

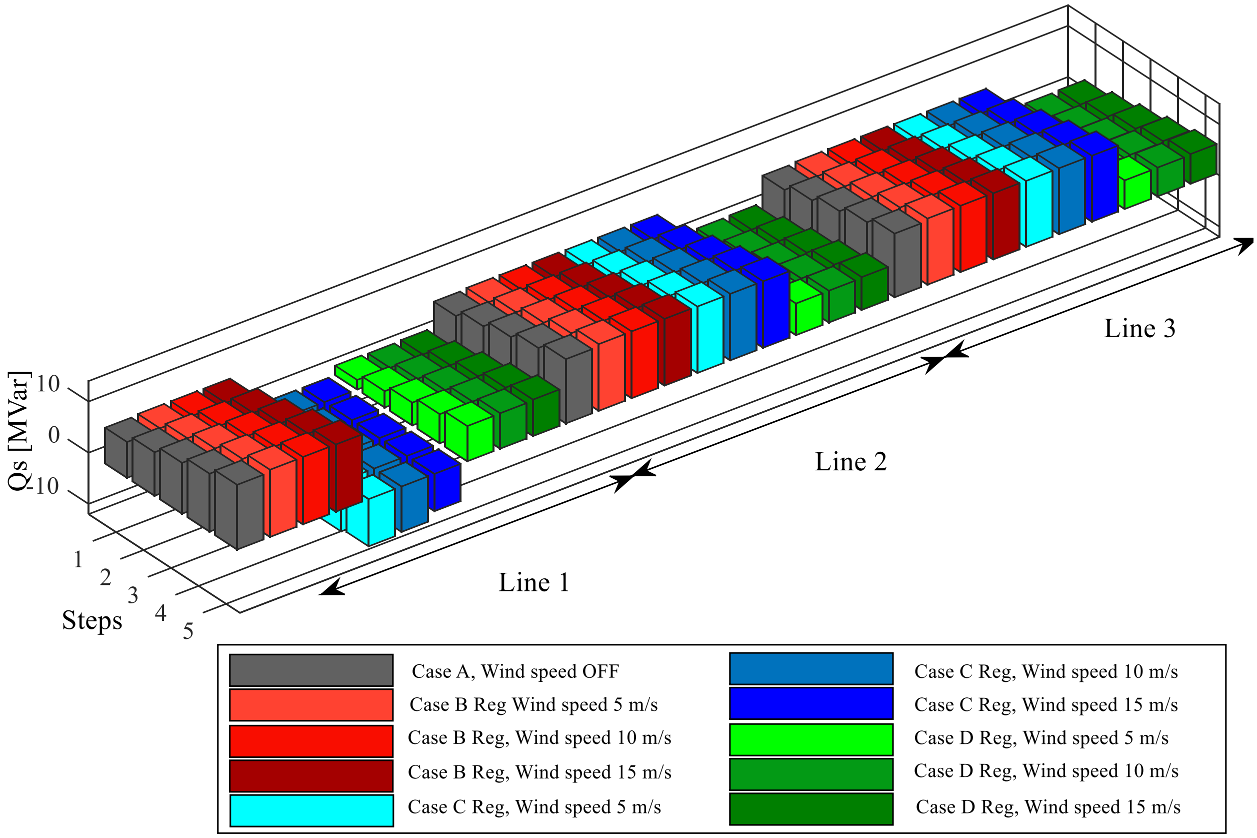


*Fig 5.26 Sending reactive power in Case A, B, C and D for wind speeds 5, 10, and 15 m/s with regulator for the 3 different length of lines.*

It is observed in fig 5.26 that the sending reactive power increases in Case B and Case C due to an increase in the sending voltage in these Cases except for line 1 where the injected reactive power value is much higher. Hence, the reactive power flow for line 1 is negative for all steps observed, except for step 1 where the injected reactive power is zero. Equally, it is noticed that the reactive power in Case D is smaller than other Cases, owing to reactive power injected onto the end of all the power lines. The influence of wind speed is not remarkable in all cases since the generated reactive power in the wind farm is independent of wind speed and active power. In addition, the differences of the power lines length affect the sending reactive power, since increasing the length of power lines will result in a corresponding increase in the impedance of the lines. Thereby, bringing about a decrease in the power flow. Fig 5.27, is in a like manner similar to fig 5.26, an increase in reactive power flow is observed in Case B and C respectively, while there is a decrease in reactive power flow observed in Case D.

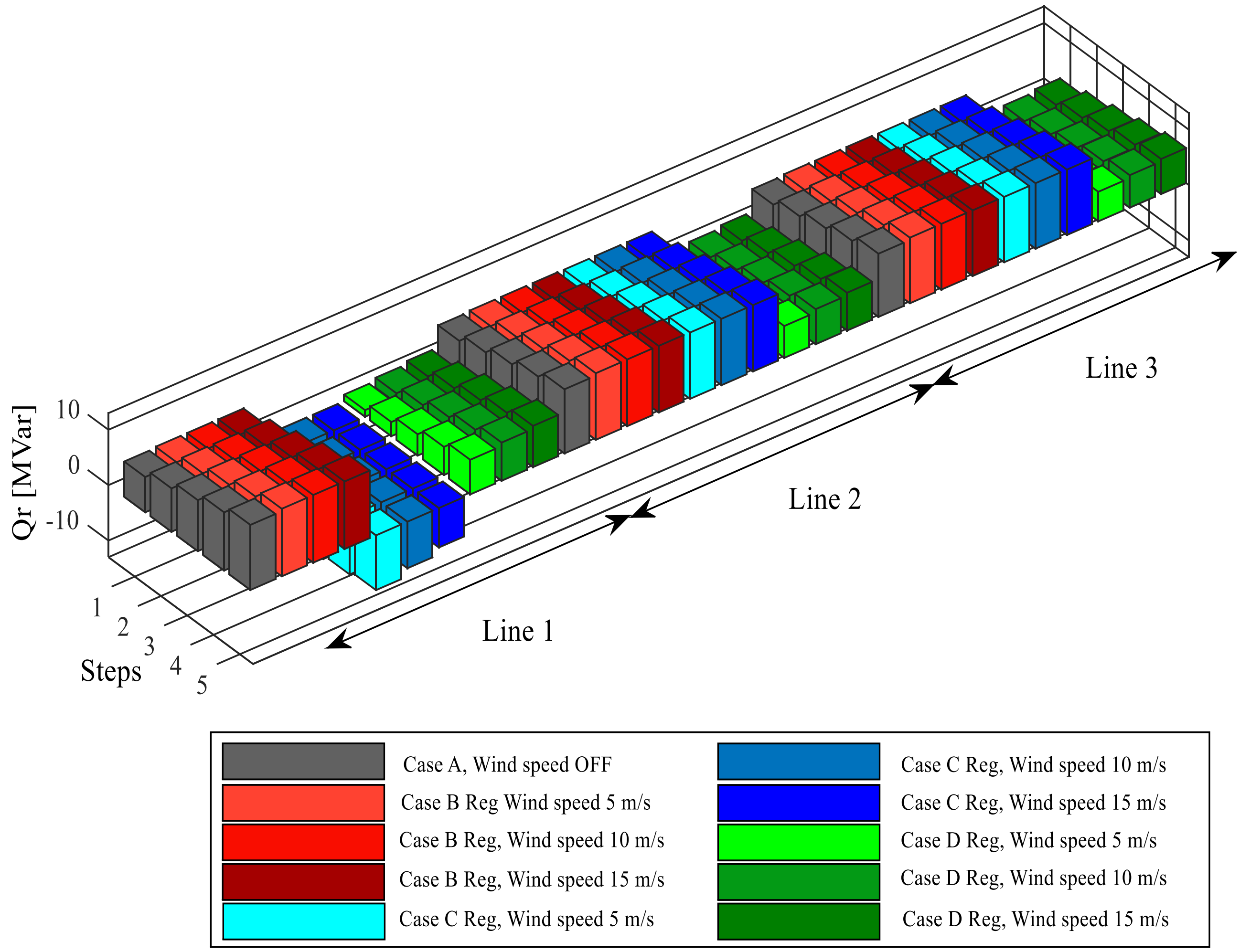


*Fig 5.27 Receiving reactive power in Case A, B, C and D for wind speeds 5, 10, and 15 m/s with regulator for the 3 different length of lines.*

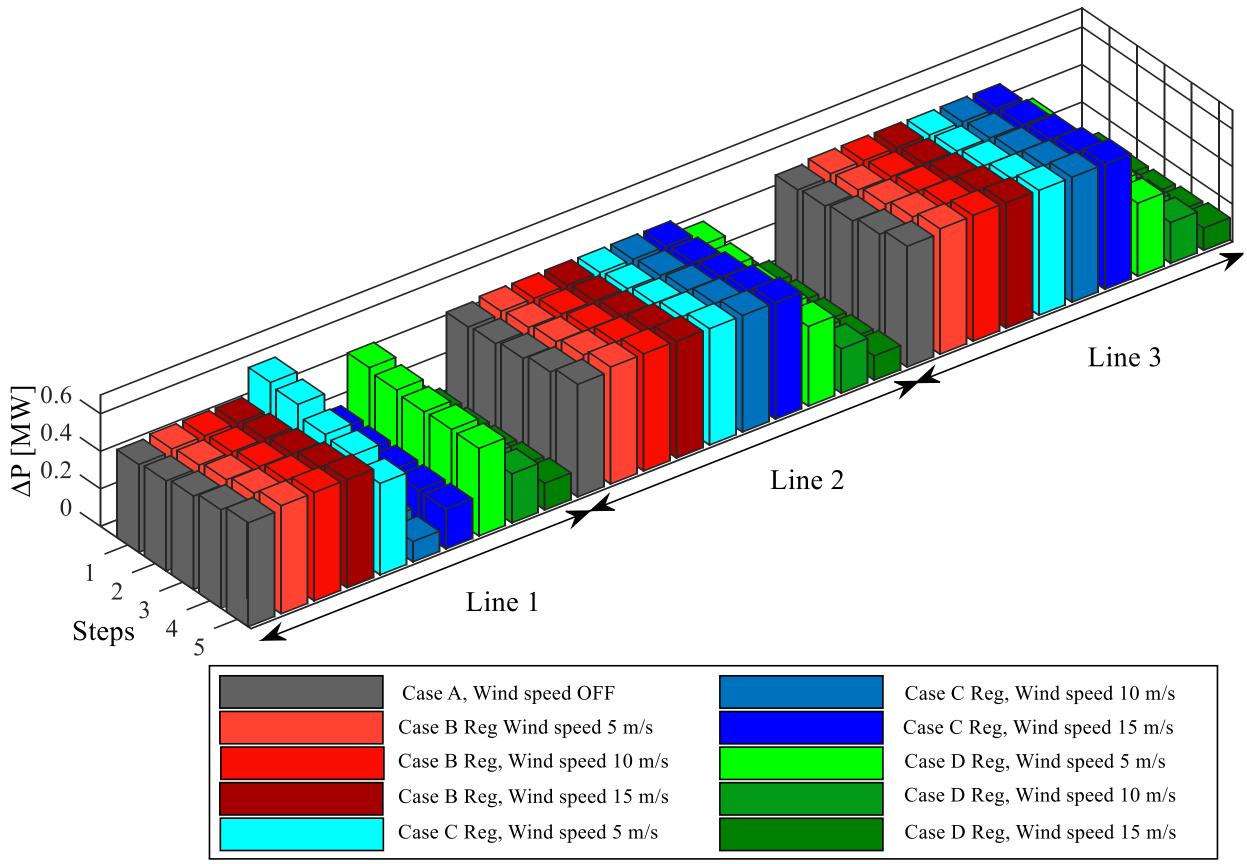


*Fig 5.28 active power losses in Cases A, B, C and D for wind speeds 5, 10, and 15 m/s with regulator for 3 different lengths lines.*

Here, fig 5.28, shows a graphical illustration of the changes in active power losses, these losses increased slightly in Case B and C respectively, except for line 1 of Case C where power losses decreases due to the active power injected onto the end of line 1. It is vividly clear that Case D is the best situation observed, since the active power losses observed here is the lowest. The impact of wind speed is remarkable only in Case D and line 1 of Case C. Whereby, increasing the wind speed bring about a corresponding increase in the generated active power, so it reduces the power flow through the power lines and power losses will be small. Increasing power losses for line 1 of Case C for wind speed of 15 m/s, since increasing the active power flow in the reverse direction of line 1 will cause active power losses to increase. It is equally observed that the effect of different steps is generally not remarkable in all cases or very insignificant. Taking that the power factor of the load is improved for the same real power, considering the various Cases observed, then the magnitude of the line current will decrease, decreasing the line losses. So, transmission efficiency will improve.

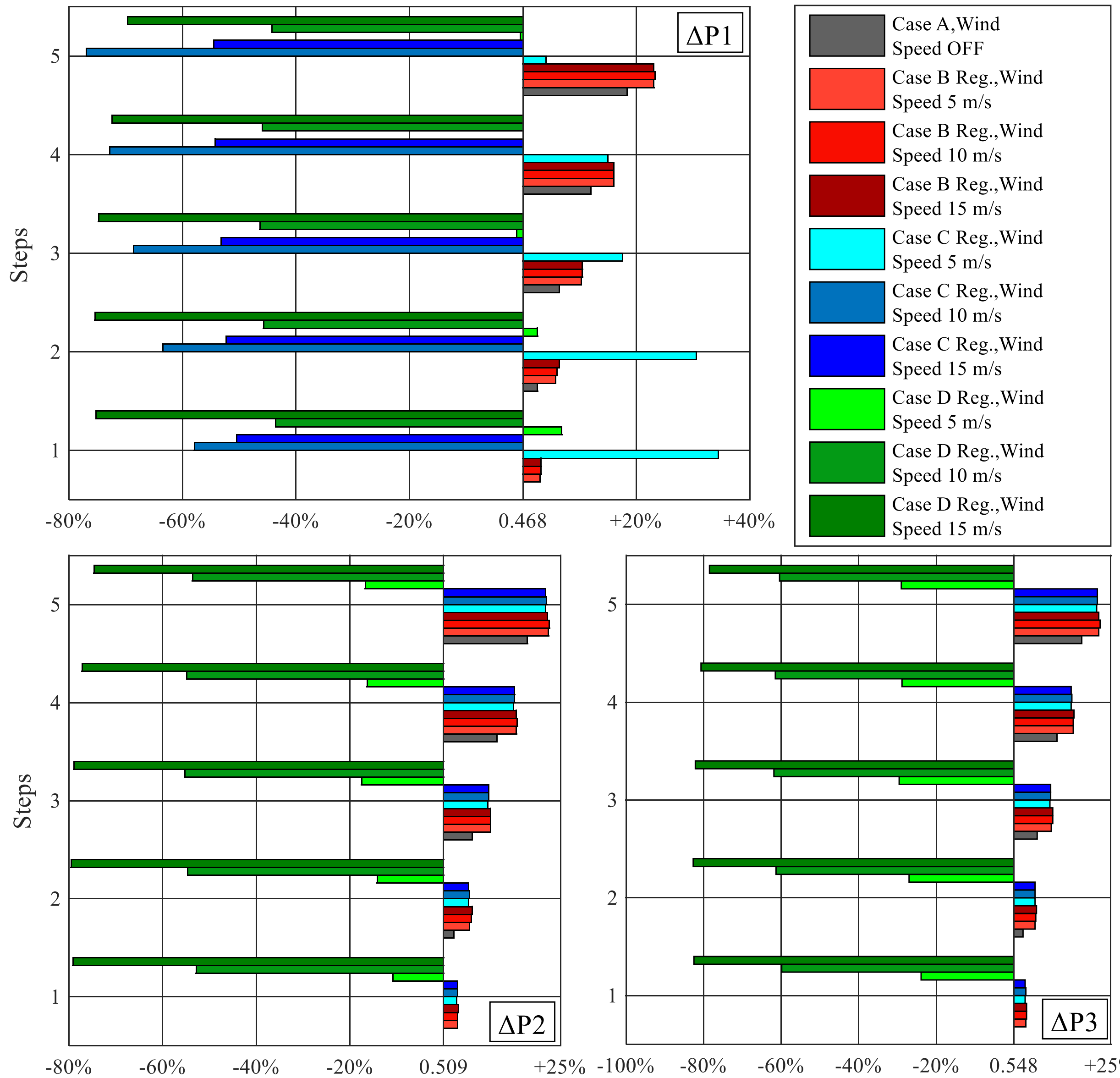


*Fig 5.29 Percentage of active power losses in Case A, B, C and D for wind speeds 5, 10, and 15 m/s with regulator to the reference active power losses of Case A.*

It is observed in fig 5.29, that the active power losses as a percentage to reference active power losses, increases gradually with the steps in all Cases observed, except for Case D and line 1 of Case C. Where the percentage of active power losses increases from 3 % in step 1 to 22 % in step 5 in Case A, B and C except for Case C of line1. while the percentage of active power losses decrease significantly in Case D. Where the decrease is about 40 % for line 1, 50 % for line 2 and 60 % for line 3. Generally, the active power losses decrease for line 1 of Case C in considerable manner from 50 % to 75 %. In addition, the effect of wind speed is remarkable in Case D, since higher wind speed causes a significant decrease in active power losses. The active power generated by the wind farm depends upon the wind speed. With the variation in active power generation, the reactive power consumption likewise varies.

### 5.4.3 Sending and Receiving Power Factor (cos $\varphi$ )

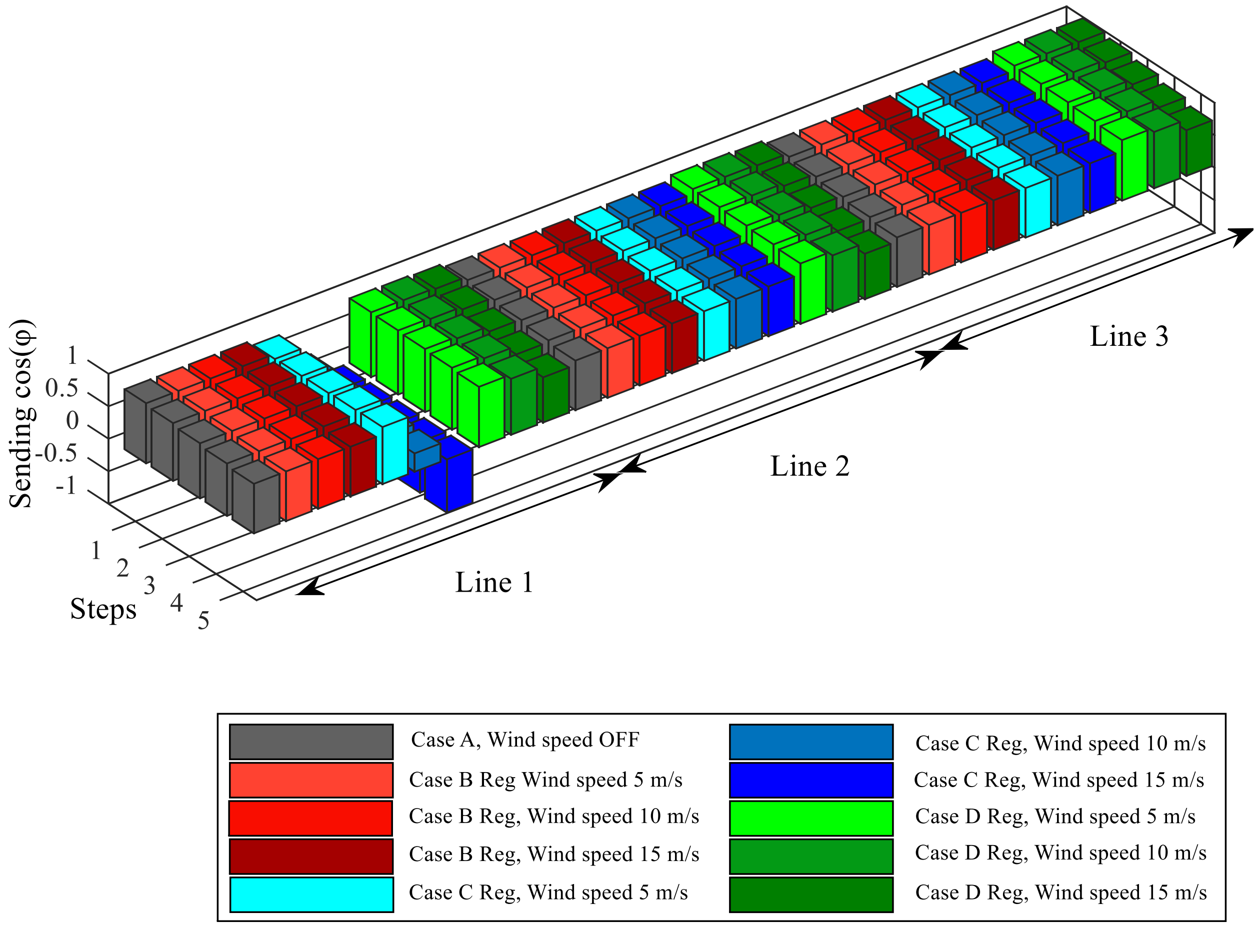


*Fig 5.30 Sending power factor in Case A, B, C and D for wind speeds 5, 10, and 15 m/s with regulator for the 3 different length of lines.*

Fig 5.30, shows the power factor in Case B and C and D except the situation for wind speed 10 and 15 m/s of line 1 of Case C and 15 m/s of Case D. Here, it is seen that the power factor for Case C and D situation monitored is higher than that for Case A due to the increase in the active power flow through the power lines where $\cos\varphi_S = \frac{P_S}{S_S}$ under the effect of increasing the sending voltage. While the power factor of line 1 of Case C for wind speeds 10 and 15 m/s is lower than that of Case A for 10 m/s and negative for 15 m/s as a result of higher active power injected to the end of the line which make the power flow in reverse direction. In Case D for wind speed 15 m/s the power factor is lower than power factor of Case A for the same previous reason cited in Fig. 5.5. The impact of wind speed could be noticed only in Case D and line 1 of Case C. In addition, the differences of the lines of lengths affects slightly the sending power factor where the power factor of long line is lower than shorter power lines, since active power losses for it will be of a higher value. With low power factor, higher rating transmission line is needed. And as current transmission is associated with joule loss. The more current means more joule loss. As such the reactive current travel from source to load and load end to source end too. Fig 5.31, is very much similar to fig 5.30, where the power factor in Case B and C and D respectively, except that of wind speed 10 and 15 m/s of line 1, for Case C and 15 m/s for Case D is higher than that of Case A.

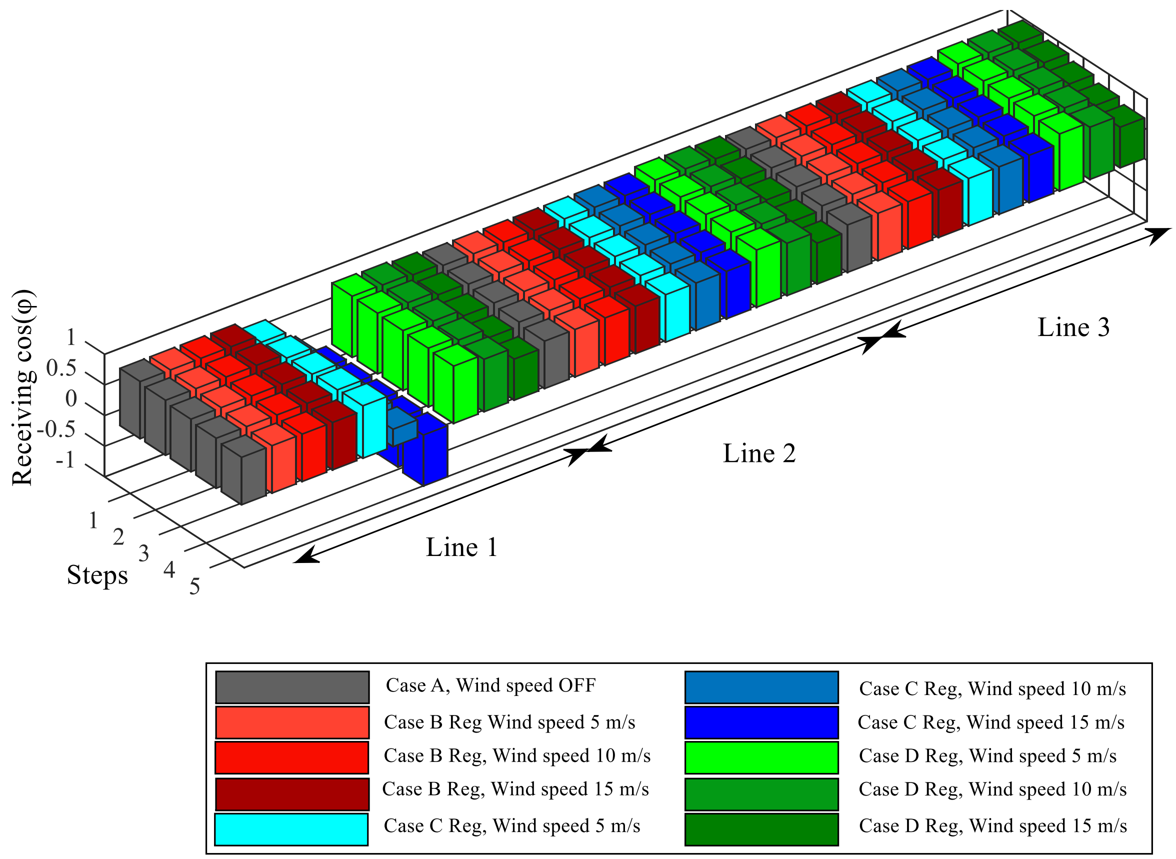


*Fig 5.31 Receiving power factor in Case A, B, C and D for wind speeds 5, 10, and 15 m/s with regulator for the 3 different length of lines.*

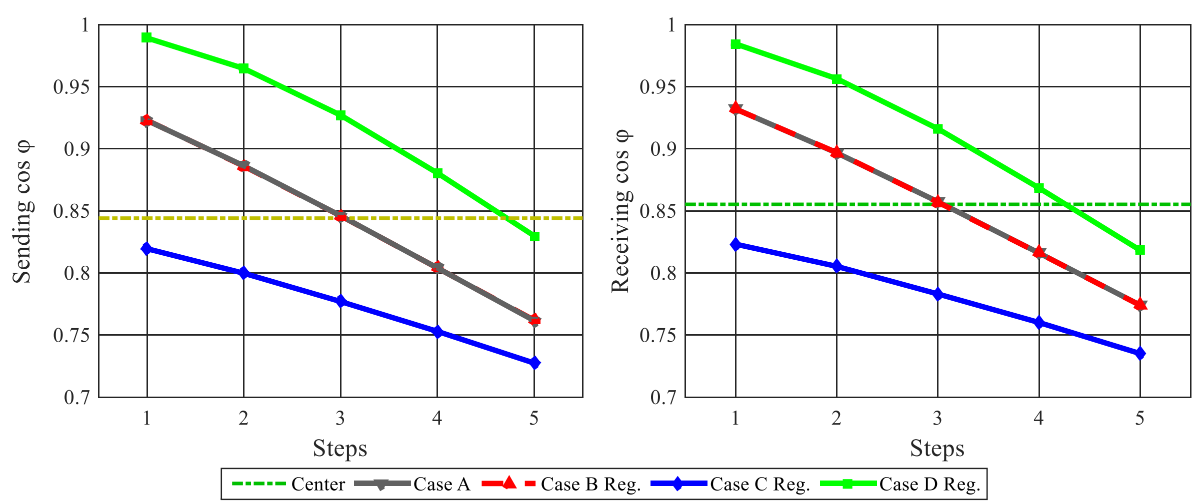


*Fig 5.32 Average value of sending and receiving power factor in Case A, B, C and D for wind speeds 5, 10, and 15 m/s with regulator*

The power factor observed is vividly clearer in fig 5.32. Here, it is observed that Case C is the worst situation and Case A and B had the same values between 0.75 and 0.92. Equally, Case D is the best scenario, owing to the fact that the power factor values observed is between 0.84 and

0.99. Hence, with low power factor the amount of apparent power is increase though the work power KW is same. This associates some significant losses both in the transmission line and in the consumer side.

## 5.5 Comparing Results Before and After Automatic Regulation

For the purpose of this thesis write-up, comparing will be for one line and one wind speed in order to specify the differences easily and clearly. So, the chosen line will be line 2, since it is generally a normal line. Although line 3 could have been chosen too, but not line 1, since Case C is different from all other lines and the chosen speed will be 5 m/s in order to study the regulation process when the generated active power is very low. Therefore, comparing will be for four parameters, which are ($V_s$ deviation%, $V_{r1}$ deviation, $\Delta V\%$ and $\Delta P\%$ ).

### 5.5.1 $V_s$ Deviation%

Fig 5.33 illustrates the sending voltage deviation as a percentage to the nominal voltage of the sub-station (66 kV) for all cases where:

- Case A (no regulation) which is the worst case and the voltage deviation is from -2.25% to -3 %.
- Case (B, Reg.) is better than Case (B) where voltage deviation for (B, Reg) is between -0.75% to -1.25%. While for Case B without regulation it is between -1.7% to -1.9%.
- Case (C, Reg) is better than Case (C) where voltage deviation for (C, Reg) is between -0.9% to -1.5%, while for Case C it is between -1.8% to -1.9%.
- Case (D, Reg) is better than Case (D), since the voltage deviation for (D, Reg) is (-1% to -1.7%) while for case D it is (-1.75% to -1.9%).

Therefore, it could be concluded that the performance of the sub-station (S.s) for these parameters after using the regulator is better than before using it.

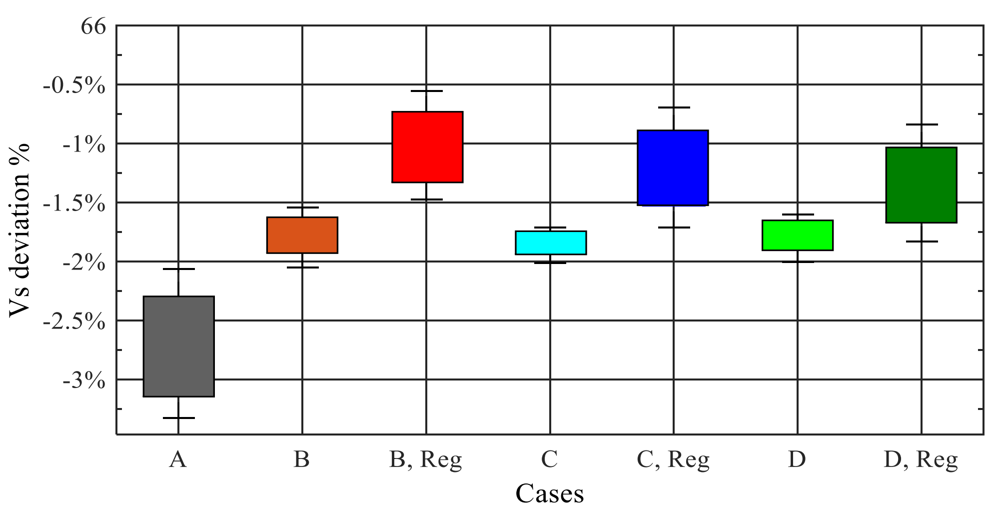


*Fig 5.33 Percentage of sending voltage deviation before and after using regulator.*

### 5.5.2 $V_{r1}$ Deviation%

Fig 5.34 illustrates the receiving voltage deviation of line 2 as a percentage of the nominal voltage of S.s (66 kV) for all Cases, the following observations were made:

- Case A (no regulation) is the worst Case and the voltage deviation is between -8% to -10.5 %.
- Case (B, Reg) is better than Case (B) where voltage deviation for (B, Reg) is between -6.5% to -8.5%, while for Case B it is between -8% to -9%.
- Case (C, Reg) is better than Case (C) where voltage deviation for (C, Reg) is between -7% to -9%, while for Case C it is between -8% to -9%.
- Case (D, Reg) is better than Case (D) where voltage deviation for (D, Reg) is between -4.5% to -6%, while for Case D, it is between -6% to -7%.

Therefore, the performance of the S.s for these parameters after using the regulator is better than before using it.

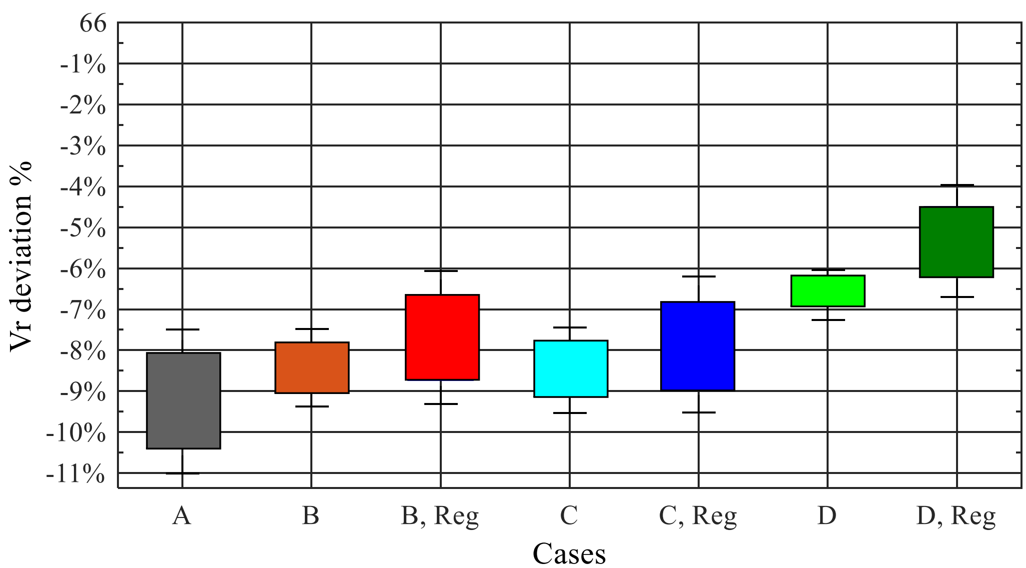


*Fig 5.34 Percentage of receiving voltage deviation before and after using regulator for line 2.*

### 5.5.3 $\Delta V$ %

Fig 5.35 illustrates the voltage drop of line 2 as a percentage of the voltage drop of step 1 of Case A (3.585 kV) for all Cases and the following observations were made:

- Cases (A), (B), (B, Reg), (C) and (C, Reg) are very similar to each other where $\Delta V\%$ is between 10% to 35%.
- Cases (D) and (D, Reg) are the best, but Case (D, Reg) is better than Case (D) since decrease of voltage drop for (D, Reg) is between -15% to -35%, while for Case D it is between -5% to -15%.

Therefore, the performance of the S.s for this parameter after using regulator is better than before using it.

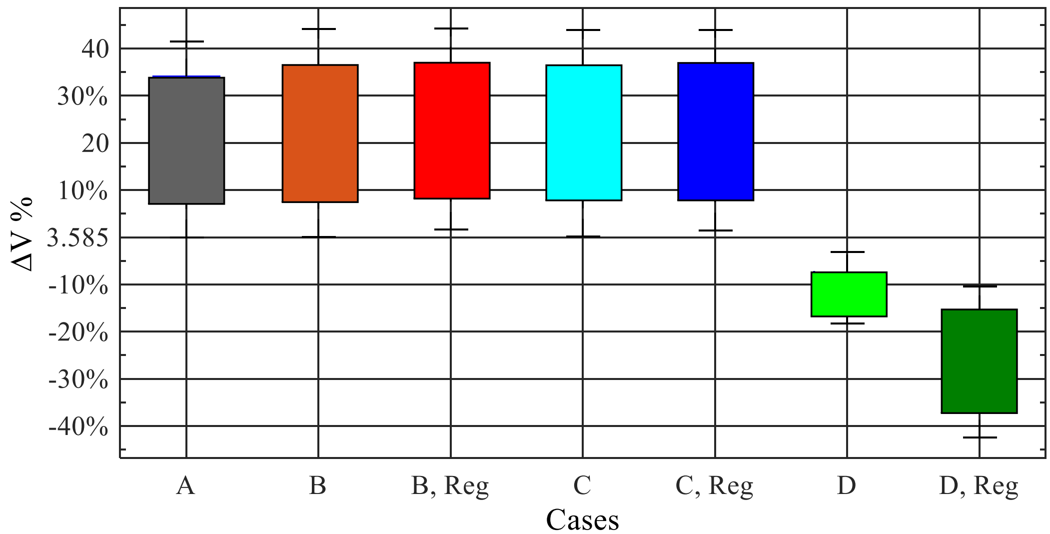


*Fig 5.35 Voltage drop of line 2 as a percentage to the voltage drop of step 1 of case A (3.585 kV)*

## 5.5.4 Δ*P* %

Fig 5.36, represents the power losses of line 2 as a percentage of the power losses of step 1 of Case A (0.509 MW) for all Cases and the following observations were made:

- Case (A), (B), (B, Reg), (C) and (C, Reg) have close values.
- Increase of power losses for Case A (no regulation) is between 2% to 12 %.
- Case (B) is better than Case (B, Reg) where increase of power losses for (B) is between 2% to 16%, while for case (B, Reg) it is between 5% to 17%.
- Case (C) is better than Case (C, Reg) where increase of power losses for (C) is between 2% to 15%, while for case (C, Reg) it is between 5% to 17%.
- Case (D, Reg) is better than Case (D) where decrease of power losses for (D, Reg) is between -13% to -17%, while for case D it is between -10% to -18%.

Therefore, the performance of the S.s for this parameter after using the regulator is better than before using the regulator for scenario D and worse than it for scenarios B and C.

So, after comparing results before and after using the regulator it can be concluded that performance of S.s after using the regulator is better than before the regulator is used in general, but the best scenario for applying the regulator on the simulation scheme of this thesis is scenario D.

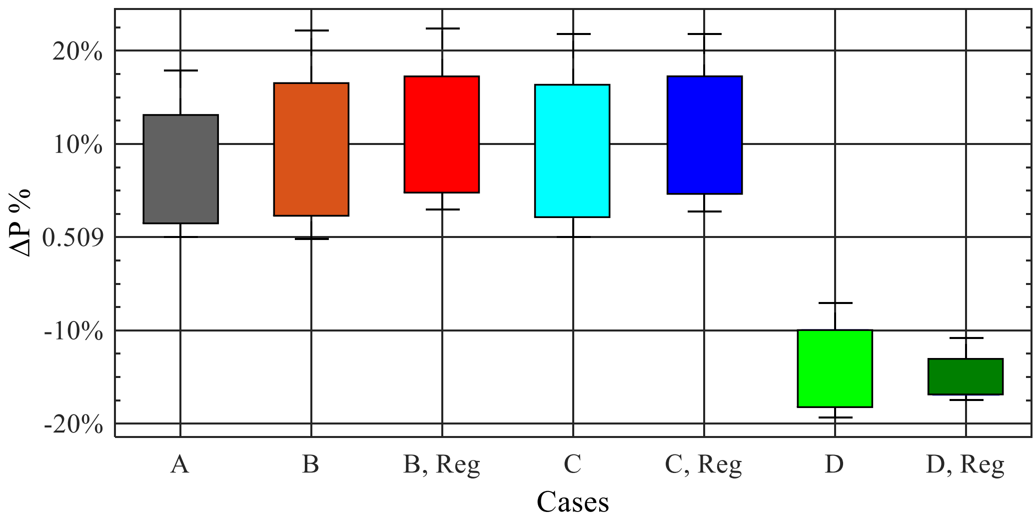


*Fig 5.36 Power losses of line 2 as a percentage to the power losses of step 1 of case A (0.509 MW)*

The power losses for one line and one speed (for example: line 2 and wind speed 10 m/s) can be analyzed by calculating power losses for each Case as a percentage of Case A for all steps with the percentage of apparent power curve as illustrated in fig 5.37. It depicts that an increase of power losses for Case B and C as a percentage of power losses of Case A is very little, that is between 2% to 4 %. Comparing and increasing of the apparent power of the line (0% in step 1 to 17% in step 5). In addition, the decrease of power losses in Case D and D, Reg is of very large value and the decrease of power losses become even larger for each new step observed. where the decrease for step 1 is (-47 % for Case D and -53% for Case D, Reg) and for step 2 (-51% for Case D and -56% for case D, Reg).

Therefore, after comparing the results before and after using the regulator it could be concluded that the performance of S.s after using the regulator is better than before it is general used, but the best scenario to apply the regulator on the simulation scheme of this thesis is the scenario for Case D.

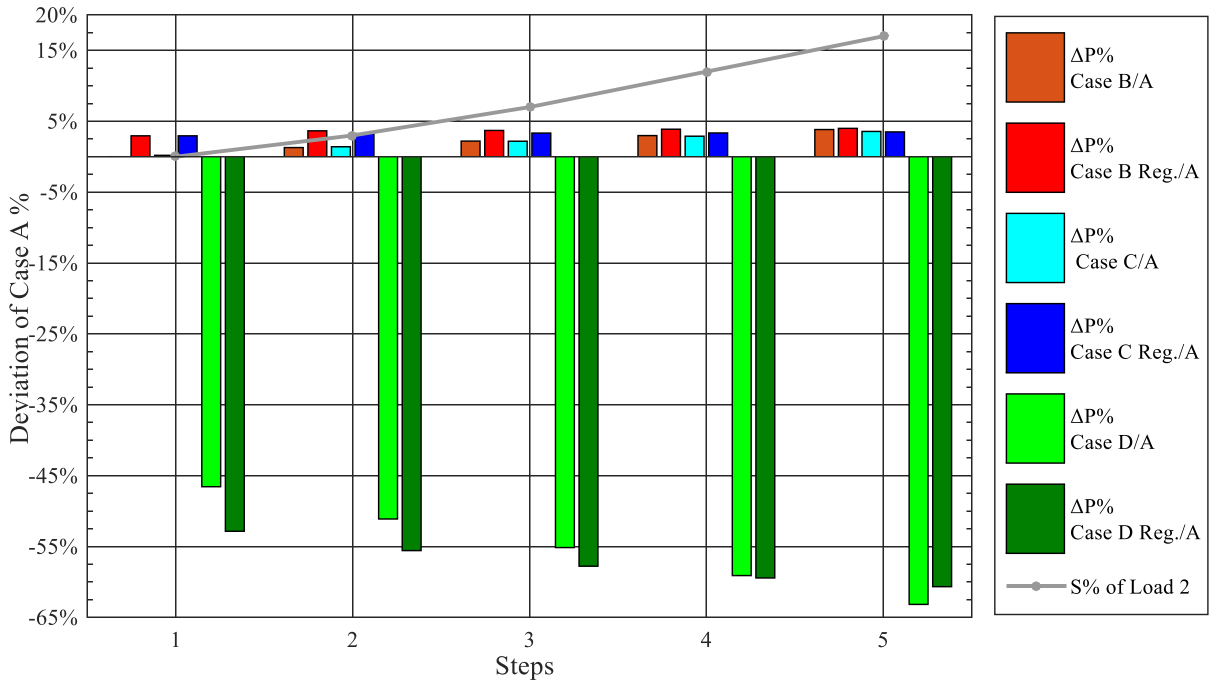


*Fig 5.37 Deviation of power losses of cases as a percentage of case A for line 2 and speed 10 m/s for all steps.*

## 5.6 General Comparing

A general comparison is needed to show the general performance of all scenarios before and after using the regulator. Therefore, fig 5.38 shows the general values of all lines and wind speeds for $V_s$, $V_r$, $\Delta V$ and $\Delta P$ parameters for each Case as a percentage to Case A. The following observations were made:

1- (Case B/ Case A) %:

Power losses and voltage drop increased slightly with about 2%, whereas the sending voltage increased significantly to between 36 % to 64%. Also, the receiving voltage increased from 10% to 17 %. In general, the performance after using the regulator is better than before using it.

2- (Case C/ Case A) %:

Power losses and voltage drop decrease between -10% to -16% for power losses and between -14% to -18% for voltage drop, while the sending voltage significantly increases from 35 % to 56%. Also, the receiving voltage increases from 32% to 48 %. In general, the performance of the scheme after using the regulator is far better than before using the regulator for sending and receiving voltage, but a worse or bad scenario is experienced for power losses and voltage drop.

3- (Case D/ Case A) %:

Power losses and voltage drop decreases, from -50% to -53% for power losses and -36% to -47% for voltage drop, while sending voltage increases significantly from 38 % to 53%. Also, receiving voltage increases from 37% to 48 %. Overall, the performance of the simulation scheme after using the regulator is far better than before using the regulator.

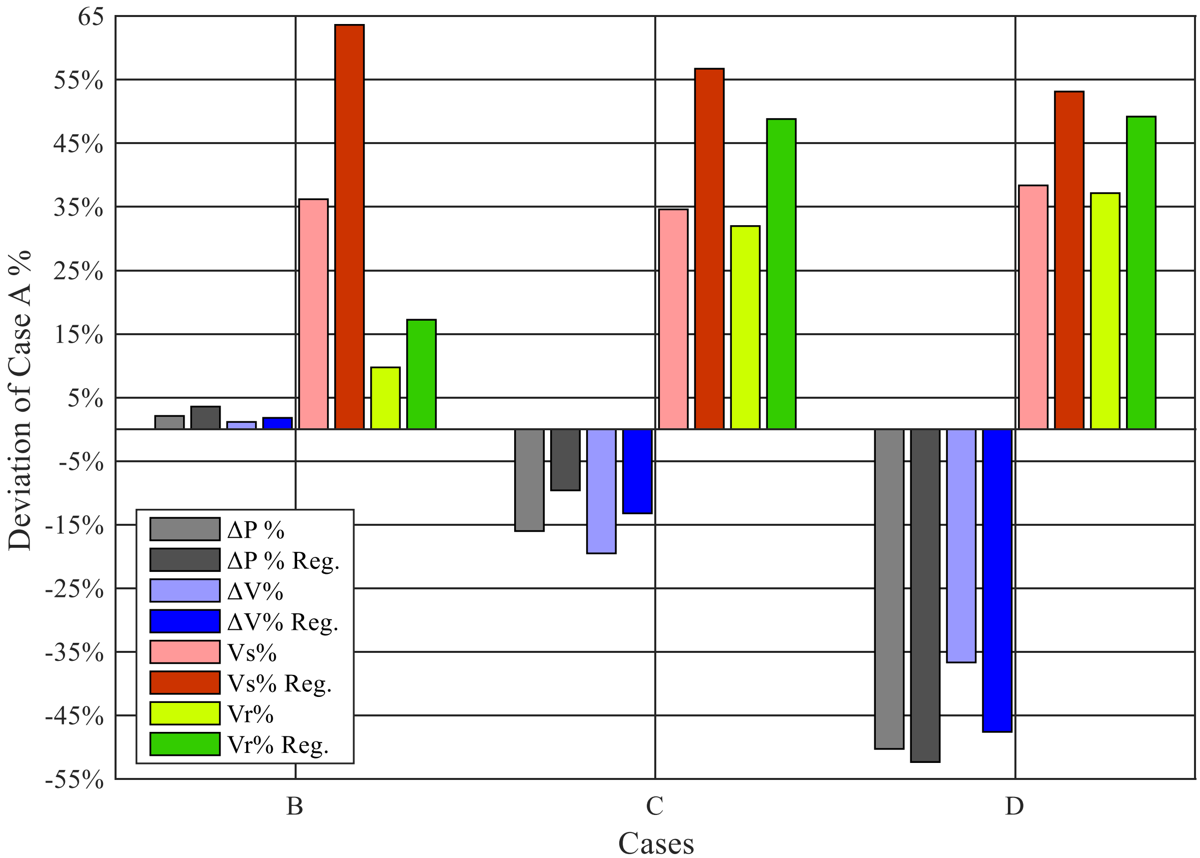


*Fig 5.38 General comparison of all Cases as a percentage to Case A for $V_s$, $V_r$, $\Delta V$ and $\Delta P$ parameters*

According to the results and function of power losses $f(losses) \vdots A_{ka}, L_{kl}, D_{kd}$ the following points can be deduced:

$A_{ka}$: The position of power injected play the most vital role in reducing power losses, which according to the results obtained from the scenario for Case D is the best, scenario for Case C is very good and the scenario for Case B is good. Also, the reactive power injected is responsible for the reduced power losses and voltage drop while the active power injected played just a small role.

$L_{kl}$ : Increasing the loads power, especially that of reactive power results in an increase of power losses, in which the power losses are directly proportional to the square of current. Also, the length of line has effect on the losses, in which the power losses is directly proportional to the length and resistance.

$D_{kd}$ : Utilizing the wind farm depends on the synchronous generator which can generate reactive power and also full scale IGBT back-to-back voltage source converter, so that it can generate reactive power independently of active power is the most suitable compensation device, since it allows the control and the injection of reactive power and voltage in wide range and in an easy manner. In addition, using a regulator depends on the values of the sending and receiving voltages and the voltage drop of all lines is a very suitable mechanism to control the reactive power injected according to the results obtained so far. It is observed that the performance of the S.s is better after utilizing the regulator.

Table 5.7 shows the performance of each Case compared to Case A. Where Case D with the regulator is adjudged the best Case.

*Table 5.7 The performance of Case B, C, and D compared to Case A*

| Case / Parameter | B | B, Reg | C | C, Reg | D | D, Reg |
|---|---|---|---|---|---|---|
| $V_s$ | Very good | Excellent | Very good | Excellent | Very good | Excellent |
| $V_r$ | Good | Good | Very good | Excellent | Very good | Excellent |
| $\Delta V$ | Acceptable | Acceptable | Good | Good | Excellent | Excellent |
| $\Delta P$ | Acceptable | Acceptable | Good | Good | Excellent | Excellent |

# Chapter 6

# 6 Validation of the Simulation Capability

MATLAB/Simulink have been well verified and validated in previous studies, as can be seen in the literature review section of this thesis. But since the simulation models of this thesis are novel, they must be verified to ensure that the capability of these simulation models is accurate. In all, two verification studies to test the accuracy of the model were carried out: The first verification exercise compared the results from the voltage/time-domain, obtaining results for the transient state, thereby showing stability of the model. Thereafter an equation was also used to validate the simulation model. The results of all the verification exercises were favorable.

## 6.1 Stability

The following figures shows the sending and receiving voltage of the simulation model, where stability of the modal is clear. Fig 6.1 shows the transient state of sending voltage where the voltage is swinging around the steady state at first then becomes stable after 0.1 seconds. Also, fig 6.2 shows the transient state of receiving voltage of line 1, where the voltage becomes stable after 0.15 seconds. Fig 6.3 represents the transient state of current of line 1. Here, the current becomes stable after 0.75 seconds. Fig 6.4 depicts the transient state of $Q_{ref}$ of line 1 where $Q_{ref}$ becomes stable after 0.15 seconds ,

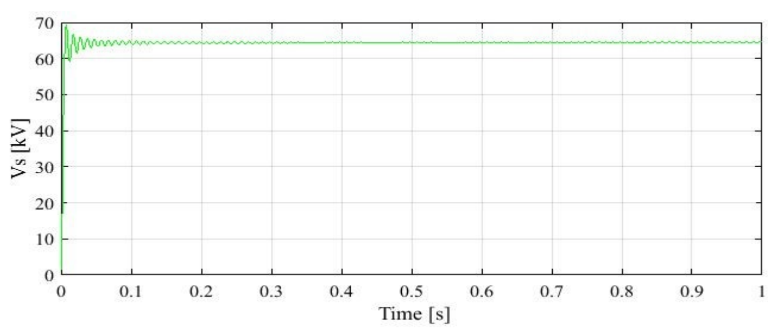


*Fig 6.1 Sending voltage curve*

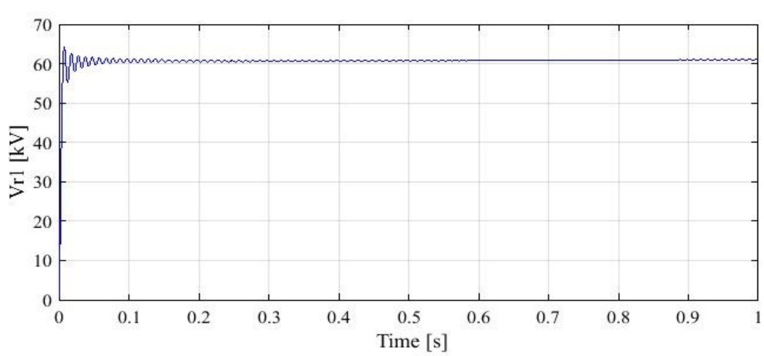


*Fig 6.2 Receiving voltage curve of line 1*

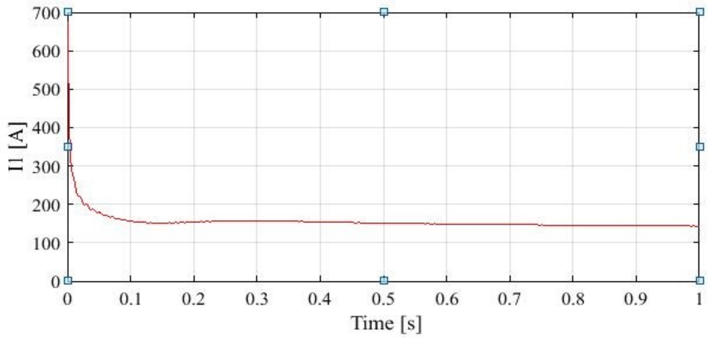


*Fig 6.3 Current curve of line 1*

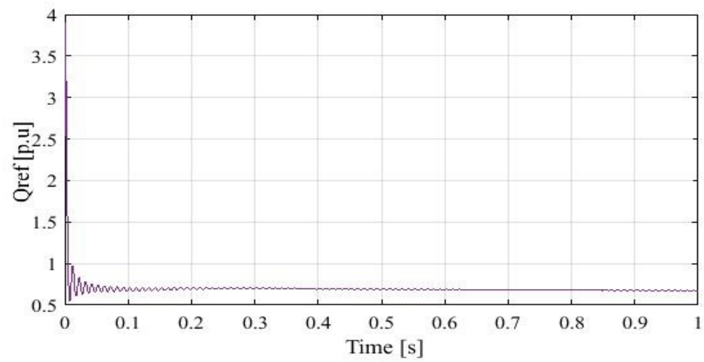


*Fig 6.4 Q $_{ref}$ of line 1*

# 6.2 Equations

Here, the value of one of the parameters is calculated and then compared with the measured value to make sure that the simulation model is valid. For example:

From measurement of (line 1, case D, wind speed 10, step 3) which has resistance $R_{1L} = 5.765\Omega$:

$$\Delta P = 251\ kW$$

$$I_{1L,M} = 120.24\ \text{A}$$

If the current of this line is calculated using the equation (4.5):

$$\Delta P = 3{I_{1L,C}}^2 \cdot R_{1L} \Longrightarrow$$

$$I_{1L,C} = \sqrt{\frac{\Delta P}{3R_{1L}}} = \sqrt{\frac{251 * 10^3}{3 * 5.765}} = 120.47\ A \Longrightarrow$$

$$I_{1L,M} \approx I_{1L,C}$$

Therefore, the measured and calculated values ($I_{1L,M}$ and $I_{1L,C}$) of current is very close. Hence, the simulation model is valid.

# Chapter 7

# 7 Conclusion and Future Research

The vast wind resource represents a potential to use wind turbines to power much of the world with renewable energy source. Many wind turbine concepts had been proposed, but few had or could have been evaluated since available modeling capabilities were limited. These limitations motivated the development of the simulation capability for modeling the scheme of this thesis. As presented in Chapter 4, the electrical, mathematical, the regulator and the wind turbine models were developed, all this combining to make up the methodologies of the wind turbine and wind farm utilized in this thesis. The simulation capability was developed with enough sophistication to address the primary limitations of the previous voltage- and time-domain studies. In addition, the simulation MATLAB/Simulink program has the features required to perform integrated loads analyses. To make it useful for examining the technical feasibility of a wind turbine concepts, the simulation capability is universal enough to analyze a variety of turbine, and support platform.

To support this and other concept studies aimed at assessing wind technology, the specifications of a representative commercial benchmark and a utility-scale wind farm was developed. In Chapter 5, the development of this wind farm has been discussed and gave an overview of the properties. Also in Chapter 5, the data of a reference benchmark is given. The wind turbine used, and data in the model-verification, loads analysis, and controls-development efforts were also given.

Through comparisons of the regulated and non-regulated data's, the newly developed simulation capability is checked to ensure correctness, as presented in Chapter 5. Finally, the results from voltage/time-domain analysis were shown to agree with results generated from an equation-calculated-domain approach. The results of all the verification exercises were favorable as presented in Chapter 6.

In summary of the accomplishments of this thesis, it has satisfied the thesis objectives by

- Using wind farm to reduce losses in a substation and regulating the voltage do not always lead to the required goal, where it is related in a significant way is by positioning it correctly. When connected to the wrong position, it will increase the power losses and voltage drop.
- When the wind farm is connected to one line the high demand of reactive power will cause a problem on the first line where the voltage at the injection point will increase significantly especially when the wind speed is high.
- Using regulator rely on algorithm takes into accounts sending and receiving voltages and drop voltage of all lines is very important when a wind farm with synchronous generator and full scale converter is being used, since such wind farms could cause in some situations high reactive power demand or line faults, resulting in high voltage values to one or more lines.

- Using the regulator is suitable when the substation is supplied from different sources or other renewable energy like another wind farm or solar farm.

To arrive at a technically and economically feasible concept, modifications to the system designs in this thesis are still required. Suggested design modifications and active and passive regulated features that could potentially improve the turbine response, and eliminate any instabilities. The recommended future research entails:

- Research about the effect of using solar farm with wind farm to the same substation, which will be very useful to finding the best method of positioning each farm and also the best regulator for such system.
- Development of regulator characteristics for transient events (faulted states) in the system and regulator settings possibilities in case of system configuration change or several generation outages.

# Chapter 8

# 8 Literatures

## 8.1 References

[1] Darrell M. Dodge, Illustrated History of Wind Power Development, Littleton, Colorado, [Online] Available from: http://telosnet.com
[2] Shepherd, Dennis G. Historical development of the windmill. Wind Turbine Technology, Cornell University, Ithaca, New York, 1990.
[3] History of Wind Energy, [Online] Available from: http://energy.gov
[4] History of Wind Energy, [Online] Available from: http://www.iowaenergycenter.org
[5] Christine Meisner Rosen and Christopher C. Sellers, "The Nature of the Firm: Towards a Ecocultural History of Business", Business History Review, 73 (1999), pp.577-606
[6] Hartmutt Berghoff and Mathias Mutz, "Missing Links? Business History and Environmental Change," Jahrbuch für wirtschaftsgeschichte, 2 (2009), pp.9-21.
[7] Andre J. Hoffman, From Heresy to Dogma. An Institutional History of Corporate Environmentalism (Stanford: Stanford University Press, 2001.
[8] Daniel Boullet, Entreprises et Environnement en France de 1960 a 1990.
[9] Les Chemins d'une prise de conscience, Geneva and Paris: Librairie Droz, 2006.
[10] Ion Bogdan Vasi, Winds of Change; The Environmental Movement and the Global Development of the Wind Energy Industry (Oxford: Oxford University Press, 2011), pp. 3-5.
[11] U.S. Department of Energy, "Wind Powering America: Installed U.S. Wind Capacity," and Global Wind Energy Council, Global Wind 2007 Report, p. 10.
[12] OECD/IEA, World Energy Outlook 2010, p. 306
[13] Janet L. Sawin, "Mainstreaming Renewable Energy in the 21st Century," Worldwatch Paper 169 (May 2004) p. 8 Vasi, Winds, p. 4.
[14] Katherine L. Dykes and John D. Sterman, "Boom and Bust Cycles in Wind Energy Diffusion Due to Inconsistency and Short-term Bias in National Energy Policies," ICSD 2010 Conference Proceedings, July 25-30, 2010.
[15] Clayton M. Christensen, Shuman Talukdar, Richard Alton and Michael B. Horn, "Picking Green Tech‟s Winners and Losers," Stanford Social Innovation Review, Spring 2011, p. 33.
[16] Richard Vietor, "Supergrid", Harvard Business School Case No 9-707-016, November 4, 2008, p. 2.
[17] Paul Gipe, Wind Energy Comes of Age, John Wiley: New York, 1995, p. 14.
[18] Wesley D. Sine and Brandon H. Lee, "Tilting at Windmills? The Environmental Movement and the Emergence of the US Wind Energy Sector," Administrative Science Quarterly, 54, 2009, pp. 123-155.
[19] Jones, Geoffrey Gareth, and Loubna Bouamane. "Historical trajectories and corporate competences in wind energy." Harvard Business School Entrepreneurial Management Working Paper 11-112 (2011).
[20] Zachary Shahan, History of Wind Turbines, Renewable energy world, Nov 21, 2014.
[21] Andy Biggs, A short history of photovoltaic solar power, August 5, 2012, [Online] Available from: http://www.evwind.es

[22] Photovoltaic (Solar Electric), [Online] Available from: http://www.seia.org
[23] Sunlight Electric, Photovoltaic History, [Online] Available from: http://www.sunlightelectric.com
[24] The Florida Solar Energy Center (FSEC), History of Photovoltaics, University of Central Florida, [Online] Available from: http://www.fsec.ucf.edu
[25] Perlin J. A history of photovoltaics. University of Southern California. 2009.
[26] Mary Bellis, History: Photovoltaics Timeline, [Online] Available from: http://inventors.about.com
[27] History of Photovoltaic (PV) Solar Energy, [Online] Available from: http://ariseenergy.com
[28] The History of Solar, [Online] Available from: https://www1.eere.energy.gov
[29] A Short History of Photovoltaic (PV) Cells, [Online] Available from: http://www.schoolgen.co.nz
[30] Paula Mints, The Solar PV Ecosystem, A Brief History and a Look Ahead, Renewable Energy World, November 20th, 2012.
[31] Dosoglu, M. K.; Arsoy, A. B. Enhancement of a reduced order doubly fed induction generator model for wind farm transient stability analyses. Turk J Elec Eng & Comp Sci 2016; 24: 2124 – 2134.
[32] Michalke, G; Hansen, A. D.; Hartkopf, T. Control strategy of a variable speed wind turbine with multipole permanent magnet synchronous generator. In Proceedings of European Wind Energy Conference and Exhibition, Milan, Italy, 7–10 May 2007.
[33] Merabet, A.; Keeble, R.; Rajasekaran, V.; Beguenane, R.; Ibrahim, H.; Thongam, J. S. Power Management System for Load Banks Supplied by Pitch Controlled Wind Turbine System. Appl. Sci. 2012; 2(4): 801-815.
[34] Shaaban, M.; Usman, M. D. Quantitative risk associated with intermittent wind generation. Turk J Elec Eng & Comp Sci 2016; 24: 3144 – 3157.
[35] Izgi, E.; Kaymak, M. K.; Oztopal, A.; Durna, B.; Sahin, A. D. Variations and relations of meteorological parameters between upwind and downwind small-scale wind turbine rotor area. Turk J Elec Eng & Comp Sci 2016; 24: 1091 – 1098.
[36] Stiel, A.; Skyllas-Kazacos, M. Feasibility Study of Energy Storage Systems in Wind/Diesel Applications Using the HOMER Model. Appl. Sci. 2012; 2(4): 726-737.
[37] Ghosh, S.; Saha, P. K.; Panda, G. K. Wind Energy Conversion System Connected with Grid Using Permanent Magnet Synchronous Generator (PMSG). International Journal of Advanced Research in Electrical, Electronics and Instrumentation Engineering 2015; Vol. 4, Issue 1: 120 – 127.
[38] Karki, R.; Dhungana, D.; Billinton, R. An Appropriate Wind Model for Wind Integrated Power Systems Reliability Evaluation Considering Wind Speed Correlations. Appl. Sci. 2013; 3(1): 107-121.
[39] Ahmed, M. A.; Pan, J.; Song, M.; Kim, Y. Communication Network Architectures Based on Ethernet Passive Optical Network for OffshoreWind Power Farms. Appl. Sci. 2016; 6, 81: 1 – 14.
[40] Fandi, G.; Igbinovia, F. O.; Müller, Z.; Švec, J.; Tlusty, J. Using renewable wind energy resource to supply reactive power in medium voltage distribution network. In: IEEE 2015 16th International Scientific Conference on Electric Power Engineering (EPE); 20-22 May 2015, Ostrava, Czech Republic: IEEE. 169 – 173.

[41] Fandi, G.; Igbinovia, F. O.; Švec, J.; Müller, Z, Tlustý J. Advantageous positioning of wind turbine generating system in MV distribution network. In: IEEE 2016 17th International Scientific Conference on Electric Power Engineering (EPE); 16– 18 May 2016: Paper L123.
[42] Yukon Government, Independent Power Production, Energy, Mines and Resources, 27th October, 2015. [Online] Available from: http://www.energy.gov.yk.ca
[43] M. Abdel-Akher, M. M. Aly, Z. Ziadi, H. El-kishky, and M. A. Abdel-Warth, “Voltage stability modeling and analysis of unbalanced distribution systems with wind turbine energy systems,” IEEE International Conference on Industrial Technology (ICIT), Feb. 26 - Mar. 1, 2014, Busan, Korea, pp. 565 – 570.
[44] J. Tamura, “Calculation method of losses and efficiency of wind generators,” S. M. Muyeen (ed.), Wind Energy Conversion Systems, Green Energy and Technology, Springer-Verlag London Limited 2012, pp. 25-51.
[45] Wirth H, Schneider K. Recent facts about photovoltaics in Germany. Report from Fraunhofer Institute for Solar Energy Systems, Germany. April 22, 2016.
[46] Makrides, G., Zinsser, B., Norton, M., Georghiou, G.E., Schubert, M., Werner, J.H., Potential of photovoltaic systems in Countries with high solar irradiation. Renewable Sustainable Energy Rev. 14, 2010, pp. 754–762.
[47] Kumar BS, Sudhakar K. Performance evaluation of 10 MW grid connected solar photovoltaic power plant in India. Energy Reports. 2015 Nov 30; Vol. 1: pp. 184-192.
[48] Nykamp S. Integrating renewables in distribution grids: storage, regulation and the interactions of different stakeholders in future grids, PhD thesis, University of Twente; Oct 18th, 2013.
[49] Klose F, Kofluk M, Lehrke S, Rubner H., Toward a distributed-power world. Renewables and smart grids will reshape the energy sector. The Boston Consulting Group Report. Jun 2010.
[50] Nicholas Abi-Samra, Renewables challenge transmission and distribution paradigms, Smart Grid News, A publication of Fierce Markets, a division of Questex, LLC. November 13, 2012.
[51] Watson, G., et al, “A Framework for Offshore Wind Energy Development in the United States,” Massachusetts Technology Collaborative (MTC); U.S. Department of Energy; GE Energy, September 2005.
[52] Henderson, A. R., Morgan, C. S., Smith, B., Sørensen, H. C., Barthelmie, R. J., and Boesmans, B., “Offshore Wind Energy in Europe — A Review of the State-of-the-Art,” Wind Energy, Vol. 6, No. 1, February 2003, pp. 35–52.
[53] Musial, W. and Butterfield, S., “Future for Offshore Wind Energy in the United States,” Energy Ocean Proceedings, June 2004, Palm Beach Florida, USA, NREL/CP-500-36313, Golden, CO: National Renewable Energy Laboratory.
[54] John Ware, Power Factor Correction, IEE Wiring Matters, Spring 2006, www.iee.org. pp. 22-24.
[55] Antonia Nasiakou, Manolis Vavalis, and Dimitrios Bargiotas, Simulating Active and Reactive Energy Markets, http://ireteth.certh.gr
[56] Ray Sladky, Tom Gilmore, Glenn Frazier, Dan Jaszkowski, Distribution System Disturbances and its Effects on Voltage Source Inverter Drives. Allen-Bradley Co. https://www.ab.com July 1995.
[57] George G. Karady, Saurabh Saksena, Baozhuang Shi, Nilanjan Senroy, Effects of Voltage Sags on Loads in a Distribution System, Power Systems Engineering Research Center (PSERC) Publication 05-63. Cornell University, Ithaca, New York, October 2005.

[58] Ken Kutsmeda, Specifying medium-voltage distribution, Consulting-Specifying Engineer, 19th September 2012.
[59] Power supply at medium voltage, Electrical Installation, [Online] Available from: http://www.electrical-installation.org
[60] Power Distribution Systems, EATON, CA08104001E, April 2016
[61] Michael Mosman, Medium Voltage Electrical System for Data Centers CCG Facilities Integration Incorporated 15 September 2012. http://www.ccgfacilities.com
[62] Farah Saeed, Overview of the Medium Voltage Power Distribution Equipment Market, Utility Products, http://www.utilityproducts.com
[63] Ziari, I., 2011. Planning of Distribution Networks for Medium Voltage and Low Voltage (Doctoral dissertation, Queensland University of Technology).
[64] Burman K, Olis D, Gevorgian V, Warren A, Butt R, Lilienthal P, Glassmire J. Integrating renewable energy into the transmission and distribution system of the us virgin islands. National Renewable Energy Laboratory (NREL), Golden, CO., Tech. Rep. 2011 Sep 1.
[65] Skov T, Sales S. Trending Toward Distributed Voltage Optimization: A Simple Solution Overlooked. Proceedings of the Newsletters of Transmission & Distribution World, New York, NY, USA. 2013 Jun;4.
[66] Camacho EF, Samad T, Garcia-Sanz M, Hiskens I. Control for renewable energy and smart grids. The Impact of Control Technology, Control Systems Society. 2011 Feb:69-88.
[67] Phuangpornpitak N, Tia S. Opportunities and challenges of integrating renewable energy in smart grid system. Energy Procedia. 2013 Dec 31;34:282-90.
[68] Frederic Dubois, Voltage control of distribution systems: the modern grid, DNV.GL, 14 May 2015.
[69] I. Erlich, M.Wilch, and C. Feltes, "Reactive power generation by DFIG based wind farms with AC grid connection," in Proc. 2007 Eur. Conf. Power Electronics and Applications, 2007, pp. 1–10.
[70] Arslan Ashraf. On Reactive Power Compensation of Wind Farms – Impact of Wind Farm Controller Delays. Master of Science Thesis in Electric Power Engineering. Department of Energy and Environment. Division of Electric Power Engineering. Chalmers University of Technology. Gothenburg, Sweden. June, 2012.
[71] M. P. Kazmierkowski, R. Krishnan, and F. Blaabjerg, Control in Power Electronics Selected Problems. San Francisco, CA, USA: Academic, 2002.
[72] Fandi, G, Švec, J, Müller, Z. The converter choice and its control circuit design for synchronous generators. In: 14th International Scientific Conference on Electric Power Engineering 2013; Ostrava, Czech Republic: pp. 697-701.
[73] Gonzialez F. D, Martinez-Rojas M, Sumper A, Gomis-Bellmunt O, Trilla L. Strategies for Reactive Power Control in Wind Farms with STATCOM. EPE Wind Energy Chapter, 3rd Seminar, 15-16 April 2010, Staffordshire University, UK.
[74] Yousuf S. M, Arthi S. Reactive Power Improvement in Wind Farm by Using UPQC. International Journal of Science and Research (IJSR) 2014; Volume 3 Issue 4: April 2014. 403-408.
[75] M. Milligan, K. Porter, E. DeMeo, P. Denholm, H. Holttinen, B. Kirby, N. Miller, A. Mills, M. O'Malley, M. Schuerger, and L. Soder, "Wind power myths debunked," IEEE Power Energy Mag., vol. 7, no. 6, pp. 89–99, Nov./Dec. 2009.
[76] F. Blaabjerg, M. Liserre, and K. Ma, "Power electronics converters for wind turbine systems," IEEE Trans. Ind. Appl., vol. 48, no. 2, pp. 708–719, Mar./Apr. 2012.

[77] Fandi G, Igbinovia F. O, Müller Z, Švec J, Tlusty J. Using renewable wind energy resource to supply reactive power in medium voltage distribution network. In: IEEE 2015 16th International Scientific Conference on Electric Power Engineering (EPE); 20-22 May 2015, Ostrava, Czech Republic: IEEE. pp. 169 – 173.
[78] Fandi G, Igbinovia F. O, Švec J, Müller Z, Tlustý J. Advantageous positioning of wind turbine generating system in MV distribution network. In: IEEE 2016 17th International Scientific Conference on Electric Power Engineering (EPE); 16– 18 May 2016.
[79] Electrical Power Distribution System | Radial and Ring Main. [Online] Available from: http://www.electrical4u.com
[80] Chan F.C. Electric Power Distribution Systems. Electrical Engineering, Vol. III, Encyclopedia of Life Support Systems (EOLSS), [Online] Available from: http://www.eolss.net
[81] Electricity Distribution. Institute for Energy Research. 2nd September, 2014. [Online] Available from: http://instituteforenergyresearch.org
[82] Pathway to Power. Mayfield Electric & Water Systems. [Online] Available from: http://www.mayfieldews.com
[83] What is the Smart Grid? US Department of Energy's Office of Electricity Delivery and Energy Reliability (OE). [Online] Available from: https://www.smartgrid.gov
[84] Eurelectric, "The role of electricity," The Union of the Electricity Industry, Bruxelles, Belgium, 2007, Tech. Rep.
[85] M. Prodanovic and T. Green, "High-quality power generation through distributed control of a power park microgrid," IEEE Trans. Ind. Electron. , vol. 53, no. 5, pp. 1471–1482, Oct. 2006.
[86] Palensky, P. Dietrich, D. Demand side management: Demand response, intelligent energy systems, and smart loads. IEEE transactions on industrial informatics, 2011, 7.3: 381-388.
[87] Balaji R. Dispersed Generation - Future Evolution of Distribution System. 5th November 2004. [Online] Available from: https://www.frost.com
[88] Pentland W. America's Most Dispersed Power System. [Online] Available from: 7TH April, 2013. http://www.forbes.com
[89] Haskard J. What is Dispersed Generation & How Might it Work in My Region of MN? 26th June, 2008. [Online] Available from: http://www.cleanenergyresourceteams.org
[90] Forsyth T, Baring-Gould I. Learn About Distributed Wind. National Renewable Energy Laboratory, Distributed Wind Energy Association (DWEA) 2007. [Online] Available from: http://distributedwind.org
[91] What is Distributed Wind, US Department of Energy, Office of Energy Efficiency & Renewable Energy. [Online] Available from: http://www.energy.gov
[92] Forsyth T. Baring-Gould I. Distributed Wind Market Applications, Technical Report, National Renewable Energy Laboratory, A national laboratory of the U.S. Department of Energy, Office of Energy Efficiency & Renewable Energy November 2007. [Online] Available from: http://www.nrel.gov
[93] (2012, Jun.). REN21—Renewables 2012 Global Status Report [Online]. Available: http://www.ren21.net
[94] (2010, Sep.). Green Energy—The Road to a Danish Energy System Without Fossil Fuels [Online]. Available: http://www.klimakommissionen.dk/en-US
[95] Blaabjerg F, Ma K. Future on power electronics for wind turbine systems. IEEE Journal of Emerging and Selected Topics in Power Electronics. 2013 Sep;1(3):139-52.
[96] Vestas Wind Power, Aarhus, Denmark. (2011, Apr.). Wind Turbines Overview [Online]. Available: www.vestas.com

[97] M. Liserre, R. Cardenas, M. Molinas, and J. Rodriguez, “Overview of multi-MW wind turbines and wind parks,” IEEE Trans. Ind. Electron., vol. 58, no. 4, pp. 1081–1095, Apr. 2011.
[98] Z. Chen, J. M. Guerrero, and F. Blaabjerg, “A review of the state of the art of power electronics for wind turbines,” IEEE Trans. Power Electron., vol. 24, no. 8, pp. 1859–1875, Aug. 2009.
[99] F. Blaabjerg, Z. Chen, and S. B. Kjaer, “Power electronics as efficient interface in dispersed power generation systems,” IEEE Trans. Power Electron., vol. 19, no. 5, pp. 1184–1194, Sep. 2004.
[100] A. D. Hansen, F. Iov, F. Blaabjerg, and L. H. Hansen, “Review of contemporary wind turbine concepts and their market penetration,” J. Wind Eng., vol. 28, no. 3, pp. 247–263, 2004.
[101] Rafi, S. H.; Ferdous, R. A.; Sheikh, M. R. I. Modeling and control strategy for variable speed wind turbine using permanent magnet synchronous generator. Rajshahi University Journal of Science & Engineering 2015; Vol. 43: 89-100.
[102] Vijayalakshmi, S. Modeling and control of A wind turbine using permanent magnet synchronous generator. International Journal of Engineering Science and Technology 2011; Vol. 3 No. 3: March 2011.
[103] Jöckel, S. High energy production plus builtin reliability – The new Vensys 70 / 77 gearless wind turbines in the 1.5 MW class. European Wind Energy Conference EWEC 2006; 27 February - 2 March 2006, Athens, Greece: Paper no. 0583.
[104] Binder, A.; Schneider, T. Permanent magnet synchronous generators for regenerative energy conversion – a survey. European Conference on Power Electronics and Applications (EPE) 2005; 11-14 Sept. 2005, Dresden, Germany: 10-P.10.
[105] Hussein, M. M.; Senjyu, T.; Orabi, M.; Wahab, M. A. A.; Hamada, M. M. Control of a Stand-Alone Variable Speed Wind Energy Supply System. Appl. Sci. 2013; 3(2): 437-456.
[106] Zhou, D.; Blaabjerg, F.; Franke, T.; Tønnes, M.; Lau, M. Comparison of wind power converter reliability with low-speed and medium-speed permanent-magnet synchronous generators. IEEE Transactions on Industrial Electronics 2015; Vol. 62, No. 10: 6575- 6584.
[107] Musial, W., Butterfield, S. and McNiff, B. “Improving Wind Turbine Gearbox Reliability”, EWEC 2007, Milan, Italy, May 7–10, 2007.
[108] Feng, Y., Qiu, Y., Crabtree, C. J., Long, H. and Tavner, P. J. “Use of SCADA AND CMS Signals for Failure Detection and Diagnosis of a Wind Turbine Gearbox”, Brussels, Belgium, 14-17 March 2011.
[109] Feng, Y., Qiu, Y., Crabtree, C. J., Long, H. and Tavner, P. J. “Monitoring wind turbine gearboxes, Wind Energy”, Published online in Wiley Online Library (wileyonlinelibrary.com). DOI: 10.1002/we.1521. 2012.
[110] Zipp, K. “Gears & Gearboxes 101”, Wind Power Engineering and Development, January 18, 2012. [Online]. Available from: http://www.windpowerengineering.com [Accessed: 29th July, 2016].
[111] Land and Sea Wind Turbines, [Online]. Available from: http://www.vassili-group.com [Accessed: 29th July, 2016].
[112] Patel, P. “GE Grabs Gearless Wind Turbines”, MIT Technology Review, September 23, 2009.
[113] 1.5 MW - The most popular wind turbine in its class, [Online]. Available from: http://www.regenpowertech.com [Accessed: 29th July, 2016].
[114] Direct Drive (Gearless) Wind Turbine Market, By Permanent Magnet (PMSG) & Electrically Excited (EESG) Generator Technology, Turbine Size/Capacity Range – Global

Trends & Forecasts to 2017, Markets and Markets, Report Code: EP 1269, October 2012, http://www.marketsandmarkets.com [Accessed: 29th July, 2016].
[115] Ragheb, M. "Modern Wind Generators", 2/28/2014, [Online]. Available from: http://mragheb.com [Accessed: 30th July, 2016].
[116] Courtice, B. "Rare earth magnets: not all new turbines are using them", March 6th, 2012. [Online]. Available from: https://yes2renewables.org [Accessed: 30th July, 2016].
[117] Blaabjerg F, Chen Z. Power electronics for modern wind turbines. Synthesis Lectures on Power Electronics. 2005 Dec 1;1(1):1-68.
[118] Gertmar L. Power Electronics and Wind Power. InProc. of EPE 2003.
[119] Iov F, Ciobotaru M, Blaabjerg F. Power electronics control of wind energy in distributed power systems. In Optimization of Electrical and Electronic Equipment, 2008. OPTIM 2008. 11th International Conference on 2008 May 22 (pp. XXIX-XLIV). IEEE.
[120] Hansen LH, Helle L, Blaabjerg F, Ritchie E, Munk-Nielsen S, Bindner HW, Sørensen PE, Bak-Jensen B. Conceptual survey of generators and power electronics for wind turbines. 2002.
[121] A. D. Hansen, F. Iov, F. Blaabjerg, and L. H. Hansen, "Review of contemporary wind turbine concepts and their market penetration," J. Wind Eng., vol. 28, no. 3, pp. 247–263, 2004.
[122] F. Blaabjerg, R. Teodorescu, M. Liserre, and A. V. Timbus, "Overview of control and grid synchronization for distributed power generation systems," IEEE Trans. Ind. Electron., vol. 53, no. 5, pp. 1398–1409, Oct. 2006.
[123] R. Teodorescu, M. Liserre, and P. Rodriguez, *Grid Converters for Photovoltaic and Wind Power Systems*. New York, NY, USA: Wiley, 2011.
[124] Hansen, A.D.; Michalke, G. Multi-pole permanent magnet synchronous generator wind turbines' grid support capability in uninterrupted operation during grid faults. Renew. Power Gener. 2009; Vol. 3, Iss. 3: 333–348.
[125] Wang, P.; Wang, H.; Cai, X.; Han, Z. Passivity-based robust controller design for a variable speed wind energy conversion system. Turk J Elec Eng & Comp Sci 2016; 24: 558 – 570.
[126] Jony, K. Beitrag zur Modellbildung dezentraler Elektroenergieversor. 1999 Germany: 50-125.
[127] Heier, S. Grid Integration of Wind Energy Conversion System. Germany: Wiley 2006.
[128] Brosh, P. F. Moderne Stromrichterantriebe. Vogel- Buchverlage 2008; Germany: 300.
[129] Singh, B.; Al-Haddad, K.; Chandra, A. Active power filter with sliding mode control. Proc. Inst. Electr. Eng. Gener. Transmiss. Distrib 1997; vol. 144, no. 6: 564–568.
[130] Ali, H.; Alaboudy, K.; Daoud, A. A.; Desouky, S. S.; Salem, A. A. Converter controls and flicker study of PMSG-based grid connected wind turbines. Ain Shams Engineering Journal, Elsevier B.V. 2013; 4: 75–91.
[131] C. H. Ng, M. A. Parker, L. Ran, P. J. Tavner, J. R. Bumby, and E. Spooner, "A multilevel modular converter for a large, light weight wind turbine generator," IEEE Trans. Power Electron., vol. 23, no. 3, pp. 1062–1074, May 2008.
[132] M. Liserre, F. Blaabjerg, and S. Hansen, "Design and control of an LCLfilter- based three-phase active rectifier," *IEEE Trans. Ind. Appl.*, vol. 41, no. 5, pp. 1281–1291, Sep./Oct. 2005.
[133] A. Rockhill, M. Liserre, R. Teodorescu, and P. Rodriguez, "Grid filter design for a multi-megawatt medium-voltage voltage source inverter," IEEE Trans. Ind. Electron., vol. 58, no. 4, pp. 1205–1217, Apr. 2011.

[134] Islam M R, Guo Y G, Zhu J G. A medium frequency transformer with multiple secondary windings for medium voltage converter based wind turbine power generating systems. Journal of Applied Physics. 2013; 113:17A324–17A324-3

[135] Islam MR, Guo YG, Zhu JG. Power converters for wind turbines: current and future development. Materials and processes for energy: communicating current research and technological developments. Energy Book Series-2013 edn. Spain. 2013:559-571.

[136] Gao R, Husain I, Wang F, Huang AQ. Solid-state transformer interfaced PMSG wind energy conversion system. In2015 IEEE Applied Power Electronics Conference and Exposition (APEC) 2015 Mar 15 (pp. 1310-1317). IEEE.

[137] J. Rebollo, I. Cortés, X. Perpiñà, and J. A. Millán, "Review of Si MOS-Gated Power Switches and PiN Rectifiers," AUTOMATIKA: časopis za automatiku, mjerenje, elektroniku, računarstvo i komunikacije. Jun. 2012, vol. 53, no. 2, pp. 117-127.

[138] B. K. Bose, "Evaluation of Modern Power Semiconductor Devices and Future Trends of Converters", IEEE Transactions on Industry Applications, 1992, vol. 28, no.2, pp. 403-413.

[139] S. A. Mohammed, M. A. Abdel-Moamen, and B. Hasanin, "A Review of the State-Of-The-Art of Power Electronics For Power System Applications," Journal of Electronics and Communication Engineering Research, 2013, vol. 1, no. 1, pp: 43-52.

[140] Insulated Gate Bipolar Transistor, Electronics Tutorials, [Online]. Available from: http://www.electronics-tutorials.ws/power/insulated-gate-bipolar-transistor.html

[141] M. T. Rahimo, A. Kopta and S. Linder. "Novel enhancedplanar IGBT technology rated up to 6.5kV for low losses and higher SOA capability". Proc. Int. Symp. Power Devices and ICs, ISPSD'2006, pp. 33-36

[142] M. T. Rahimo, U. Schlapbach, A. Kopta, J. Vobecky, D. Schneider and A. Baschnagel. "A high current 3300V module employing reverse conducting IGBTs setting a new benchmark in output power capability". Proc. Int. Symp. Power Devices and ICs, ISPSD'2008, pp. 68-71.

[143] Ji B, Song X, Sciberras E, Cao W, Hu Y, Pickert V. Multiobjective design optimization of IGBT power modules considering power cycling and thermal cycling. IEEE Transactions on Power Electronics. May 2015, vol. 30, no. 5, pp. 2493-2504.

[144] C. Busca, R. Teodorescu, F. Blaabjerg, S. Munk-Nielsen, L. Helle, T. Abeyasekera, and P. Rodriguez, "An overview of the reliability prediction related aspects of high power IGBTs in wind power applications," Microelectron. Reliab., vol. 51, no. 9–11, pp. 1903–1907, Sep.–Nov. 2011.

[145] R. Alvarez, F. Filsecker, and S. Bernet, "Comparison of press-pack IGBT at hard switching and clamp operation for medium voltage converters," in Proc. EPE 2011, 2011, pp. 1–7.

[146] Website of heraeus. [Online]. Available from: http://www.heraeus.com

[147] Website of Semikron. [Online]. Available from: http://www.semikron.com

[148] Luna A, Lima FD, Santos D, Rodríguez P, Watanabe EH, Arnaltes S. Simplified modeling of a DFIG for transient studies in wind power applications. IEEE Transactions on Industrial Electronics. 2011 Jan;58(1): 9-20.

[149] Tohidi S, Behnam MI. A comprehensive review of low voltage ride through of doubly fed induction wind generators. Renewable and Sustainable Energy Reviews. 2016 May 31;57: 412-419.

[150] Zhan TS, Chen JL, Chen SJ, Huang CH, Lin CH. Design of a chaos synchronisation-based maximum power tracking controller for a wind-energy-conversion system. IET Renewable Power Generation. 2014 Aug;8(6): 590-597.

[151] Baloch MH, Wang J, Kaloi GS. Stability and nonlinear controller analysis of wind energy conversion system with random wind speed. International Journal of Electrical Power & Energy Systems. 2016 Jul 31; 79:75-83.
[152] Yang L, Xu Z, Ostergaard J, Dong ZY, Wong KP. Advanced control strategy of DFIG wind turbines for power system fault ride through. IEEE Transactions on Power Systems. 2012 May; 27(2): 713-722.
[153] Ghulam Sarwar Kaloi, Jie Wang, Mazhar Hussain Baloch. Active and reactive power control of the doubly fed induction generator based on wind energy conversion system, Elsevier Energy Reports, Volume 2, November 2016, pp. 194–200.
[154] S. Muller, M. Deicke, and R. W. De Doncker, "Doubly fed induction generator systems for wind turbines," IEEE Ind. Appl. Mag., vol. 8, no. 3, pp. 26–33, May/Jun. 2002.
[155] D. Xiang, L. Ran, P. J. Tavner, and S. Yang, "Control of a doubly fed induction generator in a wind turbine during grid fault ride-through," IEEE Trans. Energy Convers., vol. 21, no. 3, pp. 652–662, Sep. 2006.
[156] S. Grabic, N. Celanovic, and V. A. Katic, "Permanent magnet synchronous generator cascade for wind turbine application," IEEE Trans. Power Electron., vol. 23, no. 3, pp. 1136–1142, May 2008.
[157] Wind turbine converters, ABB, [Online]. Available from: http://new.abb.com
[158] K. Ma, Power Electronics for the Next Generation Wind Turbine System, Research Topics in Wind Energy 5, Springer International Publishing Switzerland, 2015. DOI 10.1007/978-3-319-21248-7_2 [Online]. Available from: http://www.springer.com/978-3-319-21247-0 pp. 19 – 29.
[159] A. Faulstich, J. K. Stinke, and F. Wittwer, "Medium voltage converter for permanent magnet wind power generators up to 5 MW," in Proc. EPE, 2005, pp. 1–9.
[160] D. S. Oliveira, M. M. Reis, C. Silva, L. B. Colado, F. Antunes, and B. L. Soares, "A three-phase high-frequency semicontrolled rectifier for PM WECS," IEEE Trans. Power Electron., vol. 25, no. 3, pp. 677–685, Mar. 2010.
[161] B.Wu, Y. Lang, N. Zargari, and S. Kouro, Power Conversion and Control of Wind Energy Systems. Hoboken, NJ: Wiley, 2011.
[162] J. Dai, D. D. Xu, and B. Wu, "A novel control scheme for current-sourceconverter- based PMSG wind energy conversion systems," IEEE Trans. Power Electron., vol. 24, no. 4, pp. 963–972, Apr. 2009.
[163] P. Tenca, A. A. Rockhill, T. A. Lipo, and P. Tricoli, "Current source topology for wind turbines with decreased mains current harmonics, further reducible via functional minimization," IEEE Trans. Power Electron., vol. 23, no. 3, pp. 1143–1155, May 2008.
[164] J. Rodriguez, S. Bernet, W. Bin, J. O. Pontt, and S. Kouro, "Multilevel voltage-source converter topologies for industrial medium-voltage drives," IEEE Trans. Ind. Electron., vol. 54, no. 6, pp. 2930–2945, Dec. 2007.
[165] S. Kouro, M. Malinowski, K. Gopakumar, J. Pou, L. G. Franquelo, B.Wu, J. Rodriguez, M. A. Perez, and J. I. Leon, "Recent advances and industrial applications of multilevel converters," IEEE Trans. Power Electron., vol. 57, no. 8, pp. 2553–2580, Aug. 2010.
[166] R. Pena, J. C. Clare, and G. M. Asher, "Doubly fed induction generator using back-to-back PWM converters and its application to variable speed wind-energy generation," Proc. Inst. Elect. Eng.—Elect. Power Appl., vol. 143, no. 3, pp. 231–241, May 1996.
[167] K. Ma, F. Blaabjerg, and D. Xu, "Power devices loading in multilevel converters for 10 MW wind turbines," in *Proc. ISIE*, Jun. 2011, pp. 340–346.

[168] K. Ma and F. Blaabjerg, "Multilevel converters for 10MWwind turbines," in *Proc. EPE*, Birmingham, U.K., 2011, pp. 1–10.
[169] J. M. Carrasco, L. G. Franquelo, J. T. Bialasiewicz, E. Galvan, R. Portillo, M. M. Prats, J. I. Leon, and N. Moreno-Alfonso, "Power electronic systems for the grid integration of renewable energy sources: A survey," *IEEE Trans. Ind. Electron.*, vol. 53, no. 4, pp. 1002–1016, Jun. 2006.
[170] J. Rodriguez, S. Bernet, P. K. Steimer, and I. E. Lizama, "A survey on neutral-point-clamped inverters," *IEEE Trans. Ind. Electron.*, vol. 57, no. 7, pp. 2219–2230, Jul. 2010.
[171] R. Teichmann and S. Bernet, "A comparison of three-level converters versus two-level converters for low-voltage drives, traction, and utility applications," *IEEE Trans. Ind. Appl.*, vol. 41, no. 3, pp. 855–865, May/Jun. 2005.
[172] T. Bruckner, S. Bernet, and H. Guldner, "The active NPC converter and its loss-balancing control," *IEEE Trans. Ind. Electron.*, vol. 52, no. 3, pp. 855–868, Jun. 2005.
[173] O. S. Senturk, L. Helle, S. Munk-Nielsen, P. Rodriguez, and R. Teodorescu, "Medium voltage three-level converters for the grid connection of a multi-MW wind turbine," in *Proc. EPE*, 2009, pp. 1–8.
[174] H. Hosoda and S. Peak, "Multi-level converters for large capacity motor drive," in Proc. IPEC, 2010, pp. 516–522.
[175] M. Altin, O. Goksu, R. Teodorescu, P. Rodriguez, B. Bak-Jensen, and L. Helle, "Overview of recent grid codes for wind power integration," in *Proc. OPTIM*, 2010, pp. 1152–1160.
[176] M. Malinowski, K. Gopakumar, J. Rodriguez, and M. A. Peérez, "A survey on cascaded multilevel inverters," *IEEE Trans. Ind. Electron.*, vol. 57, no. 7, pp. 2197–2206, Jul. 2010.
[177] B. Engel, M. Victor, G. Bachmann, and A. Falk, "15 kV/16.7 Hz energy supply system with medium frequency transformer and 6.5 kV IGBTs in resonant operation," in *Proc. EPE*, Toulouse, France, Sep. 2–4, 2003.
[178] S. Inoue and H. Akagi, "A bidirectional isolated DC-DC converter as a core circuit of the next-generation medium-voltage power conversion system," *IEEE Trans. Power Electron.*, vol. 22, no. 2, pp. 535–542, Mar. 2007.
[179] F. Iov, F. Blaabjerg, J. Clare, O. Wheeler, A. Rufer, and A. Hyde, "UNIFLEX-PM-A key-enabling technology for future European electricity networks," *EPE J.*, vol. 19, no. 4, pp. 6–16, 2009.
[180] D. Schreiber, "Power converter circuit arrangement for generators with dynamically variable power output," U.S. Patent 6 680 856, Jan. 20, 2004.
[181] B. Andresen and J. Birk, "A high power density converter system for the Gamesa G10x 4.5 MW Wind turbine," in *Proc. EPE*, Aalborg, Denmark, 2007, pp. 1–7.
[182] R. Jones and P. Waite, "Optimised power converter for multi-MW direct drive permanent magnet wind turbines," in *Proc. EPE*, 2011, pp. 1–10.
[183] J. Kang, N. Takada, E. Yamamoto, and E. Watanabe, "High power matrix converter for wind power generation applications," in *Proc. ICPE ECCEAsia*, 2011, pp. 1331–1336.
[184] M. S. El-Moursi, B. Bak-Jensen, and M. H. Abdel-Rahman, "Novel STATCOM controller for mitigating SSR and damping power system oscillations in a series compensated wind park," *IEEE Trans. Power Electron.*, vol. 25, no. 2, pp. 429–441, Feb. 2010.
[185] X. Yuan, F. Wang, D. Boroyevich, Y. Li, and R. Burgos, "DC-link voltage control of a full power converter for wind generator operating in weak-grid systems," *IEEE Trans. Power Electron.*, vol. 24, no. 9, pp. 2178–2192, Sep. 2009.

[186] P. Rodriguez, A. V. Timbus, R. Teodorescu, M. Liserre, and F. Blaabjerg, “Flexible active power control of distributed power generation systems during grid faults,” *IEEE Trans. Ind. Electron.*, vol. 54, no. 5, pp. 2583–2592, Oct. 2007.
[187] P. Rodriguez, A. Timbus, R. Teodorescu, M. Liserre, and F. Blaabjerg, “Reactive power control for improving wind turbine system behavior under grid faults,” *IEEE Trans. Power Electron.*, vol. 24, no. 7, pp. 1798–1801, Jul. 2009.
[188] A. Timbus, M. Liserre, R. Teodorescu, P. Rodriguez, and F. Blaabjerg, “Evaluation of current controllers for distributed power generation systems,” *IEEE Trans. Power Electron.*, vol. 24, no. 3, pp. 654–664, Mar. 2009.
[189] F. K. A. Lima, A. Luna, P. Rodriguez, E. H. Watanabe, and F. Blaabjerg, “Rotor voltage dynamics in the doubly fed induction generator during grid faults,” *IEEE Trans. Power Electron.*, vol. 25, no. 1, pp. 118–130, Jan. 2010.
[190] D. Santos-Martin, J. L. Rodriguez-Amenedo, and S. Arnaltes, “Providing ride-through capability to a doubly fed induction generator under unbalanced voltage dips,” *IEEE Trans. Power Electron.*, vol. 24, no. 7, pp. 1747–1757, Jul. 2009.
[191] M. Tsili, “A review of grid code technical requirements for wind farms,” *IET J. Renew. Power Generat.*, vol. 3, no. 3, pp. 308–332, 2009.
[192] *Wind Turbines Connected to Grids with Voltages Below 100 kV*, Energinet, Fredericia, Denmark, Jan. 2003.
[193] *Technical Regulation 3.2.5 for Wind Power Plants with a Power Output Greater than 11 kW*, Energinet, Fredericia, Denmark, Sep. 2010.
[194] *Requirements for Offshore Grid Connections in the E.ON Netz Network*, E.ON-Netz, Bayreuth, Germany, Apr. 2008.
[195] Remus, T.; Marco, L.; Pedro, R. Grid converters for photovoltaic and wind power systems. Chichester, West Sussex, United Kingdom: Wiley, 2011.
[196] Hong, S. Studies on integrated variable-speed constant-frequency wind turbine mode application. Ph.D.dissertation, Electric Power Research Institute, Beijing, China, 2003, 11-40.
[197] Camm EH, Behnke MR, Bolado O, Bollen M, Bradt M, Brooks C, Dilling W, Edds M, Hejdak WJ, Houseman D, Klein S. et al, Characteristics of Wind Turbine Generators for Wind Power Plants. In2009 IEEE Power & Energy Society General Meeting 2009 Jul 26 (pp. 1-7). IEEE.
[198] Rather ZH, Chen Z, Thøgersen P, Lund P. Dynamic reactive power compensation of large-scale wind integrated power system. IEEE Transactions on Power Systems. 2015 Sep;30(5):2516-26.
[199] Dizdarevic N, Majstrovic M. FACTS-based reactive power compensation of wind energy conversion system. InPower Tech Conference Proceedings, 2003 IEEE Bologna 2003 Jun 23 (Vol. 2, pp. 8-pp). IEEE.
[200] M. Behnke, A. Ellis, Y. Kazachkov, T. McCoy, E. Muljadi, W. Price, and J. Sanchez-Gasca, “Development and validation of WECC variable speed wind turbine dynamic models for grid integration studies,” in *Proc. AWEA WindPower Conf.*, 2007.
[201] Camm EH, Behnke MR, Bolado O, Bollen M, Bradt M, Brooks C, Dilling W, Edds M, Hejdak WJ, Houseman D, Klein S. et al, Reactive power compensation for wind power plants. In2009 IEEE Power & Energy Society General Meeting 2009 Jul 26 (pp. 1-7). IEEE.
[202] FERC Order No. 661-A, *Interconnection for Wind Energy*, Docket No. RM05-4-001, December 2005.

[203] WECC PRC-024-WECC-1, *Generator Low Voltage Ride-Through Criterion*, Post Draft, September 2008.
[204] The Grid Code, UK issued by National Grid Electricity Transmission plc, Electricity codes regulatory Frameworks.
[205] Energinet.dk Ancillary Services Strategy, Energinet.dk, Aug. 2011.
[206] System Plan, Energinet.dk, Oct. 2007.
[207] International Review of Grid Codes, Task 1.1. of Wind on the Grid Report, Mar. 2007.
[208] P. Cartwright, L. Holdsworth, J. B. Ekanayake, and N. Jenkins, "Co-ordinated voltage control strategy for a doubly-fed induction generator (DFIG)-based wind farm," *Proc. Inst. Elect. Eng., Gen., Transm., Distrib.*, vol. 151, no. 4, pp. 495–502, Jul. 2004.
[209] M. Kayikci and J. V. Milanovic, "Reactive power control strategies for DFIG-based plants," *IEEE Trans. Energy Convers.*, vol. 22, no. 2, pp. 389–396, Jun. 2007.
[210] L. G. Meegahapola, D. Flynn, J. Kennedy, and T. Littler, "Active use of DFIG based wind farms for transient stability improvement during grid disturbances," in *Proc. IEEE PES GeneralMeeting 2009*, Calgary, AB, Canada, Jul. 2009.
[211] L. G. Meegahapola, S. Durairaj, D. Flynn, and B. Fox, "Coordinated utilisation of wind farm reactive power capability for system loss optimization," *Eur. Trans. Elect. Power*, 2009.
[212] W.L. Kling, J.G. Slootweg, "Wind Turbines as Power Plants" IEEE/Cigré Workshop on Wind Power and the Impacts on Power Systems, June 2002, Oslo, Norway.
[213] WECC Undervoltage Load Shedding Task Force, Technical Studies Subcommittee. *Under-Voltage Load Shedding Guidelines.* July 1999.
[214] WECC Reactive Power Reserve Work Group, Technical Studies Subcommittee. *Voltage Stability Criteria, Under-Voltage Load Shedding Strategy, and Reactive Power Reserve Monitoring Methodology.* May 2008.
[215] Muljadi E, Zhang YC. Wind Power Plant Voltage Stability Evaluation. InInternational Conference on Wind Energy Grid-Adaptive Technologies 2014 Sep 20.
[216] Igbinovia FO, Fandi G, Švec J, Müller Z, Tlusty J. Comparative review of reactive power compensation technologies. InElectric Power Engineering (EPE), 2015 16th International Scientific Conference on 2015 May 20 (pp. 2-7). IEEE.
[217] Famous O. Igbinovia, Ghaeth Fandi, Zdeněk Müller, Jan Švec, Josef Tlustý, "Optimal Location of the Synchronous Condenser in Electric-Power System Networks". 17th International Scientific Conference on Electric Power Engineering (EPE). Brno University of Technology and Czech Technical University in Prague, Czech Republic. 16th – 18th May, 2016. Publisher: IEEE 2016.
[218] Famous O. Igbinovia, Ghaeth Fandi, Jan Svec, Zdenek Muller, Josef Tlusty, Progressive Usage of the Synchronous Machine in Electrical Power Systems, Journal of Engineering Science and Technology Review (JESTR), Volume XX Issue XX, pp. XX – XX. Publisher: Kavala Institute of Technology, Lucas, Kavala, Greece, ISSN:1791-2377
[219] Ghaeth Fandi, Famous O. Igbinovia, Zdenek Muller, Jan Svec, Josef Tlusty, Reactive Power Producing Capability of Wind Turbine Systems with IGBT Power Electronics Converters, Journal of Engineering Science and Technology Review (JESTR), Volume XX Issue XX, pp. XX – XX. Publisher: Kavala Institute of Technology, Lucas, Kavala, Greece, ISSN:1791-2377
[220] A. L. P. de Oliveira, "The Definitions and Benefits of the Mechanically Switched Capacitors (MSC) for Power Transmission and Distribution Systems– (in Portuguese)", in XVII SNPTEE - Electrical Energy Production and Transmission National Seminar (Cigré), Curitiba-PR, Brazil, 2005.

[221] de Oliveira A. L. P, Pereira A. L. M. Introduction of the mechanically switched capacitors (MSCs) application on power transmission systems. In IEEE Transmission and Distribution Conference and Exposition: Latin America (T&D-LA), 2010 IEEE/PES 2010 Nov 8 (pp. 452-457). IEEE.
[222] Mechanical Switched Capacitor (MSC/MSCDN) [Online]. Available from: http://www.energy.siemens.com/co/en/power-transmission/facts/mechanical-switched-capacitor/
[223] Wenzel T, Leibfried T. Voltage Stability with Mechanically Switched Capacitors using Vacuum Circuit Breakers in the High-Voltage Grid, In IEEE12th International Conference on Optimization of Electrical and Electronic Equipment (OPTIM) 2010, Brasov, Romania, pp. 41 – 47.
[224] Wenzel T, Leibfried T. Vacuum circuit breakers in flexible AC transmission systems. IEEE Transactions on Power Delivery. 2012 Jan;27(1):236-244.
[225] McGraw-Hill Concise Encyclopedia of Engineering. S.v. "static var compensator." [Online]. Available from: http://encyclopedia2.thefreedictionary.com
[226] Siemens, “Static Var Compensator (SVC “Classic”), [Online]. Available from: http://www.energy.siemens.com
[227] R. Alves, M. Montilla, and E. Mora, "Increase of voltage stability and power limits using a static var compenstor". Universidad Simón Bolívar- Caracas, Venezuela, and Universidad de Los Andes-Mérida, Venezuela. [Online]. Available from: http://www.icrepq.com
[228] E. Csanyi, “ What is the Static Var Compensator (SVC),” Electrical Engineering Portal (EEP), Sep. 2011. [Online]. Available from: http://electrical-engineering-portal.com
[229] E. V. Liberado, W. A. Souza, J. A. Pomilio, H. K. M. Paredes, F. P. Marafão, “ Design of Static VAr Compensator using a General Reactive Energy Definition,” XI International School on Nonsinusoidal Currents and Compensation (ISNCC), Zielona Gora, Poland, ISBN: 978-1-4673-6312-9 Jun. 2013.
[230] Festo Didactic, Static Synchronous Compensator (STATCOM), Electricity and New Energy, Courseware Sample, Festo Didactic Ltée/Ltd, Quebec, Canada, ISBN 978-2-89640-572-5, 2012.
[231] P. Mattavelli, G. C. Verghese, and A. M. Stankovic, “Phasor dynamics of thyristor-controlled series capacitor systems,” IEEE Trans. Power Syst., vol. 3, no. 12, pp. 1259–1267, Aug. 1997.
[232] Genc MS. Economic analysis of large-scale wind energy conversion systems in central anatolian Turkey. Clean energy systems and experiences. 2010:131-154.
[233] European Wind Energy Association. The economics of wind energy. EWEA; 2009.
[234] J. Beurskens, and P. H. Jensen, “Economics of wind energy prospects and directions”, Renewable Energy World, vol. 4, no. 4, pp. 103-121, Apr. 2001.
[235] Jaber S. Environmental impacts of wind energy. Journal of Clean Energy Technologies. 2013 Jul;1(3):251-254.
[236] Wind Energy Development Environmental Concerns, [Online]. Available from: http://www.windeis.anl.gov/guide/concern/index.cfm
[237] Mohammad SN, Das NK, Roy S. A review of the state of the art of generators and power electronics for wind energy conversion systems. In IEEE 3rd International Conference on the Developments in Renewable Energy Technology (ICDRET) 2014, 2014 May 29 (pp. 1-6).
[238] Lew DJ. Environmental Impacts of Wind Power - D. J. Lew. INTERACTIONS: ENERGY/ENVIRONMENT, http://www.eolss.net/sample-chapters/c09/e4-23-04-02.pdf

# 8.2 Author's Publications

## 8.2.1 Publications in the Framework of the Thesis

### 8.2.1.1 Publications in Impact Factor Journals

1. Fandi, G., Igbinovia, F., Tlustý, J., Mahmoud, R. Voltage regulation and power losses reduction in a wind farm integrated mv distribution network. (Journal of Electrical Engineering, 2017, IF=0,498) , ISSN: 1335-3632.

### 8.2.1.2 Publications in Reviewed Journals

### 8.2.1.3 Patents

### 8.2.1.4 Publications in WoS and Scopus

1. Fandi, G.; Švec, J.; Müller, Z. The Converter Choice and its Control Circuit Design for Synchronous Generators In: Electric Power Engineering 2013. Ostrava: VŠB - Technical University of Ostrava, 2013, ISBN 978-80-248-2988-3.
2. Fandi, G.; Müller, Z.; Straka, L.; Švec, J. FACTS Devices Influence on Power Losses in Transmission Systems In: Proceedings of the 2014 15th International Scientific Conference on Electric Power Engineering. Brno: Vysoké učení technické v Brně, 2014, pp. 29-33. ISBN 978-1-4799-3806-3.
3. Fandi, G.; Igbinovia, F.; Müller, Z.; Švec, J.; Tlustý, J. Using renewable MV wind energy resource to supply reactive power in MV distribution network In: 2015 16th International Scientific Conference on Electric Power Engineering (EPE). Ostrava: VŠB - Technical University of Ostrava, 2015, pp. 169-173. ISBN 978-1-4673-6788-2.
4. Igbinovia, F.; Fandi, G.; Švec, J.; Müller, Z.; Tlustý, J. Comparative review of reactive power compensation technologies In: 2015 16th International Scientific Conference on Electric Power Engineering (EPE). Ostrava: VŠB - Technical University of Ostrava, 2015, pp. 2-7. ISBN 978-1-4673-6788-2.
5. Fandi, G.; Igbinovia, F.; Švec, J.; Müller, Z.; Tlustý, J. Advantageous Positioning of Wind Turbine Generating System in MV Distribution Network In: 2016 17th International Scientific Conference on Electric Power Engineering (EPE 2016). New York: IEEE, 2016, pp. 124-129. International Scientific Conference on Electric Power Engineering. ISSN 2376-5623. ISBN 978-1-5090-0908-4.
6. Igbinovia, F.; Fandi, G.; Müller, Z.; Švec, J.; Tlustý, J. Cost Implication and Reactive Power Generating Potential of the Synchronous Condenser In: The Proceedings of the 2nd International Conference on Intelligent Green Building and Smart Grid (IGBSG). Praha: IEEE Czechoslovakia Section, 2016. pp. 212-217. ISBN 978-1-4673-8473-5.
7. Igbinovia, F.; Fandi, G.; Müller, Z.; Švec, J.; Tlustý, J. Optimal Location of the Synchronous Condenser in Electric-Power System Networks In: 2016 17th International Scientific Conference on Electric Power Engineering (EPE 2016). New York: IEEE, 2016, pp. 85-90. International Scientific Conference on Electric Power Engineering. ISSN 2376-5623. ISBN 978-1-5090-0908-4.

#### 8.2.1.5 Publications are not in WoS and Scopus


1. Fandi, G. Study of MV Renewable Wind Energy Sources in Integrated MV Distrbution Networks , In: Proceedings of ELEN 2014. Praha: ČVUT FEL, Katedra elektroenergetiky, 2014, ISBN 978-80-01-05654-7.
2. Sengar, A.; Chhajer, R.; Fandi, G.; Igbinovia, F. Comparison of the Operational Theory and Features of SVC and STATCOM In: Poster 2015. Praha: České vysoké učení technické v Praze, 2015, ISBN 978-80-01-05728-5.
3. Dusane, P.; Dang, M.; Igbinovia, F.; Fandi, G. Analysis of the Synchronous Machine in its Operational Modes: Motor, Generator and Compensator In: Poster 2015. Praha: České vysoké učení technické v Praze, 2015, ISBN 978-80-01-05728-5.


### 8.2.2 Other Publications

#### 8.2.2.1 Publications in Impact Factor Journals

#### 8.2.2.2 Publications in Reviewed Journals


1. Igbinovia, F.; Fandi, G.; Mahmoud, R.; Tlustý, J. A review of electric vehicles emissions and its smart charging techniques influence on power distribution grid Journal of Engineering Science and Technology Review. 2016, 9(3), 80-85. ISSN 1791-9320. (scopus IF=0,16)


#### 8.2.2.3 Patents

#### 8.2.2.4 Publications in WoS and Scopus


1. Müller, Z.; Bejvl, M.; Simek, P.; Tlusty, J.; Valouch, V.; Fandi, G.; Cernan, M.; Muller, M., Contribution to Control Strategies for Converter Connected to Unbalanced Grid. In: 2016 SETIT Conference [online]. IEEE, 2016, s. 1-7. ISBN: 978-1-5090-4712-3.
2. Straka, Libor, and Ghaeth Fandi. Distance protection based on Artificial Neural Networks.: Proceedings of the 2014 15th International Scientific Conference on Electric Power Engineering. Brno: Vysoké učení technické v Brně, 2014, pp. 29-33. ISBN 978-1-4799-3806-3.


#### 8.2.2.5 Publications are not in WoS and Scopus


1. Fandi, G. Comparison of Simulation and Standard Method for Computation of Inductance In: POSTER 2014 - 18th International Student Conference on Electrical Engineering. Prague: Czech Technical University, 2014, ISBN 978-80-01-05499-4.

## 8.2.3 Submitted Publications

1. 2017 IEEE PES Power Africa Conference (Modeling and Simulation of a Gearless Variable Speed Wind Turbine System with PMSG), Accra, Ghana, June 27-30, 2017.
2. The Iranian Journal of Science and Technology, Transactions of Electrical Engineering - springer-
(A Novel IGBT Power Converter Control Scheme for Active and Reactive Power Utilized in Gearless Variable Speed Wind Turbine System with PMSG Connected to the Grid), Date: 15 -Jun -2016, , Impact Factor :0.107, (ISSN) is 2228-6179.

## 8.2.4 Awards

1. Engineering students of universities compete in the Prix ČEZ Foundation, 2013, Second place.
2. Engineering students of universities compete in the Prix ČEZ Foundation, 2015, Third place.
3. POSTER 2015 ,19th International Student Conference on Electrical Engineering,2015, Second place
4. Engineering students of universities compete in the Prix ČEZ Foundation, 2016, Second place.

# Chapter 9

# 9 Appendix

## 9.1 Results Before Using Regulator

### 9.1.1 Generated Active and Reactive Power of Wind Farm

*Table 9.1 Values of $Q_{ref}$, active and reactive power of various steps and speeds of wind farm.*

| Step | $Q_{ref}$ (p.u.) | Generated $Q$(MVAr) | Generated $P$(MW) for wind speed 15 m/s | Generated $P$(MW) for wind speed 10 m/s | Generated $P$(MW) for wind speed 5 m/s |
|---|---|---|---|---|---|
| 1 | 0 | 0 | 30 | 16.3 | 1.8 |
| 2 | 0.207 | 6.941 | 30 | 16.3 | 1.8 |
| 3 | 0.387 | 12.960 | 30 | 16.3 | 1.8 |
| 4 | 0.567 | 19.200 | 30 | 16.3 | 1.8 |
| 5 | 0.747 | 23.810 | 30 | 16.3 | 1.8 |

### 9.1.2 Sending and Receiving Voltages and Voltage Drop for all Cases

*Table 9.2 Measured values of sending and receiving voltage for Case A*

| Case A | | | | |
|---|---|---|---|---|
| Step | Line | $U_s$ (kV) | $U_r$ (kV) | $\Delta V$ (kV) |
| 1 | 1 | 64.640 | 61.365 | 3.275 |
| | 2 | 64.640 | 61.055 | 3.585 |
| | 3 | 64.640 | 60.745 | 3.895 |
| 2 | 1 | 64.425 | 60.785 | 3.640 |
| | 2 | 64.425 | 60.446 | 3.979 |
| | 3 | 64.425 | 60.110 | 4.315 |
| 3 | 1 | 64.210 | 60.228 | 3.982 |
| | 2 | 64.210 | 59.860 | 4.350 |
| | 3 | 64.210 | 59.492 | 4.718 |
| 4 | 1 | 64.005 | 59.685 | 4.320 |
| | 2 | 64.005 | 59.285 | 4.720 |
| | 3 | 64.005 | 58.895 | 5.110 |
| 5 | 1 | 63.805 | 59.160 | 4.645 |
| | 2 | 63.805 | 58.734 | 5.071 |
| | 3 | 63.805 | 58.315 | 5.490 |

*Table 9.3 Measured values of sending and receiving voltage for Case B (15, 10 and 5 m/s)*

| Case B (15 m/s) | | | | | Case B (10 m/s) | | | Case B (5 m/s) | | |
|---|---|---|---|---|---|---|---|---|---|---|
| Step | Line | $U_s$ (kV) | $U_r$(kV) | $\Delta V$(kV) | $U_s$(kV) | $U_r$(kV) | $\Delta V$(kV) | $U_s$(kV) | $U_r$(kV) | $\Delta V$(kV) |
| 1 | 1 | 64.729 | 61.447 | 3.382 | 64.700 | 61.420 | 3.280 | 64.648 | 61.371 | 3.277 |
| | 2 | 64.729 | 61.136 | 3.593 | 64.700 | 61.108 | 3.592 | 64.648 | 61.060 | 3.588 |
| | 3 | 64.729 | 60.827 | 3.902 | 64.700 | 60.800 | 3.900 | 64.648 | 60.752 | 3.896 |
| 2 | 1 | 64.842 | 61.182 | 3.660 | 64.813 | 61.155 | 3.658 | 64.763 | 61.107 | 3.656 |
| | 2 | 64.842 | 60.839 | 4.003 | 64.813 | 60.811 | 4.002 | 64.763 | 60.764 | 3.999 |
| | 3 | 64.842 | 60.499 | 4.343 | 64.813 | 60.472 | 4.341 | 64.763 | 60.425 | 4.338 |
| 3 | 1 | 64.912 | 60.885 | 4.027 | 64.884 | 60.858 | 4.026 | 64.835 | 60.812 | 4.023 |
| | 2 | 64.912 | 60.510 | 4.402 | 64.884 | 60.484 | 4.400 | 64.835 | 60.438 | 4.397 |
| | 3 | 64.912 | 60.141 | 4.771 | 64.884 | 60.115 | 4.769 | 64.835 | 60.069 | 4.766 |
| 4 | 1 | 64.945 | 60.597 | 4.388 | 64.957 | 60.571 | 4.386 | 64.908 | 60.526 | 4.382 |
| | 2 | 64.945 | 60.193 | 4.792 | 64.957 | 60.167 | 4.790 | 64.908 | 60.122 | 4.786 |
| | 3 | 64.945 | 59.795 | 5.190 | 64.957 | 59.769 | 5.188 | 64.908 | 59.724 | 5.184 |
| 5 | 1 | 64.985 | 60.213 | 4.732 | 65.033 | 60.294 | 4.739 | 64.984 | 60.249 | 4.735 |
| | 2 | 64.985 | 59.780 | 5.165 | 65.033 | 59.861 | 5.172 | 64.984 | 59.817 | 5.168 |
| | 3 | 64.985 | 59.355 | 5.590 | 65.033 | 59.435 | 5.598 | 64.984 | 59.391 | 5.593 |

*Table 9.4 Measured values of sending and receiving voltage for Case C (15,10 and 5 m/s)*

| Case C (15 m/s) | | | | | Case C (10 m/s) | | | Case C (5 m/s) | | |
|---|---|---|---|---|---|---|---|---|---|---|
| Step | Line | $U_s$ (kV) | $U_r$(kV) | $\Delta V$(kV) | $U_s$(kV) | $U_r$(kV) | $\Delta V$(kV) | $U_s$(kV) | $U_r$(kV) | $\Delta V$(kV) |
| 1 | 1 | 64.731 | 63.871 | 0.860 | 64.749 | 62.955 | 1.794 | 64.674 | 61.647 | 3.027 |
| | 2 | 64.731 | 61.138 | 3.593 | 64.749 | 61.155 | 3.594 | 64.674 | 61.083 | 3.591 |
| | 3 | 64.731 | 60.830 | 3.901 | 64.749 | 60.846 | 3.903 | 64.674 | 60.775 | 3.899 |
| 2 | 1 | 64.825 | 65.156 | -0.331 | 64.839 | 64.243 | 0.596 | 64.765 | 62.970 | 1.795 |
| | 2 | 64.825 | 60.822 | 4.003 | 64.839 | 60.836 | 4.003 | 64.765 | 60.766 | 3.999 |
| | 3 | 64.825 | 60.483 | 4.342 | 64.839 | 60.497 | 4.342 | 64.765 | 60.427 | 4.338 |
| 3 | 1 | 64.865 | 66.110 | -1.245 | 64.879 | 65.212 | -0.333 | 64.806 | 63.967 | 0.839 |
| | 2 | 64.865 | 60.466 | 4.399 | 64.879 | 60.479 | 4.400 | 64.806 | 60.411 | 4.395 |
| | 3 | 64.865 | 60.097 | 4.768 | 64.879 | 60.110 | 4.769 | 64.806 | 60.042 | 4.764 |
| 4 | 1 | 64.899 | 67.008 | -2.109 | 64.912 | 66.122 | -1.210 | 64.841 | 64.903 | -0.062 |
| | 2 | 64.899 | 60.113 | 4.786 | 64.912 | 60.125 | 4.787 | 64.841 | 60.059 | 4.782 |
| | 3 | 64.899 | 59.715 | 5.184 | 64.912 | 59.728 | 5.184 | 64.841 | 59.662 | 5.179 |
| 5 | 1 | 64.915 | 67.791 | -2.876 | 64.941 | 66.988 | -2.048 | 64.870 | 65.790 | -0.920 |
| | 2 | 64.915 | 59.753 | 5.162 | 64.941 | 59.776 | 5.165 | 64.870 | 59.711 | 5.159 |
| | 3 | 64.915 | 59.328 | 5.587 | 64.941 | 59.351 | 5.590 | 64.870 | 59.286 | 5.584 |

*Table 9.5 Measured values of sending and receiving voltage for Case D (15, 10 and 5 m/s)*

| Case D (15 m/s) | | | | | Case D (10 m/s) | | | Case D (5 m/s) | | |
|---|---|---|---|---|---|---|---|---|---|---|
| Step | Line | $U_s$ (kV) | $U_r$(kV) | $\Delta V$(kV) | $U_s$(kV) | $U_r$(kV) | $\Delta V$(kV) | $U_s$(kV) | $U_r$(kV) | $\Delta V$(kV) |
| 1 | 1 | 64.861 | 62.306 | 2.555 | 64.795 | 61.813 | 2.982 | 64.678 | 61.206 | 3.472 |
| | 2 | 64.861 | 62.306 | 2.555 | 64.795 | 61.813 | 2.982 | 64.678 | 61.206 | 3.472 |
| | 3 | 64.861 | 62.306 | 2.555 | 64.795 | 61.813 | 2.982 | 64.678 | 61.206 | 3.472 |
| 2 | 1 | 64.955 | 62.587 | 2.368 | 64.893 | 62.105 | 2.788 | 64.781 | 61.513 | 3.268 |
| | 2 | 64.955 | 62.587 | 2.368 | 64.893 | 62.105 | 2.788 | 64.781 | 61.513 | 3.268 |
| | 3 | 64.955 | 62.587 | 2.368 | 64.893 | 62.105 | 2.788 | 64.781 | 61.513 | 3.268 |
| 3 | 1 | 65.002 | 62.735 | 2.267 | 64.944 | 62.263 | 2.681 | 64.838 | 61.686 | 3.152 |
| | 2 | 65.002 | 62.735 | 2.267 | 64.944 | 62.263 | 2.681 | 64.838 | 61.686 | 3.152 |
| | 3 | 65.002 | 62.735 | 2.267 | 64.944 | 62.263 | 2.681 | 64.838 | 61.686 | 3.152 |
| 4 | 1 | 65.044 | 62.868 | 2.176 | 64.993 | 62.415 | 2.578 | 64.892 | 61.851 | 3.041 |
| | 2 | 65.044 | 62.868 | 2.176 | 64.993 | 62.415 | 2.578 | 64.892 | 61.851 | 3.041 |
| | 3 | 65.044 | 62.868 | 2.176 | 64.993 | 62.415 | 2.578 | 64.892 | 61.851 | 3.041 |
| 5 | 1 | 64.856 | 62.361 | 2.495 | 65.042 | 62.566 | 2.476 | 64.945 | 62.014 | 2.931 |
| | 2 | 64.856 | 62.361 | 2.495 | 65.042 | 62.566 | 2.476 | 64.945 | 62.014 | 2.931 |
| | 3 | 64.856 | 62.361 | 2.495 | 65.042 | 62.566 | 2.476 | 64.945 | 62.014 | 2.931 |

### 9.1.3 Sending and Receiving Active and Reactive Power- Active and Reactive Power Losses for all Cases

*Table 9.6 Measured values of sending and receiving active and reactive power of Line 1, 2, and 3 for the various steps of Case A*

| Case A | | | | | | | |
|---|---|---|---|---|---|---|---|
| Step | Line | $P_s$(MW) | $P_r$ (MW) | $Q_s$ (MVAr) | $Q_r$ (MVAr) | $\Delta P$(MW) | $\Delta Q$ (MVAr) |
| 1 | 1 | 16.876 | 16.408 | 7.007 | 6.376 | 0.468 | 0.631 |
| | 2 | 16.751 | 16.242 | 6.992 | 6.311 | 0.509 | 0.681 |
| | 3 | 16.627 | 16.079 | 6.977 | 6.248 | 0.548 | 0.729 |
| 2 | 1 | 16.337 | 15.857 | 8.501 | 7.827 | 0.480 | 0.674 |
| | 2 | 16.200 | 15.680 | 8.466 | 7.740 | 0.520 | 0.726 |
| | 3 | 16.066 | 15.505 | 8.429 | 7.653 | 0.561 | 0.776 |
| 3 | 1 | 15.382 | 15.334 | 9.939 | 9.202 | 0.498 | 0.737 |
| | 2 | 15.686 | 15.146 | 9.882 | 9.089 | 0.540 | 0.793 |
| | 3 | 15.542 | 14.961 | 9.824 | 8.979 | 0.581 | 0.845 |
| 4 | 1 | 15.359 | 14.835 | 11.323 | 10.506 | 0.524 | 0.817 |
| | 2 | 15.205 | 14.638 | 11.245 | 10.366 | 0.567 | 0.879 |
| | 3 | 15.054 | 14.445 | 11.166 | 10.230 | 0.609 | 0.936 |
| 5 | 1 | 14.915 | 14.361 | 12.657 | 11.744 | 0.554 | 0.913 |
| | 2 | 14.755 | 14.155 | 12.556 | 11.575 | 0.600 | 0.981 |
| | 3 | 14.598 | 13.954 | 12.456 | 11.411 | 0.644 | 1.045 |

*Table 9.7 Measured values of sending and receiving active and reactive power of Line 1, 2, and 3 for the various steps of Case B (15 m/s)*

| Case B (15 m/s) | | | | | | | |
|---|---|---|---|---|---|---|---|
| Step | Line | $P_s$ (MW) | $P_r$ (MW) | $Q_s$ (MVAr) | $Q_r$ (MVAr) | $\Delta P$(MW) | $\Delta Q$ (MVAr) |
| 1 | 1 | 16.919 | 16.451 | 7.025 | 6.392 | 0.468 | 0.633 |
| | 2 | 16.794 | 16.284 | 7.010 | 6.327 | 0.510 | 0.683 |
| | 3 | 16.670 | 16.120 | 6.994 | 6.263 | 0.55 | 0.731 |
| 2 | 1 | 16.550 | 16.063 | 8.612 | 7.929 | 0.487 | 0.683 |
| | 2 | 16.411 | 15.884 | 8.576 | 7.840 | 0.527 | 0.736 |
| | 3 | 16.275 | 15.707 | 8.539 | 7.752 | 0.568 | 0.787 |
| 3 | 1 | 16.181 | 15.671 | 10.158 | 9.405 | 0.510 | 0.753 |
| | 2 | 16.032 | 15.479 | 10.100 | 9.290 | 0.553 | 0.810 |
| | 3 | 15.885 | 15.291 | 10.041 | 9.176 | 0.594 | 0.865 |
| 4 | 1 | 15.839 | 15.299 | 11.677 | 10.834 | 0.540 | 0.843 |
| | 2 | 15.680 | 15.095 | 11.596 | 10.690 | 0.585 | 0.906 |
| | 3 | 15.525 | 14.896 | 11.515 | 10.549 | 0.629 | 0.966 |
| 5 | 1 | 15.484 | 14.909 | 13.140 | 12.192 | 0.575 | 0.948 |
| | 2 | 15.318 | 14.695 | 13.035 | 12.017 | 0.623 | 1.018 |
| | 3 | 15.155 | 14.487 | 12.931 | 11.847 | 0.668 | 1.084 |

*Table 9.8 Measured values of sending and receiving active and reactive power of Line 1, 2, and 3 for the various steps of Case B (10 m/s)*

| Case B (10 m/s) | | | | | | | |
|---|---|---|---|---|---|---|---|
| Step | Line | $P_s$ (MW) | $P_r$ (MW) | $Q_s$ (MVAr) | $Q_r$ (MVAr) | $\Delta P$(MW) | $\Delta Q$ (MVAr) |
| 1 | 1 | 16.904 | 16.435 | 7.019 | 6.386 | 0.469 | 0.633 |
| | 2 | 16.778 | 16.269 | 7.004 | 6.322 | 0.509 | 0.682 |
| | 3 | 16.654 | 16.105 | 6.988 | 6.257 | 0.549 | 0.731 |
| 2 | 1 | 16.532 | 16.047 | 8.603 | 7.920 | 0.485 | 0.683 |
| | 2 | 16.394 | 15.867 | 8.566 | 7.831 | 0.527 | 0.735 |
| | 3 | 16.258 | 15.690 | 8.529 | 7.744 | 0.568 | 0.785 |
| 3 | 1 | 16.162 | 15.652 | 10.146 | 9.393 | 0.510 | 0.753 |
| | 2 | 16.013 | 15.461 | 10.088 | 9.278 | 0.552 | 0.810 |
| | 3 | 15.866 | 15.273 | 10.029 | 9.165 | 0.593 | 0.864 |
| 4 | 1 | 15.815 | 15.276 | 11.660 | 10.818 | 0.539 | 0.842 |
| | 2 | 15.657 | 15.073 | 11.579 | 10.674 | 0.584 | 0.905 |
| | 3 | 15.501 | 14.874 | 11.497 | 10.534 | 0.627 | 0.963 |
| 5 | 1 | 15.490 | 14.914 | 13.145 | 12.196 | 0.576 | 0.949 |
| | 2 | 15.324 | 14.701 | 13.040 | 12.022 | 0.623 | 1.018 |
| | 3 | 15.161 | 14.492 | 12.936 | 11.851 | 0.669 | 1.085 |

*Table 9.9 Measured values of sending and receiving active and reactive power of Line 1, 2, and 3 for the various steps of Case B (5 m/s)*

| Case B (5 m/s) | | | | | | | |
|---|---|---|---|---|---|---|---|
| Step | Line | $P_s$ (MW) | $P_r$ (MW) | $Q_s$ (MVAr) | $Q_r$ (MVAr) | $\Delta P$(MW) | $\Delta Q$ (MVAr) |
| 1 | 1 | 16.875 | 16.408 | 7.007 | 6.375 | 0.467 | 0.632 |
| | 2 | 16.750 | 16.242 | 6.992 | 6.311 | 0.508 | 0.681 |
| | 3 | 16.626 | 16.078 | 6.976 | 6.247 | 0.548 | 0.729 |
| 2 | 1 | 16.504 | 16.019 | 8.587 | 7.906 | 0.485 | 0.681 |
| | 2 | 16.366 | 15.840 | 8.551 | 7.818 | 0.526 | 0.733 |
| | 3 | 16.230 | 15.664 | 8.514 | 7.730 | 0.566 | 0.784 |
| 3 | 1 | 16.139 | 15.631 | 10.133 | 9.381 | 0.508 | 0.752 |
| | 2 | 15.990 | 15.439 | 10.074 | 9.266 | 0.551 | 0.808 |
| | 3 | 15.844 | 15.251 | 10.016 | 9.153 | 0.593 | 0.863 |
| 4 | 1 | 15.789 | 15.251 | 11.639 | 10.799 | 0.538 | 0.840 |
| | 2 | 15.631 | 15.048 | 11.558 | 10.656 | 0.583 | 0.902 |
| | 3 | 15.476 | 14.849 | 11.477 | 10.515 | 0.627 | 0.962 |
| 5 | 1 | 15.468 | 14.893 | 13.128 | 12.180 | 0.575 | 0.948 |
| | 2 | 15.302 | 14.680 | 13.023 | 12.006 | 0.622 | 1.017 |
| | 3 | 15.139 | 14.472 | 12.919 | 11.836 | 0.667 | 1.083 |

*Table 9.10 Measured values of sending and receiving active and reactive power of Line 1, 2, and 3 for the various steps of Case C (15 m/s)*

| Case C (15 m/s) | | | | | | | |
|---|---|---|---|---|---|---|---|
| Step | Line | $P_s$ (MW) | $P_r$ (MW) | $Q_s$ (MVAr) | $Q_r$ (MVAr) | $\Delta P$(MW) | $\Delta Q$ (MVAr) |
| 1 | 1 | -11.494 | -11.766 | 7.696 | 7.655 | 0.272 | 0.041 |
| | 2 | 16.794 | 16.284 | 7.010 | 6.327 | 0.510 | 0.683 |
| | 3 | 16.670 | 16.120 | 6.994 | 6.263 | 0.550 | 0.731 |
| 2 | 1 | -11.106 | -11.288 | 2.620 | 2.854 | 0.182 | -0.234 |
| | 2 | 16.404 | 15.876 | 8.571 | 7.836 | 0.528 | 0.735 |
| | 3 | 16.268 | 15.700 | 8.534 | 7.749 | 0.568 | 0.785 |
| 3 | 1 | -10.816 | -10.977 | -1.283 | -0.981 | 0.161 | -0.302 |
| | 2 | 16.010 | 15.459 | 10.086 | 9.277 | 0.551 | 0.809 |
| | 3 | 15.864 | 15.270 | 10.027 | 9.164 | 0.594 | 0.863 |
| 4 | 1 | -10.514 | -10.696 | -4.973 | -4.713 | 0.182 | -0.260 |
| | 2 | 15.639 | 15.056 | 11.565 | 10.662 | 0.583 | 0.903 |
| | 3 | 15.484 | 14.857 | 11.484 | 10.521 | 0.627 | 0.963 |
| 5 | 1 | -10.183 | -10.416 | -8.491 | -8.367 | 0.233 | -0.124 |
| | 2 | 15.287 | 14.665 | 13.009 | 11.993 | 0.622 | 1.016 |
| | 3 | 15.124 | 14.457 | 12.904 | 11.822 | 0.667 | 1.082 |

*Table 9.11 Measured values of sending and receiving active and reactive power of Line 1, 2, and 3 for the various steps of Case C (10 m/s)*

| Case C (10 m/s) | | | | | | | |
|---|---|---|---|---|---|---|---|
| Step | Line | $P_s$ (MW) | $P_r$ (MW) | $Q_s$ (MVAr) | $Q_r$ (MVAr) | $\Delta P$(MW) | $\Delta Q$ (MVAr) |
| 1 | 1 | 1.249 | 1.182 | 6.481 | 7.014 | 0.067 | -0.533 |
| | 2 | 16.799 | 16.289 | 7.013 | 6.329 | 0.510 | 0.684 |
| | 3 | 16.675 | 16.125 | 6.997 | 6.265 | 0.550 | 0.732 |
| 2 | 1 | 1.679 | 1.671 | 1.466 | 2.183 | 0.008 | -0.717 |
| | 2 | 16.408 | 15.880 | 8.574 | 7.838 | 0.528 | 0.736 |
| | 3 | 16.271 | 15.704 | 8.537 | 7.751 | 0.567 | 0.786 |
| 3 | 1 | 2.009 | 1.998 | -2.404 | -1.683 | 0.011 | -0.721 |
| | 2 | 16.014 | 15.463 | 10.089 | 9.279 | 0.551 | 0.810 |
| | 3 | 15.867 | 15.274 | 10.030 | 9.166 | 0.593 | 0.864 |
| 4 | 1 | 2.371 | 2.319 | -6.063 | -5.447 | 0.052 | -0.616 |
| | 2 | 15.640 | 15.057 | 11.567 | 10.663 | 0.583 | 0.904 |
| | 3 | 15.485 | 14.858 | 11.485 | 10.522 | 0.627 | 0.963 |
| 5 | 1 | 2.742 | 2.617 | -9.555 | -9.139 | 0.125 | -0.416 |
| | 2 | 15.288 | 14.667 | 13.010 | 11.994 | 0.621 | 1.016 |
| | 3 | 15.126 | 14.459 | 12.906 | 11.824 | 0.667 | 1.082 |

*Table 9.12 Measured values of sending and receiving active and reactive power of Line 1, 2, and 3 for the various steps of Case C (5 m/s)*

| Case C (5 m/s) | | | | | | | |
|---|---|---|---|---|---|---|---|
| Step | Line | $P_s$ (MW) | $P_r$ (MW) | $Q_s$ (MVAr) | $Q_r$ (MVAr) | $\Delta P$(MW) | $\Delta Q$ (MVAr) |
| 1 | 1 | 15.119 | 14.738 | 6.939 | 6.539 | 0.381 | 0.400 |
| | 2 | 16.759 | 16.250 | 6.997 | 6.315 | 0.509 | 0.682 |
| | 3 | 16.635 | 16.087 | 6.981 | 6.251 | 0.548 | 0.730 |
| 2 | 1 | 15.669 | 15.316 | 1.900 | 1.639 | 0.353 | 0.261 |
| | 2 | 16.364 | 15.838 | 8.550 | 7.816 | 0.526 | 0.734 |
| | 3 | 16.228 | 15.662 | 8.513 | 7.729 | 0.566 | 0.784 |
| 3 | 1 | 16.200 | 15.840 | -1.977 | -2.280 | 0.360 | 0.303 |
| | 2 | 15.975 | 15.424 | 10.064 | 9.256 | 0.551 | 0.808 |
| | 3 | 15.829 | 15.237 | 10.005 | 9.143 | 0.592 | 0.862 |
| 4 | 1 | 16.584 | 16.165 | -6.660 | -6.098 | 0.419 | -0.562 |
| | 2 | 15.602 | 15.020 | 11.537 | 10.636 | 0.581 | 0.901 |
| | 3 | 15.447 | 14.822 | 11.456 | 10.496 | 0.625 | 0.960 |
| 5 | 1 | 16.589 | 16.103 | -9.218 | -9.840 | 0.486 | -0.622 |
| | 2 | 15.252 | 14.632 | 12.980 | 11.966 | 0.620 | 1.014 |
| | 3 | 15.090 | 14.425 | 12.876 | 11.796 | 0.665 | 1.080 |

*Table 9.13 Measured values of sending and receiving active and reactive power of Line 1, 2, and 3 for the various steps of Case D (15 m/s)*

| Case D (15 m/s) | | | | | | | |
|---|---|---|---|---|---|---|---|
| Step | Line | $P_s$ (MW) | $P_r$ (MW) | $Q_s$ (MVAr) | $Q_r$ (MVAr) | $\Delta P$(MW) | $\Delta Q$ (MVAr) |
| 1 | 1 | 7.872 | 7.710 | 7.139 | 7.394 | 0.162 | -0.255 |
| | 2 | 7.157 | 7.010 | 6.420 | 6.789 | 0.147 | -0.369 |
| | 3 | 6.561 | 6.426 | 5.814 | 6.290 | 0.135 | -0.476 |
| 2 | 1 | 7.748 | 7.602 | 6.642 | 6.767 | 0.146 | -0.125 |
| | 2 | 7.044 | 6.911 | 5.803 | 6.219 | 0.133 | -0.416 |
| | 3 | 6.458 | 6.336 | 5.249 | 5.769 | 0.122 | -0.520 |
| 3 | 1 | 7.564 | 7.428 | 6.117 | 6.455 | 0.136 | -0.338 |
| | 2 | 6.877 | 6.753 | 5.490 | 5.935 | 0.124 | -0.445 |
| | 3 | 6.304 | 6.191 | 4.961 | 5.509 | 0.113 | -0.548 |
| 4 | 1 | 7.391 | 7.266 | 5.752 | 6.121 | 0.125 | -0.369 |
| | 2 | 6.720 | 6.606 | 5.158 | 5.633 | 0.114 | -0.475 |
| | 3 | 6.160 | 6.056 | 4.657 | 5.231 | 0.104 | -0.574 |
| 5 | 1 | 6.967 | 6.834 | 6.635 | 6.976 | 0.133 | -0.341 |
| | 2 | 6.334 | 6.213 | 5.961 | 6.409 | 0.121 | -0.448 |
| | 3 | 5.807 | 5.696 | 5.393 | 5.942 | 0.111 | -0.549 |

*Table 9.14 Measured values of sending and receiving active and reactive power of Line 1, 2, and 3 for the various steps of Case D (10 m/s)*

| Case D (10 m/s) | | | | | | | |
|---|---|---|---|---|---|---|---|
| Step | Line | $P_s$ (MW) | $P_r$ (MW) | $Q_s$ (MVAr) | $Q_r$ (MVAr) | $\Delta P$(MW) | $\Delta Q$ (MVAr) |
| 1 | 1 | 12.629 | 12.330 | 7.256 | 7.114 | 0.299 | 0.142 |
| | 2 | 11.482 | 11.210 | 6.526 | 6.533 | 0.272 | -0.007 |
| | 3 | 10.526 | 10.277 | 5.912 | 6.055 | 0.249 | -0.143 |
| 2 | 1 | 12.513 | 12.233 | 6.550 | 6.466 | 0.280 | 0.084 |
| | 2 | 11.376 | 11.122 | 5.884 | 5.945 | 0.254 | -0.061 |
| | 3 | 10.429 | 10.196 | 5.323 | 5.516 | 0.233 | -0.193 |
| 3 | 1 | 12.337 | 12.071 | 6.173 | 6.130 | 0.266 | 0.043 |
| | 2 | 11.217 | 10.974 | 5.541 | 5.640 | 0.243 | -0.099 |
| | 3 | 10.283 | 10.061 | 5.009 | 5.237 | 0.222 | -0.228 |
| 4 | 1 | 12.179 | 11.923 | 5.808 | 5.802 | 0.256 | 0.006 |
| | 2 | 11.072 | 10.840 | 5.209 | 5.341 | 0.232 | -0.132 |
| | 3 | 10.151 | 9.938 | 4.704 | 4.963 | 0.213 | -0.259 |
| 5 | 1 | 12.026 | 11.783 | 5.448 | 5.476 | 0.243 | -0.028 |
| | 2 | 10.934 | 10.713 | 4.882 | 5.046 | 0.221 | -0.164 |
| | 3 | 10.024 | 9.821 | 4.403 | 4.693 | 0.203 | -0.290 |

*Table 9.15 Measured values of sending and receiving active and reactive power of Line 1, 2, and 3 for the various steps of Case D (5 m/s)*

| Case D (5 m/s) | | | | | | | |
|---|---|---|---|---|---|---|---|
| Step | Line | $P_s$ (MW) | $P_r$ (MW) | $Q_s$ (MVAr) | $Q_r$ (MVAr) | $\Delta P$(MW) | $\Delta Q$ (MVAr) |
| 1 | 1 | 17.734 | 17.215 | 7.694 | 6.903 | 0.519 | 0.791 |
| | 2 | 16.124 | 15.651 | 6.925 | 6.340 | 0.473 | 0.585 |
| | 3 | 14.781 | 14.348 | 6.278 | 5.877 | 0.433 | 0.401 |
| 2 | 1 | 17.547 | 17.048 | 6.933 | 6.221 | 0.499 | 0.712 |
| | 2 | 15.953 | 15.499 | 6.233 | 5.721 | 0.454 | 0.512 |
| | 3 | 14.625 | 14.209 | 5.643 | 5.310 | 0.416 | 0.333 |
| 3 | 1 | 17.521 | 17.036 | 6.537 | 5.858 | 0.485 | 0.679 |
| | 2 | 15.930 | 15.489 | 5.873 | 5.391 | 0.441 | 0.482 |
| | 3 | 14.603 | 14.199 | 5.313 | 5.008 | 0.404 | 0.305 |
| 4 | 1 | 17.219 | 16.756 | 6.119 | 5.507 | 0.463 | 0.612 |
| | 2 | 15.655 | 15.234 | 5.492 | 5.073 | 0.421 | 0.419 |
| | 3 | 14.352 | 13.966 | 4.964 | 4.716 | 0.386 | 0.248 |
| 5 | 1 | 17.193 | 16.741 | 5.739 | 5.156 | 0.452 | 0.583 |
| | 2 | 15.631 | 15.221 | 5.147 | 4.753 | 0.410 | 0.394 |
| | 3 | 14.330 | 13.954 | 4.647 | 4.424 | 0.376 | 0.223 |

### 9.1.4 Sending and Receiving Power Factor for all Cases

*Table 9.16 Measured values of power factor for the start and end of each line for Case A*

| Step | Line | $cos\,\varphi_s$ | $cos\,\varphi_r$ |
|---|---|---|---|
| 1 | 1 | 0.924 | 0.932 |
| | 2 | 0.923 | 0.932 |
| | 3 | 0.922 | 0.932 |
| 2 | 1 | 0.887 | 0.896 |
| | 2 | 0.886 | 0.896 |
| | 3 | 0.885 | 0.896 |
| 3 | 1 | 0.847 | 0.857 |
| | 2 | 0.846 | 0.857 |
| | 3 | 0.845 | 0.857 |
| 4 | 1 | 0.805 | 0.816 |
| | 2 | 0.804 | 0.816 |
| | 3 | 0.803 | 0.816 |
| 5 | 1 | 0.763 | 0.774 |
| | 2 | 0.762 | 0.774 |
| | 3 | 0.761 | 0.774 |

*Table 9.17 Measured values of power factor for the start and end of each line for Case B (15, 10 and 5 m/s)*

| Case B (15 m/s) | | | | Case B (10 m/s) | | Case B (5 m/s) | |
|---|---|---|---|---|---|---|---|
| Step | Line | $cos\ \varphi_s$ | $cos\ \varphi_r$ | $cos\ \varphi_s$ | $cos\ \varphi_r$ | $cos\ \varphi_s$ | $cos\ \varphi_r$ |
| 1 | 1 | 0.924 | 0.932 | 0.924 | 0.932 | 0.924 | 0.932 |
| | 2 | 0.923 | 0.932 | 0.923 | 0.932 | 0.923 | 0.932 |
| | 3 | 0.922 | 0.932 | 0.922 | 0.932 | 0.922 | 0.932 |
| 2 | 1 | 0.887 | 0.896 | 0.887 | 0.896 | 0.887 | 0.896 |
| | 2 | 0.886 | 0.896 | 0.886 | 0.896 | 0.886 | 0.896 |
| | 3 | 0.885 | 0.896 | 0.885 | 0.896 | 0.885 | 0.896 |
| 3 | 1 | 0.847 | 0.857 | 0.847 | 0.857 | 0.847 | 0.857 |
| | 2 | 0.846 | 0.857 | 0.846 | 0.857 | 0.846 | 0.857 |
| | 3 | 0.845 | 0.857 | 0.845 | 0.857 | 0.845 | 0.857 |
| 4 | 1 | 0.805 | 0.816 | 0.805 | 0.816 | 0.805 | 0.816 |
| | 2 | 0.804 | 0.816 | 0.804 | 0.816 | 0.804 | 0.816 |
| | 3 | 0.803 | 0.816 | 0.803 | 0.816 | 0.803 | 0.816 |
| 5 | 1 | 0.763 | 0.774 | 0.763 | 0.774 | 0.762 | 0.774 |
| | 2 | 0.762 | 0.774 | 0.762 | 0.774 | 0.762 | 0.774 |
| | 3 | 0.761 | 0.774 | 0.761 | 0.774 | 0.761 | 0.774 |

*Table 9.18 Measured values of power factor for the start and end of each line for Case C (15, 10 and 5 m/s)*

| Case C (15 m/s) | | | | Case C (10 m/s) | | Case C (5 m/s) | |
|---|---|---|---|---|---|---|---|
| Step | Line | $cos\ \varphi_s$ | $cos\ \varphi_r$ | $cos\ \varphi_s$ | $cos\ \varphi_r$ | $cos\ \varphi_s$ | $cos\ \varphi_r$ |
| 1 | 1 | -0.831 | -0.838 | 0.189 | 0.166 | 0.909 | 0.914 |
| | 2 | 0.923 | 0.932 | 0.923 | 0.932 | 0.923 | 0.932 |
| | 3 | 0.922 | 0.932 | 0.922 | 0.932 | 0.922 | 0.932 |
| 2 | 1 | -0.973 | -0.969 | 0.753 | 0.607 | 0.993 | 0.994 |
| | 2 | 0.886 | 0.896 | 0.886 | 0.896 | 0.886 | 0.896 |
| | 3 | 0.885 | 0.896 | 0.885 | 0.896 | 0.885 | 0.896 |
| 3 | 1 | -0.993 | -0.996 | 0.641 | 0.764 | 0.993 | 0.989 |
| | 2 | 0.846 | 0.857 | 0.846 | 0.857 | 0.846 | 0.857 |
| | 3 | 0.845 | 0.857 | 0.845 | 0.857 | 0.845 | 0.857 |
| 4 | 1 | -0.904 | -0.915 | 0.364 | 0.391 | 0.946 | 0.935 |
| | 2 | 0.804 | 0.816 | 0.804 | 0.816 | 0.804 | 0.816 |
| | 3 | 0.803 | 0.816 | 0.803 | 0.816 | 0.803 | 0.816 |
| 5 | 1 | -0.768 | -0.779 | 0.276 | 0.275 | 0.874 | 0.853 |
| | 2 | 0.762 | 0.774 | 0.762 | 0.774 | 0.762 | 0.774 |
| | 3 | 0.761 | 0.774 | 0.761 | 0.774 | 0.761 | 0.774 |

*Table 9.19 Measured values of power factor for the start and end of each line for Case D (15,10 and 5 m/s)*

| Case D (15 m/s) | | | | Case D (10 m/s) | | Case D (5 m/s) | |
|---|---|---|---|---|---|---|---|
| Step | Line | $cos\,\varphi_s$ | $cos\,\varphi_r$ | $cos\,\varphi_s$ | $cos\,\varphi_r$ | $cos\,\varphi_s$ | $cos\,\varphi_r$ |
| 1 | 1 | 0.740 | 0.721 | 0.867 | 0.866 | 0.917 | 0.928 |
| | 2 | 0.744 | 0.718 | 0.869 | 0.864 | 0.918 | 0.926 |
| | 3 | 0.748 | 0.714 | 0.871 | 0.861 | 0.920 | 0.925 |
| 2 | 1 | 0.768 | 0.746 | 0.886 | 0.884 | 0.930 | 0.939 |
| | 2 | 0.771 | 0.743 | 0.888 | 0.881 | 0.931 | 0.938 |
| | 3 | 0.77 | 0.739 | 0.890 | 0.879 | 0.932 | 0.936 |
| 3 | 1 | 0.777 | 0.754 | 0.894 | 0.891 | 0.936 | 0.945 |
| | 2 | 0.781 | 0.751 | 0.896 | 0.889 | 0.938 | 0.944 |
| | 3 | 0.785 | 0.747 | 0.899 | 0.887 | 0.939 | 0.943 |
| 4 | 1 | 0.789 | 0.764 | 0.902 | 0.899 | 0.942 | 0.950 |
| | 2 | 0.793 | 0.760 | 0.904 | 0.897 | 0.943 | 0.948 |
| | 3 | 0.797 | 0.756 | 0.907 | 0.894 | 0.945 | 0.947 |
| 5 | 1 | 0.724 | 0.699 | 0.910 | 0.906 | 0.948 | 0.955 |
| | 2 | 0.728 | 0.696 | 0.913 | 0.904 | 0.949 | 0.954 |
| | 3 | 0.732 | 0.692 | 0.915 | 0.902 | 0.951 | 0.953 |

# 9.2 Results After Using Regulator

## 9.2.1 Sending and Receiving Voltages and Voltage Drop for all Cases

*Table 9.20 Measured values of sending and receiving voltage for Case A*

| Case A | | | | |
|---|---|---|---|---|
| Step | Line | $U_s$ (kV) | $U_r$ (kV) | $\Delta V$ (kV) |
| 1 | 1 | 64.640 | 61.365 | 3.275 |
| | 2 | 64.640 | 61.055 | 3.585 |
| | 3 | 64.640 | 60.745 | 3.895 |
| 2 | 1 | 64.425 | 60.785 | 3.640 |
| | 2 | 64.425 | 60.446 | 3.979 |
| | 3 | 64.425 | 60.110 | 4.315 |
| 3 | 1 | 64.210 | 60.228 | 3.982 |
| | 2 | 64.210 | 59.860 | 4.350 |
| | 3 | 64.210 | 59.492 | 4.718 |
| 4 | 1 | 64.005 | 59.685 | 4.320 |
| | 2 | 64.005 | 59.285 | 4.720 |
| | 3 | 64.005 | 58.895 | 5.110 |
| 5 | 1 | 63.805 | 59.160 | 4.645 |
| | 2 | 63.805 | 58.734 | 5.071 |
| | 3 | 63.805 | 58.315 | 5.490 |

*Table 9.21 Measured values of sending and receiving voltage for Case B (15, 10 and 5 m/s)*

| Case B (15 m/s) | | | | | Case B (10 m/s) | | | Case B (5 m/s) | | |
|---|---|---|---|---|---|---|---|---|---|---|
| Step | Line | $U_s$ (kV) | $U_r$(kV) | $\Delta V$(kV) | $U_s$(kV) | $U_r$(kV) | $\Delta V$(kV) | $U_s$(kV) | $U_r$(kV) | $\Delta V$(kV) |
| 1 | 1 | 65.714 | 62.383 | 3.331 | 65.685 | 62.355 | 3.330 | 65.636 | 62.309 | 3.327 |
| | 2 | 65.714 | 62.066 | 3.648 | 65.685 | 62.039 | 3.646 | 65.636 | 61.993 | 3.643 |
| | 3 | 65.714 | 61.753 | 3.961 | 65.685 | 61.726 | 3.959 | 65.636 | 61.680 | 3.956 |
| 2 | 1 | 65.544 | 61.845 | 3.699 | 65.525 | 61.827 | 3.698 | 65.477 | 61.782 | 3.695 |
| | 2 | 65.544 | 61.498 | 4.046 | 65.525 | 61.479 | 4.046 | 65.477 | 61.435 | 4.042 |
| | 3 | 65.544 | 61.155 | 4.389 | 65.525 | 61.136 | 4.389 | 65.477 | 61.092 | 4.385 |
| 3 | 1 | 65.380 | 61.324 | 4.056 | 65.370 | 61.314 | 4.056 | 65.323 | 61.270 | 4.053 |
| | 2 | 65.380 | 60.947 | 4.433 | 65.370 | 60.937 | 4.433 | 65.323 | 60.893 | 4.430 |
| | 3 | 65.380 | 60.574 | 4.806 | 65.370 | 60.565 | 4.805 | 65.323 | 60.521 | 4.802 |
| 4 | 1 | 65.167 | 60.767 | 4.400 | 65.220 | 60.816 | 4.404 | 65.173 | 60.773 | 4.400 |
| | 2 | 65.167 | 60.361 | 4.806 | 65.220 | 60.410 | 4.810 | 65.173 | 60.367 | 4.806 |
| | 3 | 65.167 | 59.962 | 5.205 | 65.220 | 60.010 | 5.210 | 65.173 | 59.968 | 5.205 |
| 5 | 1 | 64.957 | 60.224 | 4.733 | 65.073 | 60.331 | 4.742 | 65.028 | 60.290 | 4.738 |
| | 2 | 64.957 | 59.791 | 5.166 | 65.073 | 59.898 | 5.175 | 65.028 | 59.857 | 5.171 |
| | 3 | 64.957 | 59.365 | 5.592 | 65.073 | 59.472 | 5.601 | 65.028 | 59.430 | 5.598 |

*Table 9.22 Measured values of sending and receiving voltage for Case C (15,10 and 5 m/s)*

| Case C (15 m/s) | | | | | Case C (10 m/s) | | | Case C (5 m/s) | | |
|---|---|---|---|---|---|---|---|---|---|---|
| Step | Line | $U_s$ (kV) | $U_r$(kV) | $\Delta V$(kV) | $U_s$(kV) | $U_r$(kV) | $\Delta V$(kV) | $U_s$(kV) | $U_r$(kV) | $\Delta V$(kV) |
| 1 | 1 | 65.588 | 68.844 | -3.256 | 65.602 | 68.038 | -2.436 | 65.543 | 66.964 | -1.421 |
| | 2 | 65.588 | 61.947 | 3.641 | 65.602 | 61.961 | 3.641 | 65.543 | 61.905 | 3.638 |
| | 3 | 65.588 | 61.635 | 3.953 | 65.602 | 61.648 | 3.954 | 65.543 | 61.592 | 3.951 |
| 2 | 1 | 65.404 | 68.518 | -3.114 | 65.423 | 67.723 | -2.300 | 65.368 | 66.663 | -1.295 |
| | 2 | 65.404 | 61.366 | 4.038 | 65.423 | 61.384 | 4.039 | 65.368 | 61.332 | 4.036 |
| | 3 | 65.404 | 61.024 | 4.380 | 65.423 | 61.041 | 4.382 | 65.368 | 60.990 | 4.378 |
| 3 | 1 | 65.225 | 68.201 | -2.976 | 65.248 | 67.416 | -2.168 | 65.198 | 66.369 | -1.171 |
| | 2 | 65.225 | 60.802 | 4.423 | 65.248 | 60.824 | 4.424 | 65.198 | 60.777 | 4.421 |
| | 3 | 65.225 | 60.431 | 4.794 | 65.248 | 60.452 | 4.796 | 65.198 | 60.406 | 4.792 |
| 4 | 1 | 65.052 | 67.893 | -2.841 | 65.079 | 67.118 | -2.039 | 65.033 | 66.084 | -1.051 |
| | 2 | 65.052 | 60.258 | 4.794 | 65.079 | 60.280 | 4.799 | 65.033 | 60.237 | 4.796 |
| | 3 | 65.052 | 59.856 | 5.196 | 65.079 | 59.881 | 5.198 | 65.033 | 59.839 | 5.194 |
| 5 | 1 | 64.878 | 67.561 | -2.683 | 64.914 | 66.827 | -1.913 | 64.872 | 65.805 | -0.933 |
| | 2 | 64.878 | 59.718 | 5.160 | 64.914 | 59.752 | 5.162 | 64.872 | 59.713 | 5.159 |
| | 3 | 64.878 | 59.293 | 5.585 | 64.914 | 59.326 | 5.588 | 64.872 | 59.288 | 5.584 |

*Table 9.23 Measured values of sending and receiving voltage for Case D (15,10 and 5 m/s)*

| Case D (15 m/s) | | | | | Case D (10 m/s) | | | Case D (5 m/s) | | |
|---|---|---|---|---|---|---|---|---|---|---|
| Step | Line | $U_s$ (kV) | $U_r$(kV) | $\Delta V$(kV) | $U_s$(kV) | $U_r$(kV) | $\Delta V$(kV) | $U_s$(kV) | $U_r$(kV) | $\Delta V$(kV) |
| 1 | 1 | 65.555 | 64.234 | 1.321 | 65.522 | 63.852 | 1.670 | 65.446 | 63.382 | 2.064 |
| | 2 | 65.555 | 64.234 | 1.321 | 65.522 | 63.852 | 1.670 | 65.446 | 63.382 | 2.064 |
| | 3 | 65.555 | 64.234 | 1.321 | 65.522 | 63.852 | 1.670 | 65.446 | 63.382 | 2.064 |
| 2 | 1 | 65.374 | 63.748 | 1.626 | 65.345 | 63.371 | 1.974 | 65.275 | 62.91 | 2.365 |
| | 2 | 65.374 | 63.748 | 1.626 | 65.345 | 63.371 | 1.974 | 65.275 | 62.91 | 2.365 |
| | 3 | 65.374 | 63.748 | 1.626 | 65.345 | 63.371 | 1.974 | 65.275 | 62.91 | 2.365 |
| 3 | 1 | 65.200 | 63.282 | 1.918 | 65.173 | 62.904 | 2.269 | 65.109 | 62.451 | 2.658 |
| | 2 | 65.200 | 63.282 | 1.918 | 65.173 | 62.904 | 2.269 | 65.109 | 62.451 | 2.658 |
| | 3 | 65.200 | 63.282 | 1.918 | 65.173 | 62.904 | 2.269 | 65.109 | 62.451 | 2.658 |
| 4 | 1 | 65.026 | 62.814 | 2.212 | 65.006 | 62.450 | 2.556 | 64.947 | 62.006 | 2.941 |
| | 2 | 65.026 | 62.814 | 2.212 | 65.006 | 62.450 | 2.556 | 64.947 | 62.006 | 2.941 |
| | 3 | 65.026 | 62.814 | 2.212 | 65.006 | 62.450 | 2.556 | 64.947 | 62.006 | 2.941 |
| 5 | 1 | 64.853 | 62.351 | 2.502 | 64.844 | 62.011 | 2.833 | 64.792 | 61.579 | 3.213 |
| | 2 | 64.853 | 62.351 | 2.502 | 64.844 | 62.011 | 2.833 | 64.792 | 61.579 | 3.213 |
| | 3 | 64.853 | 62.351 | 2.502 | 64.844 | 62.011 | 2.833 | 64.792 | 61.579 | 3.213 |

### 9.2.2 Sending and Receiving Active and Reactive Power- Active and Reactive Power Losses for all Cases

*Table 9.24 Measured values of sending and receiving active and reactive power of Line 1, 2, and 3 for the various steps of Case A*

| Case A | | | | | | | |
|---|---|---|---|---|---|---|---|
| Step | Line | $P_s$(MW) | $P_r$ (MW) | $Q_s$ (MVAr) | $Q_r$ (MVAr) | $\Delta P$(MW) | $\Delta Q$ (MVAr) |
| 1 | 1 | 16.876 | 16.408 | 7.007 | 6.376 | 0.468 | 0.631 |
| | 2 | 16.751 | 16.242 | 6.992 | 6.311 | 0.509 | 0.681 |
| | 3 | 16.627 | 16.079 | 6.977 | 6.248 | 0.548 | 0.729 |
| 2 | 1 | 16.337 | 15.857 | 8.501 | 7.827 | 0.480 | 0.674 |
| | 2 | 16.200 | 15.680 | 8.466 | 7.740 | 0.520 | 0.726 |
| | 3 | 16.066 | 15.505 | 8.429 | 7.653 | 0.561 | 0.776 |
| 3 | 1 | 15.382 | 15.334 | 9.939 | 9.202 | 0.498 | 0.737 |
| | 2 | 15.686 | 15.146 | 9.882 | 9.089 | 0.540 | 0.793 |
| | 3 | 15.542 | 14.961 | 9.824 | 8.979 | 0.581 | 0.845 |
| 4 | 1 | 15.359 | 14.835 | 11.323 | 10.506 | 0.524 | 0.817 |
| | 2 | 15.205 | 14.638 | 11.245 | 10.366 | 0.567 | 0.879 |
| | 3 | 15.054 | 14.445 | 11.166 | 10.230 | 0.609 | 0.936 |
| 5 | 1 | 14.915 | 14.361 | 12.657 | 11.744 | 0.554 | 0.913 |
| | 2 | 14.755 | 14.155 | 12.556 | 11.575 | 0.600 | 0.981 |
| | 3 | 14.598 | 13.954 | 12.456 | 11.411 | 0.644 | 1.045 |

*Table 9.25 Measured values of sending and receiving active and reactive power of Line 1, 2, and 3 for the various steps of Case B (15 m/s)*

| Case B (15 m/s) | | | | | | | |
|---|---|---|---|---|---|---|---|
| Step | Line | $P_s$ (MW) | $P_r$ (MW) | $Q_s$ (MVAr) | $Q_r$ (MVAr) | $\Delta P$(MW) | $\Delta Q$ (MVAr) |
| 1 | 1 | 17.437 | 16.954 | 7.240 | 6.588 | 0.483 | 0.652 |
| | 2 | 17.308 | 16.783 | 7.225 | 6.521 | 0.525 | 0.704 |
| | 3 | 17.180 | 16.614 | 7.209 | 6.455 | 0.566 | 0.754 |
| 2 | 1 | 16.920 | 16.422 | 8.804 | 8.106 | 0.498 | 0.698 |
| | 2 | 16.778 | 16.238 | 8.767 | 8.015 | 0.540 | 0.752 |
| | 3 | 16.638 | 16.058 | 8.729 | 7.926 | 0.580 | 0.803 |
| 3 | 1 | 16.411 | 15.894 | 10.302 | 9.538 | 0.517 | 0.764 |
| | 2 | 16.260 | 15.700 | 10.243 | 9.421 | 0.560 | 0.822 |
| | 3 | 16.111 | 15.508 | 10.183 | 9.307 | 0.603 | 0.876 |
| 4 | 1 | 15.948 | 15.405 | 11.758 | 10.910 | 0.543 | 0.848 |
| | 2 | 15.788 | 15.200 | 11.677 | 10.765 | 0.588 | 0.912 |
| | 3 | 15.632 | 14.999 | 11.594 | 10.626 | 0.633 | 0.968 |
| 5 | 1 | 15.484 | 14.908 | 13.139 | 12.191 | 0.576 | 0.948 |
| | 2 | 15.317 | 14.695 | 13.035 | 12.017 | 0.622 | 1.018 |
| | 3 | 15.154 | 14.486 | 12.931 | 11.846 | 0.668 | 1.085 |

*Table 9.26 Measured values of sending and receiving active and reactive power of Line 1, 2, and 3 for the various steps of Case B (10 m/s)*

| Case B (10 m/s) | | | | | | | |
|---|---|---|---|---|---|---|---|
| Step | Line | $P_s$ (MW) | $P_r$ (MW) | $Q_s$ (MVAr) | $Q_r$ (MVAr) | $\Delta P$(MW) | $\Delta Q$ (MVAr) |
| 1 | 1 | 17.422 | 16.939 | 7.234 | 6.582 | 0.483 | 0.652 |
| | 2 | 17.292 | 16.768 | 7.218 | 6.515 | 0.524 | 0.703 |
| | 3 | 17.165 | 16.599 | 7.202 | 6.450 | 0.566 | 0.752 |
| 2 | 1 | 16.897 | 16.401 | 8.793 | 8.095 | 0.496 | 0.698 |
| | 2 | 16.756 | 16.217 | 8.756 | 8.004 | 0.539 | 0.752 |
| | 3 | 16.616 | 16.037 | 8.718 | 7.915 | 0.579 | 0.803 |
| 3 | 1 | 16.405 | 15.888 | 10.298 | 9.535 | 0.517 | 0.763 |
| | 2 | 16.253 | 15.693 | 10.239 | 9.418 | 0.560 | 0.821 |
| | 3 | 16.105 | 15.502 | 10.180 | 9.303 | 0.603 | 0.877 |
| 4 | 1 | 15.942 | 15.399 | 11.754 | 10.905 | 0.543 | 0.849 |
| | 2 | 15.783 | 15.194 | 11.672 | 10.760 | 0.589 | 0.912 |
| | 3 | 15.626 | 14.994 | 11.590 | 10.618 | 0.632 | 0.972 |
| 5 | 1 | 15.509 | 14.932 | 13.16 | 12.211 | 0.577 | 0.949 |
| | 2 | 15.342 | 14.718 | 13.056 | 12.036 | 0.624 | 1.020 |
| | 3 | 15.179 | 14.509 | 12.951 | 11.865 | 0.670 | 1.086 |

*Table 9.27 Measured values of sending and receiving active and reactive power of Line 1, 2, and 3 for the various steps of Case B (5 m/s)*

| Case B (5 m/s) | | | | | | | |
|---|---|---|---|---|---|---|---|
| Step | Line | $P_s$ (MW) | $P_r$ (MW) | $Q_s$ (MVAr) | $Q_r$ (MVAr) | $\Delta P$(MW) | $\Delta Q$ (MVAr) |
| 1 | 1 | 17.394 | 16.912 | 7.222 | 6.571 | 0.482 | 0.651 |
| | 2 | 17.265 | 16.741 | 7.207 | 6.505 | 0.524 | 0.702 |
| | 3 | 17.137 | 16.572 | 7.191 | 6.439 | 0.565 | 0.752 |
| 2 | 1 | 16.869 | 16.374 | 8.778 | 8.081 | 0.495 | 0.697 |
| | 2 | 16.728 | 16.191 | 8.741 | 7.991 | 0.537 | 0.750 |
| | 3 | 16.589 | 16.011 | 8.703 | 7.902 | 0.578 | 0.801 |
| 3 | 1 | 16.381 | 15.865 | 10.284 | 9.521 | 0.516 | 0.763 |
| | 2 | 16.230 | 15.670 | 10.225 | 9.404 | 0.560 | 0.821 |
| | 3 | 16.081 | 15.480 | 10.165 | 9.297 | 0.601 | 0.868 |
| 4 | 1 | 15.921 | 15.378 | 11.738 | 10.891 | 0.543 | 0.847 |
| | 2 | 15.761 | 15.173 | 11.657 | 10.746 | 0.588 | 0.911 |
| | 3 | 15.605 | 14.973 | 11.575 | 10.604 | 0.632 | 0.971 |
| 5 | 1 | 15.484 | 14.908 | 13.139 | 12.191 | 0.576 | 0.948 |
| | 2 | 15.318 | 14.695 | 13.034 | 12.016 | 0.623 | 1.018 |
| | 3 | 15.155 | 14.487 | 12.930 | 11.846 | 0.668 | 1.084 |

*Table 9.28 Measured values of sending and receiving active and reactive power of Line 1, 2, and 3 for the various steps of Case C (15 m/s)*

| Case C (15 m/s) | | | | | | | |
|---|---|---|---|---|---|---|---|
| Step | Line | $P_s$ (MW) | $P_r$ (MW) | $Q_s$ (MVAr) | $Q_r$ (MVAr) | $\Delta P$(MW) | $\Delta Q$ (MVAr) |
| 1 | 1 | -8.520 | -8.752 | -10.375 | -10.231 | 0.232 | -0.144 |
| | 2 | 17.251 | 16.727 | 7.201 | 6.499 | 0.524 | 0.702 |
| | 3 | 17.123 | 16.559 | 7.185 | 6.434 | 0.564 | 0.751 |
| 2 | 1 | -9.030 | -9.253 | -9.563 | -9.403 | 0.223 | -0.160 |
| | 2 | 16.702 | 16.166 | 8.728 | 7.979 | 0.536 | 0.749 |
| | 3 | 16.564 | 15.986 | 8.690 | 7.890 | 0.578 | 0.800 |
| 3 | 1 | -9.503 | -9.722 | -8.774 | -8.604 | 0.219 | -0.170 |
| | 2 | 16.190 | 15.632 | 10.199 | 9.381 | 0.558 | 0.818 |
| | 3 | 16.041 | 15.441 | 10.140 | 9.266 | 0.600 | 0.874 |
| 4 | 1 | -9.977 | -10.191 | -8.008 | -7.836 | 0.214 | -0.172 |
| | 2 | 15.709 | 15.123 | 11.617 | 10.710 | 0.586 | 0.907 |
| | 3 | 15.553 | 14.924 | 11.536 | 10.569 | 0.629 | 0.967 |
| 5 | 1 | -10.403 | -10.616 | -7.291 | -7.120 | 0.213 | -0.171 |
| | 2 | 15.260 | 14.640 | 12.986 | 11.972 | 0.620 | 1.014 |
| | 3 | 15.098 | 14.432 | 12.882 | 11.802 | 0.666 | 1.080 |

*Table 9.29 Measured values of sending and receiving active and reactive power of Line 1, 2, and 3 for the various steps of Case C (10 m/s)*

| Case C (10 m/s) | | | | | | | |
|---|---|---|---|---|---|---|---|
| Step | Line | $P_s$ (MW) | $P_r$ (MW) | $Q_s$ (MVAr) | $Q_r$ (MVAr) | $\Delta P$(MW) | $\Delta Q$ (MVAr) |
| 1 | 1 | 4.495 | 4.298 | -11.663 | -11.432 | 0.197 | -0.231 |
| | 2 | 17.256 | 16.732 | 7.203 | 6.502 | 0.524 | 0.701 |
| | 3 | 17.129 | 16.564 | 7.187 | 6.436 | 0.565 | 0.751 |
| 2 | 1 | 3.992 | 3.821 | -10.933 | -10.632 | 0.171 | -0.301 |
| | 2 | 16.710 | 16.173 | 8.732 | 7.983 | 0.537 | 0.749 |
| | 3 | 16.571 | 15.993 | 8.694 | 7.894 | 0.578 | 0.800 |
| 3 | 1 | 3.512 | 3.364 | -10.225 | -9.863 | 0.147 | -0.362 |
| | 2 | 16.199 | 15.641 | 10.205 | 9.386 | 0.558 | 0.819 |
| | 3 | 16.051 | 15.451 | 10.146 | 9.272 | 0.600 | 0.874 |
| 4 | 1 | 3.051 | 2.924 | -9.538 | -9.121 | 0.127 | -0.417 |
| | 2 | 15.721 | 15.135 | 11.626 | 10.718 | 0.586 | 0.908 |
| | 3 | 15.565 | 14.935 | 11.545 | 10.577 | 0.630 | 0.968 |
| 5 | 1 | 2.606 | 2.498 | -8.870 | -8.406 | 0.108 | -0.464 |
| | 2 | 15.273 | 14.652 | 12.997 | 11.982 | 0.621 | 1.015 |
| | 3 | 15.111 | 14.445 | 12.893 | 11.812 | 0.666 | 1.081 |

*Table 9.30 Measured values of sending and receiving active and reactive power of Line 1, 2, and 3 for the various steps of Case C (5 m/s)*

| Case C (5 m/s) | | | | | | | |
|---|---|---|---|---|---|---|---|
| Step | Line | $P_s$ (MW) | $P_r$ (MW) | $Q_s$ (MVAr) | $Q_r$ (MVAr) | $\Delta P$(MW) | $\Delta Q$ (MVAr) |
| 1 | 1 | 18.591 | 17.962 | -11.721 | -12.764 | 0.629 | 1.043 |
| | 2 | 17.227 | 16.704 | 7.192 | 6.491 | 0.523 | 0.701 |
| | 3 | 17.100 | 16.536 | 7.175 | 6.426 | 0.564 | 0.749 |
| 2 | 1 | 18.248 | 17.637 | -11.053 | -11.994 | 0.611 | 0.941 |
| | 2 | 16.679 | 16.143 | 8.715 | 7.967 | 0.536 | 0.748 |
| | 3 | 16.541 | 15.963 | 8.677 | 7.879 | 0.578 | 0.798 |
| 3 | 1 | 17.590 | 17.040 | -10.447 | -11.272 | 0.550 | 0.825 |
| | 2 | 16.176 | 15.619 | 10.191 | 9.374 | 0.557 | 0.817 |
| | 3 | 16.028 | 15.429 | 10.132 | 9.260 | 0.599 | 0.872 |
| 4 | 1 | 17.360 | 16.822 | -9.809 | -10.561 | 0.538 | 0.752 |
| | 2 | 15.697 | 15.112 | 11.608 | 10.701 | 0.585 | 0.907 |
| | 3 | 15.541 | 14.912 | 11.526 | 10.560 | 0.629 | 0.966 |
| 5 | 1 | 16.835 | 16.348 | -9.224 | -9.885 | 0.487 | 0.661 |
| | 2 | 15.255 | 14.635 | 12.983 | 11.969 | 0.620 | 1.014 |
| | 3 | 15.093 | 14.428 | 12.879 | 11.799 | 0.665 | 1.080 |

*Table 9.31 Measured values of sending and receiving active and reactive power of Line 1, 2, and 3 for the various steps of Case D (15 m/s)*

| Case D (15 m/s) | | | | | | | |
|---|---|---|---|---|---|---|---|
| Step | Line | $P_s$ (MW) | $P_r$ (MW) | $Q_s$ (MVAr) | $Q_r$ (MVAr) | $\Delta P$(MW) | $\Delta Q$ (MVAr) |
| 1 | 1 | 9.029 | 8.913 | 1.932 | 2.348 | 0.116 | -0.416 |
| | 2 | 8.209 | 8.103 | 1.683 | 2.205 | 0.106 | -0.522 |
| | 3 | 7.526 | 7.430 | 1.470 | 2.092 | 0.096 | -0.622 |
| 2 | 1 | 8.435 | 8.320 | 3.323 | 3.738 | 0.115 | -0.415 |
| | 2 | 7.669 | 7.565 | 2.950 | 3.467 | 0.104 | -0.517 |
| | 3 | 7.03 | 6.935 | 2.631 | 3.248 | 0.095 | -0.617 |
| 3 | 1 | 7.872 | 7.754 | 4.677 | 5.072 | 0.118 | -0.395 |
| | 2 | 7.157 | 7.050 | 4.181 | 4.680 | 0.107 | -0.499 |
| | 3 | 6.561 | 6.463 | 3.761 | 4.358 | 0.098 | -0.597 |
| 4 | 1 | 7.347 | 7.218 | 5.961 | 6.321 | 0.129 | -0.360 |
| | 2 | 6.679 | 6.563 | 5.348 | 5.814 | 0.116 | -0.466 |
| | 3 | 6.123 | 6.017 | 4.831 | 5.398 | 0.106 | -0.567 |
| 5 | 1 | 6.867 | 6.725 | 7.124 | 7.439 | 0.142 | -0.315 |
| | 2 | 6.243 | 6.114 | 6.406 | 6.830 | 0.129 | -0.424 |
| | 3 | 5.723 | 5.605 | 5.801 | 6.328 | 0.118 | -0.527 |

*Table 9.32 Measured values of sending and receiving active and reactive power of Line 1, 2, and 3 for the various steps of Case D (10 m/s)*

| Case D (10 m/s) | | | | | | | |
|---|---|---|---|---|---|---|---|
| Step | Line | $P_s$ (MW) | $P_r$ (MW) | $Q_s$ (MVAr) | $Q_r$ (MVAr) | $\Delta P$(MW) | $\Delta Q$ (MVAr) |
| 1 | 1 | 13.870 | 13.606 | 1.786 | 1.774 | 0.264 | 0.012 |
| | 2 | 12.611 | 12.371 | 1.551 | 1.682 | 0.240 | -0.131 |
| | 3 | 11.561 | 11.341 | 1.350 | 1.612 | 0.220 | -0.262 |
| 2 | 1 | 13.280 | 13.026 | 3.140 | 3.148 | 0.254 | -0.008 |
| | 2 | 12.074 | 11.843 | 2.783 | 2.931 | 0.231 | -0.148 |
| | 3 | 11.069 | 10.857 | 2.479 | 2.756 | 0.212 | -0.277 |
| 3 | 1 | 12.724 | 12.473 | 4.446 | 4.457 | 0.251 | -0.011 |
| | 2 | 11.568 | 11.340 | 3.970 | 4.119 | 0.228 | -0.149 |
| | 3 | 10.605 | 10.396 | 3.568 | 3.844 | 0.209 | -0.276 |
| 4 | 1 | 12.199 | 11.946 | 5.705 | 5.703 | 0.253 | 0.002 |
| | 2 | 11.091 | 10.861 | 5.115 | 5.251 | 0.230 | -0.136 |
| | 3 | 10.168 | 9.957 | 4.618 | 4.881 | 0.211 | -0.263 |
| 5 | 1 | 11.704 | 11.443 | 6.920 | 6.891 | 0.261 | 0.029 |
| | 2 | 10.640 | 10.404 | 6.221 | 6.331 | 0.236 | -0.110 |
| | 3 | 9.755 | 9.538 | 5.632 | 5.870 | 0.217 | -0.238 |

*Table 9.33 Measured values of sending and receiving active and reactive power of Line 1, 2, and 3 for the various steps of Case D (5 m/s)*

| Case D (5 m/s) | | | | | | | |
|---|---|---|---|---|---|---|---|
| Step | Line | $P_s$ (MW) | $P_r$ (MW) | $Q_s$ (MVAr) | $Q_r$ (MVAr) | $\Delta P$(MW) | $\Delta Q$ (MVAr) |
| 1 | 1 | 19.132 | 18.632 | 1.887 | 1.196 | 0.500 | 0.691 |
| | 2 | 17.394 | 16.940 | 1.643 | 1.156 | 0.454 | 0.487 |
| | 3 | 15.947 | 15.530 | 1.434 | 1.129 | 0.417 | 0.305 |
| 2 | 1 | 18.433 | 17.953 | 3.185 | 2.552 | 0.480 | 0.663 |
| | 2 | 16.759 | 16.322 | 2.824 | 2.388 | 0.437 | 0.436 |
| | 3 | 15.364 | 14.964 | 2.517 | 2.257 | 0.400 | 0.260 |
| 3 | 1 | 17.844 | 17.381 | 4.455 | 3.850 | 0.463 | 0.605 |
| | 2 | 16.223 | 15.803 | 3.979 | 3.567 | 0.420 | 0.412 |
| | 3 | 14.873 | 14.487 | 3.576 | 3.338 | 0.386 | 0.238 |
| 4 | 1 | 17.469 | 17.001 | 5.694 | 5.073 | 0.468 | 0.621 |
| | 2 | 15.882 | 15.456 | 5.105 | 4.678 | 0.426 | 0.427 |
| | 3 | 14.560 | 14.170 | 4.609 | 4.355 | 0.390 | 0.254 |
| 5 | 1 | 16.975 | 16.509 | 6.880 | 6.252 | 0.466 | 0.628 |
| | 2 | 15.434 | 15.010 | 6.184 | 5.749 | 0.424 | 0.435 |
| | 3 | 14.149 | 13.760 | 5.599 | 5.336 | 0.389 | 0.263 |

### 9.2.3 Sending and Receiving Power Factor for all Cases

*Table 9.34 Measured values of power factor for the start and end of each line for Case B (15, 10 and 5 m/s)*

| Case B (15 m/s) | | | | | Case B (10 m/s) | | | Case B (5 m/s) | | |
|---|---|---|---|---|---|---|---|---|---|---|
| Step | Line | $cos\ \varphi_s$ | $cos\ \varphi_r$ | $I_L$(A) | $cos\ \varphi_s$ | $cos\ \varphi_r$ | $I_L$(A) | $cos\ \varphi_s$ | $cos\ \varphi_r$ | $I_L$(A) |
| 1 | 1 | 0.924 | 0.932 | 165.912 | 0.924 | 0.932 | 165.838 | 0.924 | 0.932 | 165.716 |
| | 2 | 0.923 | 0.932 | 164.812 | 0.923 | 0.932 | 164.739 | 0.923 | 0.932 | 164.617 |
| | 3 | 0.922 | 0.932 | 163.720 | 0.922 | 0.932 | 163.647 | 0.922 | 0.932 | 163.527 |
| 2 | 1 | 0.887 | 0.897 | 167.918 | 0.887 | 0.897 | 167.867 | 0.887 | 0.897 | 167.746 |
| | 2 | 0.886 | 0.897 | 166.664 | 0.886 | 0.897 | 166.614 | 0.886 | 0.897 | 166.493 |
| | 3 | 0.885 | 0.897 | 165.422 | 0.885 | 0.897 | 165.372 | 0.885 | 0.897 | 165.253 |
| 3 | 1 | 0.847 | 0.857 | 171.137 | 0.847 | 0.857 | 171.110 | 0.847 | 0.857 | 170.987 |
| | 2 | 0.846 | 0.857 | 169.728 | 0.846 | 0.857 | 169.701 | 0.846 | 0.857 | 169.579 |
| | 3 | 0.845 | 0.857 | 168.334 | 0.845 | 0.857 | 168.307 | 0.845 | 0.857 | 168.186 |
| 4 | 1 | 0.805 | 0.816 | 175.241 | 0.805 | 0.816 | 175.382 | 0.805 | 0.816 | 175.258 |
| | 2 | 0.804 | 0.816 | 173.675 | 0.804 | 0.816 | 173.816 | 0.804 | 0.816 | 173.692 |
| | 3 | 0.803 | 0.816 | 172.128 | 0.803 | 0.816 | 172.267 | 0.803 | 0.816 | 172.145 |
| 5 | 1 | 0.763 | 0.774 | 180.183 | 0.763 | 0.774 | 180.509 | 0.763 | 0.774 | 180.384 |
| | 2 | 0.762 | 0.774 | 178.462 | 0.762 | 0.774 | 178.781 | 0.762 | 0.774 | 178.657 |
| | 3 | 0.761 | 0.774 | 176.760 | 0.761 | 0.774 | 177.076 | 0.761 | 0.774 | 176.954 |

*Table 9.35 Measured values of power factor for the start and end of each line for Case C (15,10 and 5 m/s)*

| Case C (15 m/s) | | | | | Case C (10 m/s) | | | Case C (5 m/s) | | |
|---|---|---|---|---|---|---|---|---|---|---|
| Step | Line | $cos\,\varphi_s$ | $cos\,\varphi_r$ | $I_L$(A) | $cos\,\varphi_s$ | $cos\,\varphi_r$ | $I_L$(A) | $cos\,\varphi_s$ | $cos\,\varphi_r$ | $I_L$(A) |
| 1 | 1 | -0.635 | -0.650 | 121.530 | 0.360 | 0.352 | 111.209 | 0.846 | 0.815 | 194.617 |
| | 2 | 0.923 | 0.932 | 164.496 | 0.923 | 0.932 | 164.531 | 0.923 | 0.932 | 164.382 |
| | 3 | 0.922 | 0.932 | 163.406 | 0.922 | 0.932 | 163.441 | 0.922 | 0.932 | 163.293 |
| 2 | 1 | -0.687 | -0.701 | 119.901 | 0.343 | 0.338 | 104.219 | 0.855 | 0.827 | 188.572 |
| | 2 | 0.886 | 0.897 | 166.307 | 0.886 | 0.897 | 166.354 | 0.886 | 0.897 | 166.215 |
| | 3 | 0.885 | 0.897 | 165.067 | 0.885 | 0.897 | 165.115 | 0.885 | 0.897 | 164.976 |
| 3 | 1 | -0.735 | -0.749 | 118.723 | 0.325 | 0.323 | 97.510 | 0.86 | 0.834 | 182.775 |
| | 2 | 0.846 | 0.857 | 169.326 | 0.846 | 0.857 | 169.385 | 0.846 | 0.857 | 169.255 |
| | 3 | 0.845 | 0.857 | 167.935 | 0.845 | 0.857 | 167.994 | 0.845 | 0.857 | 167.865 |
| 4 | 1 | -0.780 | -0.793 | 118.354 | 0.305 | 0.305 | 91.080 | 0.871 | 0.847 | 177.220 |
| | 2 | 0.804 | 0.816 | 173.368 | 0.804 | 0.816 | 173.440 | 0.804 | 0.816 | 173.318 |
| | 3 | 0.803 | 0.816 | 171.824 | 0.803 | 0.816 | 171.896 | 0.803 | 0.816 | 171.775 |
| 5 | 1 | -0.819 | -0.831 | 117.870 | 0.282 | 0.285 | 84.932 | 0.877 | 0.856 | 171.899 |
| | 2 | 0.762 | 0.774 | 178.244 | 0.762 | 0.774 | 178.345 | 0.762 | 0.774 | 178.230 |
| | 3 | 0.761 | 0.774 | 176.545 | 0.761 | 0.774 | 176.643 | 0.761 | 0.774 | 176.531 |

*Table 9.36 Measured values of power factor for the start and end of each line for Case D (15, 10 and 5 m/s)*

| Case D (15 m/s) | | | | | Case D (10 m/s) | | | Case D (5 m/s) | | |
|---|---|---|---|---|---|---|---|---|---|---|
| Step | Line | $cos\,\varphi_s$ | $cos\,\varphi_r$ | $I_L$(A) | $cos\,\varphi_s$ | $cos\,\varphi_r$ | $I_L$(A) | $cos\,\varphi_s$ | $cos\,\varphi_r$ | $I_L$(A) |
| 1 | 1 | 0.978 | 0.967 | 80.368 | 0.991 | 0.992 | 124.003 | 0.995 | 0.998 | 169.367 |
| | 2 | 0.980 | 0.965 | 72.938 | 0.992 | 0.991 | 112.664 | 0.996 | 0.998 | 153.926 |
| | 3 | 0.981 | 0.963 | 66.742 | 0.993 | 0.990 | 103.213 | 0.996 | 0.997 | 141.058 |
| 2 | 1 | 0.930 | 0.912 | 79.204 | 0.973 | 0.972 | 121.390 | 0.985 | 0.990 | 166.287 |
| | 2 | 0.933 | 0.909 | 71.780 | 0.975 | 0.971 | 110.223 | 0.986 | 0.990 | 151.08 |
| | 3 | 0.937 | 0.906 | 65.578 | 0.976 | 0.970 | 100.910 | 0.987 | 0.989 | 138.403 |
| 3 | 1 | 0.860 | 0.837 | 80.186 | 0.944 | 0.942 | 120.240 | 0.970 | 0.976 | 164.272 |
| | 2 | 0.864 | 0.833 | 72.583 | 0.946 | 0.940 | 109.115 | 0.971 | 0.976 | 149.203 |
| | 3 | 0.868 | 0.829 | 66.224 | 0.948 | 0.938 | 99.831 | 0.972 | 0.975 | 136.637 |
| 4 | 1 | 0.777 | 0.752 | 83.187 | 0.906 | 0.902 | 120.452 | 0.951 | 0.958 | 163.256 |
| | 2 | 0.781 | 0.749 | 75.234 | 0.908 | 0.900 | 109.250 | 0.952 | 0.957 | 148.236 |
| | 3 | 0.785 | 0.744 | 68.576 | 0.911 | 0.898 | 99.895 | 0.953 | 0.956 | 135.707 |
| 5 | 1 | 0.694 | 0.671 | 87.961 | 0.861 | 0.857 | 121.817 | 0.927 | 0.935 | 163.083 |
| | 2 | 0.698 | 0.667 | 79.513 | 0.863 | 0.854 | 110.438 | 0.928 | 0.934 | 148.039 |
| | 3 | 0.702 | 0.663 | 72.436 | 0.866 | 0.852 | 100.931 | 0.930 | 0.932 | 135.485 |

## 9.2.4 Generated and Supplied Reactive Power and $Q_{ref}$ for all Cases

*Table 9.37 Generated and supplied reactive power for the cases B (15, 10 and 5 m/s)*

| Case B (15 m/s) | | | | Case B (10 m/s) | | | Case B (5 m/s) | | |
|---|---|---|---|---|---|---|---|---|---|
| Step | $Q_{Gen}$ (MVAr) | $Q_{Sup}$ (MVAr) | $Q_{ref}$ (p.u) | $Q_{Gen}$ (MVAr) | $Q_{Sup}$ (MVAr) | $Q_{ref}$ (p.u) | $Q_{Gen}$ (MVAr) | $Q_{Sup}$ (MVAr) | $Q_{ref}$ (p.u) |
| 1 | 20.635 | 19.398 | 0.624 | 20.67 | 20.081 | 0.625 | 20.742 | 20.317 | 0.628 |
| 2 | 22.214 | 21.174 | 0.663 | 21.939 | 21.313 | 0.664 | 22.006 | 21.544 | 0.666 |
| 3 | 22.797 | 21.735 | 0.700 | 23.179 | 22.516 | 0.701 | 23.229 | 22.732 | 0.703 |
| 4 | 24.034 | 22.932 | 0.739 | 24.379 | 23.677 | 0.737 | 24.429 | 23.896 | 0.739 |
| 5 | 23.815 | 22.714 | 0.777 | 25.553 | 24.81 | 0.772 | 25.599 | 25.019 | 0.774 |

*Table 9.38 Generated and supplied reactive power for the cases C (15, 10 and 5 m/s)*

| Case C (15 m/s) | | | | Case C (10 m/s) | | | Case C (5 m/s) | | |
|---|---|---|---|---|---|---|---|---|---|
| Step | $Q_{Gen}$ (MVAr) | $Q_{Sup}$ (MVAr) | $Q_{ref}$ (p.u) | $Q_{Gen}$ (MVAr) | $Q_{Sup}$ (MVAr) | $Q_{ref}$ (p.u) | $Q_{Gen}$ (MVAr) | $Q_{Sup}$ (MVAr) | $Q_{ref}$ (p.u) |
| 1 | 19.161 | 18.262 | 0.575 | 19.83 | 19.281 | 0.595 | 20.772 | 20.376 | 0.623 |
| 2 | 20.284 | 19.355 | 0.609 | 20.94 | 20.358 | 0.628 | 21.881 | 21.401 | 0.656 |
| 3 | 21.374 | 20.401 | 0.641 | 22.018 | 21.404 | 0.661 | 22.932 | 22.473 | 0.688 |
| 4 | 22.431 | 21.434 | 0.673 | 23.065 | 22.419 | 0.692 | 23.974 | 23.433 | 0.719 |
| 5 | 23.491 | 22.454 | 0.705 | 24.082 | 23.405 | 0.722 | 24.962 | 24.441 | 0.749 |

*Table 9.39 Generated and supplied reactive power for the cases D (15, 10 and 5 m/s)*

| Case D (15 m/s) | | | | Case D (10 m/s) | | | Case D (5 m/s) | | |
|---|---|---|---|---|---|---|---|---|---|
| Step | $Q_{Gen}$ (MVAr) | $Q_{Sup}$ (MVAr) | $Q_{ref}$ (p.u) | $Q_{Gen}$ (MVAr) | $Q_{Sup}$ (MVAr) | $Q_{ref}$ (p.u) | $Q_{Gen}$ (MVAr) | $Q_{Sup}$ (MVAr) | $Q_{ref}$ (p.u) |
| 1 | 15.197 | 14.296 | 0.456 | 16.127 | 15.632 | 0.484 | 17.247 | 16.899 | 0.157 |
| 2 | 16.277 | 15.344 | 0.488 | 17.192 | 16.67 | 0.516 | 18.302 | 17.924 | 0.549 |
| 3 | 17.285 | 16.318 | 0.519 | 18.226 | 17.673 | 0.547 | 19.313 | 18.923 | 0.580 |
| 4 | 18.33 | 17.328 | 0.550 | 19.229 | 18.645 | 0.577 | 20.298 | 19.861 | 0.609 |
| 5 | 19.583 | 18.539 | 0.581 | 20.202 | 19.587 | 0.606 | 21.243 | 20.783 | 0.638 |

# 9.3 Regular Model

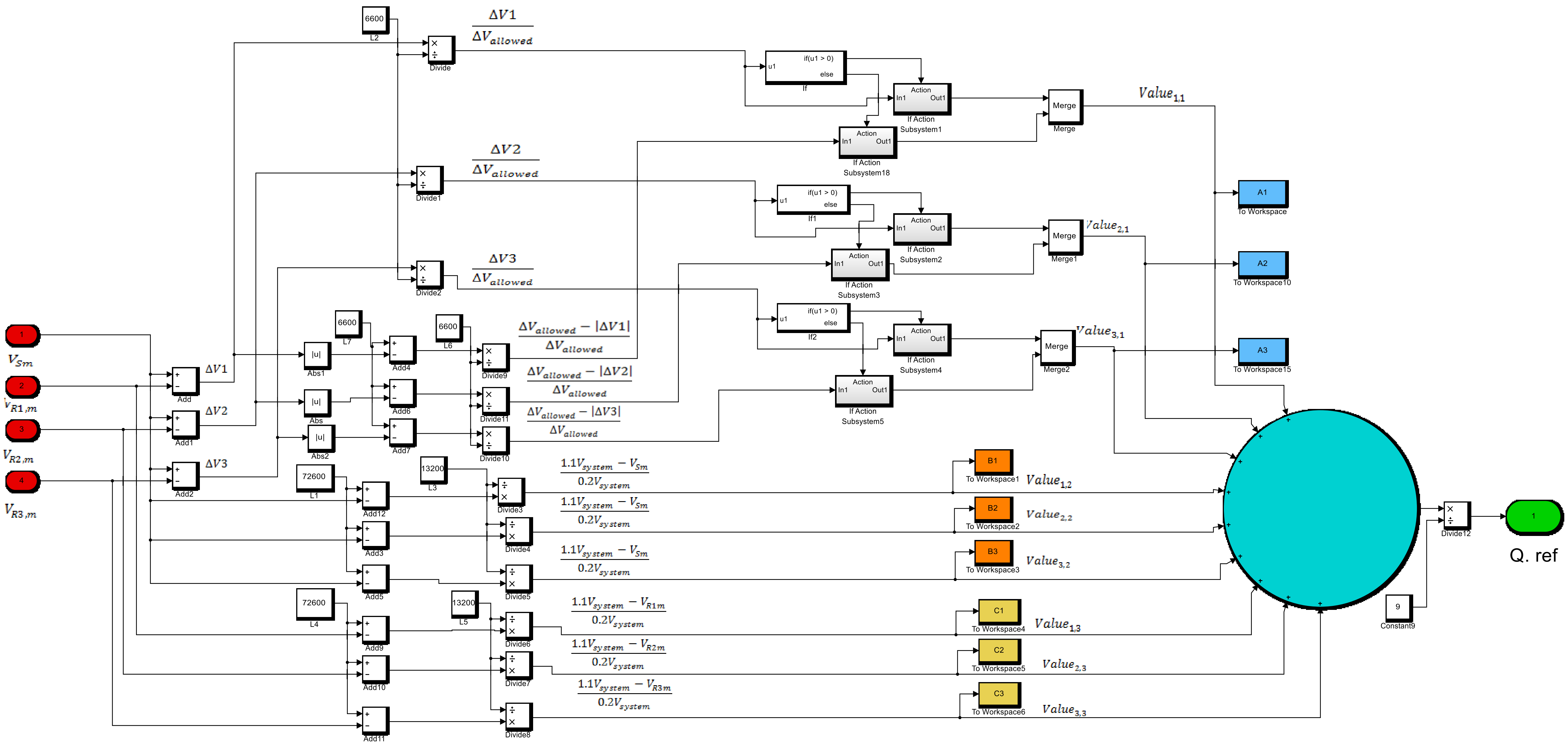


*Fig 9.1 Regulator model*